Thesis Title

Wax Flow Assurance, an Extensive Experimental Study on Risk Evaluation and Deposition Monitoring

Mohsen Hoopanah

Submitted for the degree of Doctor of Philosophy

In

Petroleum Engineering

Heriot-Watt University

Institute of Petroleum Engineering

November 2017

ABSTRACT

Flow assurance involves ensuring fluid flow in well and pipelines. In a deep cold environment wax deposition can form and easily reduce the flow. When the temperature drops below wax appearance temperature, wax particles precipitate out of solution, crystallize and form a gel. Deposition of these gels makes flow through pipelines difficult and challenging which leads to increases in operational and remedial costs. Pipeline failures in this condition is a potential threat in some cases such as restart of the production. Reliable experimental approaches mimicking pipeline conditions for wax studies are critical to reduce the cost of production and transportation of crude oil.

This thesis presents a rigorous investigation using a high-pressure rheometer aimed at identifying the optimum starting temperature for wax studies. The technique can also be used for measuring the proper temperature in terms of wax inhibitor injection. The next step in laboratory wax studies is cooling down the sample from initial temperature to a test temperature. Since pipeline passes through different environments with different temperatures from well head to the production unit which fluid poses to different cooling/heating rate when crosses these areas. The impact of cooling rate on the various wax parameters including wax appearance temperature (WAT), wax disappearance temperature (WDT) and viscosity was investigated using a rheometer. A coaxial shearing cold finger was used to study the effect of test time and shear rate on deposition with a blank oil sample. In addition, the impact of subcooling on the performance of a number of wax inhibitors was studied by a coaxial apparatus.

The main work of this thesis was aimed at investigating the reason for discrepancies between results from different conventional experimental techniques in terms of wax inhibitor screening. The result in some devices contradict with other devices which make it difficult to decide which one is more realistic and applicable in the field. The equipment included Quartz Crystal Microbalance (QCM) technique, rheometer, coaxial shearing cold finger, Near InfraRed (NIR) spectroscopy and an in-house built flowloop. A wide variety of different approaches were used to obtain reliable data with different apparatus such as employing different ageing times, flow/shear rates, subcooling, presence of impurities, test geometries, water cuts, the impact of circulation in the loop, the influence of thermal cycle, conditioning time, etc.

In addition, the dependency of wax deposition on subcooling in the presence of a watercut, various thermodynamic hydrate inhibitors and two different commercial low

dosage anti-agglomeration (AA), were investigated using a flowloop. The adhesion tendency of wax particles and the rheology of fluids were also studied in the presence of AA's using both QCM and rheometer. All the tested parameters will be experienced during the well/field life cycle.

Downhole samples which are the more likely source of crude for testing pre-development will in many instances have some degree of mud contamination. The possibility of using several wax related parameters including WAT, WDT, adhesion tendency and viscosity obtained by rheometer and QCM, to determine levels of oil based mud contamination in downhole samples was investigated.

DEDICATION

First of all, I wish to dedicate this thesis to Imam-e-Zaman (AS), and then to my lovely family, my parents, Samad and Rouh angis, my brother, Vahid, and my cute sisters, Mahdieh and Mahsa.

ACKNOWLEDGEMENTS

Firstly, I would like to express my sincere gratitude to my supervisors Prof Bahman Tohidi and Dr. Rod Burgass, for their continuous support of my PhD study and related research, for their patience, motivation, and immense knowledge. Their guidance helped me in all the time of research and writing of this thesis. I could not have imagined having a better advisors and mentors for my PhD study.

My profound thanks are also extended to Dr Grant Paterson who has been a best friend and was there whenever I needed his help no matter time or day. He also constantly supports me with his valuable suggestions. On personal side, I really loved working with him.

I wish to deeply thank Dr Jinhai Yang, Dr Antonin Chapoy and Mr Alastair Reid for their technical advices and helpful discussions during the course of this thesis.

Additionally, I greatly appreciate the reviewers and examiners of this thesis, Dr Antonin Chapoy, Dr Houra Mozaffar, Dr Rod Farquhar, Dr David Harbottle and Dr Jingsheng Ma, for their precious times and valuable suggestions.

I am also grateful to all my friends and colleagues at the Hydrates, Flow Assurance & Phase Equilibria Research Group at Heriot-Watt University and Hydrafact Ltd. who made my stay in Edinburgh very pleasant and memorable.

Last but not the least, I want to thank the members of my lovely family, my father, mother, brother and two cute sisters for their prayers, selfless support, dedication, patience, love and encouragement, not only during this program, but throughout my life. I couldn't have done it without you!

Alhamdu lillahi rabbi alAAalameen (All praises and thanks be to Allah, the Lord of the Worlds).

DECLARATION STATEMENT

(Research Thesis Submission Form should be placed here)

TABLE OF CONTENTS

LISTS OF TABLES AND FIGURES

Abbreviation

AA	*Anti-agglomerant*
Approx	*Approximately*
ASTM	*American society for testing and materials*
CAPEX	*Capital expenditure*
cm	*Centimetre*
cP	*Centipoise*
CPM	*cc per minutes*
DSC	*Differential scanning calorimetry*
FTIR	*Fourier transform infrared*
gr	*Gram*
HPLC	*High Performance Liquid Chromatography*
hrs	*Hours*
Hz	*Hertz*
INH	*Inhibitor*
LT	*Light transmittance*
Max	*Maximum*
MEG	*Mono ethylene glycol*
Min	*Minimum*
Min	*Minute*
Mrad	*Milliradian*
MW	*Molecular weight*
NIR	*Near infrared*
OPEX	*Operational expenditure*
PPD	*Pour point depressant*
Ppm	*Part per million*
QCM	*Quartz crystal microbalance*
Rad	*Radian*
RF	*Resonant frequency*
RPM	*Revolution per minute*
SARA	*saturates, aromatics, resins, and asphaltenes*
SEM	*Scanning Electron Microscopy*
St.dev	*Standard deviation*
WAT	*Wax appearance temperature*

WDT	*Wax disappearance temperature*
WFT	*Wax formation temperature*
WPT	*Wax precipitation temperature*
ΔP	*Differential pressure*
ΔRF	*Differential resonant frequency*

Chapter 1: Introduction

The deposition of paraffin wax on the internal walls of pipelines transporting reservoir fluids, especially in offshore facilities, presents a major engineering challenge to the petroleum industry, as any course of action to remediate them is very expensive. The precipitated wax has complex non-Newtonian characteristics. The presence of some impurities in the pipeline may also influence the deposition problem and therefore evaluating the effect of each parameter is a necessity for obtaining a good understanding of the wax deposition and precipitation. A number of techniques are available which can be used to control and reduce wax deposition along a pipeline including insulation, pigging, heating, and chemical methods. Chemical methods have been widely used in subsea tie-lines over long distances due to relatively lower CAPEX/OPEX. Studies show that while different methods have been applied, so far there has not been a consistent method that can be used for the evaluation of the performance of these chemicals in the field to give reliable and reproducible results from one setup to another. The initial step for developing any successful flow assurance strategy in the field is a laboratory scale study mimicking the field conditions to employ the required techniques and information for optimising design strategies to reduce wax deposition [1-16].

This work presents an extensive experimental study on wax precipitation/deposition and evaluation of the effect of different impurities which might be involved in this process using a number of different experimental equipment. The aim of this thesis is to develop an optimum approach for each setup to obtain consistent data at different conditions. Furthermore, in this thesis results obtained from different setups have been compared and linked to one another to develop and select the more reliable techniques for this evaluation. This thesis is comprised of seven chapters. The content presented in each individual chapter is described below. In addition, at the beginning of Chapters 3 to 6, there is an introduction which maps out and presents an outline of the work.

An extensive review of the existing literature on wax deposition is presented in **Chapter 2**. This chapter includes a wax overview, classification, crystallisation, and description of some physical properties of wax particles. Furthermore, the deposition, precipitation, some related mechanisms and parameters associated to this study are explained in this chapter. Moreover, the most important wax related concepts are

detailed in addition to some related laboratory techniques to measure WAT/WDT. Finally, some of the conventional methods used for control and remediation of wax precipitation and deposition in field conditions, and detailed overview of the chemical methods used are mentioned in this section.

A summary of different types of experimental apparatus used in this work is described in detail in **Chapter 3**. These equipment are Quartz Crystal Microbalance (QCM) technique, coaxial shearing cold finger, mini benchtop flowloop, rheometer and Near InfraRed (NIR) spectroscopy. The properties of the materials, the experimental procedure and analysing data is also discussed in detail in this chapter.

In wax studies, a sample is usually exposed to a thermal cycle which starts with a conditioning temperature and is cooled to a so-called test temperature. The test temperature is usually set lower than the wax appearance temperature (WAT) and is relatively close to the seabed temperature. The choice of the starting temperature, however, is poorly understood. In the laboratory, it is normal to set a temperature to mimic the worst possible results in the field. The worst-case scenario is the condition that results in the highest possible WAT, pour point and viscosity. **Chapter 4** describes a robust way using a rheometer to obtain the optimum starting condition temperature for the samples used in the following chapters. In addition to that, it is required to investigate whether this measured optimum temperature is also suitable and meets the injection condition requirements for the optimum performance of some paraffin inhibitors. For this purpose, a number of measurements with two different samples dosed with various inhibitors were conducted to obtain the optimum injection temperature necessary for the inhibitors to cover/prohibit wax precipitation/deposition. To optimize the test conditions, the impact of cooling rate on WAT, WDT and viscosity using atmospheric geometry launched was also investigated in this section. Moreover, the impacts of test time and shear rate on the wax deposition was investigated using coaxial shearing cold finger on a blank oil sample. Finally, the performance of selected chemical wax inhibitors on a specified sample under various differential temperatures was studied.

There are many approaches to assessing the risk of wax deposition and screening chemical inhibitors in the laboratory. A major obstacle for laboratory-based techniques is the inability to directly reproduce field conditions. Consequently, the results obtained from laboratory do not always guarantee to prohibit wax deposition in the field. In

addition, different devices are observed to give different results which in some cases contradict one another. **Chapter 5** presents a series of laboratory-based tests (QCM, coaxial cold finger, flowloop, rheometer and NIR) to evaluate and rank the performance of 11 different commercial inhibitors with three different real waxy oils and a model synthetic sample. Different scenarios are also investigated with the aim of demonstrating how the choice of conditions for testing inhibitors can have a substantial impact on their measured performance using coaxial and flowloop, including different ageing time, flow/shear rate, subcooling, impurities, test geometry, watercut, circulation loop and the method of inhibitor injection. In addition, visual monitoring of morphological behaviour on treated wax particles using the synthetic oil sample was conducted. Using a synthetic fluid gave an opportunity to neglect the effect of impurities, asphaltene and resin on the result. Moreover, a series of measurements were carried out using high-pressure geometry with the rheometer to investigate the performance of a specified inhibitor after several consecutive thermal cycle tests, as well as extended conditioning time. High pressure geometry in rheometer consists of a high pressure closed cell which has the ability to avoid the risk of component evaporation in a long period of measurements.

Produced oil is often commingled with water which may lead to gas hydrate problems due to the temperatures encountered, at which wax solids will also be present. Injection of hydrate inhibitors to prevent hydrates may have a negative impact on the wax problem [17-18]. In **Chapter 6** a series of measurements were conducted to study the effect of subcooling on wax deposition in the presence of watercut, some thermodynamic hydrate inhibitors and two different commercial low dosage anti-agglomeration hydrate inhibitors using flowloop. In addition, the adhesion tendency of wax particles and rheology of fluids in temperature sweep in the presence of low dosage anti-agglomeration was studied using QCM and Rheometer respectively. Following this chapter, a series of test is presented to explore the influence of mud filtrate from the initial sampling campaign on the wax related parameters including WAT, WDT, deposition adherent tendency and viscosity. The aim was to predict the parameters of the original/uncontaminated sample with a variety of oil types using Rheometer and QCM. Finally, the impact of the presence of impurities on QCM reading associated with the wax/screening inhibitor study in a consecutive thermal cycle test was investigated in this chapter.

The conclusions obtained from the experimental studies are summarised in **Chapter 7**. In addition, some recommendations for future work on subjects related to the current study are presented.

1.1 References

1. Burger, E., T. Perkins, and J. Striegler, *Studies of wax deposition in the trans Alaska pipeline.* Journal of Petroleum Technology, 1981. **33**(06): p. 1,075-1,086.
2. Aiyejina, A., et al., *Wax formation in oil pipelines: A critical review.* International journal of multiphase flow, 2011. **37**(7): p. 671-694.
3. del Carmen García, M., et al., *The influence of alkane class-types on crude oil wax crystallization and inhibitors efficiency.* Journal of petroleum science and engineering, 2000. **25**(3): p. 99-105.
4. Garcia, M.d.C., et al., *Paraffin deposition in oil production. Oil composition and paraffin inhibitors activity.* Petroleum science and technology, 1998. **16**(9-10): p. 1001-1021.
5. Ferworn, K.A., A. Hammami, and H. Ellis. *Control of wax deposition: an experimental investigation of crystal morphology and an evaluation of various chemical solvents*. in *International Symposium on Oilfield Chemistry*. 1997. Society of Petroleum Engineers.
6. Lee, H.S., *Computational and rheological study of wax deposition and gelation in subsea pipelines*. 2008: ProQuest.
7. Shock, D., J. Sudbury, and J. Crockett, *Studies of the mechanism of paraffin deposition and its control.* Journal of Petroleum Technology, 1955. **7**(09): p. 23-28.
8. Al-Yaari, M. *Paraffin wax deposition: Mitigation and removal techniques*. in *SPE Saudi Arabia Section Young Professionals Technical Symposium*. 2011. Society of Petroleum Engineers.
9. Funk, J.E. and D.R. Dinger, *Viscosity and Rheology*, in *Predictive Process Control of Crowded Particulate Suspensions*. 1994, Springer. p. 235-252.
10. Mezger, T.G., *The rheology handbook: for users of rotational and oscillatory rheometers*. 2006: Vincentz Network GmbH & Co KG.
11. Barnes, H.A., *A handbook of elementary rheology*. 2000.
12. Jennings, D.W. and K. Weispfennig, *Effects of shear and temperature on wax deposition: Coldfinger investigation with a Gulf of Mexico crude oil.* Energy & fuels, 2005. **19**(4): p. 1376-1386.
13. Burgass, R. and B. Tohidi. *Development and validation of small volume multi-tasking flow assurance tool*. in *SPE Asia Pacific Oil and Gas Conference and Exhibition*. 2011. Society of Petroleum Engineers.

14. Chi, Y., N. Daraboina, and C. Sarica, *Investigation of inhibitors efficacy in wax deposition mitigation using a laboratory scale flow loop.* AIChE Journal, 2016.

15. Hunt, P.K. and B. Zemel, *Method for identifying drilling mud filtrate invasion of a core sample from a subterranean formation*. 1991, Google Patents.

16. Abrams, A., *Mud design to minimize rock impairment due to particle invasion.* Journal of petroleum technology, 1977. **29**(05): p. 586-592.

17. Burgass, R.W., *Applications of quartz crystal microbalance technology in petroleum engineering, demonstrated by studies of wax, asphaltenes, hydrates, ice, diesel additives and anti-deposition coatings*. 2015, Heriot-Watt University.

18. Kelland, M.A., *History of the development of low dosage hydrate inhibitors.* Energy & Fuels, 2006. **20**(3): p. 825-847.

Chapter 2: Literature review

2.1 Introduction

Since large amounts of oil and gas have reached the mature stage and are on the decline, the petroleum industry is inevitably exploring oil fields situated in deeper water or in arctic environments. Low seabed temperature and long-distance pipelines are some characteristics of these areas. As a result, the most critical and increasing operational challenge during the late twentieth century was reported to be wax deposition while petroleum fluids shifted to these resources, though wax deposition has been an inherent challenge since 1928 in a wide range of locations including the reservoir, wellbore, tubing, flow lines, and surface facilities [1-4].

2.2 Wax Overview

In the petroleum industry, wax is a general term used to describe all kinds of solid being either precipitated or dissolved during cooling or while heat applied. In theory, a considerable proportion of petroleum known as paraffin of different chain length (C_{18}-C_{65}) is called wax. These saturated hydrocarbons can be linear or branched. They are typically dissolved in the favourable oil reservoir conditions where the temperature is relatively high and tend to form clusters and precipitate from crude oil, under suitable conditions. When wax precipitates it forms a crystalline structure, which is thermoplastic and deforms under tensile stress instead of cracking, though, it has stable crystal structure at lower temperatures [2, 5-7].

2.3 Crystallization

The crude oil leaves the reservoir at a temperature usually over ~70 °C and flows through a subsea pipeline where the water temperature is around 4 °C. At this temperature, depending upon the oil composition, wax might begin to precipitate. The process of separation of the solid phase from a homogenous solution oil is generally called crystallization [5, 8].

Two types of wax crystals have been distinguished, macro-crystalline and micro-crystalline [8-10].

2.3.1 Macro and microcrystalline

The characteristics of the wax generally depend on the oil composition. A wax composition mainly consisting of a mixture of n-alkanes (linear alkanes), and small amounts of iso-alkanes, and cycloalkanes create microcrystalline waxes which form clusters and precipitate from crude oils. Unstable wax solids are their characteristics due to its' branched nature. They also tend to delay the formation of the deposit. On the other hand, the macrocrystalline wax is mainly formed from Naphthenic (cyclic) and long-chain paraffin which is stiff and bulky in nature.[8-10].

2.3.2 Crystallization theory

While the temperature decreases, attractive and repulsive forces between molecules known as van der Waals forces is becoming more restricted, leads molecules to move closer together. As time progresses, wax molecules are hindered, leading to continuous reduction and closure of the space between the molecules and begin to have a more ordered arrangement after which wax crystallises. Therefore, smaller surface alkanes in terms of intermolecular forces such as branched alkanes result in a lower melting point compared to non-branched alkanes [11, 12]. Wax crystal formation involves two distinct stages, nucleation and growth [2, 13, 14]. These stages are described in the following sub-section.

2.3.2.1 Nucleation and growth

Crystallisation process initiates whenever solubility limit is approached. This is in line with the formation of unstable molecule clusters known as nucleation. The unstable molecules tend to re-dissolve into the solution. These clusters grow larger and become stable upon reaching a certain critical size named nuclei. They are the smallest stable particles of wax crystal. This nucleus provides suitable sites and having a higher magnitude of the attractive forces to receive other molecules preceding growth stage then wax precipitates [2, 13, 14].

The common particle size of bulk precipitated wax particles is about 2-7 μm [15].

2.3.2.1.1 Types of nucleation

There must exist tiny solid particles as a nucleation site to form crystals. These particles must be either in an oil system to form homogeneous nucleation or exist as impurities.

The impurities such as tiny elements of the reservoir rock or corroded material from production equipment form heterogeneous nucleation. A spontaneous nucleation is mainly a thermal process which needs to achieve a bigger supersaturation in comparison with existing impurities as a nucleus. Therefore, a faster crystallisation process is expected in the presence of heterogeneous nucleation [5, 13, 14, 16, 17].

2.3.3 Shape of crystals

The shape of wax crystals can be investigated using x-ray diffraction. The approach is achieved by measuring the angle among the scattered x-rays which give a better insight in wax particle-fluid behaviour. These experiments show that waxes form mainly rhombic or monoclinic in shape with a low order of symmetry [18, 19].

Generally, crystals of paraffin wax are categorised in three different characteristic forms known as plates, needles and mal/amorphous-crystalline shapes. Amorphous-crystals are usually small, underdeveloped crystals in early stages of crystallisation that often agglomerate [19-21].

The conditions of crystallisation such as cooling rate, shear stress as well as the composition of oil have a significant impact on the shape and size of a crystal. As an example, fast cooling tends to produce needles and mal-crystalline and slow cooling favours growth of plates [18, 22, 23]. Use of chemical inhibitors usually tends to change crystal shapes from plates and needles to mal crystalline which is desired in flow assurance [24-26].

2.4 Deposition vs. precipitation

To achieve a better understanding of the wax problem in the production, transportation and processing of crude oil, two important phenomena have to be considered, wax precipitation and wax deposition. In the literature, they are usually used interchangeably while they are different concepts. Wax precipitation occurs during the formation of solid wax crystals out of solution from a liquid phase. It takes place due to either evaporation of volatile light components, or if temperature falls below solubility point or wax appearance temperature. On the other hand, wax deposition is the formation of a layer of the separated solid phase on a surface. It can be formed from a current/existed precipitated solid phase. Precipitation is mainly a function of thermodynamic variables which is necessary for deposition to occur; though it does not necessarily lead to

deposition [27, 28]. Shear dispersion, gravity settling and Brownian motion are mechanisms for wax deposition [1, 29, 30].

2.4.1 Wax deposition stages

The crystallisation of the deposited paraffin on the pipe/tubing wall is followed by two stages or steps, known as wax gel formation and then ageing of deposited wax gel. Ageing is a developing process which raises the proportion of the solid wax content of the wax gel deposit [1, 23, 31]. They both have complex morphology as described in two following sub-sections.

2.4.1.1 Gelation and wax porosity

Gelling occurs when an adequate amount of solid paraffin forms a solid network of structures, Figure 2-1. The 3-D network structure of wax crystals does not only consist of wax. Studies of typical wax deposits revealed deposition structure entrapped mainly crude oil and some other substances such as water, gums, resins, sand and asphaltenes during the crystallisation and deposition process. The amount of oil in the deposit is known as the wax porosity which is calculated as the volumetric fraction of oil to the deposit total volume. The higher concentration of oil generally results in a thicker and softer deposition. The oil trapped causes diffusion of wax molecules into the gel deposit and counter-diffusion of oil out of the gel deposit. The wax porosity affects the wax deposition rate, hence it is necessary to know the concentration of oil in the wax deposit to predict the wax deposition more accurately [1, 23, 31-33].

Studies have shown that as little as 2% of precipitated paraffin wax is sufficient to form a gelled deposit. The strength of deposit increases by increasing the amount of solid wax content [28, 34]. The presence of asphaltene in the wax gel seems to have a disruption in gel structure which results in the reduction of the gelation temperature [110].

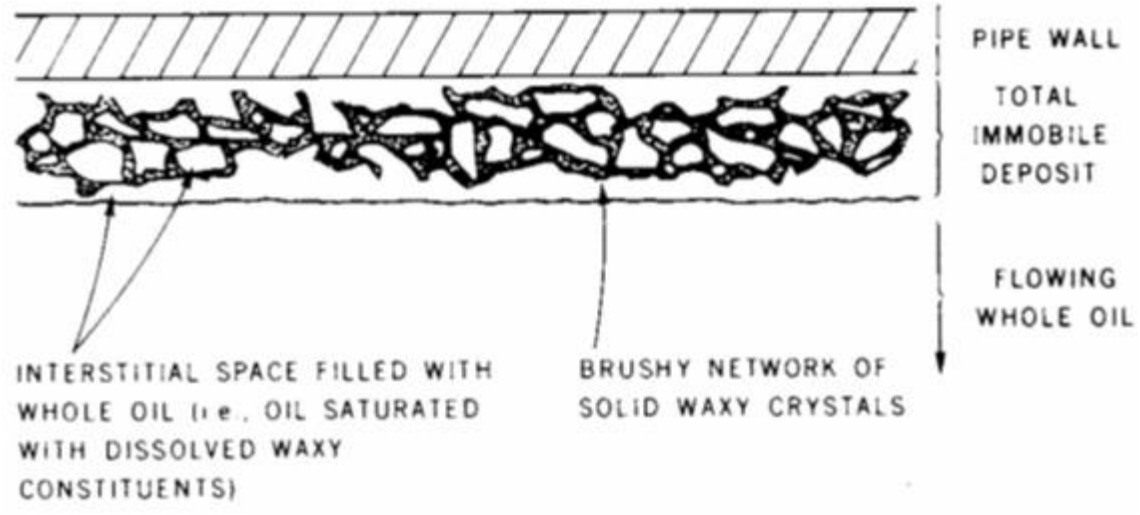

Figure 2-1. Immobile wax deposit at the pipe wall [1].

2.4.1.2 Ageing

In the gel deposited layer, the wax fraction of solid increases as time passes and substitute the trapped oil in the wax network structure by molecular diffusion. In other words, it can distinguish wax and oil by a critical carbon number. The heavier molecules, above this number, diffuse into the deposited gel through the trapped oil while those below, diffuse out of the deposit due to the counter diffusion of the trapped oil, Figure 2-2. This concept is called ageing which increases the hardness of the deposited gel over time [31-33, 35,110]. The ageing rate studies show that this parameter seems to be dependent on the oil flow rate and temperature gradient of the fluid and the pipe wall [111].

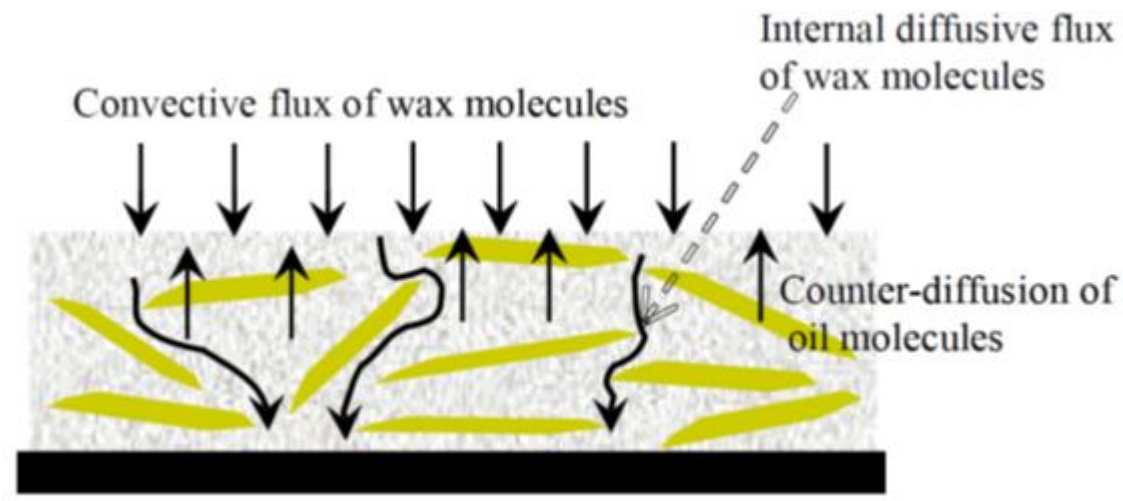

Figure 2-2. Illustration of how wax molecules diffuses into the deposit [36].

2.4.2 Mechanism of deposition

Upon precipitation, wax deposition on the components of the production system is believed to occur as a result of various mechanisms. Some of these deposition mechanisms help deposits to grow, others might prevent deposition. A number of suggested mechanisms are molecular diffusion, Brownian diffusion, shear dispersion, gravity settling, heat transfer, etc. [1, 29, 31, 37, 38].

Based on the applied experimental conditions by the work done in this thesis, most probably the prominent deposition mechanisms are molecular-Brownian diffusion and gravity settling.

2.4.2.1 Molecular and Brownian Diffusion

When oil flows in a pipeline, regardless of flow conditions, there would be a thin laminar sublayer adjacent to the pipe wall. If the pipe wall temperature is lower than the wax appearance temperature (WAT) of the oil, where solid waxy crystals start to precipitate, a thin layer of wax deposition with a lower concentration of wax particles compare to bulk oil starts to form. In other words, the temperature gradient across the pipe wall gives rise to a concentration gradient that causes the diffusion of wax from the region of higher concentration within the bulk, towards the wall where the concentration of dissolved wax is lower by molecular diffusion. This mechanism is the most widely studied and has been reported as a dominant mechanism [1, 29, 31, 39-41].

Random Brownian motion of suspended solid waxy crystals by agitating oil molecules will lead faster molecular diffusion. Therefore, the Brownian mechanism can be considered as an enhancement for deposition and growth [1, 39-41].

2.4.2.2 Gravity Settling

Since the precipitated wax crystals are denser than the rest of the bulk oil, they tend to settle in a gravity field and are deposited at the bottom of a pipe wall or other facilities. This is provided particles are not influenced by the flow regime. Gravity settling is believed to be a possible transport mechanism [1, 42-44].

2.4.3 Factors Leading to Wax Precipitation and Deposition

Wax precipitation starts to occur as soon as the pipe wall temperature reaches the solubility limit temperature. Although the solubility limit is strongly dependent on temperature, other factors are also involved in wax deposition. Such factors include oil composition and impurities, available solution gas, system pressure which directly affects the amount of gas in solution, water-oil ratio, flow conditions and shear rate, pipe wall size and roughness, etc. these factors do not necessarily shift the solubility limit but provide a favourable environment for precipitation and deposition to occur [27, 28, 45, 46].

In the following subsections some of these factors are described in more detail.

2.4.3.1 Temperature gradient

The temperature gradient in flow lines seems to be the predominant factor in wax precipitation and deposition. Though, overall temperature difference does not necessarily translate into a greater amount of deposition. In fact, the difference between the solubility limit temperature (WAT) and the temperature of the pipe wall are both important in determining the rate of wax precipitation and deposition. Wax deposition increases as the temperature gradient of the crude oil increase relative to the WAT. On the other hand, wax deposition disappears when there is no temperature gradient between the oil and the wall, even if the oil temperature is far below WAT. Reducing temperature gradient also occurs while the thickness of the wax deposit increases forming an insulating layer. As a result, the maximum thickness of the wax in flow line forms just below the WAT point where the highest temperature gradient exists [31, 32, 47-49].

2.4.3.2 Crude Oil Composition

Crude oil is generally composed of saturates, aromatics, resins, and asphaltenes (SARA) which are in thermodynamic equilibrium at initial reservoir conditions. If anything alters the original composition of the oil this might cause loss of solubility and encourage precipitation and deposition of wax. Therefore, knowledge of the oil composition gives a good idea of the wax deposit potential of the crude oil. Oil stability mainly depends on the structural distribution of saturates. Saturates are flexible in nature, especially those compounds with straight chain (n-paraffin), so this facilitates clustering and crystallisation. Iso and cycloparaffins are less flexible forming unstable wax deposition. Light saturates and aromatics, on the other hand, serve as solvents for high molecular weight saturates at the desired temperature. It is observed that adding light fractions to crude oil causes the solubility boundary region to change significantly, reducing the WAT of the crude by as much as 15 °C depending on the amount of injected light component. Polar components, especially asphaltenes, could serve as nucleation sites for additional wax deposition; though, a reduction in paraffin deposition from crude oil, in the presence of asphaltenes has been reported. The presence of impurities and other amorphous solids like formation fines and corrosion materials all contribute to wax precipitation and deposition by decreasing the energy barrier required for the formation of wax nuclei [5, 41, 50-53].

2.4.3.3 Water and emulsion

Water is inevitably found in produced oil, and increases with the lifetime of a well. The water fraction in the oil stream is known as the water-cut, and probably restricts the flow of dissolved wax especially for the case of water-in-oil dispersed flow. The wax deposition process is not thoroughly characterised in the presence of water due to the increased complexity of multiphase flow, emulsion behaviour and difficulty in obtaining consistent experimental results. Studies showed that similar to single-phase wax deposition, temperature gradient plays the predominant function of deposition. In addition, any other factors which change emulsion stability and flow patterns have an extremely significant impact on the deposition. Such factors include the water cut, the size of droplets, types of emulsion (water in oil/ oil in water), the wettability of the pipe wall, orientation of pipelines (horizontal/vertical), etc. [2, 54-57].

2.4.3.4 Pressure

In general, over time reservoir pressure declines; hence, the pressure of the flow stream from the reservoir to the surface and along the pipes drops. Light ends which act as a solvent to wax and heavy end components, start to leave the liquid phase. Therefore, the solubility of wax is reduced initiating precipitation. As a result, pressure plays a significant role in wax precipitation and deposition [51, 58, 59].

2.4.3.5 Flow rate/ Shear rate

Laboratory investigations have revealed that overall wax deposition decreases when the flow/shear rate of the crude oil or waxy mixture increases, regardless of flow being laminar or turbulent. However, wax deposition decreases as flow moves from laminar to the turbulent regime due to higher viscous nature and drags forces. One possible option for higher deposition in lower flow rate is that at low flow rates the oil has a longer residence time in the flow line, caused more heat loss to the surroundings and a higher chance of the bulk oil temperature falling below the WAT, leading to a higher wax precipitation and final deposition. Another theory is that the viscous drag exerted by higher flow/shear rate is proposed to cause a sloughing or scraping of the deposits from the pipe wall, the wax then sloughs and returns to the liquid. There is also a difference in texture between wax deposited at high flow rates and wax deposited at low flow rates. Deposits obtained from an increased flow rate appears harder, being more compact, containing lower fractions of embedded oil or solvent and is more firmly attached to the deposition surface [60-64].

2.5 Wax related concepts

In order to get a better understanding of wax thermodynamics, there are some important wax related parameters, usually assessed during the early stage of the flow assurance analysis. These are Wax Appearance Temperature (WAT), Wax Disappearance Temperature (WDT), pour point and wax content. The values of these parameters can often be found in the fluid testing conducted on the stock tank oil sample of the production fluid.

2.5.1 Wax Appearance Temperature (WAT)

As the temperature of the crude oil decreased at a controlled and specified cooling rate, the solubility limit of wax reached, then, wax starts to precipitate and form solid crystals. The highest temperature at which the first wax crystals are observed and start to drop out in the liquid bulk fluid is called the wax appearance temperature (WAT). This temperature is unique for a particular pressure as well as oil composition [65].

WAT obtained in experiments is different from thermodynamic WAT (true WAT). True WAT lies on the solid/liquid phase envelope while laboratory or experimentally measured WAT lies within the solid/liquid phase envelope. WAT is extremely important input parameter required for wax deposition modelling. All the factors that favour an increase in WAT also tend to increase wax deposition. No wax precipitation or deposition will occur as long as oil system temperature is no longer below WAT [13, 66].

Oil composition and properties such as viscosity and density of the crude change at the WAT point; hence, the WAT is often considered as one of the first parameters used in the wax study and the design of offshore facilities, because it indicates whether wax will deposit in a pipeline and approximately where this appears [28, 67, 68].

In the literature, the WAT is also called cloud point, Wax Appearance Point (WAP), Wax Formation Temperature (WFT) and Wax Precipitation Temperature (WPT) [28, 69, 70]. The term Wax Appearance Temperature (WAT) will consistently be used in this thesis.

2.5.2 Wax Disappearance Temperature (WDT)

WDT is the temperature at which all the wax crystals become completely dissolved back in solution during heating the mixture from a temperature well below its WAT. WDT is generally higher than WAT and found to be closer to the thermodynamic equilibrium temperature [70-72].

2.5.3 Pour Point

Pour point is described as the lowest temperature, considerably lower than WAT, at which a liquid remains pourable and loses its flow characteristics. In fact, while the sample oil starts cooling, wax crystals form at solubility limit point and precipitate. At

some point, the precipitates accumulate to the point where the fluid no longer can flow. In crude oils, a high paraffin content is generally expected to increase pour point of the oil[24, 26, 73, 74].

2.5.4 Wax content

Wax content is defined as the amount of wax that will precipitate in an excess amount of such solvents like dichloromethane, ethanol, diethyl ether, etc. at a very low temperature such as -20 °C to -30 °C, using a combination of distillation and extraction methods[75-77].

Wax content is a critical input for deposition prediction, though an investigation showed that higher wax content does not necessarily mean greater wax deposition risks. In fact, crude oils with more than 2% wax content and a WAT higher than the ocean floor temperature have the possibility for deposition and blockage. In addition, two different oils sharing similar wax content can show significant differences in their deposition tendency [31, 78].

2.6 WAT/WDT measurement techniques

Various experimental techniques and methods have been developed based on the change in the physical properties of the oil during the formation of solid wax crystals. The only related aspect of these devices is similar controlled cooling of the oil sample. It is considered that none of the available techniques are able to capture the very first wax crystals which lie on the solid-liquid phase boundary. Precipitated wax can be detected in different size, quantity and form. It highly depends on the sample quality, residence time of measurement, thermal history, the sensitivity of measurement techniques and user experience. Different methods inherently have different detection qualities based on various physical properties of the sample. Some are able to detect wax crystals at the nucleation stage while others at the early stage of growth. Optical techniques such as ASTM visual inspection, cross-polarized microscopy (CPM), Light Transmittance (LT), Light Scattering (NIR, FTIR); Rheological techniques such as viscometer and flow loop; thermal techniques such as differential scanning calorimetry (DSC) which is based on released heat due to crystallization of wax, and the Quartz Crystal Microbalance (QCM) which rely on wax particles adhering to a detection surface, are some common methods to measure WAT/WDT [6, 65, 72, 79-85].

From the above mentioned experimental setups ones that have been applied/optimised in this thesis for WAT/WDT measurements are detailed in Chapter 3.

2.7 Concern for Wax Deposition

The problem of wax deposition in the subsea pipeline provides significant technical and economic flow assurance issues. Over a period of time, wax deposition on the pipe wall increases; it is a very complex phenomenon which reduces the effective diameter of pipes hence increasing pressure drop along the flow channel. In the worst case, wax build up inside the pipe can be severe enough to block the pipes leading to lost production and even platform/field abandonment. Therefore, it must be diagnosed and assessed at an early stage in order to develop economically viable prevention/ mitigation strategies. Otherwise, this may lead to major consequences on the operational efficiency that would be unmanageable [35, 86, 87].

2.7.1 Control and Remediation

In order to develop economical and feasible production, it is extremely important to have a sufficient and rigorous understanding in controlling wax deposition. Wax control knowledge involves three steps, based on priority including predict/diagnose, prevent and mitigate/remediate the solid deposition. Estimation of WAT of the crude oil and the knowledge of factors that might affect deposition gives a possible understanding of prediction and prevention strategies. In such cases where complete prevention fails, remediation becomes the only viable option. Various remedial methods are being used in the industry, though most of them have limitations for longer pipelines. In general, four different methods are used to control the extent of wax deposition including pigging, pipeline insulation, chemical injection and active heating [25, 88-90].

2.7.1.1 Insulation

One of the main approaches employed to prevent potential wax deposition is pipeline insulation. Insulation limits the temperature loss, especially for short lines, leads to decreased temperature differential as a significant driving force for deposition between the bulk oil and inner pipe. Using this approach eliminates the need for continuous wax inhibition or regular pigging. However, this solution could greatly increase the production cost. Various types of thermal pipe insulation exist; generally these include external insulation coating on single pipes or pipe-in-pipe systems [90-93].

2.7.1.2 Pigging

The flow efficiency of a pipeline will begin to decrease immediately after solid such a wax start to deposit especially for long tie-back where a significant portion of the pipe is subjected to wax deposition risk. The first approach is to scrape off wax deposits by pigging [94, 95].

As seen in Figure 2-3, there are various types of pigs for which are selected based on wax properties and operating parameters. The most important factors surrounding the deployment of the pigging are internal inspection and cleaning the pipe interior in a cost-effective way. However, when the deposit is too hard or the wax layer is too thick, some problems such as stuck pigs can occur. In such cases, it could become an economic disaster costing tens of millions of dollars [96, 97].

Figure 2-3. Various types of pigs[96]

2.7.1.3 Heating

Heating is commonly used in the oil industry to move the system out of the wax stable region. There are a variety of methods used to apply heat including injection of hot water, hot oiling, steaming and continuous heating such as electrical heating element [90, 98, 99].

2.7.1.4 Chemical Method

Chemical methods include solvent, crystal modifiers and dispersant or a combination of them for controlling the deposition of paraffin wax without stopping production. Solvents are usually used for removing the deposited wax while modifiers and dispersants are used to prevent wax deposition or to reduce the amount of wax deposits. The applicability of these chemicals is highly selective for a particular composition of the crude oil as well as the environmental conditions. These additives are mostly confidential and commercially sourced. The selection of proper chemical and dosage used for crude oils has traditionally been performed using a try and error approach which is assessed through laboratory bench-top tests. However, laboratory dosage is not generally a good indication of the actual field dosage. A field trial is the best approach on this matter [100].

In following sub-sections, these three classes of chemical materials are discussed in more in detail.

2.7.1.4.1 Solvents

Escape of dissolved gases from crude oil or reduction in temperature causes a decrease in the solubility of wax leading to deposition. Solvents are applied in a frequent batch or continuously to restore the solvent properties of a crude oil hence increasing the solubility of wax. Solvents are not able to prohibit or prevent deposition, but remove existing deposited wax during oil production. Some examples of solvents most commonly used are produced condensate, white or unleaded gasoline, pentane, butane, light gas oil, aromatic compounds such as toluene and xylene, terpenes derived from pine trees, chlorinated hydrocarbons like carbon tetrachloride etc. Chlorinated hydrocarbons which have been commonly used, have been banned even in small traces due to being harmful to refinery catalysts [90, 101, 102].

2.7.1.4.2 Wax crystal modifier

Wax crystal modifiers are usually polymers with long alkyl chains which modify the crystal morphology and the way the crystals interact to inhibit the wax deposition process. However, some confusion exists about mechanisms of modifiers on wax crystals which have not yet been fully understood. There are three different ways suggested which crystal modifiers can be affected on paraffin crystals[97, 103].

First of all, they work primarily by modification of the crystal from larger sizes to smaller sizes. Smaller particles have lower molecular weights, the less energy of interaction hence solubility of crystals increases [24, 26, 97].

Furthermore, Wax crystal modifiers are substances that have a similar molecular structure to the wax which co-precipitates or co-crystallizes with the wax crystals. They are believed to alter and interfere with the growth and surface characteristics by inserting themselves in the crystals, hence, minimising the growth of wax crystals and sometimes preventing them from sticking to metal surfaces as shown in Figure 2-4 [104].

They also suppress the tendency to form a three-dimensional network and subsequently retard the rate of gelling of the crude, leading to a lower pour point and reduction in the crude oil viscosity, thereby making the transportation of the crude oil easier. In the literature, hence, crystal modifiers are usually called pour point depressant (PPD) or flow improver [97, 105].

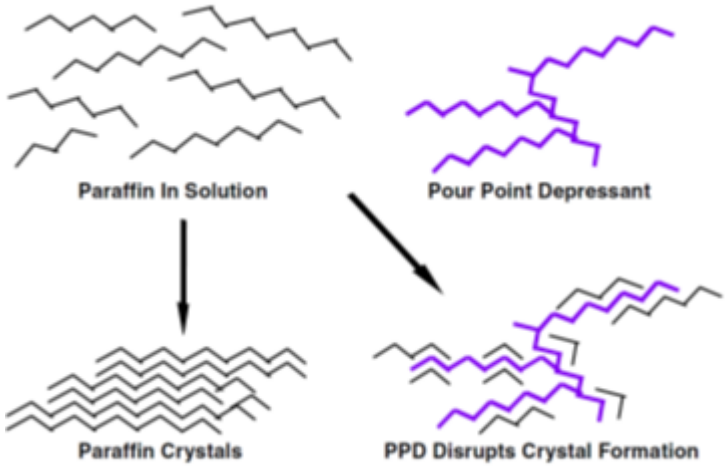

Figure 2-4. Idealised schematic of the mechanism of pour point depression [104]

In addition, these chemicals modify crystals from one type to the other. As mentioned earlier, there are three types of wax crystals known as a plate, needle and mal/amorphous. Plate and needle are progressive and growing crystals while mal crystals are like small round spheres which are newly formed wax in early stages. The interparticle and particle wall attractive forces increases by type of the crystals from mal, to the plate, to the needle crystals. Therefore, newly formed wax crystals are

desirable. Effective Wax crystal modifiers all have in common that they organised transition from needle or plate crystals to grow to resemble little spheres or particles. Therefore, the hydrodynamic drag of the flowing fluid can shear these inhibited small particles, carry them out of the flow line. Of course, these additives prevent or reduce the wax deposition rate, but, no products were found to prevent wax precipitation [97, 106].

Typical crystal modifying additives are polymeric in nature belong to the ester family of chemicals. Such modifying chemicals are included polyethylene, copolymer esters, ethylene/vinyl acetate copolymers, olefin/ester copolymers, ester/vinyl acetate copolymers, polyacrylates, polymethacrylates, alkyl phenol resins, etc. [104, 106, 107].

2.7.1.4.3 Wax dispersant

The dispersants are primarily surface-active agents and work in a similar way to surfactants. It is suggested the mechanism is such that one end of the molecule is attracted to the paraffin while the other end is soluble in oil. Then it neutralises the attractive forces between crystals keeping them dispersed as separate particles. This approach does not prevent the paraffin crystals from forming, but they are kept moving with the fluid flow.

Dispersants include sulfonates, alkyl phenol derivatives, ketones, terpenes, polyamides, naphthalene, etc. [97, 108, 109].

2.8 References

1. Burger, E., T. Perkins, and J. Striegler, *Studies of wax deposition in the trans Alaska pipeline.* Journal of Petroleum Technology, 1981. **33**(06): p. 1,075-1,086.
2. Aiyejina, A., et al., *Wax formation in oil pipelines: A critical review.* International journal of multiphase flow, 2011. **37**(7): p. 671-694.
3. del Carmen García, M., et al., *The influence of alkane class-types on crude oil wax crystallization and inhibitors efficiency.* Journal of petroleum science and engineering, 2000. **25**(3): p. 99-105.
4. Garcia, M.d.C., et al., *Paraffin deposition in oil production. Oil composition and paraffin inhibitors activity.* Petroleum science and technology, 1998. **16**(9-10): p. 1001-1021.
5. García, M.d.C., *Crude oil wax crystallization. The effect of heavy n-paraffins and flocculated asphaltenes.* Energy & fuels, 2000. **14**(5): p. 1043-1048.
6. Baltzer Hansen, A., et al., *Wax precipitation from North Sea crude oils. 3. Precipitation and dissolution of wax studied by differential scanning calorimetry.* Energy & Fuels, 1991. **5**(6): p. 914-923.
7. Dirand, M., et al., *Multicomponent paraffin waxes and petroleum solid deposits: structural and thermodynamic state.* Fuel, 1998. **77**(12): p. 1253-1260.
8. Thanh, N.X., M. Hsieh, and R. Philp, *Waxes and asphaltenes in crude oils.* Organic Geochemistry, 1999. **30**(2): p. 119-132.
9. Zaky, M.T. and N.H. Mohamed, *Comparative study on separation and characterization of high melting point macro-and micro-crystalline waxes.* Journal of the Taiwan Institute of Chemical Engineers, 2010. **41**(3): p. 360-366.
10. Kinsel, A. and J. Phillips, *Method for Classification of Petroleum Waxes.* Industrial & Engineering Chemistry Analytical Edition, 1945. **17**(3): p. 152-156.
11. Jetter, R. and M. Riederer, *In vitro Reconstitution of Epicuticular Wax Crystals: Formation of Tubular Aggregates by Long-Chain Secondary Alkanediols.* Botanica Acta, 1995. **108**(2): p. 111-120.
12. Speight, J.G., *The chemical and physical structure of petroleum: effects on recovery operations.* Journal of Petroleum Science and Engineering, 1999. **22**(1): p. 3-15.
13. Hansen, J.H., et al., *A thermodynamic model for predicting wax formation in crude oils.* AIChE Journal, 1988. **34**(12): p. 1937-1942.
14. Hammami, A. and M.A. Raines. *Paraffin deposition from crude oils: comparison of laboratory results to field data*. in *SPE Annual Technical Conference and Exhibition*. 1997. Society of Petroleum Engineers.
15. Siljuberg, M.K., *Modelling of Paraffin Wax in Oil Pipelines.* 2012.
16. Kraack, H., M. Deutsch, and E. Sirota, *n-Alkane homogeneous nucleation: Crossover to polymer behavior.* Macromolecules, 2000. **33**(16): p. 6174-6184.
17. Hennessy, A., A. Neville, and K. Roberts, *An examination of additive-mediated wax nucleation in oil pipeline environments.* Journal of crystal growth, 1999. **198**: p. 830-837.

18. Lu, X., et al., *Wax morphology in bitumen.* Journal of Materials Science, 2005. **40**(8): p. 1893-1900.

19. Koch, K. and H.-J. Ensikat, *The hydrophobic coatings of plant surfaces: epicuticular wax crystals and their morphologies, crystallinity and molecular self-assembly.* Micron, 2008. **39**(7): p. 759-772.

20. Ferris, S. and H. Cowles, *Crystal Behavior of Paraffin Wax.* Industrial & Engineering Chemistry, 1945. **37**(11): p. 1054-1062.

21. Ferris, S., H. Cowles Jr, and L. Henderson, *Composition and Crystal Form of the Petroleum Waxes.* Industrial & Engineering Chemistry, 1931. **23**(6): p. 681-688.

22. Webber, R.M., *Low temperature rheology of lubricating mineral oils: effects of cooling rate and wax crystallization on flow properties of base oils.* Journal of Rheology (1978-present), 1999. **43**(4): p. 911-931.

23. Singh, P., H.S. Fogler, and N. Nagarajan, *Prediction of the wax content of the incipient wax-oil gel in a pipeline: An application of the controlled-stress rheometer.* Journal of Rheology (1978-present), 1999. **43**(6): p. 1437-1459.

24. Pedersen, K.S. and H.P. Rønningsen, *Influence of wax inhibitors on wax appearance temperature, pour point, and viscosity of waxy crude oils.* Energy & fuels, 2003. **17**(2): p. 321-328.

25. Ferworn, K.A., A. Hammami, and H. Ellis. *Control of wax deposition: an experimental investigation of crystal morphology and an evaluation of various chemical solvents*. in *International Symposium on Oilfield Chemistry*. 1997. Society of Petroleum Engineers.

26. Taraneh, J.B., et al., *Effect of wax inhibitors on pour point and rheological properties of Iranian waxy crude oil.* Fuel processing technology, 2008. **89**(10): p. 973-977.

27. Weingarten, J. and J. Euchner, *Methods for predicting wax precipitation and deposition.* SPE Production Engineering, 1988. **3**(01): p. 121-126.

28. Roenningsen, H.P., et al., *Wax precipitation from North Sea crude oils: 1. Crystallization and dissolution temperatures, and Newtonian and non-Newtonian flow properties.* Energy & Fuels, 1991. **5**(6): p. 895-908.

29. Azevedo, L. and A. Teixeira, *A critical review of the modeling of wax deposition mechanisms.* Petroleum Science and Technology, 2003. **21**(3-4): p. 393-408.

30. Kok, M. and R. Saracoglu, *Mathematical modelling of wax deposition in crude oil pipelines (comparative study).* Petroleum science and technology, 2000. **18**(9-10): p. 1121-1145.

31. Singh, P., et al., *Formation and aging of incipient thin film wax-oil gels.* AIChE Journal, 2000. **46**(5): p. 1059-1074.

32. Singh, P., et al., *Morphological evolution of thick wax deposits during aging.* American Institute of Chemical Engineers. AIChE Journal, 2001. **47**(1): p. 6.

33. Ramirez-Jaramillo, E., C. Lira-Galeana, and O. Manero, *Modeling wax deposition in pipelines.* Petroleum science and technology, 2004. **22**(7-8): p. 821-861.

34. Bidmus, H.O. and A.K. Mehrotra, *Heat-transfer analogy for wax deposition from paraffinic mixtures.* Industrial & engineering chemistry research, 2004. **43**(3): p. 791-803.

35. Hoteit, H., R. Banki, and A. Firoozabadi, *Wax deposition and aging in flowlines from irreversible thermodynamics.* Energy & Fuels, 2008. **22**(4): p. 2693-2706.

36. Venkatesan, R., *The deposition and rheology of organic gels*. 2004: University of Michigan.

37. Huang, Z., et al., *A fundamental model of wax deposition in subsea oil pipelines.* AIChE Journal, 2011. **57**(11): p. 2955-2964.

38. Leiroz, A.T. and L.F. Azevedo, *Paraffin deposition in a stagnant fluid layer inside a cavity subjected to a temperature gradient.* Heat transfer engineering, 2007. **28**(6): p. 567-575.

39. Fasano, A., L. Fusi, and S. Correra, *Mathematical models for waxy crude oils.* Meccanica, 2004. **39**(5): p. 441-482.

40. Kok, M.V. and O. Saracoglu. *Mathematical Modelling of Wax Deposition in Crude Oil Pipeline Systems*. in *SPE Asia Pacific Oil and Gas Conference and Exhibition*. 2000. Society of Petroleum Engineers.

41. Leontaritis, K.J., *The asphaltene and wax deposition envelopes.* Fuel Science and Technology International, 1996. **14**(1-2): p. 13-39.

42. Merino-Garcia, D., M. Margarone, and S. Correra, *Kinetics of waxy gel formation from batch experiments.* Energy & fuels, 2007. **21**(3): p. 1287-1295.

43. Leiroz, A. and L. Azevedo. *Studies on the mechanisms of wax deposition in pipelines*. in *Offshore Technology Conference*. 2005. Offshore Technology Conference.

44. Correra, S., M. Andrei, and C. Carniani, *Wax diffusivity: is it a physical property or a pivotable parameter?* Petroleum science and technology, 2003. **21**(9-10): p. 1539-1554.

45. Creek, J., et al., *Wax deposition in single phase flow.* Fluid Phase Equilibria, 1999. **158**: p. 801-811.

46. Hoffmann, R. and L. Amundsen, *Single-phase wax deposition experiments.* Energy & Fuels, 2009. **24**(2): p. 1069-1080.

47. Hamouda, A. and S. Davidsen. *An approach for simulation of paraffin deposition in pipelines as a function of flow characteristics with a reference to Teesside oil pipeline*. in *SPE International Symposium on Oilfield Chemistry*. 1995. Society of Petroleum Engineers.

48. Jennings, D.W. and K. Weispfennig, *Effects of shear and temperature on wax deposition: Coldfinger investigation with a Gulf of Mexico crude oil.* Energy & fuels, 2005. **19**(4): p. 1376-1386.

49. Parthasarathi, P. and A.K. Mehrotra, *Solids deposition from multicomponent wax-solvent mixtures in a benchscale flow-loop apparatus with heat transfer.* Energy & fuels, 2005. **19**(4): p. 1387-1398.

50. Lu, X. and P. Redelius, *Compositional and structural characterization of waxes isolated from bitumens.* Energy & fuels, 2006. **20**(2): p. 653-660.

51. Pan, H., A. Firoozabadi, and P. Fotland, *Pressure and composition effect on wax precipitation: experimental data and model results.* SPE Production & Facilities, 1997. **12**(04): p. 250-258.

52. Kriz, P. and S.I. Andersen, *Effect of asphaltenes on crude oil wax crystallization.* Energy & fuels, 2005. **19**(3): p. 948-953.

53. Ray, S.S., N.K. Pandey, and A.K. Chatterjee, *Effect of aromatics and iso-alkanes on the pour point of different types of lube oils.* Fuel, 2009. **88**(9): p. 1629-1633.

54. Hoffmann, R., et al., *Wax deposition in stratified oil/water flow.* Energy & Fuels, 2012. **26**(6): p. 3416-3423.

55. Zhang, Y., et al., *Effect of emulsion characteristics on wax deposition from water-in-waxy crude oil emulsions under static cooling conditions.* Energy & Fuels, 2009. **24**(2): p. 1146-1155.

56. Zhang, Y., J. Gong, and H. Wu, *An experimental study on wax deposition of water in waxy crude oil emulsions.* Petroleum Science and Technology, 2010. **28**(16): p. 1653-1664.

57. Liu, Y., et al., *Study of deposition behavior in small-diameter gathering pipelines for water-cut oil.* Chemistry and Technology of Fuels and Oils, 2012. **48**(5): p. 386-392.

58. Hamouda, A. and B. Viken. *Wax deposition mechanism under high-pressure and in presence of light hydrocarbons*. in *SPE International Symposium on Oilfield Chemistry*. 1993. Society of Petroleum Engineers.

59. Dalirsefat, R. and F. Feyzi, *A thermodynamic model for wax deposition phenomena.* Fuel, 2007. **86**(10): p. 1402-1408.

60. Hsu, J., M. Santamaria, and J. Brubaker. *Wax deposition of waxy live crudes under turbulent flow conditions*. in *SPE Annual Technical Conference and Exhibition*. 1994. Society of Petroleum Engineers.

61. Agrawal, K., et al., *Wax deposition of Bombay high crude oil under flowing conditions.* Fuel, 1990. **69**(6): p. 794-796.

62. Lu, Y., et al., *Counterintuitive effects of the oil flow rate on wax deposition.* Energy & Fuels, 2012. **26**(7): p. 4091-4097.

63. Hsu, J. and J. Brubaker. *Wax deposition measurement and scale-up modeling for waxy live crudes under turbulent flow conditions*. in *International Meeting on Petroleum Engineering*. 1995. Society of Petroleum Engineers.

64. Wang, W. and Q. Huang, *Prediction for wax deposition in oil pipelines validated by field pigging.* Journal of the Energy Institute, 2014. **87**(3): p. 196-207.

65. Kok, M.V., et al., *Comparison of wax appearance temperatures of crude oils by differential scanning calorimetry, thermomicroscopy and viscometry.* Fuel, 1996. **75**(7): p. 787-790.

66. Coutinho, J.A. and V. Ruffier-Meray, *Experimental measurements and thermodynamic modeling of paraffinic wax formation in undercooled solutions.* Industrial & engineering chemistry research, 1997. **36**(11): p. 4977-4983.

67. Hasan, S.W., M.T. Ghannam, and N. Esmail, *Heavy crude oil viscosity reduction and rheology for pipeline transportation.* Fuel, 2010. **89**(5): p. 1095-1100.

68. Wardhaugh, L. and D. Boger, *Flow characteristics of waxy crude oils: application to pipeline design.* AIChE Journal, 1991. **37**(6): p. 871-885.

69. da Silva, J.A.L. and J.A. Coutinho, *Dynamic rheological analysis of the gelation behaviour of waxy crude oils.* Rheologica Acta, 2004. **43**(5): p. 433-441.

70. ASTM D2500-16a, S.T.M.f.C.P.o.P.P.a.L.F., ASTM International, West Conshohocken, PA, 2016, www.astm.org.

71. Mohammadi, A.H., et al. *Gas hydrates in oil systems*. in *SPE Europec/EAGE Annual Conference and Exhibition*. 2006. Society of Petroleum Engineers.

72. Burgass, R. and B. Tohidi. *Development and validation of small volume multi-tasking flow assurance tool*. in *SPE Asia Pacific Oil and Gas Conference and Exhibition*. 2011. Society of Petroleum Engineers.

73. Schlueter, K. and W. Zoellner, *Pour point depressants for paraffin solutions*. 1987, Google Patents.

74. ASTM D97-16, S.T.M.f.P.P.o.P.P., ASTM International, West Conshohocken, PA, 2016, www.astm.org.

75. *Process for separating wax from oil*. 1941, Google Patents.

76. Hiebert, G.L. and M.B. DeTar, *Pour point depressants and their use*. 1998, Google Patents.

77. Martos, C., et al., *Characterization of Brazilian Crude Oil Samples To Improve the Prediction of Wax Precipitation in Flow Assurance Problems†.* Energy & Fuels, 2010. **24**(4): p. 2221-2226.

78. Ismail, L., R.E. Westacott, and X. Ni, *On the effect of wax content on paraffin wax deposition in a batch oscillatory baffled tube apparatus.* Chemical Engineering Journal, 2008. **137**(2): p. 205-213.

79. Coutinho, J.A. and J.-L. Daridon, *The limitations of the cloud point measurement techniques and the influence of the oil composition on its detection.* Petroleum Science and Technology, 2005. **23**(9-10): p. 1113-1128.

80. Espada, J.J., J.A. Coutinho, and J.L. Pena, *Evaluation of methods for the extraction and characterization of waxes from crude oils.* Energy & Fuels, 2010. **24**(3): p. 1837-1843.

81. Roehner, R. and F. Hanson, *Determination of wax precipitation temperature and amount of precipitated solid wax versus temperature for crude oils using FT-IR spectroscopy.* Energy & fuels, 2001. **15**(3): p. 756-763.

82. Marchesini, F.v.H., et al., *Rheological characterization of waxy crude oils: Sample preparation.* Energy & Fuels, 2012. **26**(5): p. 2566-2577.

83. IJeomah, C.E., et al., *Measurement of wax appearance temperature under simulated pipeline (dynamic) conditions.* Energy & Fuels, 2008. **22**(4): p. 2437-2442.

84. Fong, N. and A.K. Mehrotra, *Deposition under turbulent flow of wax-solvent mixtures in a bench-scale flow-loop apparatus with heat transfer.* Energy & fuels, 2007. **21**(3): p. 1263-1276.

85. Jiang, Z., J. Hutchinson, and C. Imrie, *Measurement of the wax appearance temperatures of crude oils by temperature modulated differential scanning calorimetry*. Fuel, 2001. **80**(3): p. 367-371.

86. Venkatesan, R. and J. Creek. *Wax deposition during production operations: SOTA*. in *Offshore Technology Conference*. 2007. Offshore Technology Conference.

87. Brown, T., V. Niesen, and D. Erickson. *Measurement and prediction of the kinetics of paraffin deposition*. in *SPE Annual Technical Conference and Exhibition*. 1993. Society of Petroleum Engineers.

88. Lee, H.S., *Computational and rheological study of wax deposition and gelation in subsea pipelines*. 2008: ProQuest.

89. Shock, D., J. Sudbury, and J. Crockett, *Studies of the mechanism of paraffin deposition and its control.* Journal of Petroleum Technology, 1955. **7**(09): p. 23-28.

90. Al-Yaari, M. *Paraffin wax deposition: Mitigation and removal techniques*. in *SPE Saudi Arabia Section Young Professionals Technical Symposium*. 2011. Society of Petroleum Engineers.

91. Ohrn, T.R. and L.H. Taylor Jr, *Internally insulated, corrosion resistant pipeline*. 2000, Google Patents.

92. Kerr, G.W. and J.F. Stephens, *Thermal pipe insulation*. 1957, Google Patents.

93. Walter, F.D. and S.J. Henry, *Thermally insulated pipe*. 1970, Google Patents.

94. Tiratsoo, J.N., *Pipeline pigging technology*. 1992: Gulf Professional Publishing.

95. Mendes, P.S., et al., *Resistive force of wax deposits during pigging operations.* Journal of energy resources technology, 1999. **121**(3): p. 167-171.

96. Gupta, A. and A. Sircar, *Flow Assurance and Comparison of Modelling & SCADA Results for Onshore Crude Oil Trunk Line-A Case Study*.

97. Leontaritis, K.J. *Wax Flow Assurance Issues in Gas Condensate Multiphase Flowlines*. in *Offshore Technology Conference*. 2007. Offshore Technology Conference.

98. Merino-Garcia, D. and S. Correra, *Cold flow: A review of a technology to avoid wax deposition.* Petroleum Science and Technology, 2008. **26**(4): p. 446-459.

99. Esaklul, K.A., et al. *Active heating for flow assurance control in deepwater flowlines*. in *Offshore Technology Conference*. 2003. Offshore Technology Conference.

100. Towler, B.F. and S. Rebbapragada, *Mitigation of paraffin wax deposition in cretaceous crude oils of Wyoming.* Journal of Petroleum Science and Engineering, 2004. **45**(1): p. 11-19.

101. Kang, P.-S., D.-G. Lee, and J.-S. Lim. *Status of wax mitigation technologies in offshore oil production*. in *The Twenty-fourth International Ocean and Polar Engineering Conference*. 2014. International Society of Offshore and Polar Engineers.

102. Lashkarbolooki, M., F. Esmaeilzadeh, and D. Mowla, *Mitigation of wax deposition by wax-crystal modifier for Kermanshah crude oil.* Journal of Dispersion Science and Technology, 2011. **32**(7): p. 975-985.

103. Langer Jr, A.W. and W. Philippoff, *Wax crystal modifiers for petroleum oils*. 1976, Google Patents.

104. Manka, J.S., J.S. Magyar, and R.P. Smith. *A novel method to winterize traditional pour point depressants*. in *SPE annual technical conference*. 1999.

105. Zhang, H. and W.F. Xiao. *Pour Point Depressant (PPD) and Flow Improver Additives (FIA) of Crude Oil and its Study Method Progress*. in *Advanced Materials Research*. 2012. Trans Tech Publ.

106. Jafari Ansaroudi, H., et al., *Study of the morphology of wax crystals in the presence of ethylene-co-vinyl acetate copolymer.* Petroleum Science and Technology, 2013. **31**(6): p. 643-651.

107. Jung, T., J.-N. Kim, and S.-P. Kang, *Influence of polymeric additives on paraffin wax crystallization in model oils.* Korean Journal of Chemical Engineering, 2016. **33**(6): p. 1813-1822.

108. Haxell, J.P., E.A. Brown, and D.E. Wilson, *Isocyanate-modified microcrystalline wax or lignite wax dispersant*. 1991, Google Patents.

109. Groffe, D., et al., *A wax inhibition solution to problematic fields: a chemical remediation process.* Petroleum science and technology, 2001. **19**(1-2): p. 205-217.

110. Venkatesan, Ramachandran, Jenny-Ann Östlund, Hitesh Chawla, Piyarat Wattana, Magnus Nydén, and H. Scott Fogler. "*The effect of asphaltenes on the gelation of waxy oils.*" Energy & Fuels 17, no. 6 (2003): 1630-1640.

111. Singh, Probjot, Ramachandran Venkatesan, H. Scott Fogler, and Nagi Nagarajan. "*Formation and aging of incipient thin film wax-oil gels.*" AIChE Journal 46, no. 5 (2000): 1059-1074.

Chapter 3: Materials, experimental equipment and procedures

3.1 Introduction

A summary of different types of experimental apparatus and procedures on wax studies are detailed in this chapter. The properties of the materials used are also discussed in this section.

A number of experimental apparatus have been employed for generating the experimental data in this work. These set-ups are Quartz Crystal Microbalance (QCM), coaxial cold finger, flow loop, rheometer and NIR. In all of the set-ups the experiment is designed so that a thermal gradient is created which will induce wax particles to precipitate and deposit on surfaces for evaluations purposes.

The objective of using these experimental devices was to evaluate wax inhibitors and investigate the effect of some variables such as cooling rate, starting temperature, etc. on precipitation, deposition and other wax properties. The effect of impurities such as mud filtrate and hydrate inhibitors, on wax properties were also studied using these apparatus.

3.2 Material

Nine different stabilised dead oils and condensates supplied from various companies were used in this investigation designated as OIL-A, OIL-B, OIL-C, OIL-E, OIL-F, OIL-G, OIL-H, OIL-I and OIL-J. In addition, a synthetic sample was formulated by adding pure slack wax into diesel for visual observation. This sample was used to eliminate the effect of impurities, asphaltene and resin. The slack wax was a commercially available product, low melting point microcrystalline wax supplied by (Meade-King Robinson & CO.LTD, No.9543). It was mixed with diesel at 5.26 wt% denoted as OIL-D. The storage container of the oils was shaken thoroughly before the sample was taken and transferred to the corresponding equipment.

A brief description of the oils investigated, is given in Table 3-1, where the oils are listed based on decreasing API gravity. A 50-mL pycnometer was used to determine the densities of the oil samples. WAT and WDT were evaluated using a QCM and viscosity was measured using a rheometer.

Table 3-1. List of oil sample used in this work with some basic characteristics

Oil sample	Density (gr/cc)	API	WAT ±0.5 (°C)	WDT ±0.5 (°C)	Viscosity at 20°C (cP)
OIL-I	0.7770	50.61	11.7	24.4	3.2
OIL-B	0.7956	46.36	29.1	51.8	24.0
OIL-C	0.8139	42.36	27.4	43.6	10.7
OIL-A	0.8286	39.27	33.5	53.9	6.8
OIL-D	0.8310	38.78	31.3	43.2	52.4
OIL-F	0.8314	38.69	38.2	54.2	12.3
OIL-H	0.8489	35.18	34.9	39.5	107.0
OIL-G	0.8503	34.90	26.2	47.0	146.0
OIL-E	0.8852	28.34	13.2	24.1	42.5
OIL-J	0.8976	26.13	17.4	28.6	152.0

Ten different chemical additives were used as wax inhibitors and/or pour point depressants. These were commercially sourced and are denoted as INH-A, INH-B, INH-C, INH-D, INH-E, INH-F, INH-G, INH-H, INH-I and INH-J. All the inhibitors were dosed at supplier recommended ppm based on the volume of stabilised crude. Information regarding the composition and use of each inhibitor is given in Table 3-2 below.

Table 3-2. List of commercial chemical inhibitors used in this work with a brief explanation and recommended dose rates.

Inhibitors	Components	Type	Recommended dosage (ppm)
INH-A	Alcohols C8-10, Ethoxylated, 2-butoxyethanol, alkyl ether sulphate, Ethanol	pour point depressant	250
INH-B	xylene: 60-100 weight%,Ethylbenzene: 10-30 weight%	paraffin inhibitor	200
INH-C	Heavy Aromatic Naphta 60-100%, Naphtalene5-10 %, 1,2,4-Trimethylbenzene 5-10%	paraffin inhibitor	350
INH-D	contain xylene 60-100%,	pour point depressant	100
INH-E	10% active Ethylene Vinyl Acetate polymer in aromatic solvent,	paraffin inhibitor	400
INH-F	22% blend of alky resins and ethoxylated amines in aromatic hydrocarbon,	paraffin inhibitor	400
INH-G	25% active high molecular weight copolymer in aromatic solvent,	paraffin inhibitor	400
INH-H	propriety mixture of detergents and surfactants	paraffin inhibitor	400
INH-I	----	pour point depressant	600
INH-J	----	paraffin inhibitor	400

A commercial oil-based drilling fluid was used as a contaminant in initial sampling. The aim was to investigate a proper way to estimate uncontaminated waxy oil properties such as, WAT, WDT, viscosity and deposition tendency. The composition was listed in Table 3-3 below.

Table 3-3. The composition of commercial oil-based drilling fluid used in this study.

SCN	MW	Weight%	Mole%
C9s	121	0.13	0.19
C10s	134	2.10	2.69
C11s	147	11.20	13.07
C12s	161	27.65	29.46
C13s	175	28.73	28.16
C14s	190	20.44	18.45
C15s	206	7.90	6.58
C16s	222	1.54	1.19
C17s	237	0.25	0.18
C18s	251	0.05	0.03
C19s	263	0.01	0.00
Overall	172	100.00	100.00

Two different thermodynamic hydrate inhibitors, MEG and methanol, were used to study their effect on wax deposition. Two different commercial anti-agglomerations named AA-1 and AA-2 were used.

Barium sulphate was added to oil to investigate the impact of scale on QCM results. Deionised water was added to oil samples to see the effect of water cut on deposition. Toluene and n-heptane were used for cleaning purpose only. Table 3-4 below, lists specifications as stated by the supplier of the materials used in this work.

Table 3-4. Specifications as stated by the supplier of the materials used in this work

Chemical name	Supplier	Mass fraction purity
Toluene	Fischer scientific	>0.995
n-Heptane	Rathburn chemicals	>0.990
Barium sulphate	Fischer scientific	>0.975
MEG	Sigma-Aldrich	>0.998
Methanol	Sigma-Aldrich	>0.998

3.3 Experimental Equipment

3.3.1 Quartz Crystal Microbalance (QCM)

Quartz Crystal Microbalance (QCM) is an AT-cut piece of quartz with gold electrodes bonded to its surface. AT-cut is the most widely quartz cut in electronic industries which is cut the quartz at 35° 25' to the Z axis. A photo of both sides QCM surface is shown in Figure 3-1. It is a piezoelectric material which describe a relation between a mechanical stress and electrical voltage. Imposing any mechanical stress such as adhering mass to the surface is converted to the resonant frequency by an impedance analyser. This effect is only used in non-conductive material.

In ideal conditions an increase in mass of 1 nanogram will give rise to a reduction of 1 Hz in RF provided the deposited mass is rigid and distributed evenly on the surface. The RF of the QCM is also influenced by changes in pressure, density and viscosity of the surrounding medium [1-3].

Figure 3-1. A photo of both sides of QCM surface bonded with gold layers

The QCM should be submersed in non-conductive liquids to avoid shortcut current between detectors on both sides of the QCM surface. The method relies upon an increase in solid particles on forming, adhering to the surface of a QCM which gives a reduction in resonant frequency. Likewise, a reduction in the total mass of the QCM (due to the removal of solid deposits) will result in an increase in the resonant frequency. As a result, the QCM can be employed in a variety of cells to measure WAT and WDT in most crude oils apart from those of very high viscous sample which wax crystals unable to move. It also can be used to assess the effect of wax inhibitors on the wax adhesion tendency of crystal formed which is judged by observing the magnitude of ΔRF as a function of temperature[1, 3]

It must be noted that in all cases of wax and particles deposition, it is difficult to be exact regarding the amount of solids adhering due to the nature of the solid deposits such as varying degrees of viscoelasticity, and uncertainties regarding parameters such as density and evenness of deposits[1, 3]

3.3.1.1 Twin tube QCM setup

The tests using QCM in this thesis was performed by a multi-sample setup in static condition without a mixer. A multi-sample was comprised of eight different channels connected to the impedance analyser with an ability to measure eight different measurements simultaneously. However, two channels were used in this study. The setup consisted of two approximately 15 cm^3 glass test tubes, each having a QCM suspended within them, filled with the same stabilised test sample. Two different QCM were used for the entire comparative measurements in this work. The test tubes were sealed with a rubber cap and immersed in a water bath for temperature control. The temperature of the bath was monitored with a SITEC PRT (Platinum Resistance Thermometer) with the sensing part directly in contact with a test tube in the bath (Grant, GP200). The temperature probe was calibrated against a Prema 3040 precision thermometer. The uncertainty in the temperature measurements was estimated to be better than ±0.1 °C. Preliminary measurements showed that no any significant observation on QCM reading in terms of WAT-WDT measurements, and agitation to the samples resulted some noise on deposition. So it was decided to launch the setup without a mixer. Note that the test tube diameter was small enough, 12mm in diameter, to regulate temperature among bath and bulk sample while cooling and heating. In the preliminary measurements a temperature probe mounted in the middle of test tube which showed a really good match between sample in the test tube and the bath temperature. Figure 3-2 and Figure 3-3 show photo and schematic of the multi-channel QCM setup used in this study.

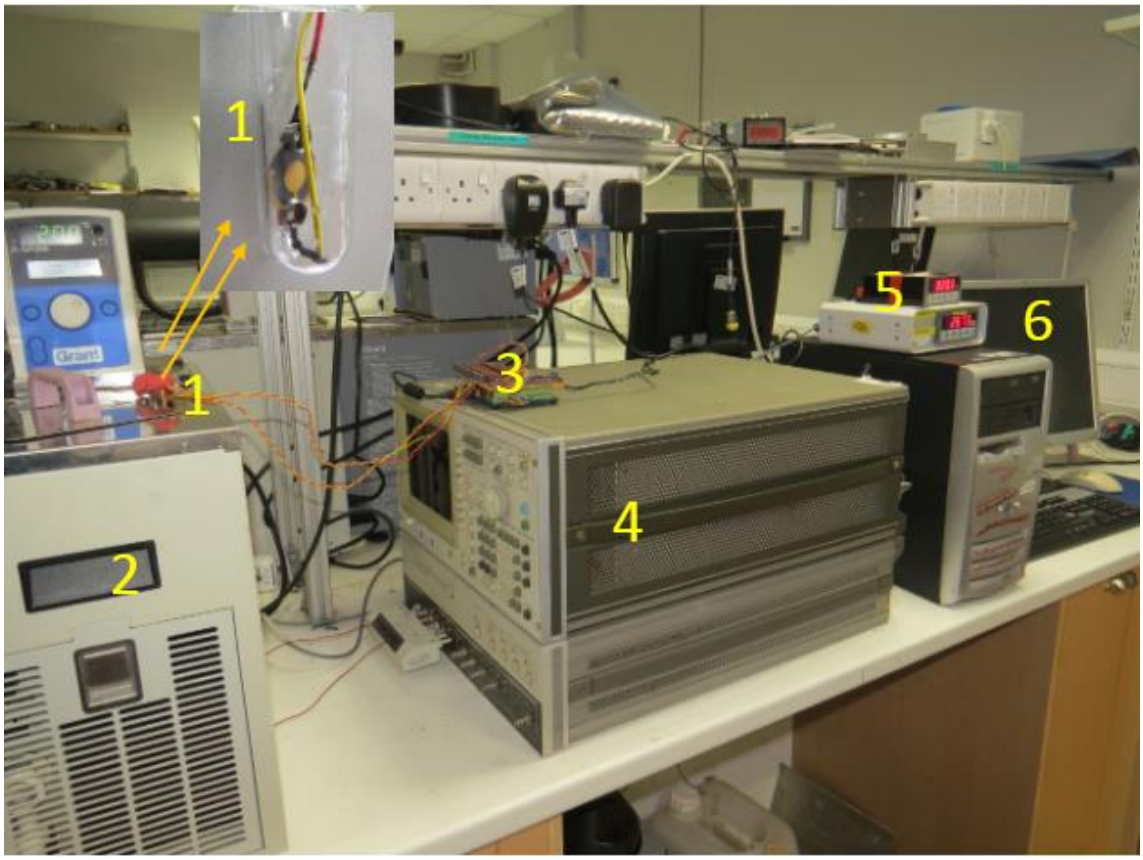

Figure 3-2. Photograph showing QCM multi-sample setup, 1) two test tube mounted a QCM, 2) Thermal cooling bath, 3) Multi-channel connection, 4) Impedance Analyser, 5) Temperature readout box, 6) LABVIEW installed on computer

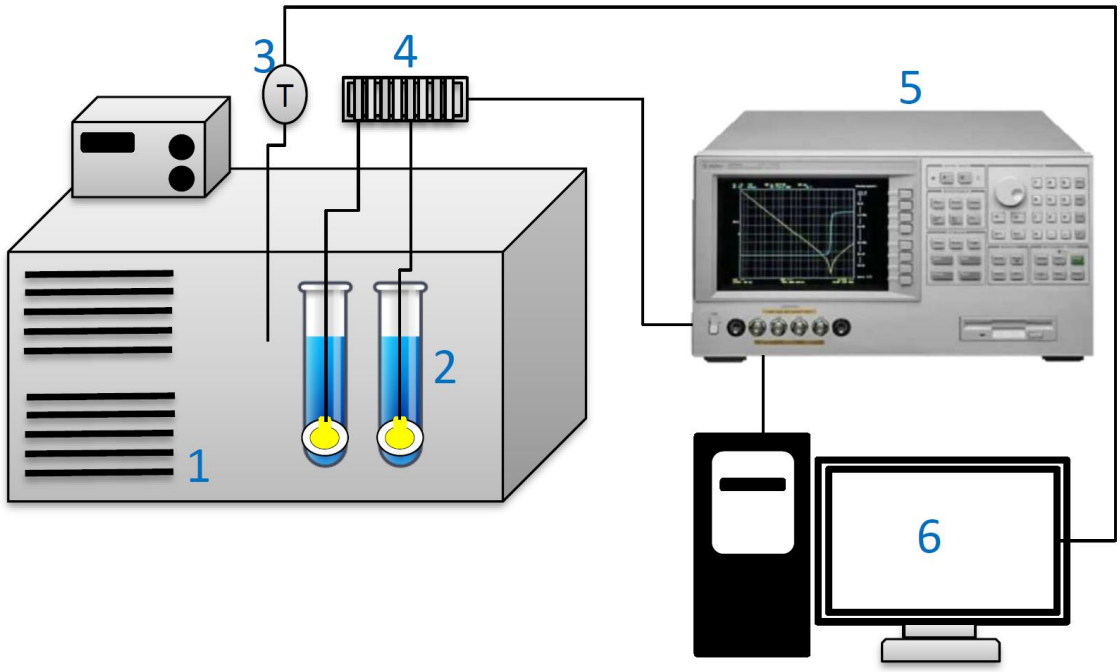

Figure 3-3. The schematic of the QCM multi-sample apparatus, 1) Thermal cooling bath, 2) two test tube mounted a QCM, 3) Temperature readout box, 4) Multi-channel connection, 5) Impedance Analyser, 6) LABVIEW installed on computer

3.3.1.2 QCM test procedure and analysis of data

The capability of the QCM to accurately measure WAT and WDT was demonstrated previously [1]. The QCM tests involved subjecting the test fluid to a temperature cycle, continuously cooling and then continuously heating whilst monitoring the resonant frequency of the QCM. The general form of the QCM procedure is as follows:

Choosing an appropriate starting temperature is the first and most important part of WAT, WDT and pour point analysis. Conventional conditioning temperatures based on standard methods (ASTM D-2500, ASTM D-97, etc.) would have been insufficient or in some cases quite high in preparing a wax-free oil sample; therefore, a rheometer analysis was used a developed technique to determine the best starting point and conditioning temperature in order to dissolve all wax, apart from asphaltene and resin. The procedure will be described in the following chapter [4, 5].

The sample bottle was shaked thoroughly before a subsample was taken. The subsample was then introduced to the cooling bath and the temperature of the bath was initially set to the specified conditioning temperature and left to equilibrate for 2-3 hrs to remove any precipitated wax. The water bath was then cooled at a constant rate of 0.5 °C/min in all cases to a temperature below the WAT point. Figure 3-4 is an illustration of the analysis procedure based on the data from one experiment.

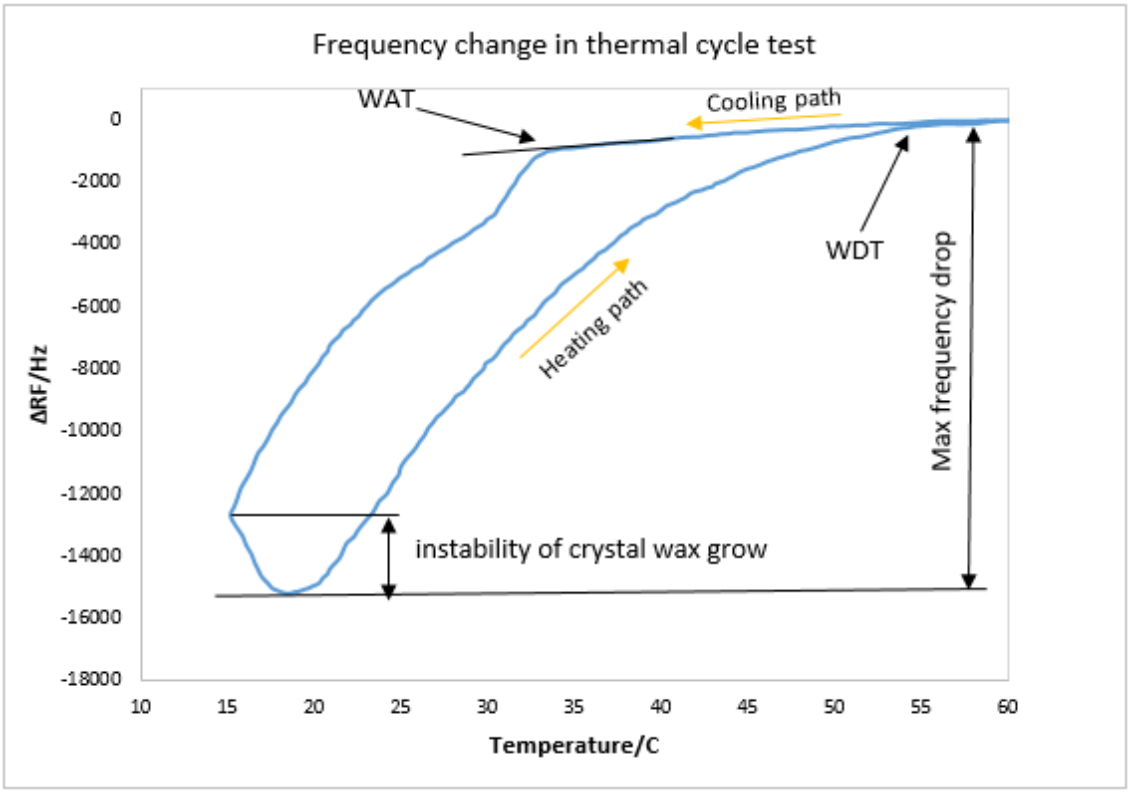

Figure 3-4. Frequency changes in a thermal cooling/heating cycle test.

On cooling from the initial temperature, in the absence of precipitated wax, there was an observed reduction in RF, which follows an approximately linear trend and the slope is related to the oil characteristics. As noted earlier, QCM is sensitive to viscosity and density of the sample, and the observed reduction in RF is attributed to the increased viscosity as the temperature was reduced.

At the WAT, the change in the resonant frequency (ΔRF), as a function of reducing temperature, became significantly greater as precipitated wax adheres to the QCM surface; this unique temperature point was identified, by finding the deviation from a linear trend.

The reduction in RF continued till the lowest temperature was reached. At this point, the sample was then heated to the conditioning temperature at the same rate of temperature change as used on cooling. After few degrees of increasing temperature, the RF was still observed to continue decreasing to reach its' maximum reduction before increasing as the wax dissolves back into the bulk oil. This reduction was probably due to a delay in achieving equilibrium at the applied cooling rate. Lower cooling rate gives more time to equilibrate and probably would minimise RF reduction in the early stages of heating [1].

The wax dissolution temperature (WDT) was detected when the RF returned to the linear trend observed during cooling in the Newtonian region. However, it was observed that the WDT was difficult to identify using this approach. For more precise evaluation of the WDT, a stepwise heating program was required, which would allow stabilisation of RF at each temperature interval. Consequently, a broader range of values for WDT compared to WAT was reported. The aim of the QCM tests was not to make precise measurements of the WDT if this was the case then step-heating would have been used.

The cooling/heating cycle was repeated several times for each test sample to measure repeatability and wax morphological behaviour during cycles. The WAT, WDT and maximum frequency drop were reported for each crude oil sample with/out inhibitors from the two test cells.

3.3.2 Coaxial shearing wax deposition

The coaxial shearing wax deposition apparatus comprises of a shear cell which dictates shear stress to the cold finger surface. This setup provides a method for quantifying the amount of wax that will be deposited on the internal wall of a pipe at a predetermined temperature gradient and flow regime.

3.3.2.1 Coaxial cold finger setup

Essentially, the apparatus consists of a stainless-steel cell/tube (approx. 300 cm^3) to hold the petroleum sample. Flanges at the top and bottom of the cell provide a high-pressure seal. A cold finger (bobbin) is suspended from the top flange and, during experiments, is immersed in the bulk fluid sample. A rotating cylinder is positioned between the outside diameter of the bob and the inside diameter of the cell.

The high-pressure cell is mounted on a magnetic stirrer then stirrer speed (rpm) is set to simulate specific pipeline conditions. The stirrer drives the rotating cylinder via a coupled magnet and allows the user to vary the shear rate of the bulk fluid relative to the bobbin. The stirrer creates a helical decaying rotating flow regime. However, it has significantly different regimes than those present in real production operations[6].

A glycol bath provides a cooling medium for the bob with sufficient heat transfer to maintain the surface of the bobbin at an adequately low temperature. The temperature of the cell wall is controlled by a thermo-electric jacket, which is controlled by a temperature relay control box. It is important to note that the thermos-electric jacket

heats only and does not cool; the lowest temperature of the cell wall achievable is, therefore, limited to the ambient temperature of the laboratory. Temperature probes monitor the temperature of the circulating fluid inside the bob and the temperature of the bulk fluid in the cell, however, the apparatus is unable to log these data. Figure 3-5 and Figure 3-6 show photo and schematic of the coaxial shearing wax deposition set-up used in this work.

Figure 3-5. Photograph illustrating the coaxial shearing wax deposition setup. 1) Coaxial, 2) Temperatures control and readout, 3) Thermal control bath 4) Bobbin inlet/outlet hoses, 5) Bobbin fluid inlet valve, 6) Electro-thermal jacket, 7) Inlet valve and pressure gauge, 8) Pressure relief valve, 9) Magnetic stirrer

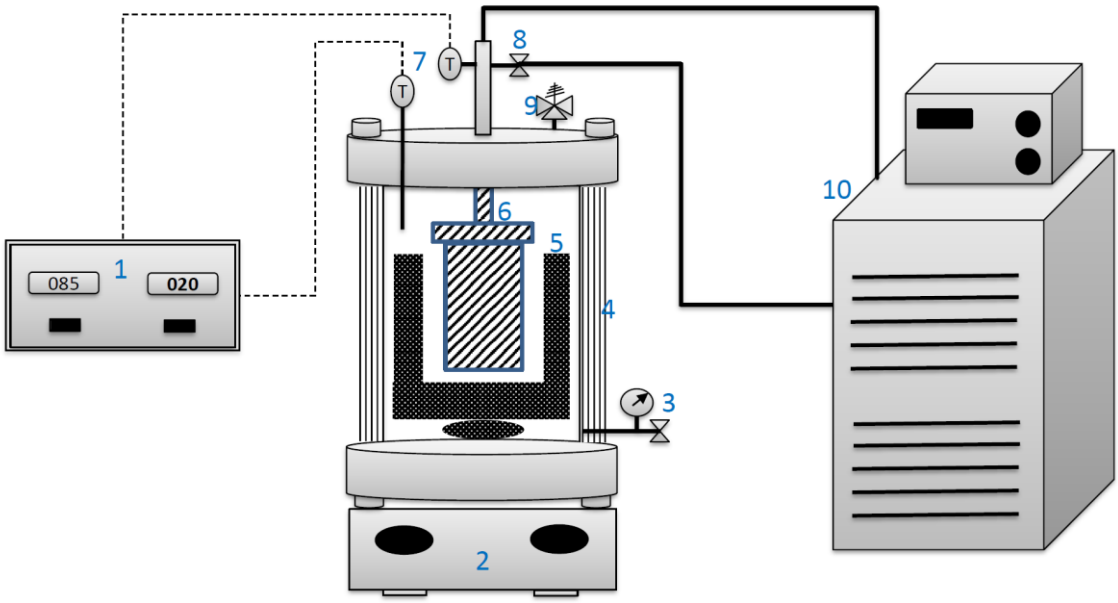

Figure 3-6. The schematic of the coaxial shearing wax deposition setup, 1) Temperatures control and readout, 2) Magnetic stirrer, 3) Inlet valve and pressure gauge, 4) Electro-thermal jacket, 5) Rotating cylinder, 6) fixed bobbin cylinder, 7) Thermal sensors, 8) Bobbin inlet/outlet hoses, 9) Pressure relief valve, 10) Thermal control bath

Wax deposition was measured gravimetrically by collecting the deposited wax from the bobbin surface alone (i.e. not the cold finger tubing and fittings) and weighed using a balance (Mettler Toledo, MS204S/01, ±0.0004 g).

Subsequent to wax deposition experiments, the deposited wax could be collected for inspecting the nature of the crystal structure and compositional analysis. Ultimately, the data generated can be used to predict the amount of wax that will be recovered from the pipeline during pigging operations and to help identify the required pigging frequency.

The drawback of this type of laboratory apparatus is difficulties to remove excess oil dripping off the bobbin without losing any wax deposition. In addition, only one data point can be measured which represents a snapshot of wax deposition versus time; sloughing and scraping off the wax layers during the test would be somewhat scattered, making it difficult in terms of comparison purposes and evaluating inhibitor additives especially in a long time.

The dimensions and test conditions are presented in Table 3-5 below.

Table 3-5: Coaxial cold finger parameters

Bobbin Diameter / cm	*3.175*
Bobbin Height / cm	***4.938***
Surface area of bobbin / cm^2	*49.23*
Oil volume required covering the cold finger(cc)	***175***
Available capacity / cm^3	*300*
Maximum shear rate / s^{-1}	***500***
*Minimum shear rate / s^{-1}**	*50**
Minimum buck oil temperature	***Ambient***
Maximum bulk oil T /^oC	*100*
Maximum working Pressure / psi	***2000***
*******Zero shear is possible with the magnetic mixer switched off*	

3.3.2.2 Coaxial procedure

The cell was loaded with sufficient volume of oil to ensure the vortex created by mixing was above the cold-finger bob and dosed with inhibitor.

The stirrer speed then was calculated and applied based on real pipeline data according to formulated Equation3-1 and Equation3-2 [7].

$$\gamma = \frac{4q}{\pi r^3} \quad \text{……. Equation 3-1}$$

$$rpm = \frac{15\gamma}{\pi}\left[1 - \left(\frac{ri}{re}\right)^2\right] \quad \text{……..……..Equation 3-2}$$

q= pipeline flowrate, cm^3/min

r= pipeline radius, mm

γ= shear rate, s^{-1}

ri= bob radius, mm

re= rotor radius, mm

The temperature of the bulk was set to a predetermined conditioning temperature, as determined by rheometer testing, and left to condition and equilibrate for a period of 30 minutes. It was necessary to ensure all wax had disappeared and any wax memory (part of high-molecular-weight wax particles which suspended as crystals in the oil) was removed.

During the conditioning period, the fluid inlet to the cold bobbin was closed. The cell wall was then reduced to the target temperature. When the cell wall (bulk fluid) reached the target temperature, the cooling inlet for the cold finger bob was opened to provide immediate cooling of the cold finger bob.

A timer was also started when the fluid inlet of the cold finger bobbin was opened to cool the bobbin. The system was then left for different test times to allow the wax to deposit on the cold finger.

The experiment is stopped and the bobbin removed. The deposit is then scraped off from the bobbin cylinder using a razor blade as shown in Figure 3-7.

Visual assessments were made of the physical characteristics of deposits and photographs were taken for documentation.

Figure 3-7. Photograph of the deposited wax and wax collection.

3.3.3 Rheometer

Before describing the rheometer, it is worth giving a short explanation about viscosity and rheology. Though, it is beyond the scope of this thesis to discuss in detail about the measurement and interpretation of fluids behaviour.

Viscosity is the mechanical property of fluids which depends on the interaction between molecules tending to resist flow. The first mathematical definition of viscosity was derived by Isaac Newton in the 1600's. He described viscosity as a constant proportionality in the plot of shear stress versus shear rate. In other words, the viscosity of the fluid is independent of shear rate and yields a straight line. Materials related to this property called Newtonian fluid such as water and solutions of single phase low molecular weight. Viscometers are instruments which are specifically limited to measure these types of fluids[8-10].

In the real word, on the other hand, a large group of fluids exhibit more complex behaviour where their viscosity strongly depends on the shear rate of fluid flow. This behaviour is known as shear thinning or pseudoplastic which decrease or increase respectively with increasing shear rate. There is also another type of material which has viscosity reduction at the time, called thixotropic. All these complex, real-world materials are categorised as non-Newtonian fluids and study of their behaviour is called rheology. The rheometer is a device used for characterising these types of fluids and uses a small sample size and provides precise control of shear rate[8-10].

Crude oil composition is very complex and heterogeneous, exhibiting both kinds of rheological behaviour. The rheology behaviour of crude oils is highly dependent on the temperature and distinguished by the WAT of the fluid. At sufficiently high temperatures above the cloud point, all crude oils with the exception of extremely asphaltene-rich oils are pure Newtonian fluids. As the temperature is reduced below the cloud point, they become highly complex non-Newtonian fluids. At this region, flow properties are difficult to measure reliably and give rise to some errors due to the presence of wax crystals; hence, this gives rise to a fundamental issue regarding operating and design of pipeline systems at low temperature where the oil displays a strong shear thinning behaviour [8, 9, 11, 12].

The rheometer was used in this thesis mainly to evaluate wax treatment additives at atmospheric pressure. It was used to monitor viscosity at a constant shear rate over a decreasing temperature gradient for comparative purposes. Measuring the onset temperature of the wax crystallisation where the liquid first exhibits non-Newtonian behaviour, was another potential of using rheometer presented in this work. Moreover, investigating a developed technique to measure the ideal starting conditioning temperature was another possibility using rheometer. In addition, the capability of

oscillation frequency was used to measure pourpoint mimic the ASTM D-97. The impact of inhibitors and conditioning temperature on pourpoint was also studied.

3.3.3.1 Rheometer setup

Rheology studies on waxy oil were carried out with temperature sweeps using a stress controlled rotational-type rheometer obtained from Anton Paar Ltd. (Physica MCR 301). It is an expensive though straightforward instrument which offers great flexibility, sensitivity and analytical power.

Almost all the measurements presented were obtained with the aid of 25mm diameter, 1° angle cone and plate geometry (Cones CP50-1). It consists of two circular plates where material under test is sandwiched between them. The bottom plate is fixed in rotational terms while the top is fitted to a shaft, floated on a sophisticated air bearing in order to keep friction to a very low level. It is then fitted to a very sensitive electric motor to control the torque of the system while rotating/oscillating according to pre-set experimental parameters.

The gap between the lower and upper test plates is defaulted to be at 0.1mm to achieve optimum measurement accuracy. The largest sized particle present in the test material recommended being at least three times lower than the gap. Since the size of wax particles formed are much lower than recommended gap, it was considered to be a suitable geometry for the tests presented in this work[9, 13].

One important reason to choose this geometry was based on the fact that this was the only geometry with the capability to generate uniform shear rate on the whole measuring surface. Therefore, it gave a homogeneous flow and eliminated particle migration alongside the measuring system. In addition, thermal equilibrium can be achieved pretty easily because of the small sample required[9].

However, loss of light components due to evaporation is a potential disadvantage of this geometry, especially with light hydrocarbons at a high conditioning temperature. Since the working basis presented in this study is the comparative approach of the samples in the same experimental condition, this drawback could be ignored or considered to have no significant influence[9].

The base plate temperature of this geometry was controlled with a Peltier system so that the temperature of the sample could be accurately controlled within 0.1°C in the range

of -40°C to +200 °C. In addition, a temperature-regulated bath was connected to the rheometer, set at a suitable constant temperature, to give more control on Peltier elements and cover the desired range of temperature; without it, Peltier unable to go beyond the desired temperature range. In this work, the bath temperature was set at 20°C to cover the routine testing regime range of -20°C to 100°C of the measuring system.

Both plates are machined from titanium for durability as well as minimising the rotational inertia. It is also equipped with TruGap technology ensuring no thermal expansion or contraction of the titanium in temperature gradient result in a change of measuring the gap.

The maximum applicable shear rate for the cone was 3,000 s^{-1}. The shear rate is one of the fundamental factors in the rheological analysis, and it must be noted that choosing the proper one was found to be elaborate especially for shear thinning materials. The recommended torque based on selecting a shear rate depends on the resolution of the rheometer sensor (0.05 µPa to 5MPa). However, in the preliminary measurement, it was observed that being in the recommended torque was not sufficient. It was found out that choosing proper shear rate was highly dependent on composition which must be found by trial and error. Overall, it was observed that low shear rate resulted in an unreliable result with scattering and very high viscosity. On the other hand, high shear rate generated a really low viscosity which was probably due to slippage of the rotating plate over the sample. Hence, choosing the optimum shear rate was found to be crucial for analysing viscosity trends especially detecting WAT-WDT.

After preliminary experimentation for the purpose of analysing waxy oil samples, it was observed that shear rate $10s^{-1}$ produced reproducible curves for the oil samples tested. It was also observed viscosity deviation in non-Newtonian region decreased with increasing shear rate. This is most probably due to reducing the size of the crystals and aggregates.

Loading the correct amount of sample was also an important part of the job which required to be carefully presented on the base plate. Too much sample oozed out from between the plates and gave scattered data especially in temperature sweep. On the other hand, loading too little sample meant the gap would not be totally filled gave underestimated viscosity. The best technique for loading was using a disposable plastic

pipette and loading slightly too much sample then carefully wiping away the excess around rotating cone plate.

A photograph of the atmospheric set-up with cone and plate geometry is shown in Figure 3-8.

Figure 3-8. Photograph of atmospheric rheometer set-up with cone and plate geometry. 1) Rheometer installed with atmospheric geometry, 2) Remote control and logged the results, 3) Temperature-regulated bath, 4) Cone and plate atmospheric geometry

The high-pressure concentric cylinder (CC30) was another geometry used in this work. The most important advantage of this geometry was the capability to avoid evaporation; hence, it was used to evaluate the effect of ageing time on a pure inhibitor, INH-C, as well as dosed with oil sample OIL-A. The shear thinning behaviour was monitored over an extended period without losing significant amounts of light components.

The temperature was controlled by an external temperature controlled bath (Grant, GP200). There was always a temperature lag between the sample and the bath temperature even at a low cooling rate, making it unreliable for temperature sweep measurements.

The sample size required to filled the geometry was 22cc and the pressure setup limited available shear rates to a maximum of 1500 s^{-1}. The maximum working pressure was 6000 psi. Figure 3-9 shows the concentric cylinder geometry.

Figure 3-9. Photograph of high-pressure rheometer in concentric cylinder geometry. 1) Rheometer installed with high pressure geometry, 2) Remote control and logged the results, 3) Temperature-regulated bath, 4) Magnetic coupling, 5) Pressure head and measuring cylinder, 6) Relief valve, 7) Inlet valve

3.3.3.2 Rotational procedure in the atmospheric condition using cone and plate geometry

The sample was initially loaded into the rheometer plate whose temperature was previously set at 20 °C. The temperature was then raised quickly thanks to the Peltier system and kept for 3 minutes at the premeasured starting point to be conditioned to erase the thermal memory of the oil by redissolving any possible waxy structure. The thermal cycle was then started right after equilibrium holding time, cooling the sample at a constant rate to reach the destination temperature; finally, without any delay, heating it back with the same rate of temperature change to the starting temperature. The applied shear rate was constant during the whole process.

The data generated were plotted in a Log μ (cP) vs. temperature (℃) based on Arrhenius principle, Equation 3-3, which shows a linear relationship for Newtonian range[14]:

$$\mu = Ae^{-E_a/RT} \quad \text{.....Equation 3-3}$$

Where

μ = Newtonian dynamic viscosity

E_a = Activation energy of viscous flow in joules

R = Universal gas constant

T = Temperature

A= Pre-exponential factor largely dependent on the entropy of activation of flow

In Figure 3-10, a semi-log variation of viscosity generated in a thermal cooling/ heating cycle test is demonstrated. In addition, the way to measure crystallisation and dissolution temperatures (WAT/WDT), as well as the maximum viscosity is shown. The maximum viscosity and WAT obtained by rheometer are the two main predominant parameters used widely in this work. Heating up the sample to obtain WDT resulted scattering viscosity and difficult to indicate the WDT, therefore, WDT was only measured for some limited cases.

Following is a brief description and interpretation of the thermal cycle plot.

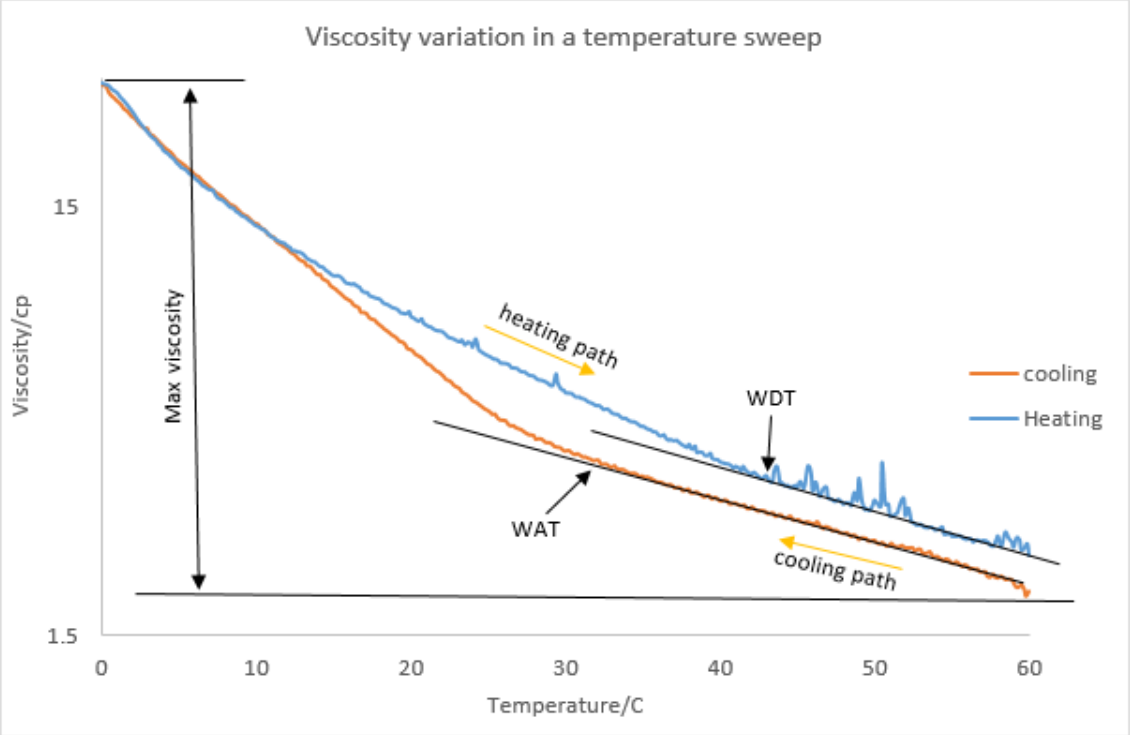

Figure 3-10. Viscosity variation in a thermal cycle test using rheometer

At the start of cooling, well above the wax appearance temperature, the viscosity increased gradually. This behaviour continued, obeying the Arrhenius temperature dependence of Newtonian fluids until wax started to precipitate out from the solution. An abrupt deviation in viscosity was then observed due to the fact that a significant amount of wax crystals began form. The point where non- Arrhenius behaviour was starting, could be related to the wax appearance temperature [13, 14].

Finding the proper point of deviation, though, was found to be a demanding job highly dependent on sample composition. Fluids with higher wax content, for example, showed a more clear-defined deviation. In addition, samples dosed with some inhibitors were observed to show a gradually increasing viscosity in the span of temperature sweep, making it a challenging task to find the exact point. Furthermore, since the oils are generally shear-thinning, the shear rate could largely govern the deviation point. The increasing shear rate was observed to show less defined deviation point. Therefore, a preliminary measurement was required to find the optimum shear rate on the samples under study. Moreover, user experience was required to find the correct deviation point.

As the temperature reduced further down the WAT, wax crystals grew, leading the waxy sample to become more and more non-Newtonian hence the viscosity increased at a higher rate. However, the rate of viscosity increase rate was found to be governed by shear rate and cooling rate in the non-Newtonian region. It may be related to the shear thinning nature of waxy oil samples which govern the amount, size, and shape of wax crystals [13, 14].

Finally, the sample was heated back to the starting conditioning temperature. Wax crystals dissolved to the solution reducing the amount of available crystals in the bulk sample. Hence, the viscosity was observed to decrease gradually until it laid on the Arrhenius straight line representing the wax dissolution point(WDT)[13, 14].

The hysteresis between Newtonian range above WAT and WDT probably results from the evaporation and loss of light components during the thermal cycle which is related to the oil characteristics. The difference between WAT and WDT was probably related to the thermal equilibrium which in principle can be avoided by cooling and heating at a low enough rate [1].

3.3.3.3 Oscillation procedure at atmospheric conditions using cone and plate geometry

The aim of this section was to investigate measurement of pour point using a rheometer.

3.3.3.3.1 Pour point and gelation point

One of the most important concepts in the flow assurance wax study is pour point temperature which is related to the deposition process. Pour point is an indicator of the gelling potential of a crude sample. It typically occurs when about 2 wt% wax is precipitated out of solution to form a wax gel network. This point is defined according to standard ASTM-D97 and consists of cooling down the sample. The lowest temperature at which the oil sample will no longer be able to flow when held in a horizontal position in a test jar for about 5 seconds, is recorded as the pour point. It is the industrial standard for referring to the point of no flow [4, 14].

Measurement of pour point is normally conducted without applied stress. From a rheological point of view, this approach fails to mimic the real field conditions where viscosity and shear stress exist under flow conditions[4].

The gelation temperature, on the other hand, is a general form of pour point which is a function of applied shear stress to the sample, hence, covers a wider range of temperature. In addition, like pour point, it highly depends on cooling rate as well as the composition of the waxy oil. It is also expected to be slightly higher than pour point and depressed by applying higher stress[15, 16].

Interpretation of gelation temperature versus pour point was beyond the scope of this work. The aim of this study was using the capability of rheometer, finding gelation temperature at realistic conditions at similar temperature to the pour point obtained by ASTM D-97.

3.3.3.3.2 Oscillation mode

The capability of the rheometer (Anton Paar, Physica MCR 301) using oscillatory mode at atmospheric conditions, enables measurement of gelation temperature with varying applied stress.

As oppose to rotation where samples are under continuous deformation in one direction, oscillation causes a back and forth movement under a particularly applied frequency and shear stress. This type of approach provides a condition to investigate the viscoelastic nature of oils. Properties such as pour point and gelation where solid-like behaviour (elasticity) of a sample oil takes predominance over its liquid-like behaviour (viscosity) [9].

It was observed in preliminary measurements that working at extremely low temperatures, resulted in scattered data in some cases. Probably the plate sensor may not be coupled well over the sample due to break up of the sample and slippage of the sensor, hence measured values should be treated with caution in this region.

3.3.3.3.3 Procedure

The procedure for loading and programming the rheometer was similar to rotation mode with the exception of applying amplitude oscillatory stress with a frequency instead of using constant shear rate.

It was observed that very low values of the stress amplitude did not provide sufficient strain so the gelation point was unrealistically high. On the other hand, high shear stress depressed drastically the point, significantly lower than the estimated pour point. Preliminary measurements showed a frequency of 1.59 Hz with an amplitude of 25 μNm resulted in values quite close to the pour point measured with ASTM, at least for the sample oils under study.

The rheometer software recorded all necessary oscillation data, though only, deflection angle, loss modulus and storage modulus were used to measure gelation point in a temperature sweep.

As seen from Figure 3-11, there were two different approaches to determine gelation point, deflection angle and storage/loss modulus. Deflection angle decreased gradually approached to 0 mrad as the temperature of the sample lowered near the gelation point. Gelation point was measured qualitatively by this approach. On the other hand, using storage and loss modulus associated with the sol–gel transition was shown to be more accurate, being very sensitive to the structure change as a result of reaching the gelation point. This method was used in this work to make gelation point measurements [17, 18].

The liquid-like behaviour of the sample is characterised by the loss modulus (viscous response) while the solid-like behaviour is characterised by the storage modulus (elastic response). When a wax-oil mixture was at a temperature above the gelation point, loss modulus was at a higher value than the storage modulus. When temperature decreased, both moduli increased in value until the sample reached to the gelation point. At gelation temperature, storage modulus is equal to loss modulus. Storage modulus increased if the mixture was subjected to a further cooling. This definition is quite close

to the conventional determination of sol-gel in complex mixtures such as a polymer. The sol-gel technique is a process which defines a transition between liquid phase and solid phase. The accuracy of using rheometer for detecting pour point was found to be ±0.2°C in comparison with ASTM D-97 method which is ±3°C [4, 17-19].

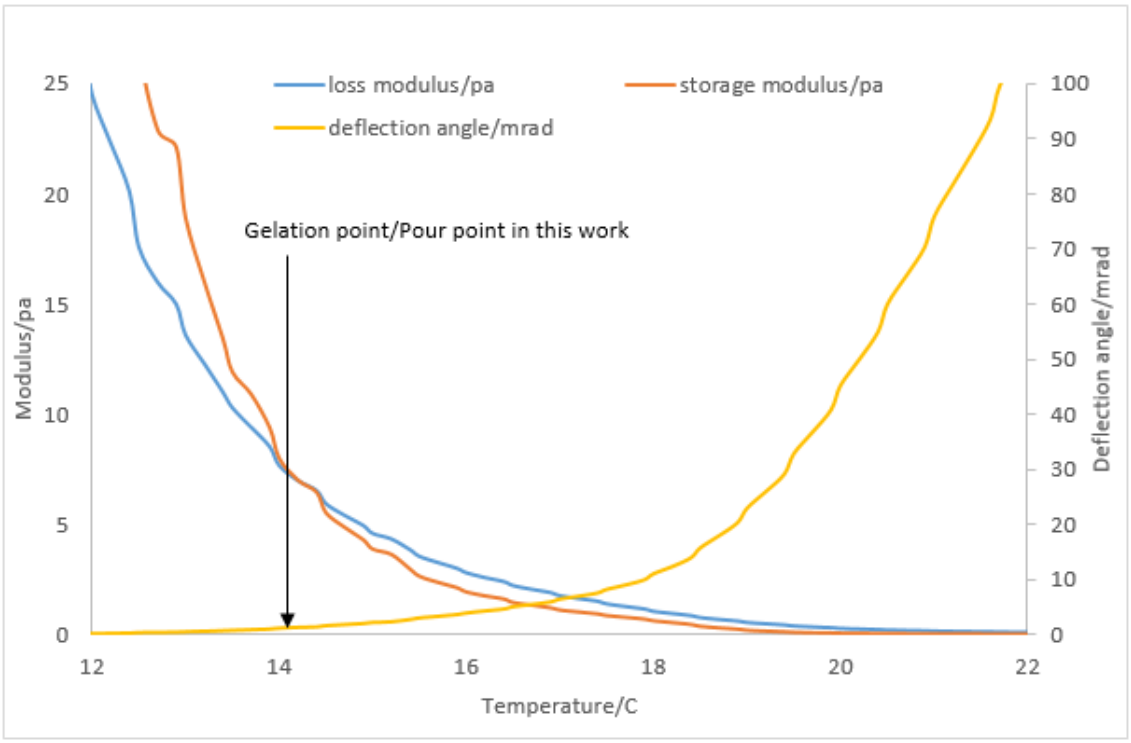

Figure 3-11. Different approaches used oscillation mode to measure pour point. Example from this work.

3.3.4 Mini-Flowloop benchtop equipment

In flow assurance associated with wax, the most important issues are related to the study of deposition under flowing conditions. Flow loops are preferred and often considered the most reliable apparatus for studies of wax deposition when compared to the other techniques; because they can simulate as near as possible the realistic dynamic conditions found in a pipeline and production system. They are usually flexible tools, where the conditions of the test such as pressure, temperature, shear rate, etc., can be varied [20, 21].

3.3.4.1 Flowloop setup

An in-house bench-scale flow loop apparatus was designed and fabricated to study the impact of some additives in comparison with the other conventional experimental instruments. Figure 3-12 and Figure 3-13 show photograph and schematic of the flow loop used in this study.

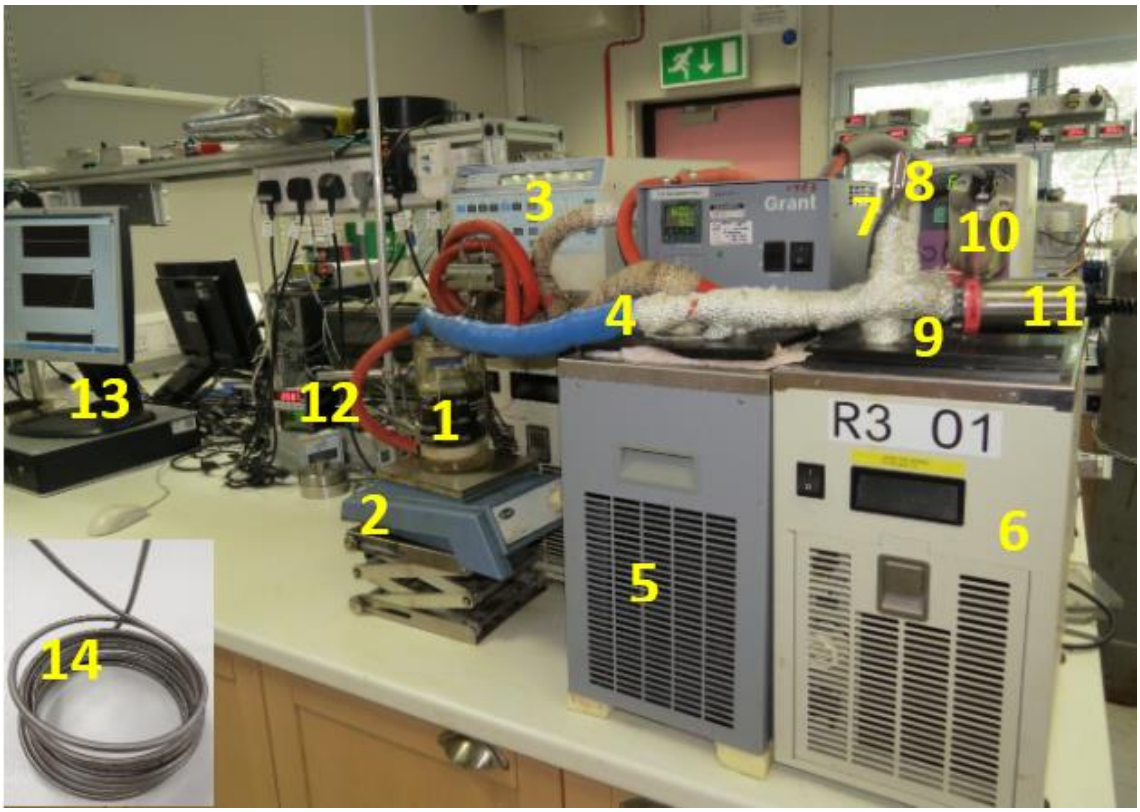

Figure 3-12. Photograph of in-house build flow loop employed in the current study, 1) Jacketed beaker(reservoir), 2) Mixer and stand, 3) HPLC pump, 4) Heater hose and insulation, 5) Conditioning bath, containing two conditioning loops, inlet and outlet of test loop, 6) Test bath, containing test loop, 7) Inlet temperature sensor, 8) Outlet temperature sensor, 9) Test bath temperature sensor, 10) Inlet pressure sensor, 11) Outlet pressure sensor, 12) 5 different readout boxes, 3 for temperature, 2 for pressure, 13) LABVIEW recording, 14) Test loop C, 2.23cm ID, 300cm length

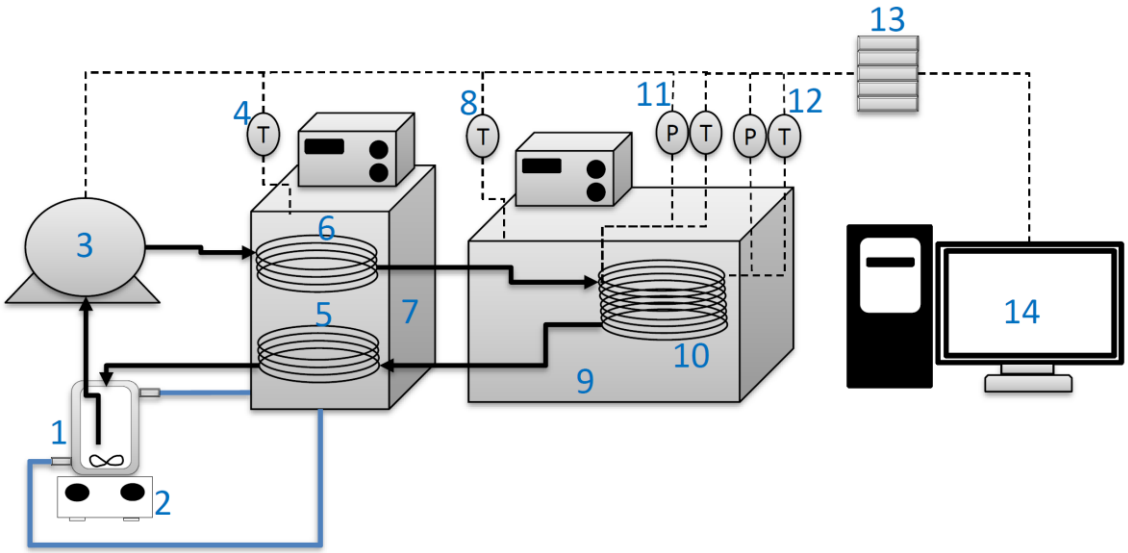

Figure 3-13. The schematic of the in-house build flow loop apparatus 1) Jacketed beaker(reservoir), 2) Mixer and stand, 3) HPLC pump, 4) Conditioning bath temperature probe, 5) Outlet conditioning loop, 6) Inlet condition loop, 7) Conditioning bath, 8) Test bath temperature sensor, 9) Test bath, 10) test loop, 11) Inlet temperature and pressure sensor, 12) Outlet temperature and pressure sensor, 13) readout boxes, 14) LABVIEW recording.

This flow loop consisted of a jacketed beaker containing a 3cm magnetic stirrer mounted on a stirrer plate as an oil reservoir feeding the flow loop. The jacketed beaker temperature was controlled by a temperature-regulated bath (Grant, LTC6-30RS) named the conditioning bath which is at a constant temperature during the test. Circulation of the mixtures at predetermined rates was accomplished by using an HPLC pump (Hitachi L6200A) which was able to deliver flow rates up to 10 cc/min providing a laminar flow regime.

The pump takes oil from the reservoir and pumps it through the conditioning loop in the conditioning bath. The 2-meter conditioning loop was made of stainless steel with a 1.47mm ID. This was considered sufficiently long to erase thermal history and dissolve back any wax in the loop. Downstream from the conditioning bath was a deposition test section.

The test section was the most important part of a flow loop where wax was encouraged to deposit on the inner pipe wall while monitoring temperatures and pressures, a similar situation to that encountered in oil and gas pipelines.

The test section was built from different sizes of stainless steel-316 tubing as described in Table 3-6, which were submerged in a temperature-regulated bath (Grant, GP200). The sample was circulated in the loop while being cooled in the test section with cold water, forcing the deposition of wax on the inner pipe wall.

Table 3-6. specification of test loops used in this work

Specification	***Loop A***	***Loop B***	***Loop C***
Length of test section loop (cm)	*50*	*239*	*300*
Inside diameter (mm)	*1.47*	*2.98*	*2.23*
Outside diameter (mm)	*3.33*	*6.02*	*3.33*
Volume of test section loop (cc)	*0.85*	*16.66*	*11.71*
Effective internal area of test section loop (cm^2)	*23*	*224*	*210*
Minimum shear rate that could be achieved based on available pump (s^{-1})	*53*	*6*	*15*
Maximum shear rate that could be achieved based on available pump (s^{-1})	*529*	*63*	*151*

The temperatures were measured by a platinum resistance thermometer located at the inlet and outlet of the test tube. The accuracy of the measured temperature was ±0.1°C.

In addition, another temperature probe was inserted to the cooling bath to monitor temperature outside the test loop.

It was also equipped with pressure transducers (Quartzdyne QS10K-B, pressure range 0-10000psi) to record the inlet and outlet pressure of the test loop. They were calibrated using a Budenberg deadweight tester. The accuracy of the pressure transducers was ±0.001psi.

All temperatures and pressures were logged via readout boxes through data acquisition LabVIEW installed on the computer in 10 seconds intervals during the experiments.

After the test section, the sample was circulated through the remaining length of the flow loop, which was submerged in a conditioning bath, before being returned to the sample reservoir to complete the closed loop. All parts of this flow loop outside the conditioning and test section baths were surrounded by a thermal tube which was connected and fed by the conditioning bath. It was also covered and insulated by a thick and dense layer of glass wool to minimise heat loss and prohibit wax deposition outside the target test section.

3.3.4.2 Test procedure and analysing data

Initially, the oil remaining in the loop as well as wax deposits in the test section from the previous experimental run were removed and cleaned by circulating toluene for about an hour.

The conditioning bath was adjusted to a predetermined conditioning temperature, as determined by rheometer tests, to erase any thermal history. The oil was then temperature conditioned for about an hour in two stages: first in the reservoir, followed by a 2-meter loop submerged in the conditioning bath immediately after the pump to ensure the oil sample temperature on the inlet side of the test section loop was still higher than WAT, hence no possibility of deposition.

A sufficient volume of oil was required to load into the reservoir to avoid any significant compositional changes whenever wax deposits in the test section. Some preliminary measurements by rheometer were done to measure viscosity change before and after the test for the oil samples used in this work, it was found that 200 cc of oil was sufficient so that the impact of depletion was negligible.

For all experiments, especially in the presence of an emulsion, it was crucial to provide sufficient agitation in the reservoir, at least 30 min, before pumping through loops as well as during the test to ensure the homogeneity of the mixture pumped through the

lines. The magnetic mixer speed in the reservoir was set to 3/10 in all cases. It was not possible to calculate the exact amount of shear applied.

In the experimental study, there are mainly two approaches in order to imitate field conditions; choosing the same Reynold number or the same shear rate, Equations 3-4 and Equation 3-5 [22-24]:

$Re = \frac{q d \rho}{\mu A}$ Reynold's number……..……Equation 3-4

$\gamma = \frac{4q}{\pi r^3}$ shear rate (s^{-1})…….……..Equation 3-5

Where

μ: fluid viscosity, $kg.m^{-1}.s^{-1}$

d: inner diameter, m

q: flow rate, m^3/second

r: inner radius, m

ρ: density, gr/cm^3

A: surface area, m^2

As the experiments are usually performed in bench top size loops with a low diameter, choosing the same Reynold number needs a high flowrate which was impossible to perform due to back flow pressure. Hence the only possible option was varying shear rate. The maximum possible shear rate with available accessories in this work was 529 s^{-1} which is in the laminar flow range.

It was observed that increasing shear rate in laminar flow, generated lower deposition as well as a smoother build up pressure which could be related to the strength of the deposited layer. It might be due to the fact that increasing oil flow rate in laminar regime could increase the shear stress at the liquid-deposit interface, which reinforced the intensity of shear stripping, leading to removal of oil from the network of deposited wax, consequently reducing the wax deposited thickness as well as increasing the deposition hardness [25].

The temperature of the test section bath was then chilled at a rate of 0.5 °C/min from the conditioning temperature to the desired target value, and held at this temperature for a predetermined ageing time.

The precipitation process was commenced as soon as oil temperature near the wall was below the WAT. Wax then started to deposit on the pipeline's inner wall reducing the inner pipe diameter which resulted in an increase in the differential pressure across the

test section loop. The differential pressure was measured and plotted against temperature.

The deviation point from the straight line in a plot of differential pressure versus temperature sweep was known as dynamic WAT, as shown in Figure 3-14 [23].

The calculated dynamic WAT was observed as expected, to be in higher value in lower loop diameter. Since a certain amount of wax is required to reduce the effective diameter.

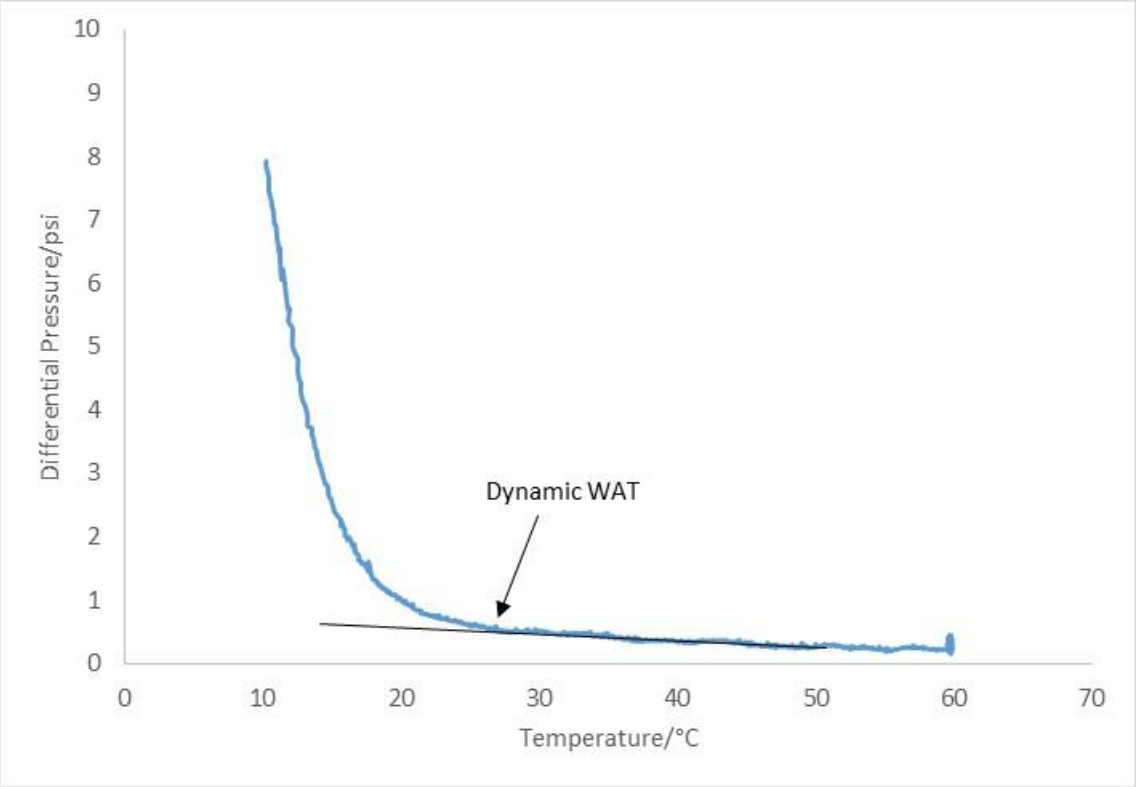

Figure 3-14. plot shows differential pressure versus temperature to measure dynamic WAT obtained by flowloop

As the deposit grows in thickness, differential temperature over the test pipeline was also expected to reduce due to the paraffin's thermal insulation property. However, the accuracy of the thermal couple was observed to interfere greatly with the oil flow; hence, they were only used to compromise flow consistency in this work as described below.

The wax thickness present in the pipe wall was then calculated by Hagen-Poiseuille equation, using the differential pressure which was monitored by transducers installed at the inlet and outlet of the test section, Equation 3-6. This equation defined for laminar flow of a Newtonian fluid through a cylindrical tube[26, 27]:

$\Delta P = \frac{8\mu LQ}{\pi r^4}$ Poiseuille's equation……Equation 3-6

Equation 3-6 rearranged to calculate the wax thickness obtained at a constant flow rate, Equation 3-7:

$$wax\ thickness = r - \sqrt[4]{\frac{8\mu LQ}{\pi \Delta P}} \quad \text{Equation 3-7}$$

Where

μ: Fluid viscosity, Pa.s

L: Length of cylindrical tube, cm

Q: Flow rate, cm^3/sec

r: Inner radius of the cylindrical tube, cm

ΔP: Pressure drop across the cylindrical tube, pascal

Having a constant flow rate is critical to measure the wax thickness. A flow meter is recommended to be used in flow loop to assure a constant flow is injected through the pipes. However, in this setup there no flow meter was used; hence the inlet temperature of test section was used as a sign of flow stability. The waxy oil sample entered the test section at a higher temperature than the cooling bath temperature, so then any interruption in flow caused reduction of the inlet temperature. As shown in Figure 3-15, the inlet temperature was smooth and almost flat representing a constant flow without any interruptions. On the other hand, Figure 3-16 shows frequent sudden reductions in the inlet temperature indicating inconsistent and interrupted flow due to blockage in pipes and/or HPLC check valve, even though, HPLC showed a constant flow. Whenever this was the case, the result was ignored and test repeated with another fresh sample.

Another parameter in Hagen-Poiseuille equation which is often associated with uncertainty was the viscosity of the oil. The fluid viscosity is determined for Newtonian fluid while the precipitated wax crystals caused non-Newtonian behaviour; hence the thickness of wax grew in the non-Newtonian region. The main approach to estimate viscosity was using the rheometer at the same shear rate and temperature applied in the flow loop. However, the discrepancy of measured viscosity compared to flow loop underestimated the wax thickness. It might be due to the fact that high residence time and variation of shear across the flow loop, changed the structure of complex test fluids where the oil almost has pseudo-plastic and shear thinning behaviour, hence viscosity is expected to be higher in flowloop.

In this work, using rearranged Hagen-Poiseuille method, Equation 3-8, with the parameters at the beginning of ageing time as shown in Figure 3-15, to measure viscosity which gave a higher to that measured with the rheometer. It was assumed that

no deposition had occurred at this point, hence the effective radius was not reduced. It was also assumed that viscosity remained during the remainder of the test. These data were not used for modelling prediction and only used for pure comparative purposes.

$$\mu = \frac{\pi r^4 \Delta P}{8LQ}$$ .....Equation 3-8

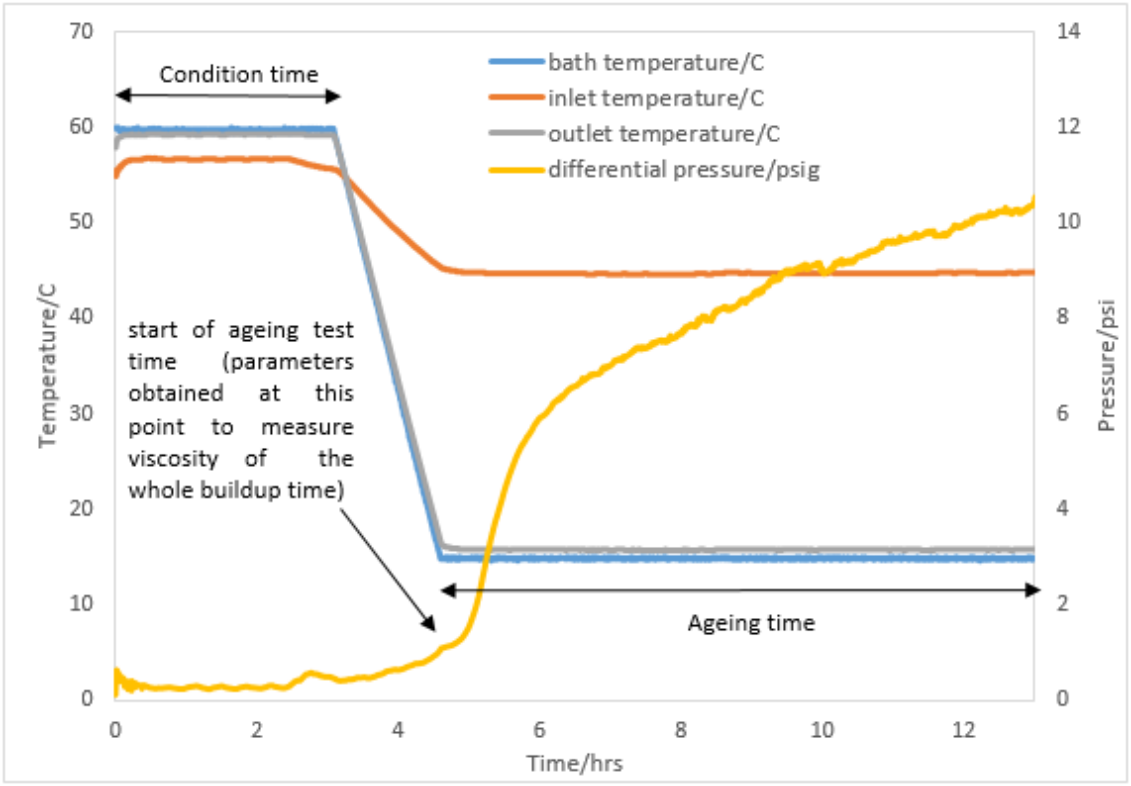

Figure 3-15. Plot shows a consistent flow fed the test loop, acceptable result

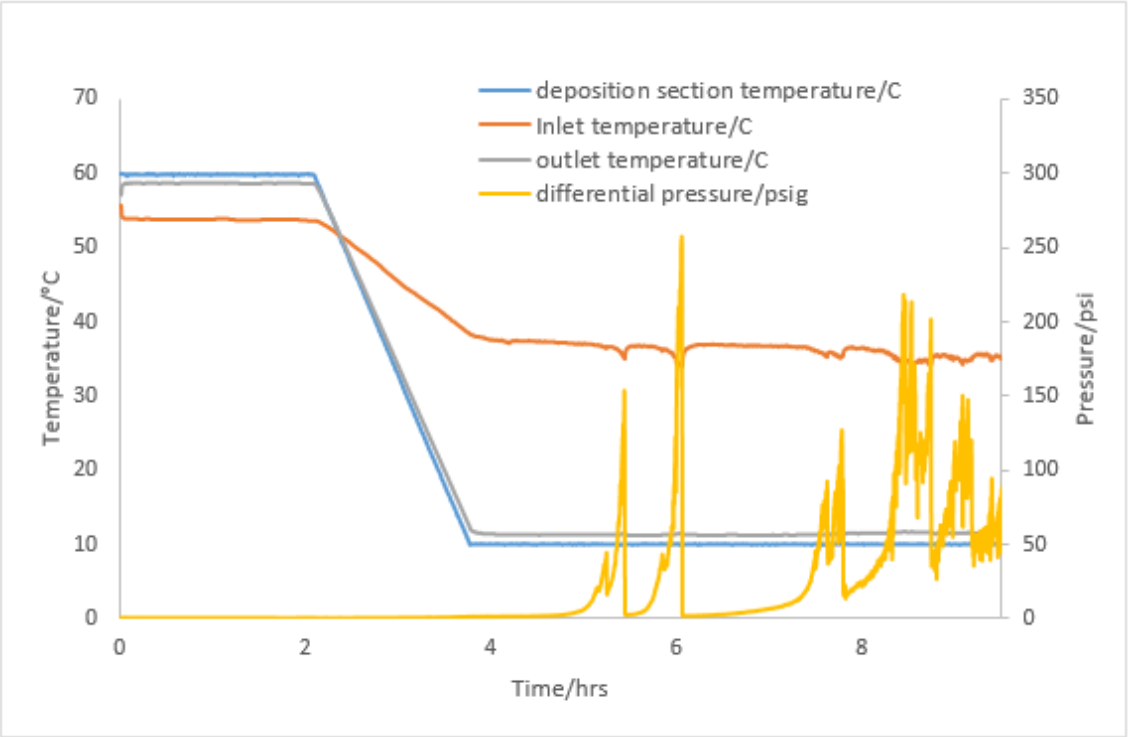

Figure 3-16. Plot shows an inconsistent flow fed the test loop, hence ignored the result

3.3.5 Near Infra-Red(NIR) spectroscopy

NIR spectroscopy is a fast and simple analytical technique to determine and monitor the change in the concentration of chemical components based on a change in the absorption in some specific regions where specific functional groups such as C-H, N-H and O-H band absorbs light. The most commonly used bands in NIR spectroscopy for hydrocarbons determination are at 1100-1200 nm, 1300-1500 nm and 1600-1800 nm [corresponding to the carbon-hydrogen (*C-H*) molecular bonds] because NIR absorption by hydrocarbons is caused by their carbon-hydrogen (*C-H)* molecular bonds. Hence, these specific regions can be used for detection of the onset of formation of wax crystals with sizes lower than 55nm [27, 28].

3.3.5.1 NIR setup

Figure 3-17 illustrates a schematic of the experimental apparatus. A broadband, 20 W tungsten-halogen light source (HL-2000-FHSA, Ocean Optics) was guided to an NIR spectrometer (Arcoptix) via a cuvette containing the test sample using fibre optic cables. The cuvette had a path length of 2 mm and internal volume of 700 µL, which was mounted in a thermal jacket that was temperature controlled by circulating fluid from a circulating water bath (Grant, GP200). A high precision PRT probe was placed inside

the cell. A Prema 3040 precision thermometer was employed to calibrate the temperature probe. Uncertainty was estimated to be within ± 0.1°C for the temperature probe. The NIR spectrometer could cover the spectral range of 900 – 2400 nm with a resolution of 8 cm^{-1}. The absorption of wavelengths across this range was measured relative to a reference spectrum measured with air. The NIR spectrometer had USB connectivity for control and data acquisition. The analysis for each measurement typically took about 50 seconds.

3.3.5.2 Test procedure and analysing data

The NIR technique was used to measure WAT and intensity drop which corresponds to wax precipitation rate. The basis of this work using NIR was for screening inhibitor performance in terms of comparative purposes, hence reference measurement with air was ignored.

The analysis was performed by first heating the sample to the predetermined conditioning temperature to dissolve wax particles only. This specified conditioning temperature for each fluid sample will be explained in the next chapter. The sample then started to cool down at a rate of 0.5°C/min and the NIR spectra, as well as temperature, were recorded using LabVIEW. Intensity change in 1100nm spectra was plotted versus temperature sweep in this work. Deviation from straight line determined precipitation point of wax particles as shown in Figure 3-18. The standard deviation for WAT measurement using NIR was obtained in ±0.5°C.

In addition, the maximum intensity drop was also considered as a precipitation rate of wax crystals. Higher intensity drop could be translated for lower inhibitor performance.

It was also attempted to measure WDT by heating back the fluid to conditioning temperature. There was not successful in preliminary measurements even by decreasing cooling rate as much as possible. Scattered values near conditioning temperature made it impossible to detect a distinct point at least for the sample used in this work.

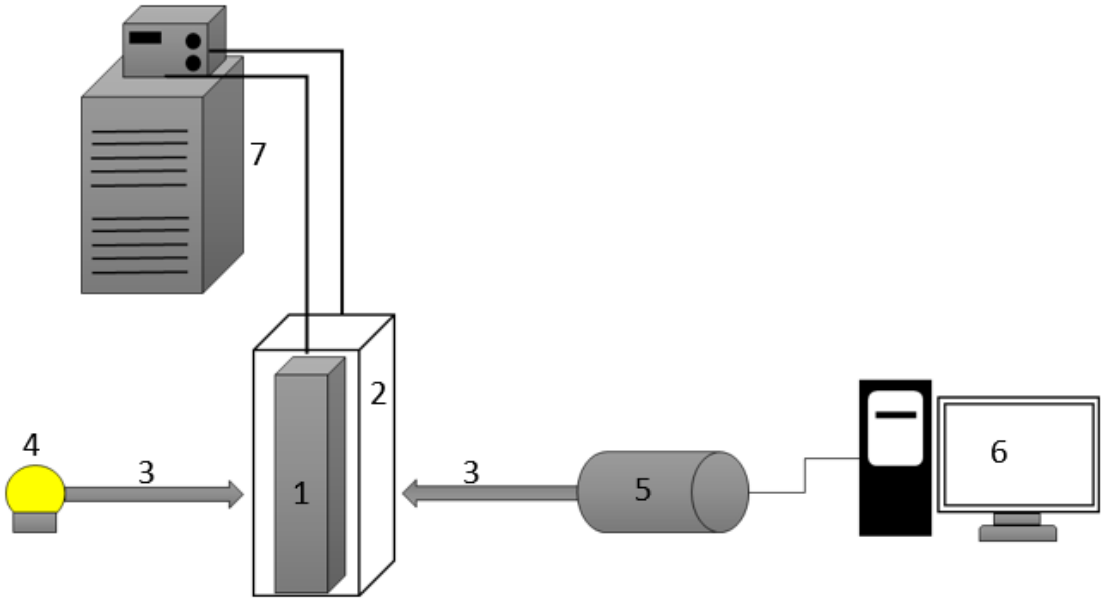

Figure 3-17. The schematic of the NIR apparatus. 1) Cuvette, 2) Thermal jacket, 3) Fibre optic, 4) NIR Light source, 5) Spectrometer, 6) LABVIEW recording, 7) Temperature controlled bath

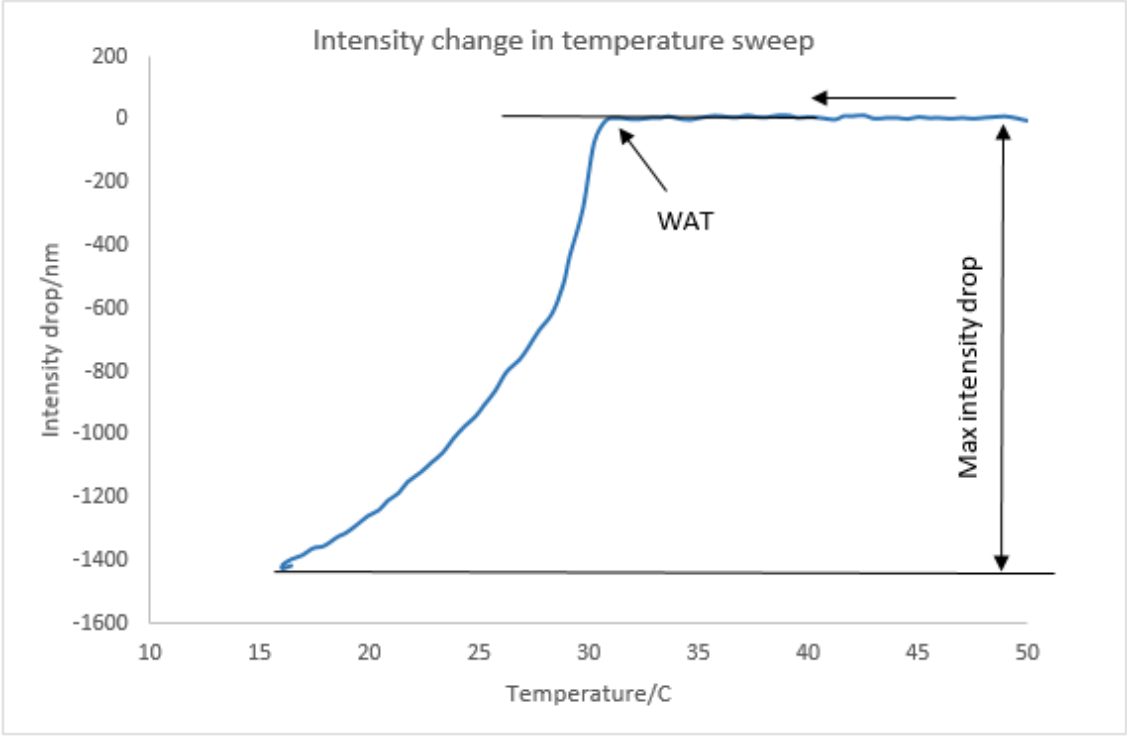

Figure 3-18. The intensity changes in temperature sweep. Measuring WAT and maximum intensity drop

3.4 References

1. Burgass, R.W., *Applications of quartz crystal microbalance technology in petroleum engineering, demonstrated by studies of wax, asphaltenes, hydrates, ice, diesel additives and anti-deposition coatings*. 2015, Heriot-Watt University.
2. Burgass, R.W., et al., *Dew point and bubble point measurement*. 2001, Google Patents.
3. Burgass, R. and B. Tohidi. *Development and validation of small volume multi-tasking flow assurance tool*. in *SPE Asia Pacific Oil and Gas Conference and Exhibition*. 2011. Society of Petroleum Engineers.
4. ASTM D97-16, S.T.M.f.P.P.o.P.P., ASTM International, West Conshohocken, PA, 2016, www.astm.org.
5. ASTM D2500-16a, S.T.M.f.C.P.o.P.P.a.L.F., ASTM International, West Conshohocken, PA, 2016, www.astm.org.
6. Alekseenko, S., et al., *Helical vortices in swirl flow.* Journal of Fluid Mechanics, 1999. **382**: p. 195-243.
7. Triantafillopoulos, N., *Measurement of Fluid Rheology and Interpretation of Rheograms" 2 nd edition. Kaltec Scientific.* Inc. USA, 1998.
8. Funk, J.E. and D.R. Dinger, *Viscosity and Rheology*, in *Predictive Process Control of Crowded Particulate Suspensions*. 1994, Springer. p. 235-252.
9. Mezger, T.G., *The rheology handbook: for users of rotational and oscillatory rheometers*. 2006: Vincentz Network GmbH & Co KG.
10. Barnes, H.A., *A handbook of elementary rheology*. 2000.
11. Rønningsen, H.P., *Rheological behaviour of gelled, waxy North Sea crude oils.* Journal of Petroleum Science and Engineering, 1992. **7**(3): p. 177-213.
12. Mohammed, R., et al., *Dewatering of crude oil emulsions 1. Rheological behaviour of the crude oil—water interface.* Colloids and Surfaces A: Physicochemical and Engineering Aspects, 1993. **80**(2): p. 223-235.
13. Marchesini, F.v.H., et al., *Rheological characterization of waxy crude oils: Sample preparation.* Energy & Fuels, 2012. **26**(5): p. 2566-2577.
14. Roenningsen, H.P., et al., *Wax precipitation from North Sea crude oils: 1. Crystallization and dissolution temperatures, and Newtonian and non-Newtonian flow properties.* Energy & Fuels, 1991. **5**(6): p. 895-908.
15. Venkatesan, R., P. Singh, and H.S. Fogler, *Delineating the pour point and gelation temperature of waxy crude oils.* SPE journal, 2002. **7**(04): p. 349-352.
16. da Silva, J.A.L. and J.A. Coutinho, *Dynamic rheological analysis of the gelation behaviour of waxy crude oils.* Rheologica Acta, 2004. **43**(5): p. 433-441.
17. Kane, M., M. Djabourov, and J.-L. Volle, *Rheology and structure of waxy crude oils in quiescent and under shearing conditions.* Fuel, 2004. **83**(11): p. 1591-1605.
18. Visintin, R.F., et al., *Rheological behavior and structural interpretation of waxy crude oil gels.* Langmuir, 2005. **21**(14): p. 6240-6249.
19. Visintin, R.F., et al., *Structure of waxy crude oil emulsion gels.* Journal of Non-Newtonian Fluid Mechanics, 2008. **149**(1): p. 34-39.

20. Parthasarathi, P. and A.K. Mehrotra, *Solids deposition from multicomponent wax-solvent mixtures in a benchscale flow-loop apparatus with heat transfer.* Energy & fuels, 2005. **19**(4): p. 1387-1398.

21. Creek, J., et al., *Wax deposition in single phase flow.* Fluid Phase Equilibria, 1999. **158**: p. 801-811.

22. Hoffmann, R. and L. Amundsen, *Single-phase wax deposition experiments.* Energy & Fuels, 2009. **24**(2): p. 1069-1080.

23. IJeomah, C.E., et al., *Measurement of wax appearance temperature under simulated pipeline (dynamic) conditions.* Energy & Fuels, 2008. **22**(4): p. 2437-2442.

24. Bidmus, H.O. and A.K. Mehrotra, *Solids deposition during "cold flow" of wax−solvent mixtures in a flow-loop apparatus with heat transfer.* Energy & Fuels, 2009. **23**(6): p. 3184-3194.

25. Singh, P., et al., *Formation and aging of incipient thin film wax-oil gels.* AIChE Journal, 2000. **46**(5): p. 1059-1074.

26. Leontaritis, K.J. and J.D. Leontaritis. *Cloud point and wax deposition measurement techniques*. in *International Symposium on Oilfield Chemistry*. 2003. Society of Petroleum Engineers.

27. Chin, W.C., *Computational Rheology for Pipeline and Annular Flow: Non-Newtonian Flow Modeling for Drilling and Production, and Flow Assurance Methods in Subsea Pipeline Design*. 2001: Gulf Professional Publishing.

28. Paso, K., H. Kallevik, and J. Sjoblom, *Measurement of wax appearance temperature using near-infrared (NIR) scattering.* Energy & Fuels, 2009. **23**(10): p. 4988-4994.

Chapter 4: Investigation of the required initial experimental conditions for the wax studies

4.1 Introduction

Most crude oil samples are understood to have been exposed to temperatures below its WAT during transportation to the laboratory. Therefore, before undertaking any wax studies it should be noted that part of high-molecular-weight wax particles, which depend on temperature conditions, remain suspended as crystals in the oil, which is referred to as thermal memory of wax. This phenomenon is known to change the wax content of the bulk oil in the given temperature range; as a result, some test results such as WAT, pour point and rheological behaviour could be influenced. Therefore, it is required to erase any previous history that might exist in such samples by applying appropriate heat to the sample to reach a wax-free homogeneous condition and consequently to eliminate the history effect on the wax under studies [1].

In wax studies, a sample is usually exposed to a thermal cycle which starts with a conditioning temperature before reaching a so-called test temperature. The test temperature in the laboratory is usually in line with the expected temperature on the sea floor in order to mimic real field conditions. However, the choice of the starting conditioning temperature is quite elaborate. According to ASTM standard D2500 for WAT measurements, the recommended conditioning temperature is at least 14°C above the expected WAT point. However, as previously mentioned, to eliminate the effect of the thermal memory, it is required to take the optimum starting temperature up to a temperature that is high enough to completely dissolve the wax, before cooling commences. This will in turn yield the highest possible WAT, pour point and flow properties, and, as a result, correspond to the worst possible conditions in the real field [1, 2].

On the other hand, to prevent the loss of light components especially for crude oils with a high gas to oil ratio, the initial conditioning temperature should not be heated to temperatures significantly higher than those of actual industrial processes. Furthermore, when the oil is reheated to a higher starting temperature, asphaltenes, together with resins and heavy oil components will dissolve or disassociate with the wax particles. These are mainly polar substances of oil and known to act as a natural pour point depressants (PPD) which can surround wax crystals and modify their morphology and

surface characteristics during cooling in a complex fashion. It is highly important then to choose the value high enough to dissolve the wax particles, but not too high to cause interactions between resin and asphaltenes and wax crystals [1, 3].

As the first step of the wax study in this work, a series of experiments using rheometer were conducted on the oil samples to identify the lowest possible initial conditioning temperature before further wax investigation which will be described in the following chapters. Furthermore, the effect of the cooling rate on wax properties was studied using the rheometer. In addition to that, the coaxial cold finger apparatus was used to perform a series of measurements to study the impact of ageing time and shear rate on a blank oil sample. Also, the effect of differential temperatures on the performance of chemical wax inhibitors was studied using this set-up. Table 4-1 gives an outline of the experimental work in this chapter.

Table 4-1. Outline of the experimental work done in this chapter

Test type	***Sample type***	***Experimental condition***	***Equipment***
Effect of conditioning	*OIL-F*	*(30, 40, 50, 60, 70) (°C)*	***Rheometer (rotation mode+ oscillation mode)***
	OIL-G	*(35, 45, 55, 65, 70, 80) (°C)*	
	OIL-H	*(40, 50, 60, 70, 80) (°C)*	
	OIL-E	*(35, 40, 50, 65) (°C)*	
	OIL-D	*(40, 45, 50, 55, 60) (°C)*	
	OIL-A	*(40, 50, 60, 70, 80) (°C)*	
	OIL-C	*(30, 40, 50, 60, 70) (°C)*	
	OIL-C, INH-C, 350ppm	*(30, 40, 50, 60, 70) (°C)*	
	OIL-C, INH-F, 400ppm	*(30, 40, 50, 60) (°C)*	
	OIL-C, INH-B, 200ppm	*(30, 40, 50, 60,70) (°C)*	
	OIL-C, INH-E, 400ppm	*(30, 40, 50, 60, 70) (°C)*	
	OIL-B	*(30, 40, 50, 60, 70) (°C)*	
	OIL-B, INH-C, 350ppm	*(40, 50, 60, 70) (°C)*	
Effect of cooling rate	*OIL-E*	*(0.2, 0.5, 0.75, 1) (°C/min)*	***Rheometer (rotation mode)***
	OIL-H	*(0.2, 0.5, 0.75, 1) (°C/min)*	
	OIL-G	*(0.2, 0.5, 0.75, 1) (°C/min)*	
	OIL_F	*(0.2, 0.5, 0.75, 1) (°C/min)*	
Effect of ageing	*OIL-E*	*(24, 42.5, 67, 143.5, 257) hrs*	***Coaxial***
Effect of shear rate	*OIL-E*	*(50, 100, 200, 250, 350, 500) (s^{-1})*	
Effect of ΔT	*OIL-A*	*(7, 15, 19, 23, 30) (°C)*	
	OIL-A, INH-C,350ppm	*(15, 19, 23, 30) (°C)*	
	OIL-A, INH-A, 250ppm	*(17, 30) (°C)*	
	OIL-A, INH-D, 100ppm	*(17, 20, 23, 30) (°C)*	
	OIL-A, INH-B, 200ppm	*(15, 30) (°C)*	

4.2 The impact of conditioning temperature on wax study

Table 4-2 and Table 4-3 show the results obtained by rotation and oscillation mode using the rheometer respectively. The cooling rate in both modes was set at a constant

rate of 1 °C/min, the reason to choose this rate is detailed in the cooling rate section. In the rotation mode, shear rate was set at 10 s^{-1} to measure WAT/WDT and viscosity. However, since WDT measurement did not result a reliable data, reheating cycle to determine WDT was only done in limited cases of OIL-E, OIL-F, OIL-G and OIL-H samples. Viscosity measured at the lowest test temperature known as the maximum viscosity was selected as the representative of rheology behaviour under WAT point; because it was the highest possible viscosity which gave clearer discrepancies among each thermal cycle measurements. Frequency and amplitude torque was set at 1.59 Hz and 25 µNm respectively in the oscillation mode to measure pour point of the sample. A temperature sweep was started after 3 minutes conditioning at different starting temperatures in all cases.

Table 4-2. The condition and results of rheometer to measure viscosity, used different fluids in different starting conditioning temperature

Fluid	***Condition T (°C)***	***Destination T (°C)***	***Cooling rate (°C/min)***	***Shear rate (s^{-1})***	***WAT (°C)***	***WDT (°C)***	***Minimum Viscosity (cP)***	***Max Viscosity (cP)***
OIL-F	*30*	*25*	*1*	*10*	*----*	*----*	*4.68*	*5.67*
	40	*25*	*1*	*10*	*----*	*----*	*3.41*	*8.96*
	50	*25*	*1*	*10*	*40.0*	*46.0*	*2.59*	*6.77*
	60	*25*	*1*	*10*	*39.5*	*48.5*	*2.42*	*6.84*
	70	*25*	*1*	*10*	*45.0*	*54.0*	*1.82*	*6.93*
OIL-G	*35*	*20*	*1*	*10*	*28.5*	*----*	*10.40*	*78.90*
	45	*20*	*1*	*10*	*30.0*	*38.5*	*6.79*	*99.00*
	55	*20*	*1*	*10*	*32.3*	*40.0*	*5.42*	*129.00*
	60	*20*	*1*	*10*	*34.0*	*45.0*	*4.90*	*151.00*
	65	*20*	*1*	*10*	*33.5*	*42.5*	*4.47*	*69.10*
	70	*20*	*1*	*10*	*37.0*	*47.0*	*4.02*	*28.20*
	80	*20*	*1*	*10*	*39.0*	*49.0*	*3.32*	*26.50*
OIL-H	*40*	*20*	*1*	*10*	*36.5*	*----*	*6.73*	*103.00*
	50	*20*	*1*	*10*	*39.0*	*47.0*	*4.59*	*118.00*
	60	*20*	*1*	*10*	*39.8*	*49.5*	*3.66*	*141.00*
	70	*20*	*1*	*10*	*40.6*	*54.0*	*2.98*	*57.80*
	80	*20*	*1*	*10*	*41.5*	*56.0*	*2.86*	*56.00*
OIL-E	*35*	*5*	*1*	*10*	*18.0*	*29.0*	*20.10*	*424.00*
	40	*5*	*1*	*10*	*19.0*	*30.0*	*17.20*	*654.00*
	50	*5*	*1*	*10*	*19.0*	*28.0*	*11.80*	*213.00*
	65	*5*	*1*	*10*	*21.0*	*29.0*	*7.95*	*197.00*
OIL-D	*40*	*15*	*1*	*10*	*34.3*	*----*	*3.05*	*22.00*
	45	*15*	*1*	*10*	*32.4*	*----*	*2.54*	*51.00*
	50	*15*	*1*	*10*	*32.7*	*----*	*2.00*	*81.70*
	55	*15*	*1*	*10*	*32.5*	*----*	*1.91*	*23.60*
	60	*15*	*1*	*10*	*32.5*	*----*	*1.96*	*12.70*
OIL-A	*50*	*15*	*1*	*10*	*28.7*	*----*	*2.25*	*17.10*
	60	*15*	*1*	*10*	*34.3*	*----*	*1.94*	*17.90*
	70	*15*	*1*	*10*	*34.0*	*----*	*1.70*	*15.20*
	80	*15*	*1*	*10*	*38.7*	*----*	*1.44*	*9.02*
OIL-C	*30*	*5*	*1*	*10*	*22.6*	*----*	*3.64*	*108.00*
	40	*5*	*1*	*10*	*26.6*	*----*	*2.84*	*125.00*

Continued Table 4-2

Fluid	Condition T (°C)	Destination T (°C)	Cooling rate (°C/min)	Shear rate (s^{-1})	WAT (°C)	WDT (°C)	Minimum Viscosity (cP)	Max Viscosity (cP)
	50	5	1	10	29.1	----	2.42	56.20
	60	5	1	10	29.6	----	1.89	51.50
	70	5	1	10	34.4	----	2.25	32.80
OIL-C, INH-C, 350ppm	30	5	1	10	23.9	----	9.17	38.60
	40	5	1	10	26.9	----	3.97	17.60
	50	5	1	10	22.5	----	2.28	12.30
	60	5	1	10	22.2	----	2.13	13.20
	60	5	1	10	21.9	----	2.45	14.50
	70	5	1	10	23.0	----	1.95	15.20
OIL-C, INH-F, 400ppm	30	5	1	10	26.6	----	6.54	22.50
	40	5	1	10	26.1	----	2.60	16.60
	50	5	1	10	27.4	----	2.43	15.80
	60	5	1	10	27.4	----	1.74	14.00
OIL-C, INH-B, 200ppm	30	5	1	10	23.1	----	5.30	123.00
	40	5	1	10	27.1	----	3.45	94.90
	50	5	1	10	28.6	----	2.36	48.60
	60	5	1	10	30.7	----	2.12	51.10
OIL-C, INH-E, 400ppm	30	5	1	10	23.6	----	5.99	85.50
	40	5	1	10	29.6	----	4.48	42.50
	50	5	1	10	21.2	----	2.43	16.20
	60	5	1	10	23.7	----	1.93	15.00
OIL-B	40	10	1	10	27.6	----	1.87	163.00
	50	10	1	10	30.9	----	1.89	187.00
	60	10	1	10	32.7	----	1.87	124.00
	70	10	1	10	33.9	----	1.62	110.00
OIL-B, INH-C, 350ppm	40	10	1	10	25.0	----	3.60	41.50
	50	10	1	10	22.7	----	1.67	15.40
	60	10	1	10	22.4	----	1.94	7.60
	70	10	1	10	26.2	----	1.36	24.40

Table 4-3. The condition and results of rheometer to measure pour point, used different fluids in different starting conditioning temperature

fluid	Condition T (°C)	Destination T (°C)	Cooling rate (°C/min)	Angular frequency (rad/s)	Frequency (Hz)	Amplitude, Torque (μNm)	pour point (°C)
OIL-F	30	-20	1	10	1.59	25	-15.10
	40	-20	1	10	1.59	25	-15.30
	50	-20	1	10	1.59	25	-14.30
	60	-20	1	10	1.59	25	-9.30
	70	-20	1	10	1.59	25	-6.96
OIL-G	35	0	1	10	1.59	25	13.20
	45	0	1	10	1.59	25	19.70
	55	0	1	10	1.59	25	22.70
	65	0	1	10	1.59	25	18.00
	70	0	1	10	1.59	25	-2.00
	80	0	1	10	1.59	25	-8.00
OIL-H	40	0	1	10	1.59	25	14.40
	50	0	1	10	1.59	25	14.40
	60	0	1	10	1.59	25	24.70
	70	0	1	10	1.59	25	9.00

Continued Table 4-3

fluid	*Condition T (°C)*	*Destination T (°C)*	*Cooling rate (°C/min)*	*Angular frequency (rad/s)*	*Frequency (Hz)*	*Amplitude, Torque (μNm)*	*pour point (°C)*
	80	*0*	*1*	*10*	*1.59*	*25*	*7.50*
OIL-E	*35*	*-10*	*1*	*10*	*1.59*	*25*	*4.54*
	40	*-10*	*1*	*10*	*1.59*	*25*	*6.37*
	50	*-10*	*1*	*10*	*1.59*	*25*	*-6.65*
	65	*-10*	*1*	*10*	*1.59*	*25*	*-15.00*
OIL-A	*40*	*-20*	*1*	*10*	*1.59*	*25*	*-14.60*
	40	*-20*	*1*	*10*	*1.59*	*25*	*-14.60*
	50	*-20*	*1*	*10*	*1.59*	*25*	*-15.90*
	60	*-20*	*1*	*10*	*1.59*	*25*	*-12.90*
	70	*-20*	*1*	*10*	*1.59*	*25*	*-6.30*
	80	*-20*	*1*	*10*	*1.59*	*25*	*-8.13*
OIL-C	*30*	*-20*	*1*	*10*	*1.59*	*25*	*-6.95*
	40	*-20*	*1*	*10*	*1.59*	*25*	*-6.28*
	50	*-20*	*1*	*10*	*1.59*	*25*	*-5.29*
	60	*-20*	*1*	*10*	*1.59*	*25*	*-3.63*
	70	*-20*	*1*	*10*	*1.59*	*25*	*-14.30*
OIL-C, INH-C, 350ppm	*30*	*-20*	*1*	*10*	*1.59*	*25*	*-10.30*
	40	*-20*	*1*	*10*	*1.59*	*25*	*-12.40*
	50	*-20*	*1*	*10*	*1.59*	*25*	*-23.00*
	60	*-20*	*1*	*10*	*1.59*	*25*	*-23.00*
OIL-C, INH-B, 200ppm	*30*	*-20*	*1*	*10*	*1.59*	*25*	*-6.11*
	40	*-20*	*1*	*10*	*1.59*	*25*	*-4.62*
	50	*-20*	*1*	*10*	*1.59*	*25*	*-5.29*
	60	*-20*	*1*	*10*	*1.59*	*25*	*-4.29*
	70	*-20*	*1*	*10*	*1.59*	*25*	*-14.30*
OIL-C, INH-E, 400ppm	*30*	*-20*	*1*	*10*	*1.59*	*25*	*-5.27*
	40	*-20*	*1*	*10*	*1.59*	*25*	*-7.79*
	50	*-20*	*1*	*10*	*1.59*	*25*	*-23.00*
	60	*-20*	*1*	*10*	*1.59*	*25*	*-15.80*
	70	*-20*	*1*	*10*	*1.59*	*25*	*-23.00*
OIL-C, INH-F, 400ppm	*30*	*-20*	*1*	*10*	*1.59*	*25*	*-19.50*
	40	*-20*	*1*	*10*	*1.59*	*25*	*-23.00*
	50	*-20*	*1*	*10*	*1.59*	*25*	*-23.00*
	60	*-20*	*1*	*10*	*1.59*	*25*	*-23.00*
OIL-B	*30*	*-10*	*1*	*10*	*1.59*	*25*	*3.21*
	40	*-10*	*1*	*10*	*1.59*	*25*	*5.54*
	50	*-10*	*1*	*10*	*1.59*	*25*	*3.19*
	60	*-10*	*1*	*10*	*1.59*	*25*	*14.20*
	70	*-10*	*1*	*10*	*1.59*	*25*	*15.40*
OIL-B, INH-C, 350ppm	*40*	*-20*	*1*	*10*	*1.59*	*25*	*1.22*
	50	*-20*	*1*	*10*	*1.59*	*25*	*-21.00*
	60	*-20*	*1*	*10*	*1.59*	*25*	*-17.90*
	70	*-20*	*1*	*10*	*1.59*	*25*	*-16.60*

For clarity, the maximum viscosity and pour point with different starting conditions are plotted in Figure 4-1 to Figure 4-9.

In all of these figures the horizontal axis shows the starting conditioning temperature, the left vertical axis is related to the maximum viscosity in centipoise and the right

vertical axis represents the pour point at each starting condition. The appropriate starting condition region for the wax study is demonstrated with orange arrows in all of the plots. It must be noted that the WAT referred in plots are measured with QCM setup. The estimated single optimum starting temperature is identified from each graph however to get a more accurate optimum starting temperature it is required to measure more points close to the estimated point. According to Table 4-2 which was ranked top to bottom based on increasing starting temperature in each individual sample, it was observed as expected that increasing the conditioning temperature led to increasing both WAT and WDT due to dissolution of more heavy components, so then they coming out or dissolve back in the bulk oil at higher temperatures during thermal cycles causing higher WAT/WDT.

Furthermore, it seemed increasing the starting temperature to the region where interact the asphaltene/resin, only disturbed the wax crystalize interlocking network resulting a lower viscosity/pour point and had no significant impact on the reduction/inhibition the precipitation of wax. Both pour point and viscosity depend upon the morphology of wax crystallization network, increased by associate more wax particles until the presence of resins and asphaltene in the crude oil interact and reduce them. As a result, the optimum conditioning temperature was chosen while maximum viscosity started to decrease in addition with an opposite trend or a sharp change in pour point. Pour points in OIL-A, OIL-E, OIL-H and OIL-G samples start decreasing at the same time as maximum viscosity reduces. As against, pour point started to increase in OIL-B, OIL-C and OIL-F samples. Overall, it appears that maximum viscosity was a more reliable indicator of the optimum conditioning temperature. An explanation of the plots is presented below.

In the case of OIL-E sample, Figure 4-1, the maximum viscosity increased up to 40°C then decreased to 230cP at 50°C, and no other points were measured between them. Similarly, pour point slightly increased up to 40°C (+2°C) then decreased at 50°C (-13°C), which could be attributed to the presence of natural PPD. As a result, the highest possible crystallization temperature without interfering natural PPD for OIL-E sample was in the region of 40°C to 50°C corresponding to WAT+27°C to WAT+37°C.

The optimum conditioning temperature for OIL-H, Figure 4-2, was in the region of WAT+25°C to WAT+35°C where both pour point and maximum viscosity decreased about 16°C and 83cP respectively.

A high optimum conditioning temperature was observed in the case of OIL-G, Figure 4-3. This temperature was found to be in the region of WAT+34°C to WAT+39°C. Maximum viscosity and pour point decreased in this area in the amount of 82cP and 3°C respectively.

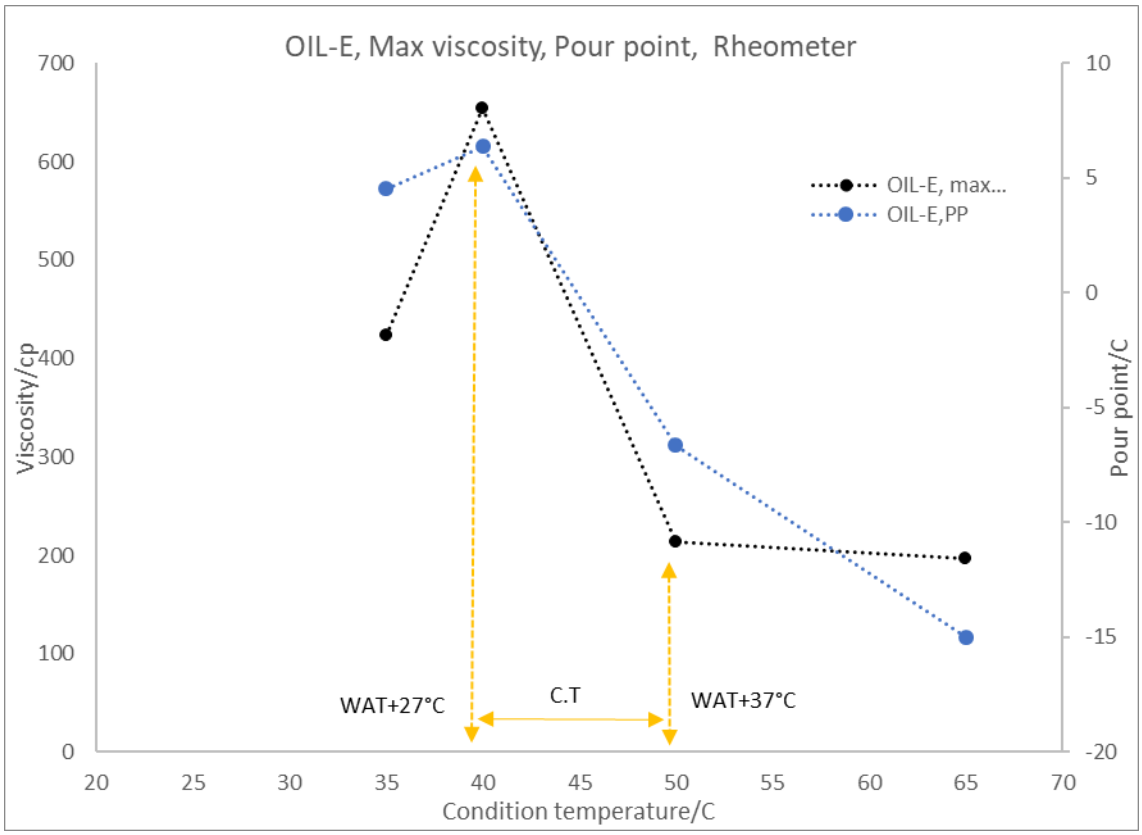

Figure 4-1. Maximum viscosity and pour point variation with different conditioning temperature measured with rheometer on OIL-E sample. Lines between points are only for visual clarification.

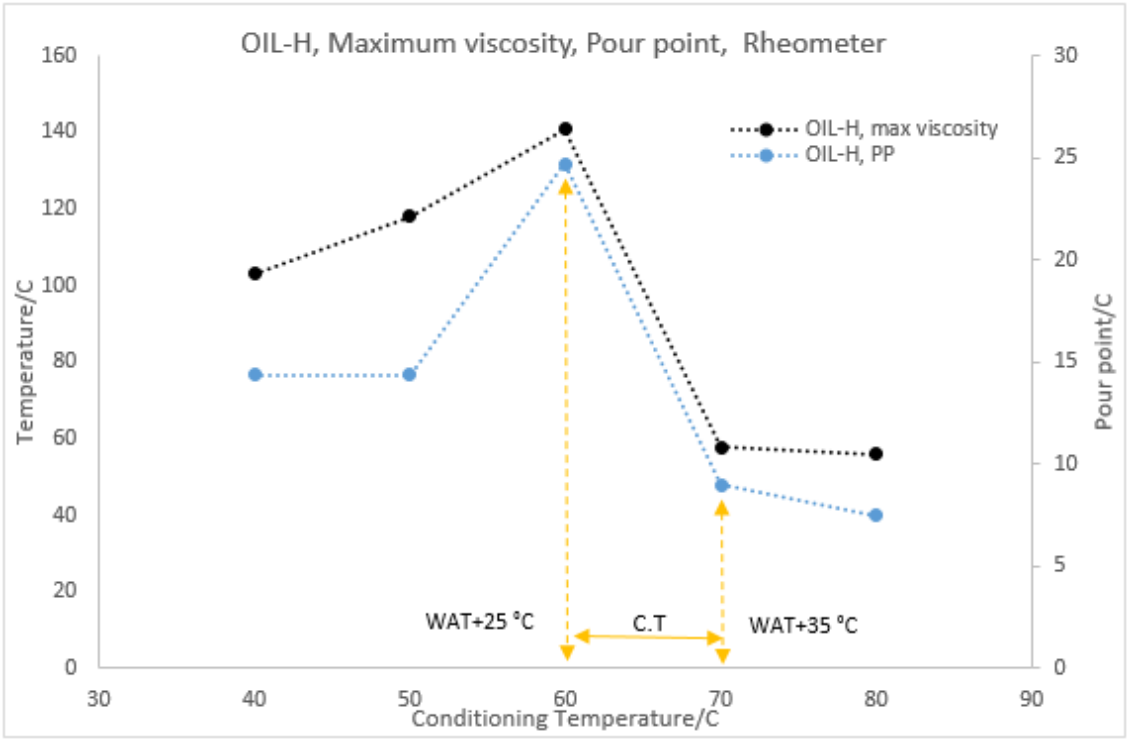

Figure 4-2. Maximum viscosity and pour point variation with different conditioning temperature measured with rheometer on OIL-H sample. Lines between points are only for visual clarification.

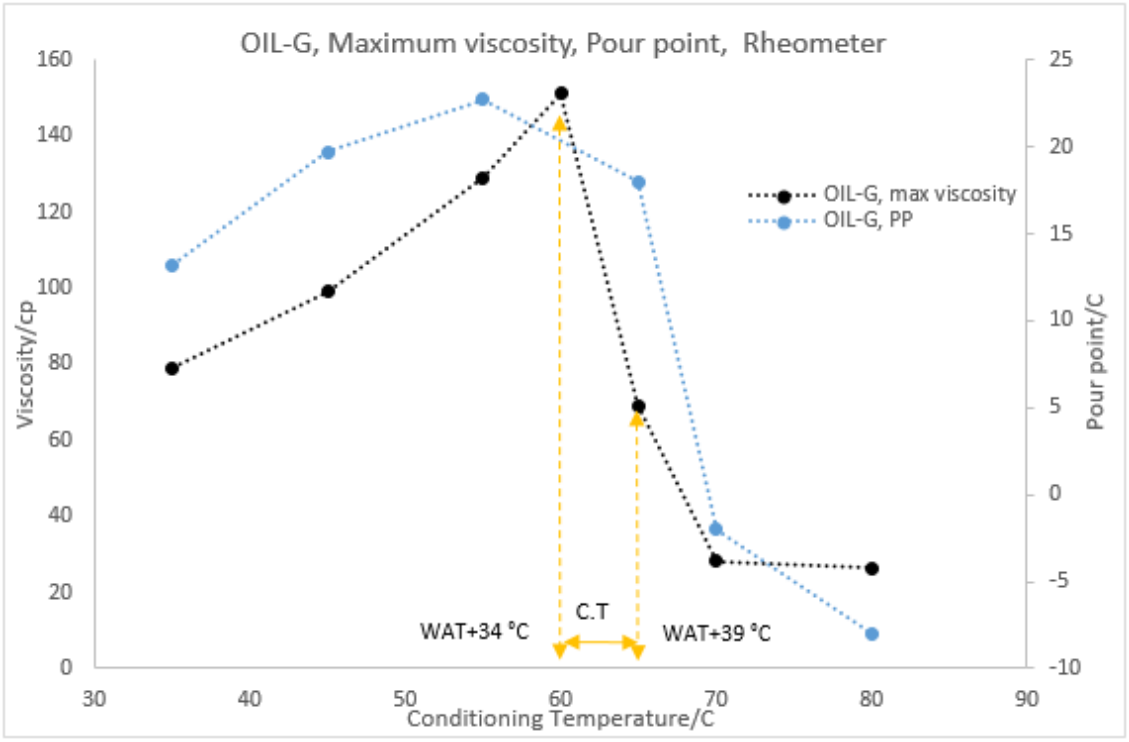

Figure 4-3. Maximum viscosity and pour point variation with different conditioning temperature measured with rheometer on OIL-G sample. Lines between points are only for visual clarification.

By analysing Figure 4-4 and Figure 4-5, it can be observed that OIL-A and OIL-F samples, had very small changes in maximum viscosity and pour point compared to other samples under study. This could be attributed to the fact that the amount of heavy components, as well as dissolved natural PPD, might not be sufficient to bring about a significant change in the wax interlocking network. Hence, it would be complex to select the best conditioning region for these samples.

A small reduction in both pour point(-2°C) and viscosity(-6cP) in OIL-A sample, Figure 4-4 seems to be an appropriate choice for the starting temperature in the region of WAT+37°C to WAT+47°C represented to temperatures between 70°C to 80°C. However, this range of temperature seems a bit high for such a light oil and to avoid evaporation in some devices, some tests in this thesis started at 60°C which did not have any significant effect on the results.

In Figure 4-5, no reduction in pour point for OIL-F sample was observed which means most probably there was not enough natural PPD present in this sample to have any impact. Maximum viscosity was steady after 50°C which confirms the lack of heavy components in this region, though pour point was still increasing which could be due to evaporation light components heating over 50°C. It seems the optimum conditioning temperature was between WAT+12°C to WAT+22°C.

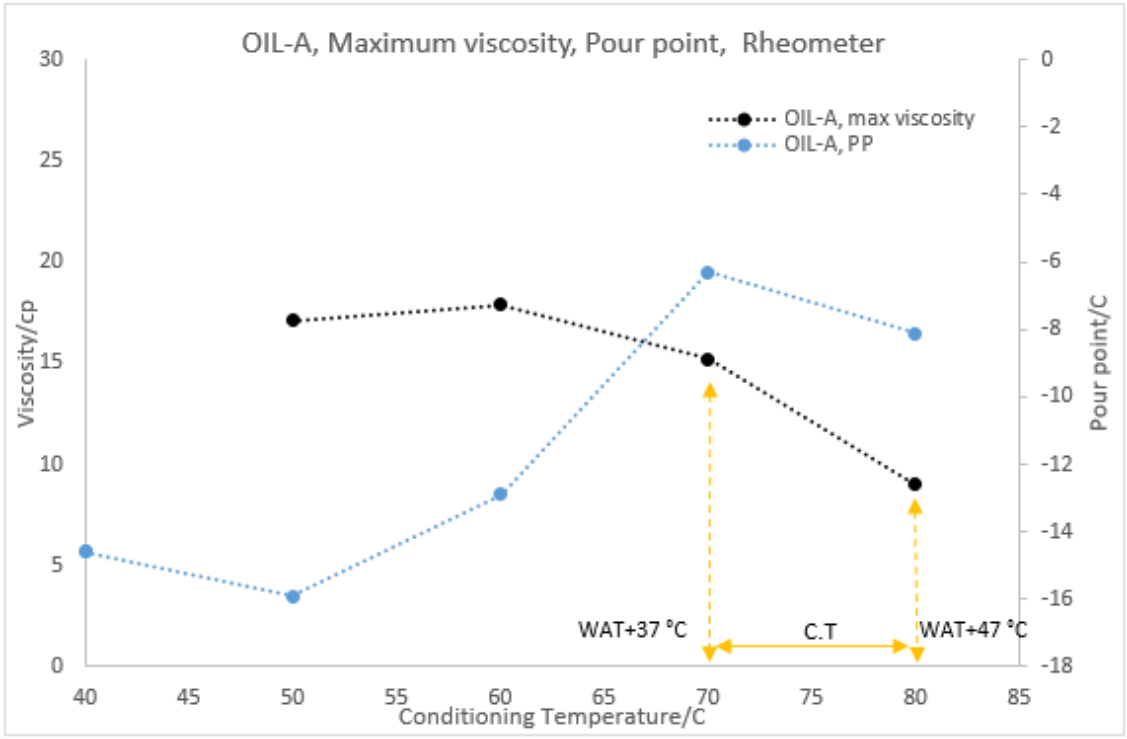

Figure 4-4. Maximum viscosity and pour point variation with different conditioning temperature measured with rheometer on OIL-A sample. Lines between points are only for visual clarification.

Ideally, a paraffin inhibitor requires to be injected at a temperature higher than WAT point to be able to cover all wax particles and prevent them coming out of solution. In order to confirm the current procedure for determining a suitable conditioning temperature, a series of measurements with two different samples OIL-B and OIL-C dosed with different inhibitors were launched. Results are plotted in Figure 4-6 to Figure 4-9.

For both samples the optimum region was chosen while maximum viscosity had a sharp reduction, though pour point increased especially in OIL-B sample with an elevation of 11°C. This region for OIL-B seems to be between WAT+22°C and WAT+32°C with a 63cP reduction in maximum viscosity.

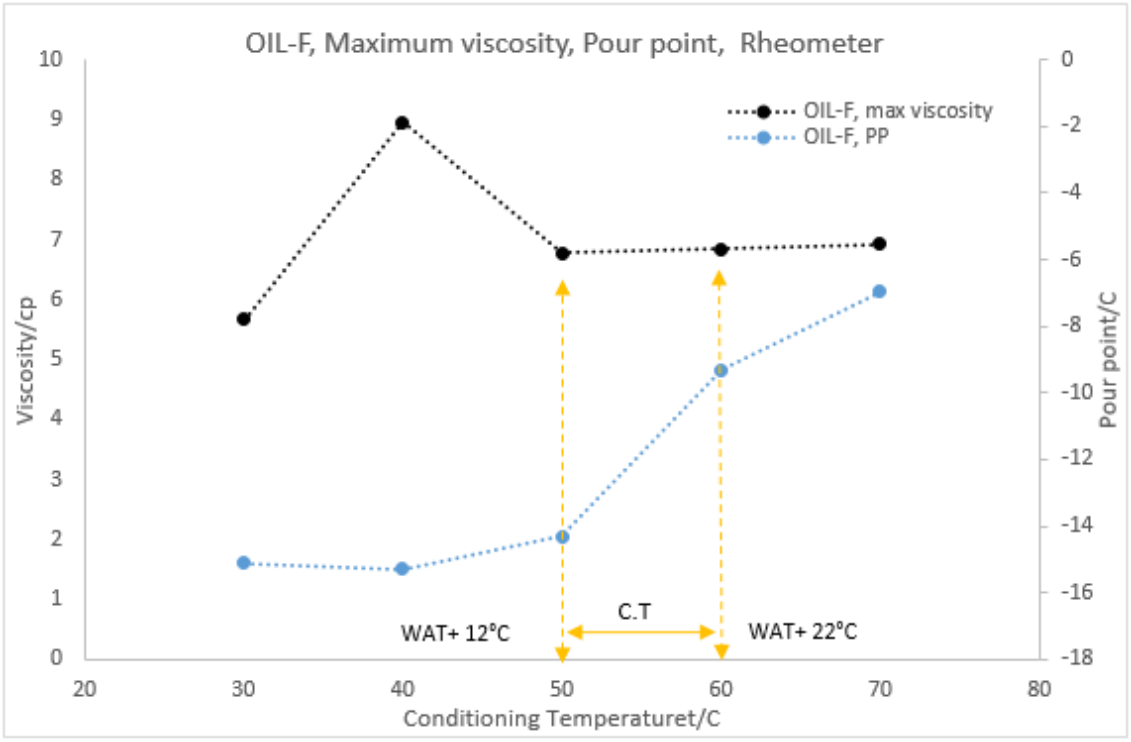

Figure 4-5. Maximum viscosity and pour point variation with different conditioning temperature measured with rheometer on OIL-F sample. Lines between points are only for visual clarification.

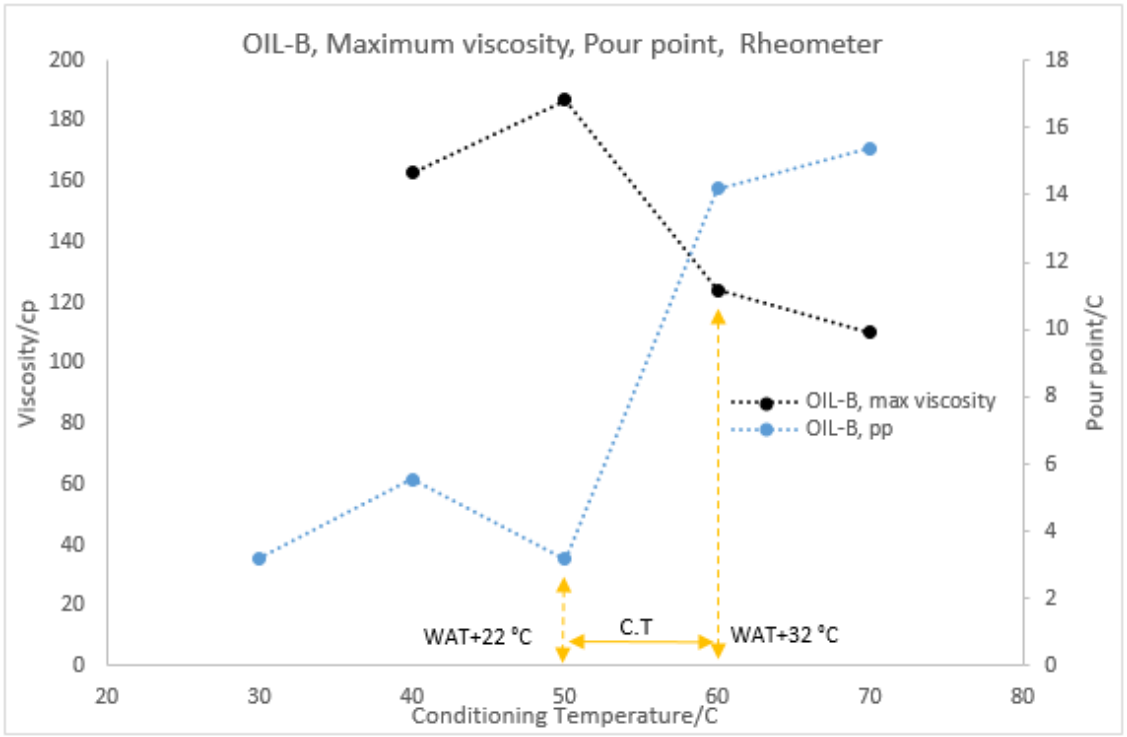

Figure 4-6. Maximum viscosity and pour point variation with different conditioning temperature measured with rheometer on OIL-B sample. Lines between points are only for visual clarification.

Figure 4-7 represents the results obtained with OIL-B dosed with 350ppm inhibitor INH-C. The lowest pour point and viscosity was obtained in a region similar with an optimum conditioning temperature.

The obtained condition for OIL-C was slightly lower than ASTM recommended temperature, between WAT+13°C to WAT+23°C where viscosity had a sharp decreasing of 59cP, Figure 4-8, while pour point had a slight increasing of about 1°C, Figure 4-9. The pour point was also observed to decline further with a starting temperature of 60°C. OIL-C sample was dosed with 200, 400, 350 and 400 ppm of inhibitors, INH-B, INH-E, INH-C and INH-F respectively.

The results obtained from these two samples dosed with inhibitors highlighted the importance of choosing maximum viscosity reduction as a basis for selecting the lowest possible temperature to cover all paraffin in the bulk oil.

It also showed that Injection of the paraffin inhibitor into the well should be deliberately controlled to be injected at the ideal temperature to gain an optimum performance.

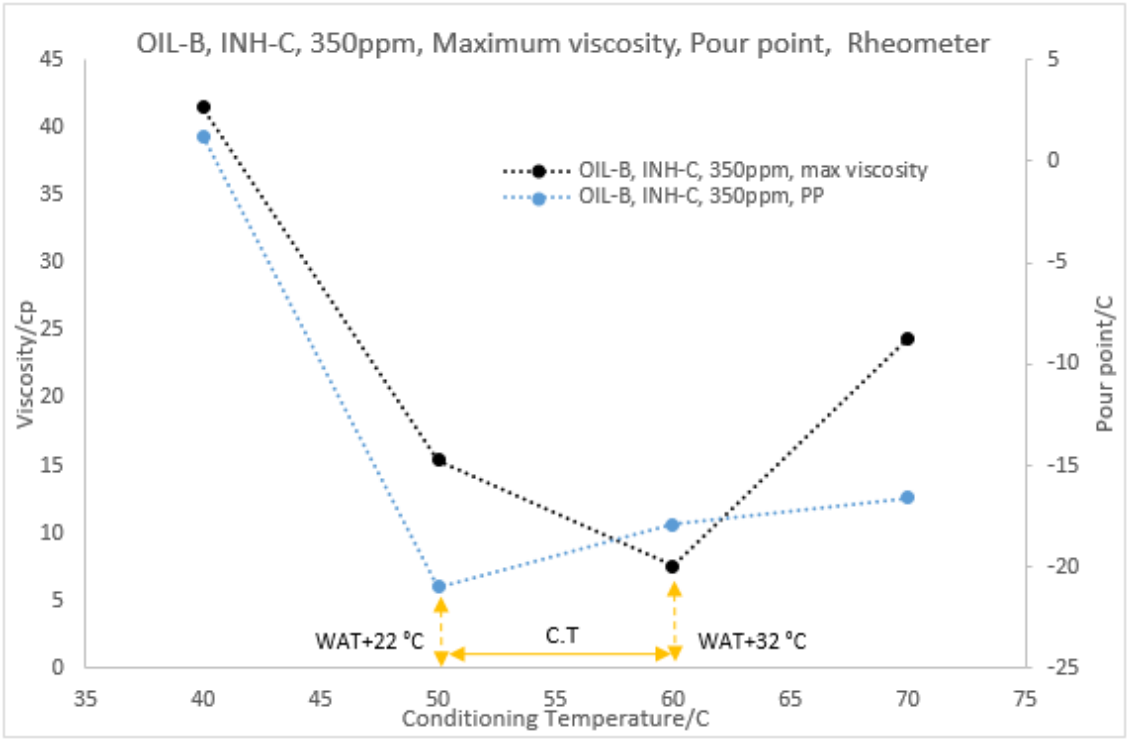

Figure 4-7. Maximum viscosity and pour point variation with different conditioning temperature measured with rheometer on OIL-B dosed with INH-C, 350ppm inhibitor. Lines between points are only for visual clarification.

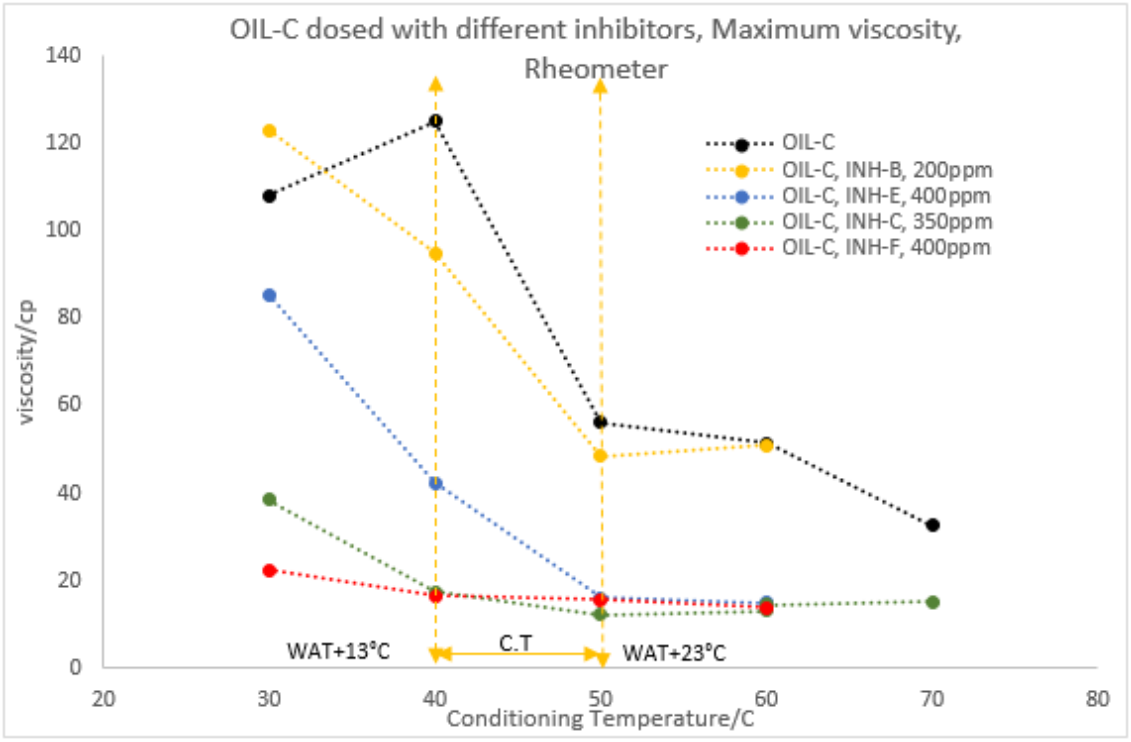

Figure 4-8. Maximum viscosity variation with different conditioning temperature measured with rheometer on OIL-C sample dosed with different inhibitors. Lines between points are only for visual clarification.

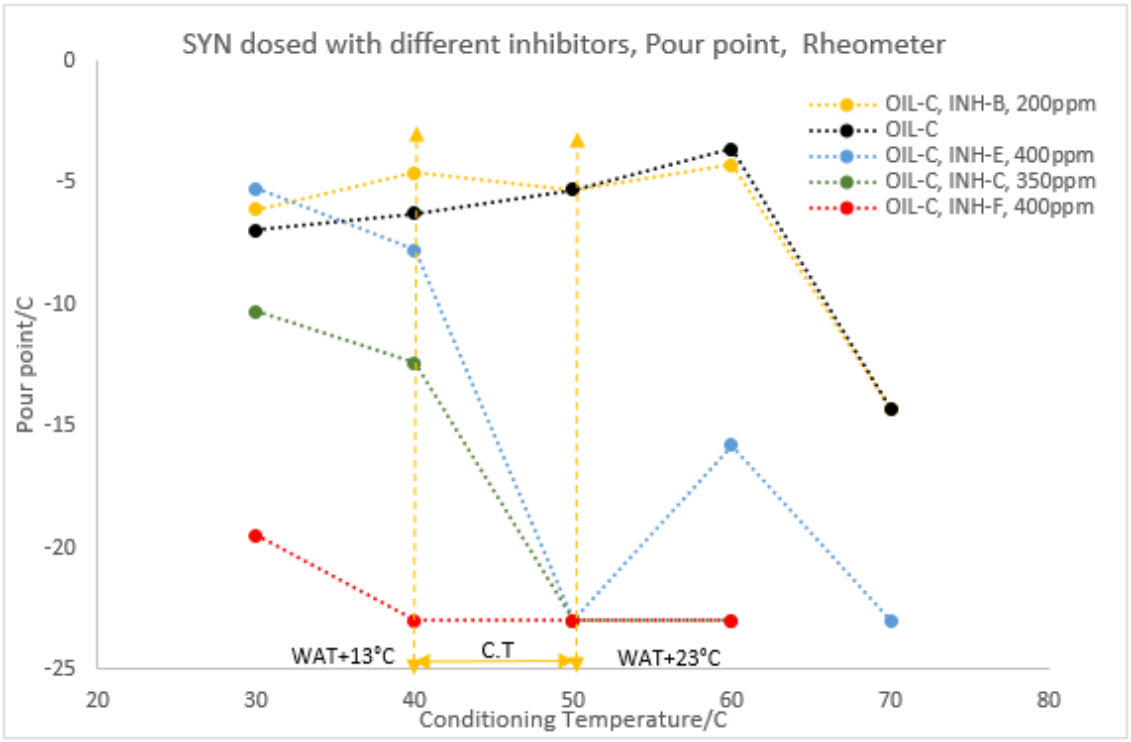

Figure 4-9. Pour point variation with different conditioning temperature measured with rheometer on OIL-C sample dosed with different inhibitors. Lines between points are only for visual clarification.

4.3 Effect of cooling/heating rate on wax studies

The main objective of this experimental section was to determine the impact of cooling/heating rate on WAT/WDT and viscosity measurements using rheometer to find an optimum rate for further investigation.

Experiments were performed at four different cooling/heating rates of 0.2, 0.5, 0.75 and 1°C/min using four different oil samples of OIL-E, OIL-F, OIL-G and OIL-H. Table 4-4 summarizes the conditions under which the experiments were performed.

The trend for WAT and WDT was the same so only WAT trend was plotted along with maximum viscosity in Figure 4-10 to Figure 4-13. The horizontal axis represents the cooling rate, the left vertical axis shows viscosity in centipoise and the right vertical axis the WAT in degree Celsius. OIL-E and OIL-H samples were measured at three and two different conditioning temperatures respectively; the same trend is seen in all cases, therefore, only the data for tests with a starting temperature of 50°C are plotted in Figure 4-12 and Figure 4-13.

Table 4-4. The condition and results of rheometer to measure viscosity, using different fluids at different cooling/heating rates

fluid	***Conditioning T (°C)***	***Destination T (°C)***	***Cooling rate (°C/min)***	***Shear rate (s^{-1})***	***WAT (°C)***	***WDT (°C)***	***Minimum. Viscosity (cP)***	***Maximum. Viscosity (cP)***
OIL-E	*35*	*5*	*0.20*	*10*	*19.0*	*29*	*20.40*	*695.00*
		5	*0.20*	*10*	*19.6*	*30*	*20.20*	*572.00*
		5	*0.50*	*10*	*18.0*	*28*	*19.80*	*480.00*
		5	*0.75*	*10*	*17.8*	*28*	*20.30*	*479.00*
		5	*0.75*	*10*	*19.0*	*30*	*20.50*	*495.00*
		5	*1.00*	*10*	*18.0*	*29*	*20.10*	*424.00*
	50	*5*	*0.20*	*10*	*21.0*	*30*	*12.00*	*274.00*
		5	*0.50*	*10*	*20.3*	*29.3*	*12.00*	*228.00*
		5	*0.75*	*10*	*19.5*	*29*	*11.70*	*211.00*
		5	*1.00*	*10*	*19.0*	*28*	*11.80*	*213.00*
	65	*5*	*0.20*	*10*	*21.0*	*31*	*8.15*	*259.00*
		5	*0.50*	*10*	*21.0*	*29*	*7.93*	*209.00*
		5	*1.00*	*10*	*21.0*	*29*	*7.95*	*197.00*
OIL-H	*50*	*20*	*0.20*	*10*	*40.0*	*48*	*4.51*	*92.90*
		20	*0.50*	*10*	*40.0*	*47*	*4.61*	*99.00*
		20	*0.75*	*10*	*38.6*	*47*	*4.42*	*108.00*
		20	*1.00*	*10*	*39.0*	*47*	*4.59*	*118.00*
	40	*20*	*0.20*	*10*	*38.0*	*----*	*6.34*	*89.30*
		20	*0.50*	*10*	*37.0*	*----*	*6.28*	*89.20*
		20	*1.00*	*10*	*36.5*	*----*	*6.73*	*103.00*
OIL-G	*60*	*20*	*0.20*	*10*	*35.5*	*46*	*4.78*	*130.00*
		20	*0.50*	*10*	*35.0*	*45*	*4.87*	*128.00*

Continued Table 4-4

fluid	*Conditioning T (°C)*	*Destination T (°C)*	*Cooling rate (°C/min)*	*Shear rate (s^{-1})*	*WAT (°C)*	*WDT (°C)*	*Minimum. Viscosity (cP)*	*Maximum. Viscosity (cP)*
		20	*0.75*	*10*	*34.5*	*45*	*4.85*	*143.00*
		20	*1.00*	*10*	*34.0*	*45*	*4.90*	*151.00*
		25	*0.20*	*10*	*41.0*	*53*	*2.52*	*7.00*
		25	*0.50*	*10*	*39.5*	*48.5*	*2.42*	*6.84*
OIL-F	*60*	*25*	*0.75*	*10*	*38.5*	*46.5*	*2.90*	*7.20*
		25	*1.00*	*10*	*38.0*	*46*	*2.49*	*7.73*

An important point to be noted here is that the variation of WAT and WDT in the range of cooling/heating rates tested was not significant, though, the trend was important to assessed for predictions at higher and lower rates. Maximum viscosity variation, on the other hand, clearly changed with the exception of OIL-F sample, Figure 4-10, most probably due to lack of heavy components as mentioned it in the previous section.

It was generally observed that a slow cooling rate resulted in higher measured values for WAT and WDT for all samples. Wax crystals should reach a certain size to be detected by rheometer as indicated by viscosity deviations from Arrhenius equation. As anticipated, the time for measurement was longer for smaller values of cooling rate which resulted in larger wax crystals and/or aggregates, hence, being detected by rheometer at higher temperatures.

Since the oils are generally shear-thinning and the wax-oil mixture under WAT point was being cooled under a constant shear stress, therefore, the sample was subjected to a longer period of shearing by decreasing cooling rate, hence, as shown in Figure 4-10 to Figure 4-12 corresponding to OIL-F, OIL-G, and OIL-H samples, the maximum viscosity was lower.

Surprisingly, the opposite trend was observed for OIL-E at all conditioning temperatures, Figure 4-13. The only reason which could lead to this behavior was that the applied shear rate $10s^{-1}$ was not high enough to break down the wax microstructure. Put simply, OIL-E was a heavy oil containing a high amount of heavy components. The maximum viscosity for this oil was significantly higher than the other oils. Since a slower cooling rate may produce larger crystals, a lower degree of degradation as a result of the applied shear rate was obtained for OIL-E sample; consequently, a higher viscosity was achieved.

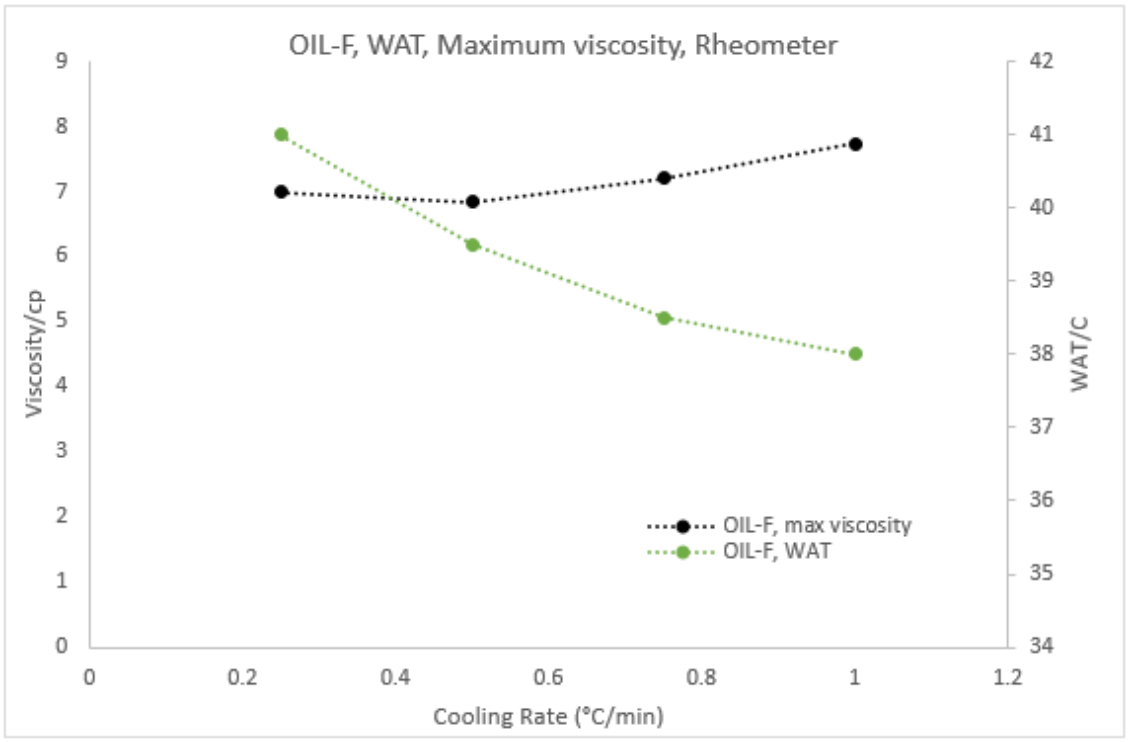

Figure 4-10. Maximum viscosity and WAT variation with different cooling rate measured with rheometer using OIL-F oil sample. Lines between points are only for visual clarification.

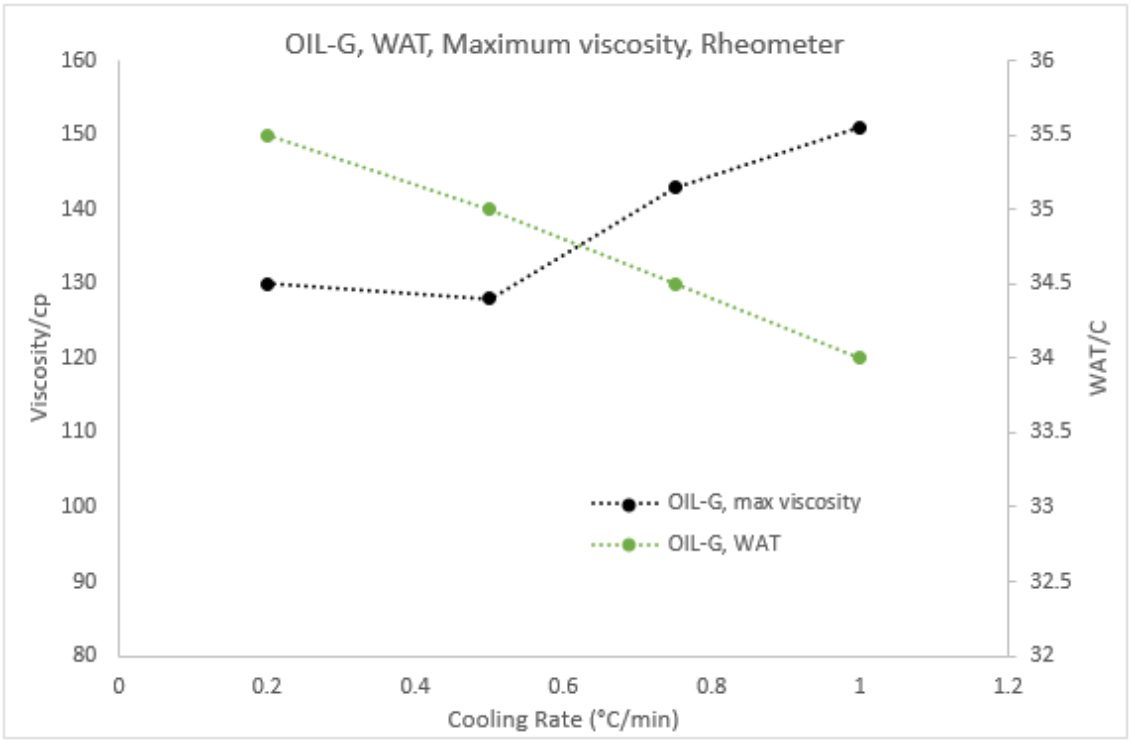

Figure 4-11. Maximum viscosity and OIL-G variation with different cooling rate measured with rheometer used OIL-F oil sample. Lines between points are only for visual clarification.

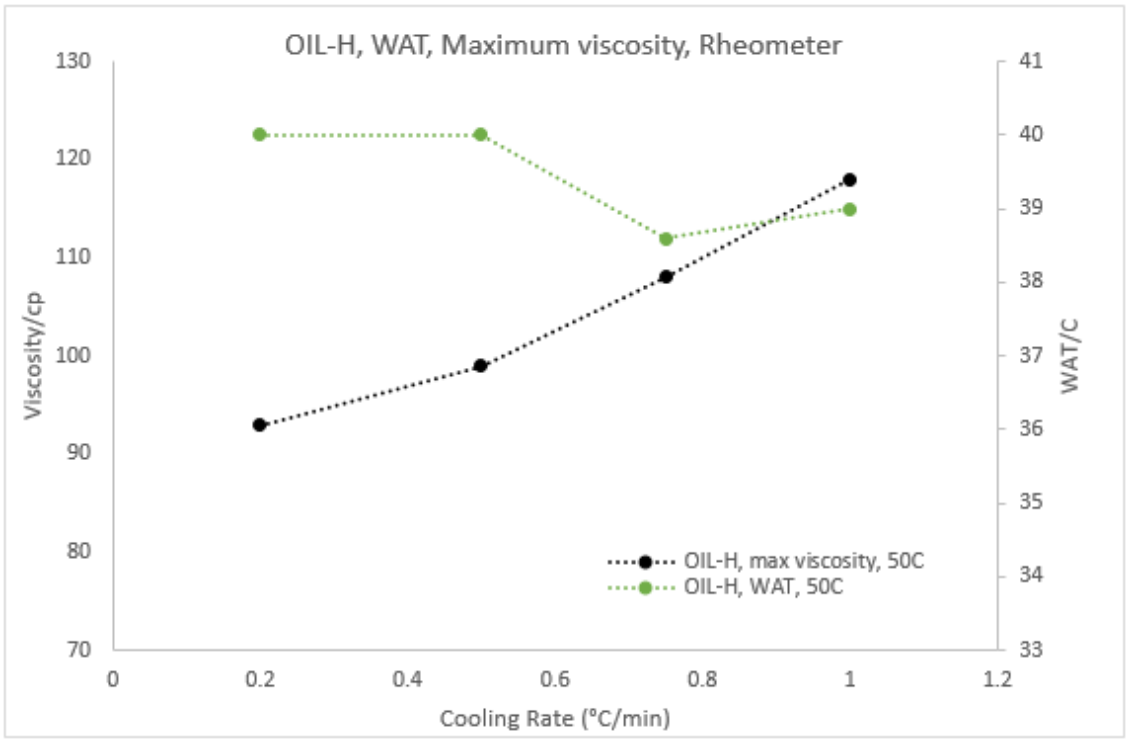

Figure 4-12. Maximum viscosity and WAT variation with different cooling rate measured with rheometer used OIL-H oil sample. Connection trend between points are only for visual clarification.

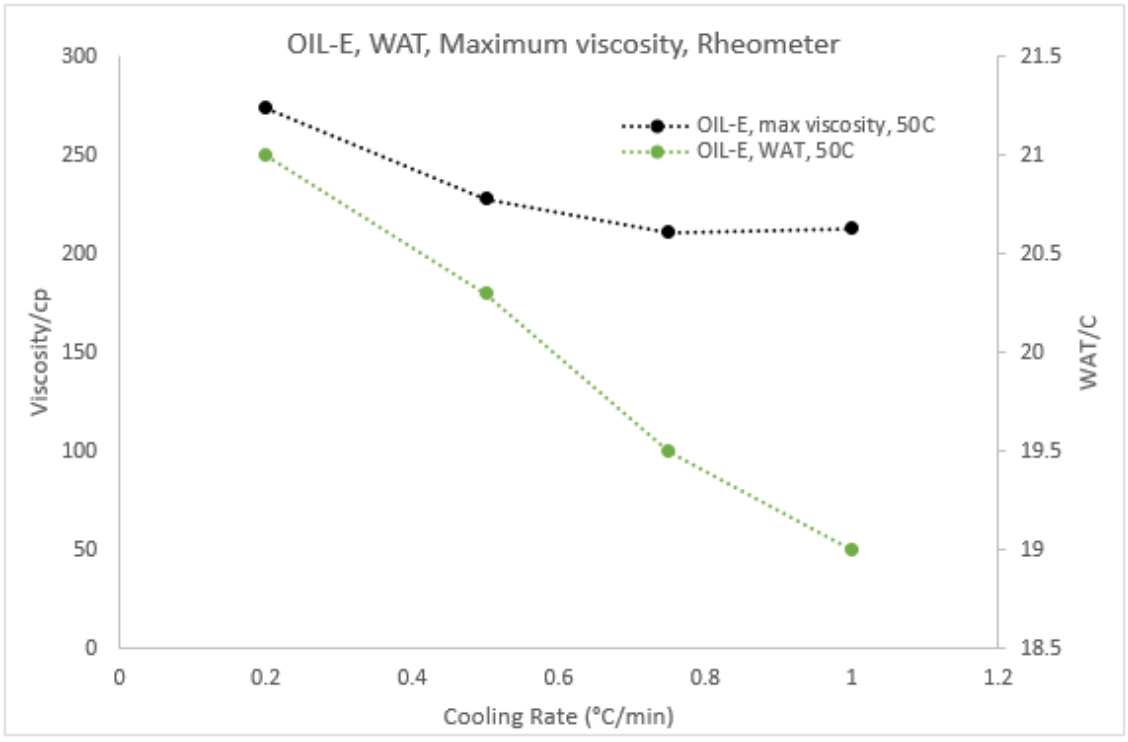

Figure 4-13. Maximum viscosity and WAT variation with different cooling rate measured with rheometer used OIL-E oil sample. Connection trend between points are only for visual clarification.

Since the evaporation of light component in samples was another issue when using atmospheric geometry in the rheometer, and it was not observed to have a significant

effect on WAT/WDT in this range, it was decided to conduct all measurements using rheometer at a cooling/heating rate of 1 °C/min in order to minimise the time for each test.

4.4 Effect of ageing time and shear rate using coaxial cold finger

A series of experiments was performed using a coaxial cold finger setup to assess the impact of elapsed experimental time and shear rate on wax deposition.

A preliminary measurement was done to select a suitable oil sample with a minimum scattering data over a long ageing time. The oil sample, OIL-E, was finally selected with a wax appearance temperature of 19 °C and wax disappearance temperature of 28 °C. The bulk oil temperature for all measurements was maintained at 30 °C and the bobbin temperature set at 0 °C which represents WAT+11°C and WAT-19°C respectively. All the conditions and results of measurements are tabulated in Table 4-5. The data are presented in increasing shear rate.

Throughout the work program, 5 tests were performed using exactly the same conditions, three with fresh aliquots of oil (Tests 1 to 3) and two tests with the same oil recombined with deposited wax (Tests 4 and 18).

Tests 1 to 3 were performed to ascertain the repeatability of the wax deposition and assess the statistical uncertainty of the measurements. For these tests, the same conditions were used and also a fresh aliquot of oil was used for each individual measurement. The purpose of Tests 4 and 18 was to investigate if re-combining the collected wax and oil could be employed as a method to re-use the wax and bulk oil from previous tests; hence, it would be possible to perform a series of subsequent tests without using large quantities of oil. In addition, recombining might reduce the uncertainty between two different samples for comparison purposes such as inhibitor evaluation which as discussed in the next chapter. The average and uncertainty of wax deposition of these five tests were measured to be 1.3079 ±0.1374 gr. These initial tests indicated an approximation for the statistical uncertainty of the measurements and that re-combining collected wax and oil could be used reliably to perform repeat test. However, it must be noted that for other oil samples used in this work, it was observed that uncertainty increased with increasing ageing time (the time when test is performed) as discussed in detail in the next chapter.

Tests 5 to 21 were performed using the re-combined wax-oil approach, and explored the effect of shear rate and experimental time on the measured wax deposition.

Table 4-5. Conditions and results of all measurements. Ranked top to bottom based on increasing aging time and shear rate.

Test	Volume of sample (cc)	Ageing time (hrs)	Shear rate (s^{-1})	Bulk T (°C)	Bulk T compare to WAT (°C)	Bobbin T (°C)	Bobbin T compare to WAT (°C)	ΔT (°C)	Deposited mass (gr)
12	200	42.5	0	30	+11	0	-19	30	Not clear
9	200	42.5	50	30	+11	0	-19	30	1.0115
10	200	67.0	50	30	+11	0	-19	30	1.3449
8	200	24.0	100	30	+11	0	-19	30	0.7643
1	200	42.5	100	30	+11	0	-19	30	1.5031
Continued Table 4-5		42.5	100	30	+11	0	-19	30	1.2730
3	200	42.5	100	30	+11	0	-19	30	1.1809
4	200	42.5	100	30	+11	0	-19	30	1.1924
18	200	42.5	100	30	+11	0	-19	30	1.3902
5	200	67.0	100	30	+11	0	-19	30	1.5421
6	200	257.0	100	30	+11	0	-19	30	2.4183
7	200	143.5	100	30	+11	0	-19	30	2.3242
11	200	42.5	200	30	+11	0	-19	30	1.7068
13	200	67.0	200	30	+11	0	-19	30	1.9046
17	200	42.5	250	30	+11	0	-19	30	2.0909
16	200	67.0	250	30	+11	0	-19	30	2.0298
21	200	143.5	250	30	+11	0	-19	30	2.2970
15	200	42.5	350	30	+11	0	-19	30	1.8220
19	200	67.0	350	30	+11	0	-19	30	1.9852
14	200	42.5	500	30	+11	0	-19	30	1.5599
20	200	67.0	500	30	+11	0	-19	30	1.8684

4.4.1 Effect of ageing time on deposition using coaxial cold finger

Presented in Figure 4-14 is dependence of mass deposition as a function of elapsed experimental time at a variety of measured shear rates. As expected, the mass deposited increased with increasing experimental time. The relationship was approximately linear between the experimental times of 50 and 150 hrs, although the data was insufficient to be rigorous with this statement, but it did indicate that a single measured point in this timeframe may be used to determine the wax deposition rate. Although not repeated for all shear rates, it did appear that the wax deposition rate decreased for times over 150 hrs, which was most likely due to wax accumulation on the cold finger bob providing a thermal insulation layer between the surface of the cold-finger bob and the bulk oil.

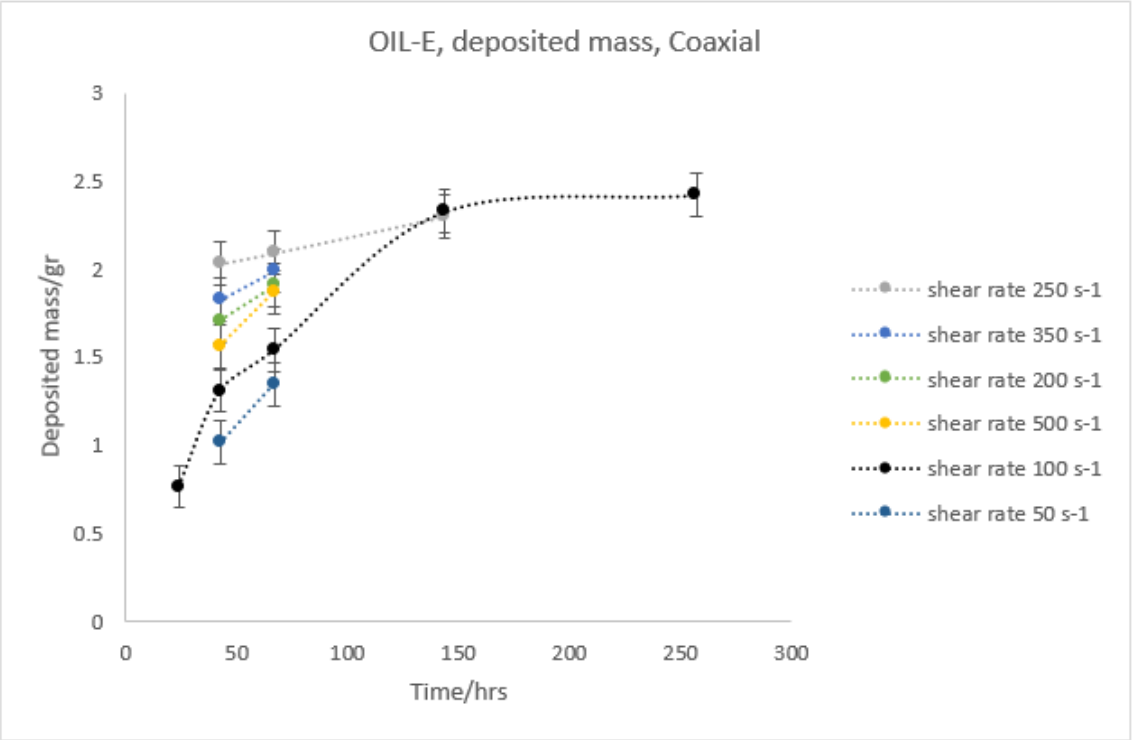

Figure 4-14. Wax deposition versus time for a variety of shear rates. Connection trend between points are only for visual clarification.

Demonstrated in Figure 4-16, from scraping the wax from the bob at the end of each test, the impact of so-called 'ageing' of the wax was observed on the hardness of deposition. For those tests with longest experimental times, the wax became gradually harder. During ageing, the gel-like structure deposited on the bob (pipeline) walls, comprised a 3-dimensional network of solid wax particles and entrapped liquid oil, became richer in heavier paraffin content while the lighter paraffin content, or the amount of entrapped oil, simultaneously diffused out of the gel layer network.

4.4.2 Effect of shear rate on deposition using coaxial cold finger

Figure 4-15 presents the results of the mass of deposited wax versus shear rate for two different experimental aging times. There is clearly a maximum point in these trends, which, for this oil, occurs at a shear rate of approximately 250 s^{-1}. Unreported experiments were also performed under static conditions, but it was difficult to discern between deposited wax (if any) from the bulk oil, most likely due to the fact that there was no shear force to promote ageing / hardening.

It was observed that wax deposition increased with increasing the shear rate. This was likely to be due to shear dispersion, an effect which is well known for laminar-flow regimes. At higher shear rates, the gradient of velocities in the coaxial cell is larger than

it is at the lower shear rates, known as shear dispersion. In other words, the velocity of oil at the cold-finger bob was lower than at the cell wall, because the rotation frequency was the same, but the circumference, or distance traveled per unit time, was smaller compared to particles traveling close to the cell wall. The wax particles in the high-velocity regions experience more drag forces, which caused displacement and the net result was a migration of solid particles towards the low-velocity region, i.e. the cold-finger bob, or pipeline wall in petroleum operations. It was, therefore, expected that the increase in wax deposition should increase linearly with increasing shear rate, as is indeed observed in Figure 4-15. However, as the shear rate approaches the shear strength of the deposited wax, the shear force could dislodge deposited wax from the bob surface: a process known as shear-transport or 'sloughing'. The maximum in the observed trend of deposition *vs.* shear rate was a consequence of two competing phenomena: shear–dispersion and shear–transport [4-6].

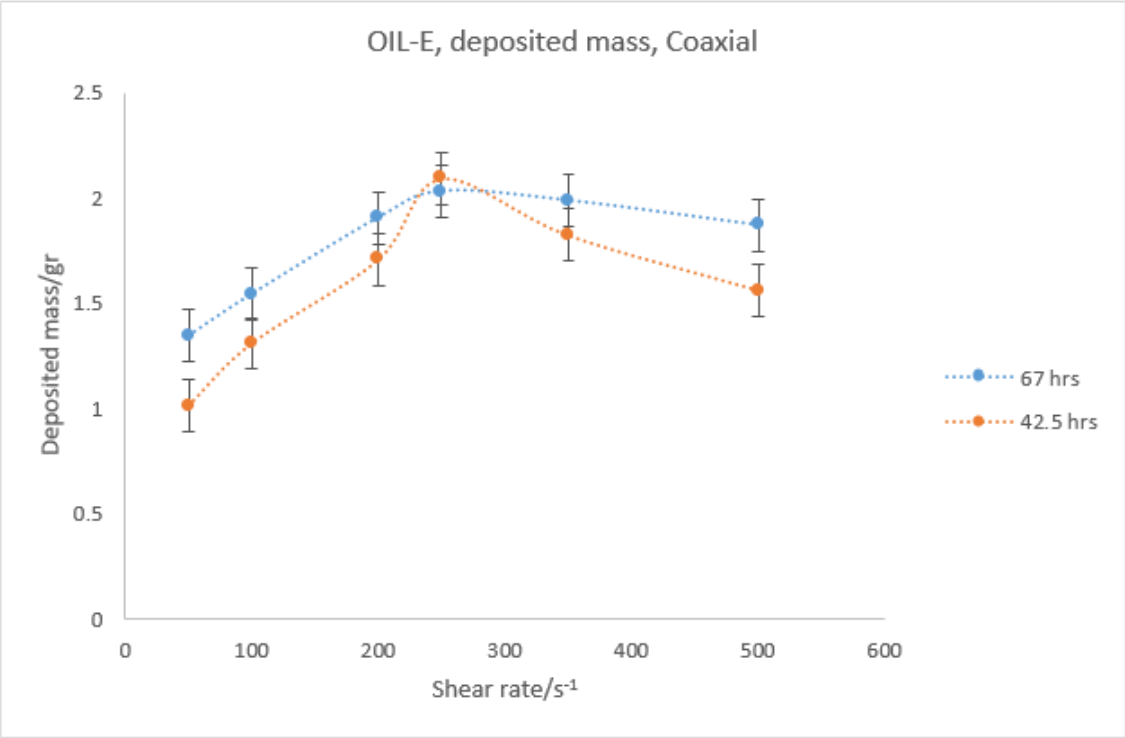

Figure 4-15. Wax deposition versus shear rate for two different ageing times. Lines between points are only for visual clarification.

The possibility that an experimental artifact is the root of the observed trends should not be neglected. It was observed that the deposited wax was thicker at the base of the bob compared to the top of the bob, which was increasingly apparent at shear rates over 250s^{-1}, Figure 4-16. This was most likely caused by the vortex created by mixing (and associated eddy currents) as well as gravity settling, but it was unclear at this stage if

this had an impact on the measured wax deposition. It must be noted that the oil level for all measurements was consistent and was ensured to be higher than the cold finger, even for the highest shear rates.

Figure 4-16. Photographs of the deposited wax on the cold finger bob. It was scrapped to see depth of deposition.

4.5 Effect of different temperature gradients on the inhibitor performance

The objective of this section was to investigate the impact of temperature gradient as a driving force on the performance of inhibitors in terms of wax deposition. The coaxial setup was used to mimic flow-line temperature gradient as well as flow behavior.

OIL-A sample was selected for this study with a WAT of 33°C and WDT of 54°C (WAT/WDT measured with QCM). The bulk temperature in all tests was set at 45°C which represents WAT+12°C during 24hrs ageing time following conditioning at 80°C for an hour. Only the bobbin temperature was varied in each individual differential temperature test.

Table 4-6 shows the results and all the experimental details. As expected, the higher degree of subcooling (temperature difference from WAT) corresponds to the greater driving force for crystallization, covering a larger amount of components, hence, higher deposition formed as shown in Figure 4-17. The photos of bobbin covered with deposited material, in all samples with/out inhibitors are shown in Figure 4-18 to Figure 4-20, for visual observation/inspection of deposited mass.

Table 4-6. The results and conditions measured with coaxial set up using OIL-A dosed with different inhibitors with different temperature gradients compare to WAT.

fluid	***Volume of sample (cc)***	***ageing time (hrs)***	***shear rate (s^{-1})***	***Bulk T (°C)***	***Bulk T compare to WAT(33°C) (°C)***	***Bobbin T (°C)***	***Bobbin T compare to WAT(33°C) (°C)***	***ΔT (°C)***	***deposited mass (gr)***
OIL-A(fresh)	*200*	*24*	*100*	*45*	*+12*	*15*	*-18*	*30*	*1.1664*
OIL-A(used)	*200*	*24*	*100*	*45*	*+12*	*15*	*-18*	*30*	*1.1160*
OIL-A(fresh)	*200*	*24*	*100*	*45*	*+12*	*15*	*-18*	*30*	*1.1758*
OIL-A(fresh)	*200*	*24*	*100*	*45*	*+12*	*22*	*-11*	*23*	*0.9305*
OIL-A(fresh)	*200*	*24*	*100*	*45*	*+12*	*26*	*-7*	*19*	*0.7835*
OIL-A(used)	*200*	*24*	*100*	*45*	*+12*	*30*	*-3*	*15*	*0.5078*
OIL-A(fresh)	*200*	*24*	*100*	*45*	*+12*	*38*	*+5*	*7*	*0.0458*
OIL-A, INH-C, 350ppm(used)	*200*	*24*	*100*	*45*	*+12*	*15*	*-18*	*30*	*1.2815*
OIL-A, INH-C,350ppm(fresh)	*200*	*24*	*100*	*45*	*+12*	*15*	*-18*	*30*	*1.3539*
OIL-A, INH-C, 350ppm(used)	*200*	*24*	*100*	*45*	*+12*	*22*	*-11*	*23*	*0.7048*
OIL-A, INH-C, 350ppm(used)	*200*	*24*	*100*	*45*	*+12*	*26*	*-7*	*19*	*0.3421*
OIL-A, INH-C, 350ppm(used)	*200*	*24*	*100*	*45*	*+12*	*30*	*-3*	*15*	*0.0173*
OIL-A, INH-A, 250ppm (fresh)	*200*	*24*	*100*	*45*	*+12*	*15*	*-18*	*30*	*1.3176*
OIL-A, INH-A, 250ppm	*200*	*24*	*100*	*45*	*+12*	*28*	*-5*	*17*	*0.8572*

Continued Table 4-6

fluid	*Volume of sample (cc)*	*ageing time (hrs)*	*shear rate (s^{-1})*	*Bulk T (°C)*	*Bulk T compare to WAT(33°C) (°C)*	*Bobbin T (°C)*	*Bobbin T compare to WAT(33°C) (°C)*	*ΔT (°C)*	*deposited mass (gr)*
(fresh)									
OIL-A, INH-D, 100ppm(fresh)	*200*	*24*	*100*	*45*	*+12*	*15*	*-18*	*30*	*1.3301*
OIL-A, INH-D, 100ppm(fresh)	*200*	*24*	*100*	*45*	*+12*	*22*	*-11*	*23*	*1.1420*
OIL-A, INH-D, 100ppm(fresh)	*200*	*24*	*100*	*45*	*+12*	*25*	*-8*	*20*	*0.9624*
OIL-A, INH-D, 100ppm(fresh)	*200*	*24*	*100*	*45*	*+12*	*28*	*-5*	*17*	*0.7504*
OIL-A, INH-B, 200ppm(fresh)	*200*	*24*	*100*	*45*	*+12*	*15*	*-18*	*30*	*0.9306*
OIL-A, INH-B, 200ppm(fresh)	*200*	*24*	*100*	*45*	*+12*	*30*	*-3*	*15*	*0.5900*

In Figure 4-17 trend of deposited mass for the blank oil is plotted in a black color. As shown in Figure 4-17, a test was done with the blank sample at 5°C above the WAT. The mass of deposit was not significant. The deposit was insoluble in toluene and heptane; hence, it was not a hydrocarbon. SEM analysis of the deposits showed the presence of impurities such as Fe-rich particles and scale such as barium sulfate.

Surprisingly, with both inhibitors INH-D and INH-A at all measured differential temperatures there was higher deposition in compared with the blank sample. Therefore, these inhibitors, regardless of temperature gradient promoted deposition. In addition, this negative impact on deposition was repeated for inhibitors INH-C at WAT-18°C and INH-B in WAT-3°C. However, INH-B reduced deposition at WAT-18°C and INH-C with lower subcooling.

INH-C showed the highest dependency on temperature gradient, giving a better performance at lower subcooling.

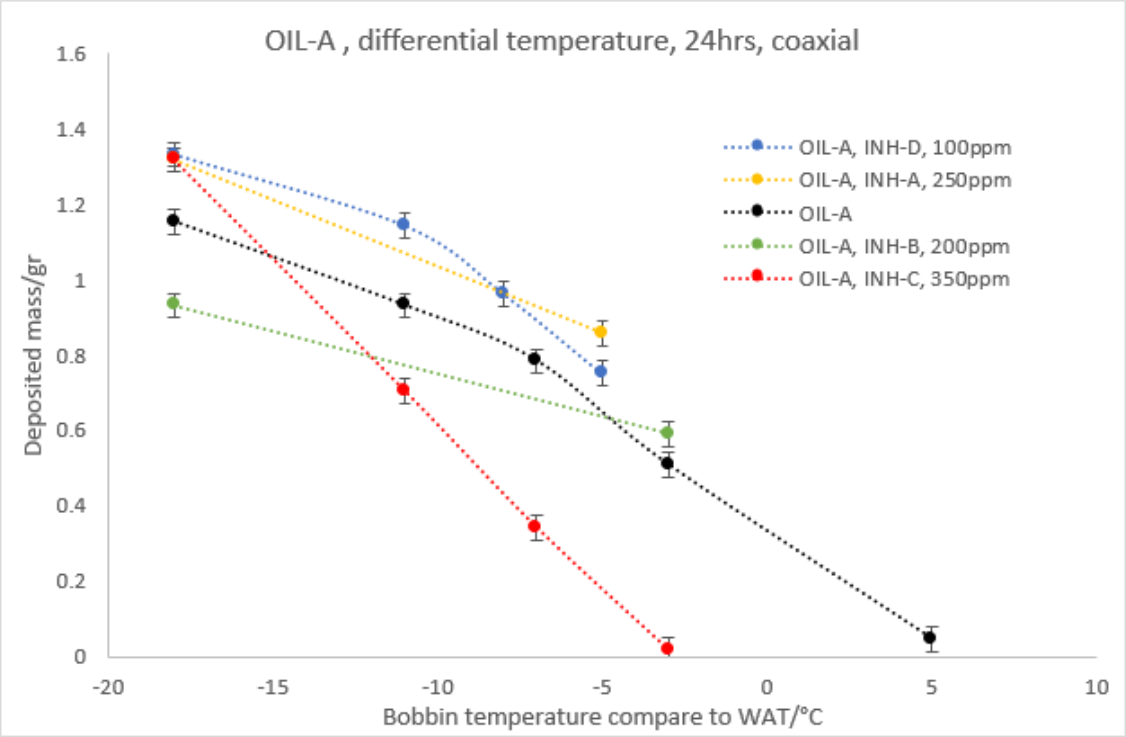

Figure 4-17. Comparison of mass deposition measured with the coaxial set up, using OIL-A dosed with different inhibitors at different temperature gradients compare to WAT. Lines between points are only for visual clarification.

In all samples except with INH-C, decreasing subcooling resulted a smoother layer of deposition, Figure 4-18 and Figure 4-19. As discussed in Chapter 2, the form of wax crystals highly depends on the oil composition. Macro crystalline which is mainly formed from Naphthenic (cyclic) and long-chain paraffin usually diffused out of the bulk sample at lower subcooling. Since these crystals are stiff and bulky in nature, causing the formation of a smoother layer[7-9].

At higher subcooling on the other hand, microcrystalline waxes tend to precipitate out of the bulk oil. They usually form clusters which are unstable wax solids represented by a small sphere(dotted) shape and uneven layers[7-9].

As shown in Figure 4-20, tests dosed with INH-C formed dotted shape at all different subcoolings. A function of wax inhibitors is crystal modification from plate and needle to mal crystalline. Mal crystals are like small round spheres and the hydrodynamic drag of the flowing fluid can shear these inhibited small particles and carry them out of the flow line easily. It appears that INH-C belongs to this group of inhibitors[10, 11].

Figure 4-18. Visual observation of the mass deposition on bobbin surface of the coaxial bobbin, using OIL-A at different temperature gradients compare to WAT after 24 hrs with 100 s^{-1}. Photos ranked from left corner down to the right corner based on decreasing deposited mass. Used samples are those tests with the same oil recombined with deposited wax.

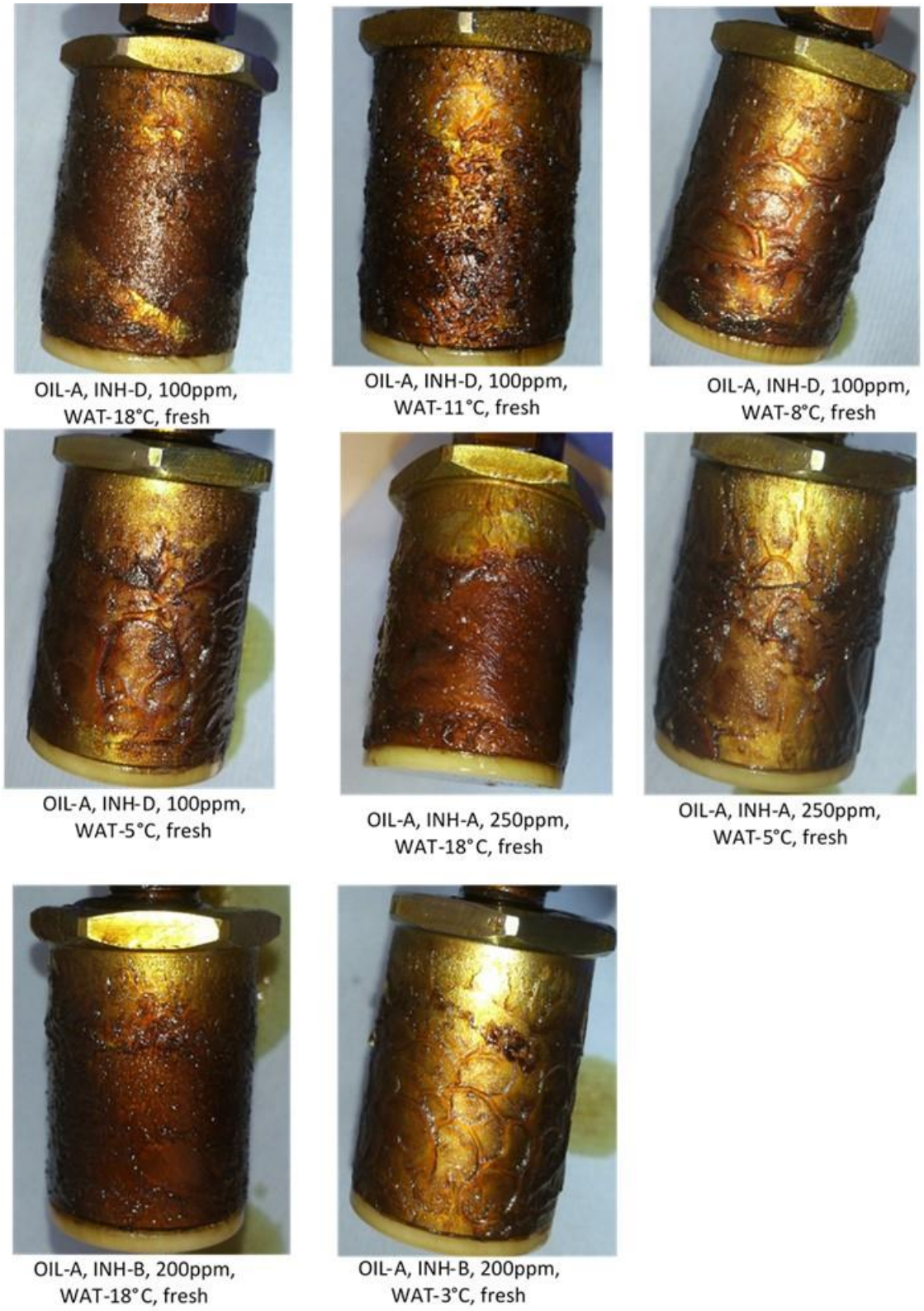

Figure 4-19. Visual observation of the mass deposition on bobbin surface of the coaxial bobbin, using OIL-A with different inhibitors at different temperature gradients compare to WAT after 24 hrs with 100 s^{-1}. Photos ranked from left corner down to the right corner based on decreasing deposited mass according to each inhibitor. Used samples are those tests with the same oil recombined with deposited wax.

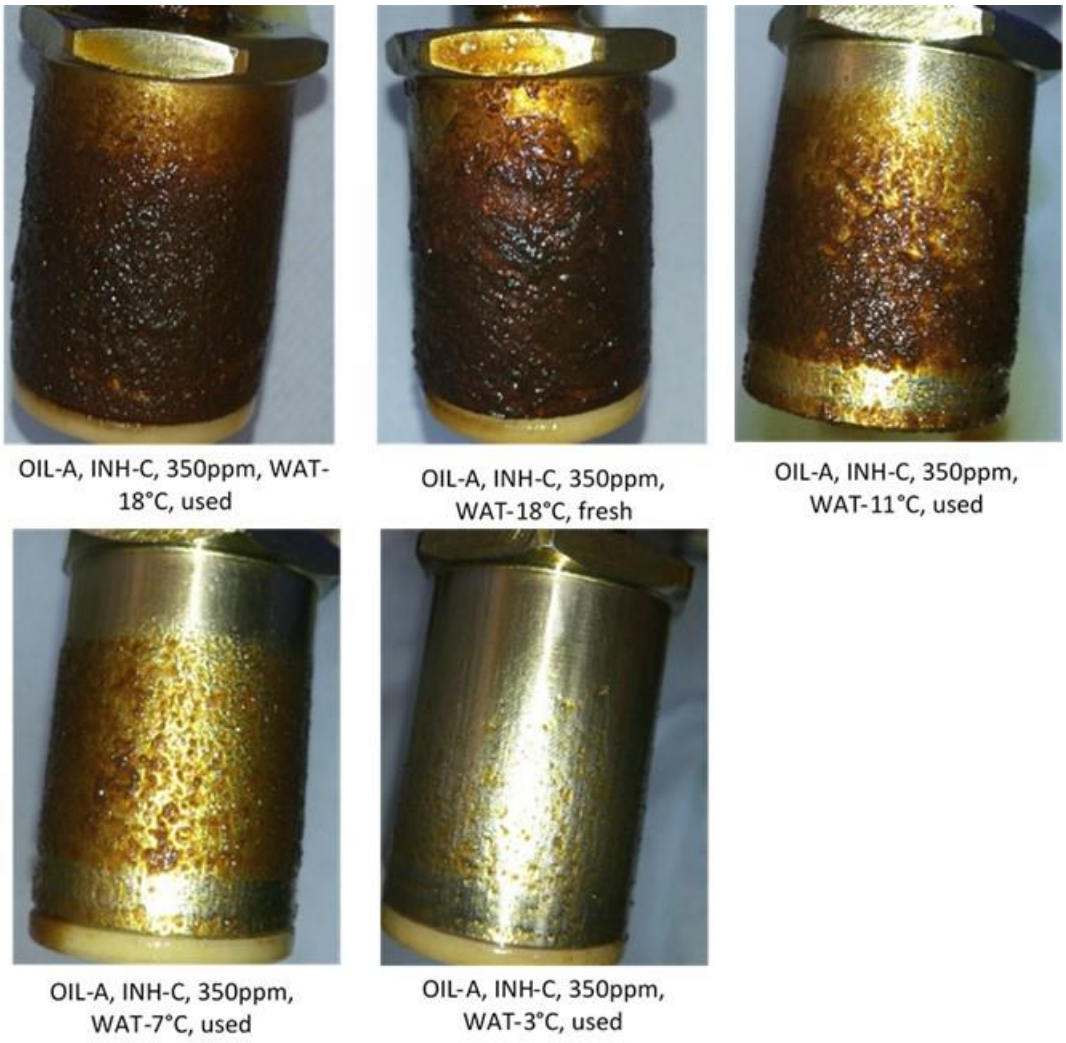

Figure 4-20. Visual observation of the mass deposition on bobbin surface of the coaxial bobbin, using OIL-A, INH-C, 350ppm at different temperature gradients compare to WAT after 24 hrs with 100 s^{-1}. Photos ranked from left corner down to the right corner based on decreasing deposited mass. Used samples are those tests with the same oil recombined with deposited wax.

4.6 References

1. Marchesini, F.v.H., et al., *Rheological characterization of waxy crude oils: Sample preparation.* Energy & Fuels, 2012. **26**(5): p. 2566-2577.
2. ASTM D2500-16a, S.T.M.f.C.P.o.P.P.a.L.F., ASTM International, West Conshohocken, PA, 2016, www.astm.org.
3. Suryanarayana, I., et al., *Infrared spectroscopic studies on the interactions of pour point depressants with asphaltene, resin and wax fractions of Bombay high crude.* Fuel, 1990. **69**(12): p. 1546-1551.
4. Hsu, J., M. Santamaria, and J. Brubaker. *Wax deposition of waxy live crudes under turbulent flow conditions*. in *SPE Annual Technical Conference and Exhibition*. 1994. Society of Petroleum Engineers.
5. Singh, P., et al., *Formation and aging of incipient thin film wax-oil gels.* AIChE Journal, 2000. **46**(5): p. 1059-1074.
6. Parthasarathi, P. and A.K. Mehrotra, *Solids deposition from multicomponent wax-solvent mixtures in a benchscale flow-loop apparatus with heat transfer.* Energy & fuels, 2005. **19**(4): p. 1387-1398.
7. Thanh, N.X., M. Hsieh, and R. Philp, *Waxes and asphaltenes in crude oils.* Organic Geochemistry, 1999. **30**(2): p. 119-132.
8. Zaky, M.T. and N.H. Mohamed, *Comparative study on separation and characterization of high melting point macro-and micro-crystalline waxes.* Journal of the Taiwan Institute of Chemical Engineers, 2010. **41**(3): p. 360-366.
9. Kinsel, A. and J. Phillips, *Method for Classification of Petroleum Waxes.* Industrial & Engineering Chemistry Analytical Edition, 1945. **17**(3): p. 152-156.
10. Leontaritis, K.J. *Wax Flow Assurance Issues in Gas Condensate Multiphase Flowlines*. in *Offshore Technology Conference*. 2007. Offshore Technology Conference.
11. Jafari Ansaroudi, H., et al., *Study of the morphology of wax crystals in the presence of ethylene-co-vinyl acetate copolymer.* Petroleum Science and Technology, 2013. **31**(6): p. 643-651.

Chapter 5: Screening inhibitors with various experimental equipment

5.1 Introduction

A routine procedure for wax deposition removal in pipelines is pigging which is technically and economically challenging especially in subsea tie-lines across long distances. Using chemical additives to control the extent of wax deposition is a substitution technique. However, inappropriate chemical inhibitor can even worsen the situation, Figure 4-17, hence choosing the suitable inhibitor is crucially important [1].

The performance of inhibitors is normally evaluated by measurements of reduction in WAT/WDT, pour point, non-Newtonian viscosity and deposition in the laboratory under pipeline condition using conventional devices such as cold finger, QCM, flowloop, etc. However, reduction of wax deposition under specific conditions in the laboratory does not necessarily guarantee reduction of wax deposition at the realistic pipeline conditions. Likewise, in some cases different devices in the lab have been found to give conflicting results and therefore relying on a single equipment and methos for inhibitor evaluation is highly risky and is not suggested [2-4].

The aim of this work was to conduct a series of screening techniques, comparing and evaluating the wax inhibition performance of a number of commercially available wax inhibitors.

The equipment used for these studies includes rheometer, QCM, coaxial cold finger, flow loop and NIR. These set ups were emplyed to evaluate the performance of 11 different commercial inhibitors named INH-A, INH-B, INH-C, INH-D, INH-E, INH-F, INH-G, INH-H, INH-I, and INH-J with three different real waxy oils with three different viscosities, named OIL-A(very low viscosity), OIL-B(high viscosity), and OIL-C(middle range viscosity). In addition to this three oil samples a model synthetic oil sample named OIL-D. OIL-D was used to eliminate the impact of asphaltene and impurities as well as enabling visual observation for evaluation purposes. Table 5-1 presents an outline of tests using different samples and inhibitors in this chapter.

Table 5-1. Wax inhibitor evaluation test matrix using different oil samples and instruments presented in this chapter. It must be noted that dose rates are vendor recommended.

Technique	Evaluated parameter	Oil sample	Characteristic	Blank	A, 250ppm	B, 200ppm	C, 350ppm	D, 100ppm	E, 400ppm	F, 400ppm	G, 400ppm	H, 400ppm	I, 600ppm	J, 400ppm
Rheometer	Viscosity-WAT	A					350, 700							
		B										400, 2000		
		C												
		D												
	Pour point	A												
		B												
		C										400, 800		
QCM	WAT-WDT, Deposition	A												
		B												
		C												
		D												
Coaxial	Deposition	A	67 hrs											
		A	24 hrs				350, 700							
		B												
		C												
		A	1 hr											
		B												
		C												
Flowloop	Deposition	A	5CPM, 10°C											
			10CPM, 10°C											
		B	5CPM, 10°C											
			10CPM, 15°C											
		C	5CPM, 5°C								400, 800, 1200			
			5CPM, 15°C											
			5CPM, 20°C											
			10CPM, 151 s^{-1}											
			10CPM, 529 s^{-1}									400, 800		
			Added INH to the blank with/out water cut											
			Single batch											
		D	10CPM, 15°C											
NIR	WAT, Deposition	B												
		C										400, 800		
		D												
Test tube photos	Deposition	D	Visual observation											

5.2 Rheometer

5.2.1 Viscosity evaluation using atmospheric cone and plate geometry

The first approach for inhibitor screening using the rheometer was based on viscosity assessment. In this approach the efficiency of an additive was evaluated based on the reduction of non-Newtonian viscosity when added to the system. In all cases, the viscosity obtained at the lowest temperature representing" maximum viscosity'' was selected for the evaluation of the inhibitor performance. The trend obtained from the maximum viscosity measurements of different samples is recognised as the baseline trend which all the other results and trends obtained from all other techniques are compared against.

Table 5-2, presents a summary of the results and conditions using the rheometer with atmospheric geometry and different oil samples dosed with various inhibitors. The choice of conditioning temperature for each oil sample was explained in detail in the previous chapter. The final temperature was selected by trial and error, well below WAT to get a clear indication of viscosity behaviour. The cooling and shear rates were set at 1°C/min and 10 s^{-1} respectively. Tabulated data was ranked top to bottom based on reduction of maximum viscosity for each individual oil sample. WAT comparison will be discussed in detail with data obtained from Rheometer, QCM and NIR later in this chapter.

Figure 5-1 to Figure 5-4 illustrate the viscosity changes with temperature for OIL-A, OIL-B, OIL-C and OIL-D respectively dosed with various inhibitors. The plots are in the linear scale for better visual observation, though WAT measurements must be taken in semi-log scale as described in detail in Chapter 3. All the legends are ranked top to bottom based on decreasing overall viscosity. As noted before, deviation from Arrhenius straight line occurred below cloud point where wax particles dropped out of bulk oil and affect the rheology led to a non-Newtonian behaviour [5].

As shown in Figure 5-1, OIL-A, presented very low viscosity with/out dosed with inhibitor in a deviation of ±0.87 cP, could be attributed to the low wax content or small wax particle size; which made it difficult to assess inhibitor performance using rheometer. In addition, some parameters in Arrhenius equation are slightly temperature dependent even in the Newtonian temperature range; hence, a small curvature was expected in all measurements which made it difficult to distinguish the deviation from Arrhenius equation, detecting WAT for OIL-A sample.

Table 5-2. The test conditions and results of rheometer tests with atmospheric geometry, using different oil samples dosed with various inhibitors, ranked based on decreasing overall viscosity in each oil sample

Fluid	Condition T (°C)	Destination T (°C)	Cooling rate (°C/min)	Shear rate (s^{-1})	WAT (°C)	Minimum Viscosity (cP)	Maximum Viscosity (cP)	% Maximum viscosity reduction compare to blank
OIL-A, INH-E, 400ppm	80	15	1	10	25.7	1.18	10.63	-17.8
OIL-A, INH-F, 400ppm	80	15	1	10	31.9	1.46	9.19	-1.9
OIL-A, INH-G, 400ppm	80	15	1	10	24.5	1.98	9.10	-0.9
OIL-A	80	15	1	10	33.8	1.44	9.02	0.0
OIL-A, INH-C, 700ppm	80	15	1	10	28	2.08	8.81	2.3
OIL-A, INH-A,250ppm	80	15	1	10	37.6	1.49	8.68	3.8
OIL-A, INH-B,200ppm	80	15	1	10	32.7	2.37	8.57	5.0
OIL-A, INH-D,100ppm	80	15	1	10	36.5	1.68	8.21	9.0
OIL-A, INH-C, 350ppm	80	15	1	10	32.6	1.67	7.38	18.2
OIL-B, INH-H, 400ppm	60	10	1	10	35.4	1.53	135	-8.9
OIL-B, INH-H, 2000ppm	60	10	1	10	35.6	1.69	133	-7.3
OIL-B	60	10	1	10	35.1	1.87	124.00	0.0
OIL-B, INH-A, 250ppm	60	10	1	10	35.2	1.83	73.90	40.4
OIL-B, INH-B, 200ppm	60	10	1	10	35.2	1.87	55.90	54.9
OIL-B, INH-I, 600ppm	60	10	1	10	34.6	1.50	34.30	72.3
OIL-B, INH-D, 100ppm	60	10	1	10	35.0	1.83	27.70	77.7
OIL-B, INH-J, 400ppm	60	10	1	10	28.7	2.23	22.70	81.7
OIL-B, INH-E, 400ppm	60	10	1	10	25.5	1.71	18.60	85.0
OIL-B, INH-F, 400ppm	60	10	1	10	35.1	1.79	16.40	86.8
OIL-B, INH-G, 400ppm	60	10	1	10	24.7	1.49	11.80	90.5
OIL-B, INH-C, 350ppm	60	10	1	10	23.5	1.94	7.60	93.9
OIL-C	50	5	1	10	29.1	2.42	56.20	0.0
OIL-C, INH-A, 250ppm	50	5	1	10	28.1	2.16	55.40	1.4
OIL-C, INH-H, 400ppm	50	5	1	10	29.2	2.71	51.90	7.7
OIL-C, INH-B, 200ppm	50	5	1	10	28.6	2.36	48.60	13.5
OIL-C, INH-D, 100ppm	50	5	1	10	31.4	2.69	30.2	46.3
OIL-C, INH-G, 400ppm	50	5	1	10	24.2	2.44	17.5	68.9
OIL-C, INH-E, 400ppm	50	5	1	10	21.2	2.43	16.2	71.2
OIL-C, INH-F, 400ppm	50	5	1	10	27.4	2.43	15.8	71.9
OIL-C, INH-C, 350ppm	50	5	1	10	22.5	2.28	12.3	78.1
OIL-D	50	15	1	10	32.7	2.00	81.7	0.0
OIL-D, INH-H, 400ppm	50	15	1	10	32.9	2.11	78.0	4.5
OIL-D, INH-B, 200ppm	50	15	1	10	32.4	2.07	57.8	29.3
OIL-D, INH-E, 400ppm	50	15	1	10	31.7	2.31	18.1	77.8
OIL-D, INH-C, 350ppm	50	15	1	10	31.2	2.42	10.5	87.1
OIL-D, INH-G, 400ppm	50	15	1	10	28.4	2.09	6.2	92.4
OIL-D, INH-D, 100ppm	50	15	1	10	29.9	2.11	5.8	92.8

Sample dosed with inhibitors INH-E, INH-F and INH-G were slightly shifted above blank oil in all temperature sweep. The reason most probably was due to sampling; because all samples were taken a long time after the other rheology measurements from the remaining oil reservoir tank which contained higher heavy components as well as

scale and corroded metal particles. The impact of these impurities contained in OIL-A on QCM reading will be discussed in detail in section 6.5.

Mixture dosed with INH-C with a dosage of 700 ppm also showed the highest shift in non- Newtonian region compared to other mixtures. The same effect was observed with high-pressure geometry, Figure 5-5. One possible explanation for this observation is that since the concentration of impurities in OIL-A is relatively high, when inhibitor is added to this oil the inhibitor molecules act as seeds for impurity molecules to gather around. This will in turn cause the impurities to form some kind of suspension in the oil phase rather than settling at the bottom of the sample and therefore result in a higher viscosity measurement.

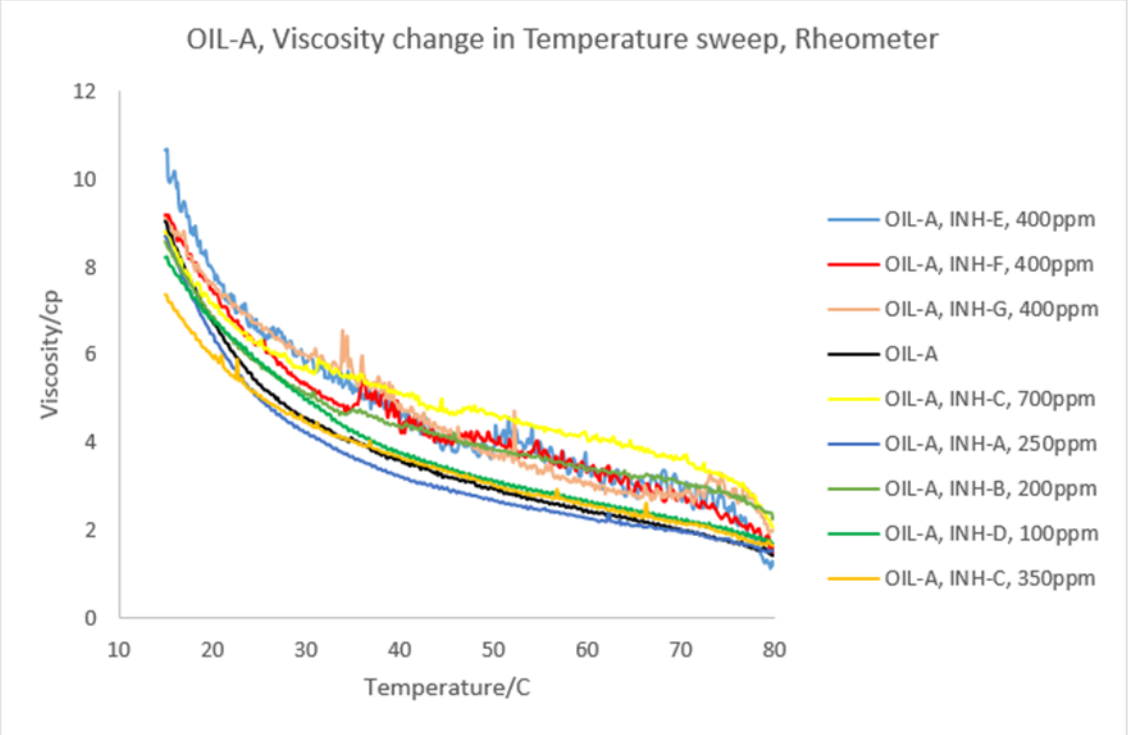

Figure 5-1. Viscosity change in temperature sweep measured with rheometer using OIL-A sample dosed with different inhibitors. The legend is ranked top to bottom based on decreasing overall viscosity

On the other hand, the viscosity variation in the mixtures with OIL-B, OIL-C and OIL-D, was identifiable. It was also observed that the viscosity in non-Newtonian region reduced in presence of all polymeric inhibitors. The only exception was adding a non-polymeric inhibitor INH-H (mixture of detergents and surfactants) in Oil-B sample which was tested with two different dosages of 400 and 2000ppm. Both dosages had almost the same impact, slightly increasing viscosity.

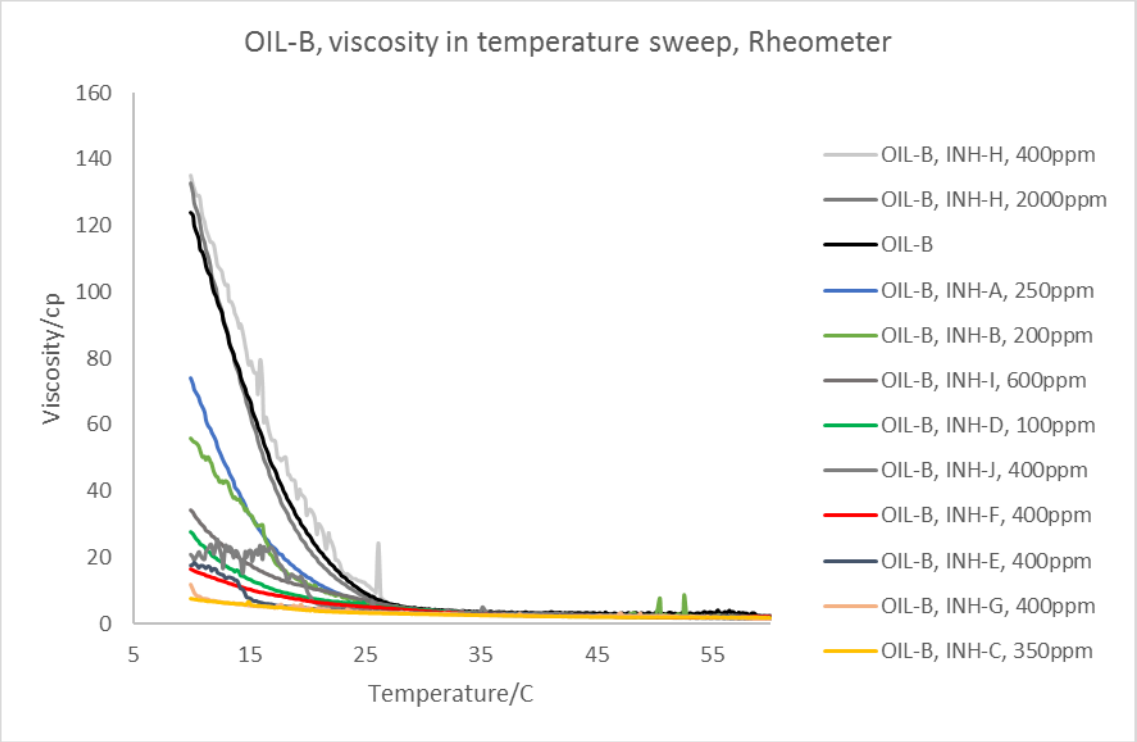

Figure 5-2. Viscosity change in temperature sweep measured with rheometer used OIL-B sample dosed with different inhibitors. The legend ranked top to bottom based on decreasing overall viscosity

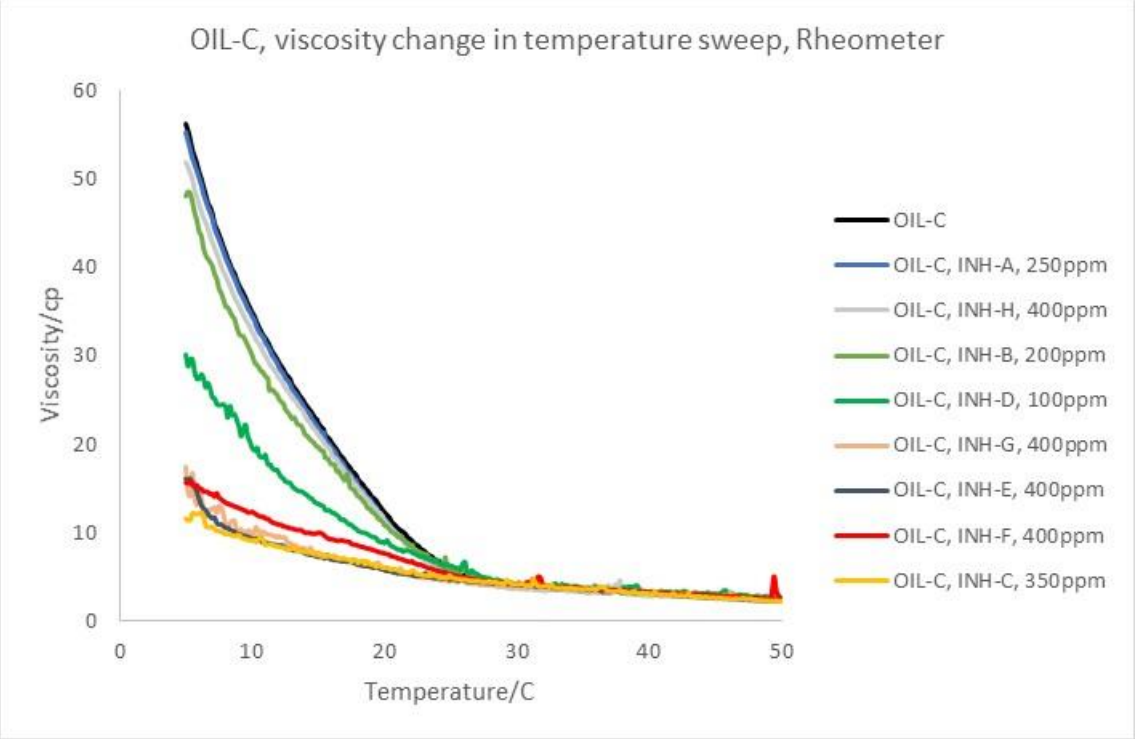

Figure 5-3. Viscosity change in temperature sweep measured with rheometer used OIL-C sample dosed with different inhibitors. The legend ranked top to bottom based on decreasing overall viscosity.

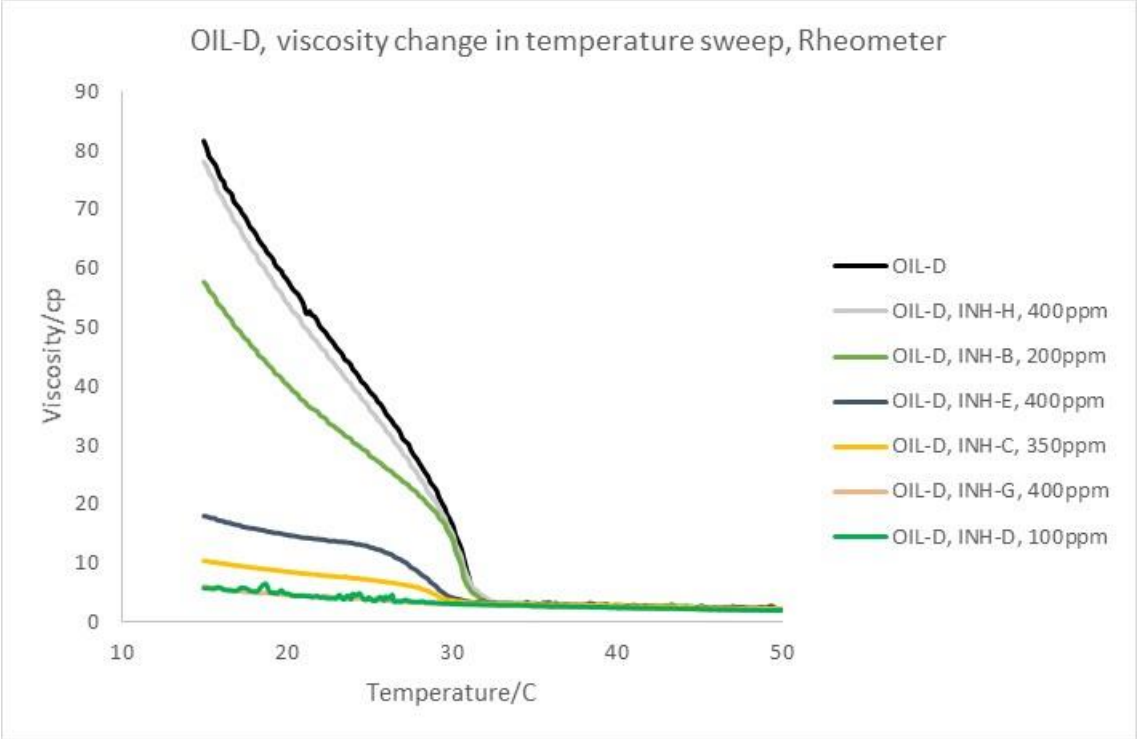

Figure 5-4. Viscosity change in temperature sweep measured with rheometer used OIL-D sample dosed with different inhibitors. The legend ranked top to bottom based on decreasing overall viscosity.

As seen above, Inhibitors performance could be ranked in three classes, 1. high viscosity reduction, 2. moderate reduction, and 3. no significant change or slightly increasing as following:

OIL-A:

As discussed, all inhibitors were almost in the same category

OIL-B:

Class1) INH- C, D, E, F, G, I, J

Class2) INH- A, B

Class3) INH- H

OIL-C:

Class1) INH- C, E, F, G

Class2) INH- D

Class3) INH- A, B, H

OIL-D:

Class1) INH- C, D, E, G

Class2) INH- B

Class3) INH- H

In overall ranking, INH-C, INH-E, INH-F and INH-G, were found to be the best viscosity reducer compare with the other screened inhibitors. It must be noted that the reason to know discrepancies among inhibitor performances are beyond the scope of this thesis. Almost all inhibitors are confidentially produced and polymeric nature. The only purpose to screen inhibitors in this thesis is to explain why and how different setup shows different results

5.2.2 High pressure geometry

Measurements were conducted over several thermal cycles using QCM and flowloop to investigate the repeatability and impact of thermal cycles on the obtained results.

To investigate the strength of inhibitor presented under several consecutive thermal cycle tests, as well as long conditioning time, a series of measurement was launched using high-pressure geometry. The purpose of using this geometry was to minimise loss of light components during analysis by the rheometer.

OIL-A with two different dosages of INH-C, 350ppm and 700ppm was used. In addition, pure INH-C was also used in thermal cycle tests. As shown in Table 5-3, the conditioning temperature was set at 80°C. The heating in high-pressure geometry as mentioned earlier, was controlled using a cooling/heating bath which was set to a cooling rate of 0.5°C/min.

Table 5-3. The test conditions and results from rheometer tests with a high-pressure geometry in consecutive thermal cycles using OIL-A dosed with INH-C with two different dosages as well as a pure inhibitor.

Fluid	Cycle	Condition time (hrs)	Condition T (°C)	Destination T (°C)	Cooling rate (°C/min)	Shear rate (S^{-1})	WAT (°C)	Minimum Viscosity (cP)	Maximum Viscosity (cP)
OIL-A, INH-C, 350ppm	1	9	80	15	0.5	1000	28.8	2.29	4.82
	2	3	80	15	0.5	1000	28.5	2.23	4.74
	3	3	80	15	0.5	1000	34	2.06	4.63
OIL-A	1	3	80	15	0.5	1000	36.1	2.35	5.46
	2	3	80	15	0.5	1000	36.6	2.06	5.4
	3	3	80	15	0.5	1000	35.3	1.96	5.86
OIL-A, INH-C, 700ppm	1	3.45	80	15	0.5	1000	----	2.32	5.59
	2	3	80	15	0.5	1000	31.2	2.72	5.81
	3	3	80	15	0.5	1000	37	2.87	5.88
pure INH-C	1	4.7	80	15	0.5	1000	----	----	190
	2	4	80	15	0.5	1000	----	----	191

Preliminary experiments have revealed that for viscous samples (viscosity greater than 100cP at ambient temperature), using a low shear rate (50-100 s^{-1}) results in a more precise viscosity measurement. On the other hand, using a high shear rate (500-1000s^{-1}) results in a more reliable viscosity measurement for samples with lower viscosity (lower than 100cP in an ambient temperature). A shear rate of 1000s^{-1} was set for all the tests on the OIL-A with/out INH-C as well as pure INH-C.

As shown in Figure 5-5, at the beginning of test with the blank sample, the viscosity reduced at a constant temperature by about 2cP which is significant in terms of OIL-A. As discussed in section 6.5, OIL-A was found to have some impurities such as scale and corroded metal particles, gradually settle down caused uneven result in viscosity. The rising viscosity at the initial stage of the test at constant temperature was observed in the mixture dosed with inhibitor as well, though, ignored to present initial period to synchronise time in a plot with the blank sample. This behaviour was not observed in following cycles.

The pure inhibitor, INH-C, was also subjected to a thermal cycle, shown in Figure 5-6.

Viscosities in all the cycles were found to be repeatable in the case of blank, pure inhibitor, and sample dosed with 350ppm INH-C. Therefore, it could be concluded that the possibility of inhibitor deterioration or morphological change in the thermal cycles and long conditioning time were insignificant, at least for the tested inhibitor.

Viscosity in double dosage INH-C to 700ppm, raised which was also observed the similar trend in the atmospheric geometry in Figure 5-1. It showed that increasing

inhibitor dosage doesn't necessarily guarantee improving the performance. Hence, dosage evaluation is important however it was not being the purpose of this project. The reason for higher viscosity might be described as follows.

As noted in the last chapter, it was found that INH-C most probably acted as a crystal modifier which formed small spherical crystals which deposit in uneven layers. In addition, it was found that OIL-A contained significant amount of impurities. This inhomogeneity, most probably, get involved with impurities in the wax crystals. The amount of impurities in the wax crystals increased by increasing inhibitor dosages which caused viscosity increase furthermore.

In addition, in the middle of heating process in each cycle, viscosity was found to have a big jump which was growing continually in the following cycles. The three hours conditioning was not sufficient to return the viscosity to the baseline. The modified particles which were sheared while formed in cooling process, initiate melting separated from crystals, resulted in an uneven distribution of impurities and crystals on the rheometer surface, most probably causing this jump.

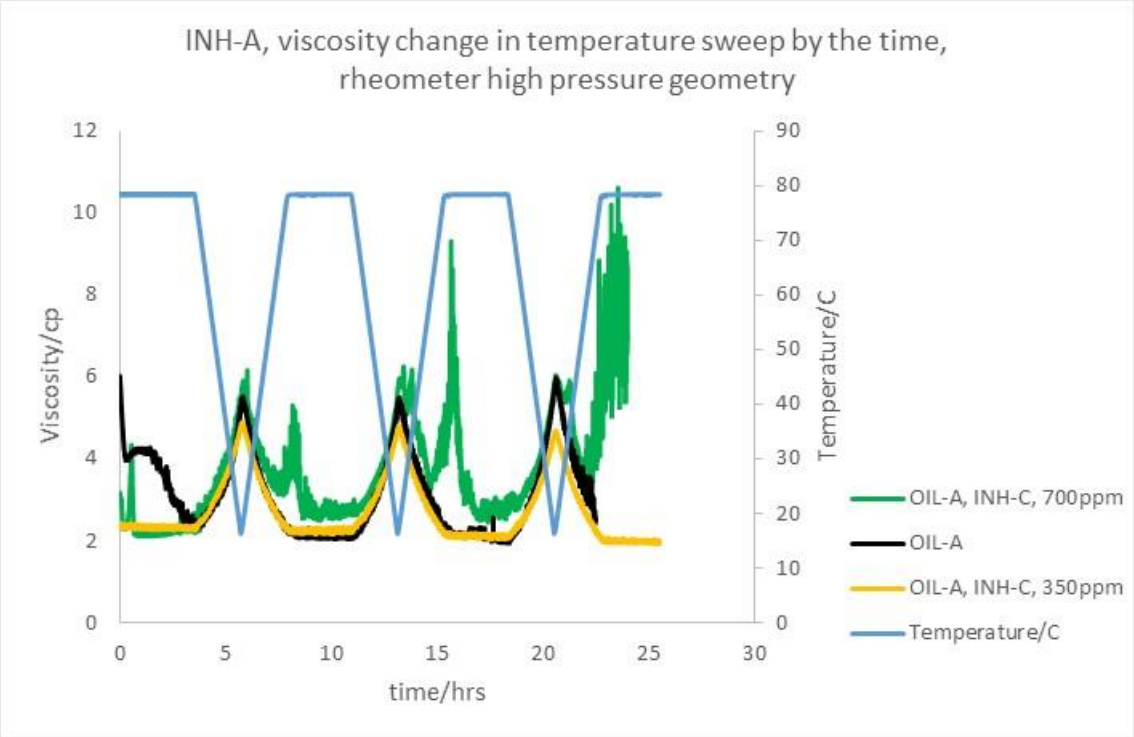

Figure 5-5. Variation of viscosity in temperature sweep measured with rheometer using OIL-A dosed with INH-C at two different dose rates. The legend ranked top to bottom based on decreasing overall viscosity.

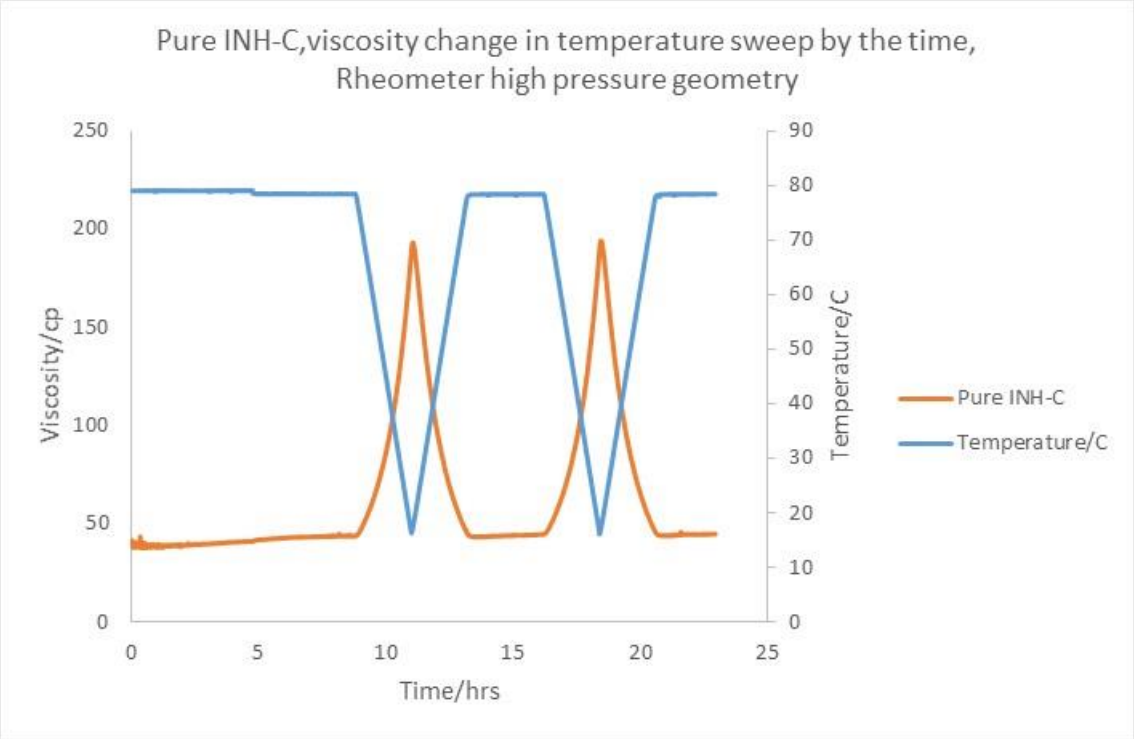

Figure 5-6. Variation of viscosity in the temperature sweep measured with rheometer used pure INH-C inhibitor.

5.2.3 Pour point evaluation using atmospheric cone and plate geometry

Pour point reduction provides a reference to evaluate the effectiveness of inhibitors. The reduction leads to higher production rates hence lower energy costs for operation [5]. A successful approach was used to measure pour point with an accuracy of ±0.2°C using the rheometer (detailed in section 3.3.3.3.3). The procedure was discussed in detail in Chapter 3. Table 5-4 summarises the experimental conditions and results of the pour points measured using the rheometer. The tabulated data was ranked from top to bottom for each individual oil sample based on decreasing pour point. The conditioning temperature was determined with the rheometer as described in the last chapter. The final temperature was chosen to be sufficiently low to reach the pour point temperature. Frequency and amplitude torque were set at 1.59 Hz and 25 µNm respectively to obtain a reliable result comparable with ASTM D-97 (section 3.3.3.3.3) [6].

Table 5-4. The test conditions and results of rheometer tests with oscillation mode, using different oil samples dosed with various inhibitors, ranked top to bottom based on decreasing pour point for each oil sample

Fluid	*Condition T (°C)*	*Destination T (°C)*	*Cooling rate (°C/min)*	*Angular frequency (rad/s)*	*Frequency (Hz)*	*Amplitude, Torque (μNm)*	*pour point (°C)*
OIL-A	60	-25	1	10	1.59	25	-14.5
OIL-A	60	-25	1	10	1.59	25	-14.6
OIL-A, INH-E, 400ppm	60	-25	1	10	1.59	25	-19.5
OIL-A, INH-F, 400ppm	60	-25	1	10	1.59	25	-21.4
OIL-A, INH-G, 400ppm	60	-25	1	10	1.59	25	-21.4
OIL-A, INH-D, 100ppm	60	-25	1	10	1.59	25	-21.4
OIL-A, INH-C, 350ppm	60	-25	1	10	1.59	25	-23.1
OIL-A, INH-A, 250ppm	60	-25	1	10	1.59	25	-24
OIL-A, INH-B, 200ppm	60	-25	1	10	1.59	25	-25
OIL-B, INH-A, 250ppm	60	-10	1	10	1.59	25	15.9
OIL-B	60	-10	1	10	1.59	25	14.2
OIL-B, INH-B, 200ppm	60	-10	1	10	1.59	25	7.19
OIL-B, INH-I, 600ppm	60	-10	1	10	1.59	25	0.52
OIL-B, INH-D, 100ppm	60	-10	1	10	1.59	25	-1.98
OIL-B, INH-J, 400ppm	60	-20	1	10	1.59	25	-7.63
OIL-B, INH-F, 400ppm	60	-20	1	10	1.59	25	-7.79
OIL-B, INH-E, 400ppm	60	-20	1	10	1.59	25	-14.1
OIL-B, INH-C, 350ppm	60	-20	1	10	1.59	25	-17.9
OIL-B, INH-G, 400ppm	60	-25	1	10	1.59	25	-23
OIL-C	50	-20	1	10	1.59	25	-5.29
OIL-C, INH-B, 200ppm	50	-20	1	10	1.59	25	-5.29
Continued Table 5-4 ***ppm***	50	-20	1	10	1.59	25	-8.95
OIL-C, INH-A, 250ppm	50	-20	1	10	1.59	25	-9.95
OIL-C, INH-H, 800ppm	50	-20	1	10	1.59	25	-12.3
OIL-C, INH-D, 100ppm	50	-20	1	10	1.59	25	-13
OIL-C, INH-F, 400ppm	50	-25	1	10	1.59	25	-21
OIL-C, INH-E, 400ppm	50	-25	1	10	1.59	25	-22.5
OIL-C, INH-C, 350ppm	50	-25	1	10	1.59	25	-23.6
OIL-C, INH-G, 400ppm	50	-25	1	10	1.59	25	-25

Figure 5-7 shows an example of the behaviour of deflection angle in oscillation mode with OIL-B dosed with different inhibitors. The legend was ranked top to bottom based on increasing overall deflection angle and decreasing pour point. Deflection angles showed almost the same curvature trend in the Newtonian region above WAT, here 35°C, and start to deviate below the cloud point temperature where wax particles form and drop out of bulk oil. As discussed it in Chapter 3, higher deflection angle represents low resistance flow, hence lower pour point.

For all measurements in this work using oscillation with different inhibitor dosage and even in various starting conditioning temperature, it was observed that deflection angle dropped down by about 20-30mrad at around 460mrad. There was no apparent reason for this behaviour and it most probably related to the rheometer setup.

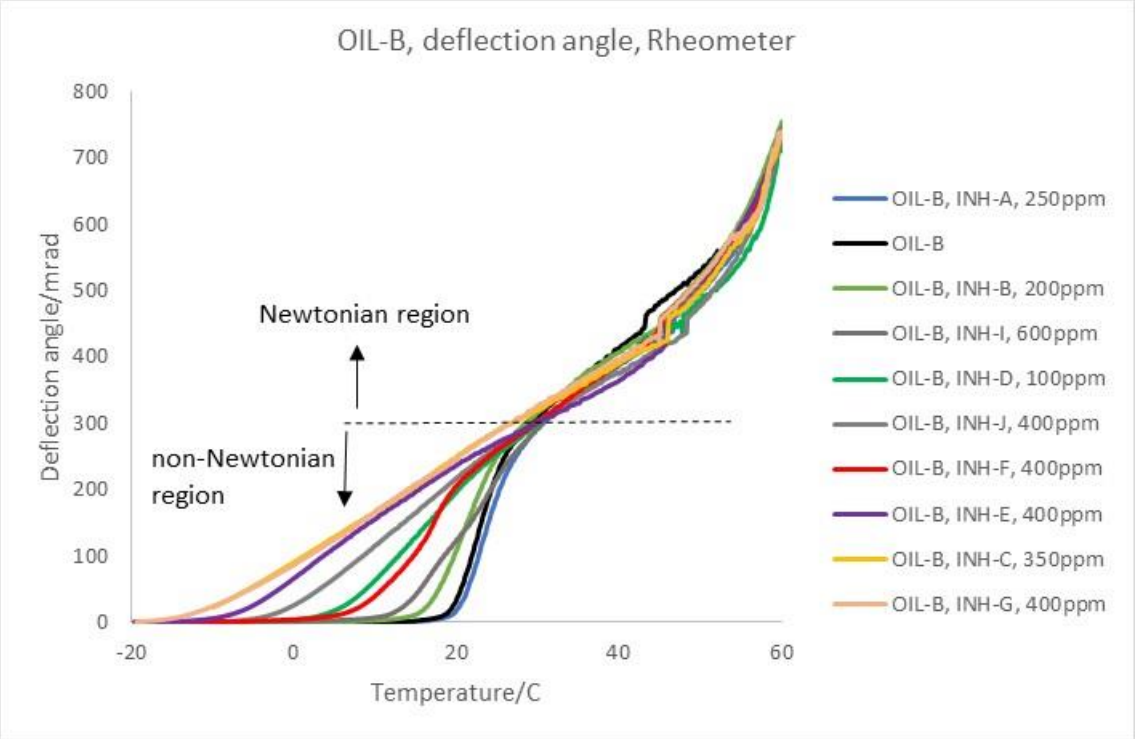

Figure 5-7. Deflection angle variation of oscillation in temperature sweep measured with rheometer using OIL-B dosed with different inhibitors. The legend is ranked top to bottom based on increasing overall deflection angle and decreasing pour point.

Pour point ranked from top to bottom in Figure 5-8, Figure 5-9 and Figure 5-10, from left to right for OIL-A, OIL-B and OIL-C respectively. The maximum viscosity of each individual mixture dosed with inhibitor are also plotted. The right-hand axis represents the viscosity in cP and left axis the pour point temperature in degree Celsius. The pour point measured for OIL-D sample was obtained at -22°C which was near the lower limit of the rheometer range, -25°C, so OIL-D was not measured as when dosed with an inhibitor it was expected to show lower pour point. All measured inhibitors reduced pour point in all three samples with the same rank as viscosity. As shown in Figure 5-8, there was a large difference between the pour point of the blank OIL-A and WAT at about 47°C which translate uneven distribution of components. It shows that OIL-A contains some component with high carbon number comes out in the high temperature while the whole wax content is quite low became solid in very low temperature. Since the instability of pour point obtained by rheometer was about ±0.2°C, it was then possible to evaluate inhibitors in low wax content oil such as OIL-A in terms of pour point reduction. The highest reduction for OIL-A was obtained with INH-B by about a 10°C. The same ranking class as described in viscosity could be observed in mixtures with OIL-B and OIL-C. The largest reductions in pour point were 19.71°C and 37.2°C achieved by adding inhibitors INH-G to the oil samples OIL-B and OIL-C respectively.

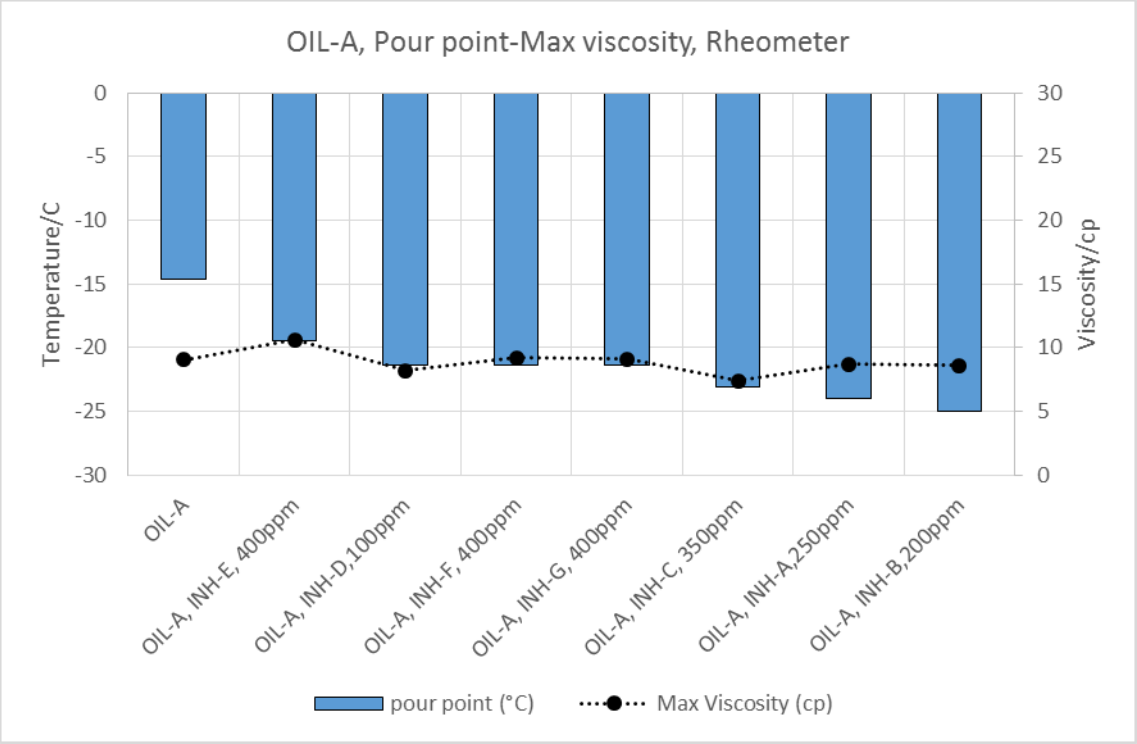

Figure 5-8. Comparison of pour point and maximum viscosity measured with the rheometer using OIL-A dosed with different inhibitors. The plot ranked from left to right based on decreasing pour point.

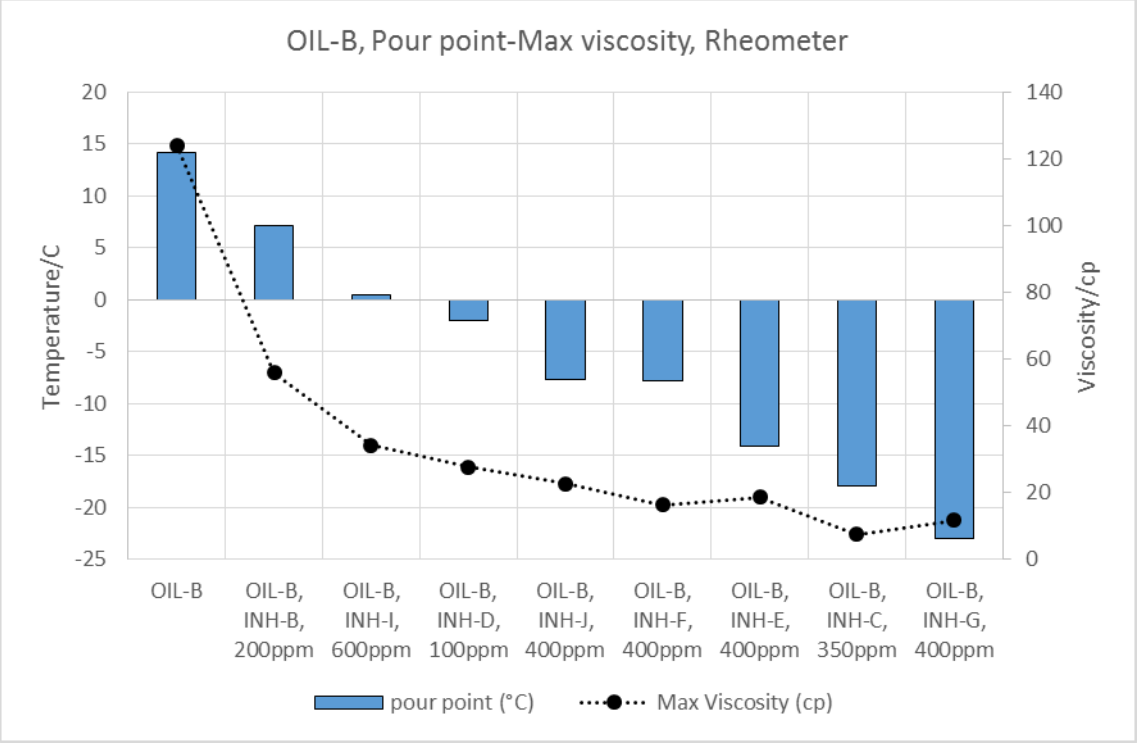

Figure 5-9. Comparison of pour point and the maximum viscosity measured with the rheometer used OIL-B oil sample dosed with different inhibitors. The plot ranked from left to right based on decreasing pour point.

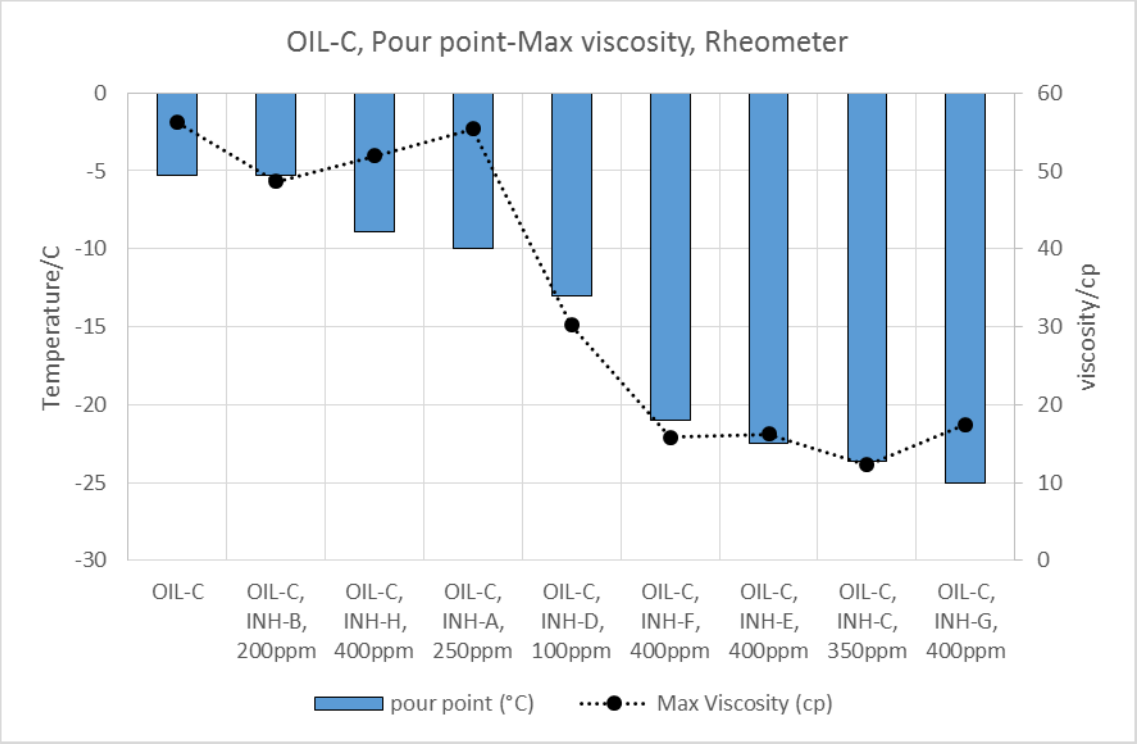

Figure 5-10. Comparison of pour point and maximum viscosity measured with the rheometer using OIL-C dosed with different inhibitors. The plot ranked from left to right based on decreasing pour point.

5.3 QCM technique

One function of wax inhibitors is to reduce the adhesion tendency of the wax solids to the pipe wall. It was noted earlier, QCM has the ability to measure adhesion tendency to the surface by reduction the resonant frequency (RF). Therefore, a reduction in overall ΔRF would be an indicative of reduced wax formation, or an indication that the wax formed has a lesser degree of agglomeration which could be assessed the influence of inhibitors. However, the value of ΔRF does not necessarily directly correlate with wax deposition, so a comparison of ΔRF cannot be used to determine or quote a percentage reduction in a wax deposition [7].

The aim of this section was to compare WAT obtained by QCM with NIR and rheometer which will be discussed later in this chapter. In addition, the relation between WAT and resonant frequency drop was investigated. Moreover, resonant frequency drop as an indication of wax deposition was compared with viscosity in each individual treated sample.

Table 5-5 to Table 5-8 list all the experimental conditions and results for two different QCM surface conducted at the same time in different thermal cycles. Conditioning

temperatures were calculated by rheometer as discussed in Chapter 3. The conditioning time for each cycle was 1, 2 and 3 hrs for OIL-A, both OIL-(C-D) and OIL-B respectively. This time was found by trial and error which was a sufficient time to dissolve the majority of precipitated wax particles remaining in previous cycles to get a reasonably repeatable frequency drop. Destination temperature for oil samples was set at 15°C except for OIL-C which was set at 5°C well below WAT point to see a clear RF drop. In addition, the average and standard deviation of WAT/WDT and frequency drop for both QCM in all cycles were tabulated. Frequency was very sensitive to the roughness of QCM surface, any scratch on the surface would change it significantly. That's why all measurements were performed with two different QCM for comparison purposes. The average overall uncertainty for all measurements with two different QCM and several consecutive cycles were 0.5°C, 1.2°C and 1600Hz for WAT, WDT and frequency drop respectively. The uncertainty for resonant frequency was measured for consecutive cycles. Thermal cycles might have an impact on the crystal morphology. Since resonant frequency is directly related to the morphology of crystals, the deviation of resonant frequency was quite high. Impurities also were found to have a significant effect on the reading, especially for frequency drop in the first and the other cycles in OIL-A. This will be discussed in the next chapter.

Table 5-5. The results and test conditions for both QCM using OIL-A dosed with different inhibitors. Conditioning time for each cycle was 1hr, and the cooling/heating rate was 0.5°C/min

Fluid	***Cycle***	***Conditioning T (°C)***	***Destination T (°C)***	***WAT1 (°C)***	***WAT2 (°C)***	***WDT1 (°C)***	***WDT2 (°C)***	***Maximum ΔRF1 (Hz)***	***Maximum ΔRF2 (Hz)***
OIL-A	1	60	15	33.2	32.9	51.5	47.9	-7686	-6974
	2	60	15	33.4	33.9	54.1	54.1	-15179	-17133
	3	60	15	33.4	33.7	55.4	55.8	-16641	-19197
	4	60	15	33.7	34.0	55.6	56.7	-17343	-19792
	average			***33.4***	***33.6***	***54.2***	***53.6***	***-14212***	***-15774***
	st.dev			***0.2***	***0.5***	***1.9***	***4.0***	***4443***	***5976***
OIL-A, INH-F, 400ppm	1	60	15	32.9	33.4	56.7	50.9	-7938	-3591
	2	60	15	33.9	34.3	57.3	56.8	-10611	-9921
	3	60	15	34.8	34.2	57.4	57.1	-11610	-13622
	4	60	15	34.4	34.4	58.0	57.3	-12565	-15385
	average			***34.0***	***34.1***	***57.4***	***55.5***	***-10681***	***-10630***
	st.dev			***0.8***	***0.5***	***0.5***	***3.1***	***1995***	***5216***
OIL-A, INH-E, 400ppm	1	60	15	25.7	25.7	29.8	24.2	-1329	-1255
	2	60	15	24.7	25.0	28.7	27.1	-2269	-2151
	3	60	15	25.3	24.4	27.3	25.0	-2327	-1843
	4	60	15	26.1	24.6	29.2	24.8	-2350	-1689
	average			***25.5***	***24.9***	***28.8***	***25.3***	***-2069***	***-1735***
	st.dev			***0.6***	***0.6***	***1.1***	***1.3***	***494***	***373***

Continued Table 5-5

Fluid	*Cycle*	*Conditioning T (°C)*	*Destination T (°C)*	*WAT1 (°C)*	*WAT2 (°C)*	*WDT1 (°C)*	*WDT2 (°C)*	*Maximum ΔRF1 (Hz)*	*Maximum ΔRF2 (Hz)*
OIL-A, INH-G, 400ppm	1	60	15	26.3	25.9	32.7	31.2	-1483	-1136
	2	60	15	25.4	25.7	36.0	31.8	-2357	-1718
	3	60	15	26.2	25.4	35.3	31.1	-2283	-1889
	4	60	15	25.6	25.6	33.4	33.7	-2320	-1900
	average			***25.9***	***25.7***	***34.4***	***32.0***	***-2111***	***-1661***
	st.dev			***0.44***	***0.21***	***1.6***	***1.2***	***420***	***360***
OIL-A, INH-C,350ppm	1	60	15	29.0	27.5	31.2	28.3	-2939	-2047
	2	60	15	26.6	26.3	33.6	30.9	-3378	-2719
	3	60	15	26.4	26.4	34.0	30.0	-2908	-2386
	4	60	15	27.3	26.8	34.5	26.8	-3172	-2629
	average			***27.3***	***26.8***	***33.3***	***29.0***	***-3099***	***-2445***
	st.dev			***1.2***	***0.5***	***1.5***	***1.8***	***220***	***300***
OIL-A, INH-A,250ppm	1	60	15	32.3	32.0	55.5	54.0	-7325	-6782
	2	60	15	32.9	32.7	55.0	54.1	-14599	-12587
	3	60	15	33.3	33.3	55.7	54.9	-15899	-13732
	4	60	15	33.4	33.4	56.3	55.1	-17243	-14973
	average			***33.0***	***32.9***	***55.6***	***54.5***	***-13767***	***-12019***
	st.dev			***0.5***	***0.6***	***0.5***	***0.6***	***4428***	***3624***
OIL-A, INH-D, 100ppm	1	60	15	32.5	32.5	57.3	56.9	-10215	-11537
	2	60	15	33.7	32.7	56.2	54.6	-16141	-16222
	3	60	15	33.1	33.1	56.1	55.4	-17485	-18124
	4	60	15	33.4	33.3	----	----	-19101	-19115
	average			***33.2***	***32.9***	***56.5***	***55.6***	***-15736***	***-16250***
	st.dev			***0.5***	***0.4***	***0.7***	***1.2***	***3874***	***3363***
OIL-A, INH-B, 200ppm	1	60	15	32.1	31.8	58.2	56.9	-13255	-10856
	2	60	15	31.8	32.1	58.5	57.8	-16185	-16185
	3	60	15	32.7	32.5	58.1	58.3	-16442	-17390
	4	60	15	32.5	32.2	----	----	-16574	-17713
	average			***32.3***	***32.2***	***58.3***	***57.7***	***-15614***	***-15536***
	st.dev			***0.4***	***0.3***	***0.2***	***0.7***	***1581***	***3189***

Table 5-6. The results and test conditions for both QCM using OIL-B dosed with different inhibitors. Conditioning time for each cycle was 3hr, and the cooling ramp was 0.5°C/min

Fluid	*Cycle*	*Conditioning T (°C)*	*Destination T (°C)*	*WAT1 (°C)*	*WAT2 (°C)*	*WDT1 (°C)*	*WDT2 (°C)*	*Maximum ΔRF1 (Hz)*	*Maximum ΔRF2 (Hz)*
OIL-B-1	1	60	15	28	28.6	50.4	52.3	-12793	-14340
	2	60	15	28.4	29.6	50.1	51.9	-12237	-15714
	3	60	15	28.3	29.9	51	52.1	-11921	-17228
	4	60	15	29.1	29.9	50.3	52.9	-11877	-18109
	average			***28.5***	***29.5***	***50.5***	***52.3***	***-12207***	***-16347***
	st.dev			***0.5***	***0.6***	***0.4***	***0.4***	***422***	***1664***
OIL-B-2	1	60	15	----	28.6	52.9	52.1	-10383	-14729
	2	60	15	----	29.3	53.1	51.1	-7660	-16118
	3	60	15	----	29.5	53.6	51.2	-7458	-17076
	4	60	15	----	29.9	52.9	51.6	-7575	-17807
	average			***----***	***29.3***	***53.1***	***51.5***	***-8269***	***-16432***
	st.dev			***----***	***0.5***	***0.3***	***0.5***	***1411***	***1329***
OIL-B-3	1	60	15	29.3	29	50.7	51.7	-12419	-15054
	2	60	15	28.1	29.9	52.2	51.1	-12476	-16142

Continued Table 5-6

Fluid	*Cycle*	*Conditioning T (°C)*	*Destination T (°C)*	*WAT1 (°C)*	*WAT2 (°C)*	*WDT1 (°C)*	*WDT2 (°C)*	*Maximum ΔRF1 (Hz)*	*Maximum ΔRF2 (Hz)*
	3	60	15	28.2	30.3	51.9	51.9	-11634	-17003
	4	60	15	28.3	29.9	50.8	51.6	-11018	-17722
	5	60	15	28.3	30.7	----	----	-10805	-18543
	average			***28.4***	***30.0***	***51.4***	***51.6***	***-11670***	***-16892***
	st.dev			***0.5***	***0.6***	***0.8***	***0.3***	***772***	***1357***
OIL-B, INH-J, 400ppm	1	60	15	23.9	24.2	39.3	46.9	-1703	-2713
	2	60	15	24.2	24.2	38.5	48.9	-1710	-3751
	3	60	15	24.6	24.6	38.1	48.8	-1742	-4728
	average			***24.2***	***24.3***	***38.6***	***48.2***	***-1718***	***-3730***
	st.dev			***0.4***	***0.2***	***0.6***	***1.1***	***20***	***1007***
OIL-B, INH-C, 350ppm	1	60	15	22	22.4	29.5	29	-1530	-2146
	2	60	15	22.6	22.4	32.4	32.4	-1636	-2380
	3	60	15	22.6	22.9	37.1	32.4	-1678	-2316
	average			***22.4***	***22.6***	***33.0***	***31.3***	***-1614***	***-2280***
	st.dev			***0.3***	***0.3***	***3.8***	***2.0***	***76***	***120***
OIL-B, INH-I, 600ppm	1	60	15	28.6	28.6	49.8	50.5	-10597	-13796
	2	60	15	28.3	28.7	46.9	50.6	-7366	-13572
	3	60	15	27.7	29	48.4	49.2	-5822	-14726
	4	60	15	27.7	29.5	50	49.7	-5206	-14881
	average			***28.1***	***29.0***	***48.8***	***50.0***	***-7247***	***-14243***
	st.dev			***0.5***	***0.4***	***1.4***	***0.7***	***2410***	***655***
OIL-B, INH-B, 200ppm	1	60	15	----	27	----	50	----	-11054
	2	60	15	27.7	27.2	48	52.7	-3570	-12526
	3	60	15	29.4	27.5	47.2	52.7	-3176	-14269
	4	60	15	29.9	27.8	47.1	53.2	-3051	-15525
	average			***29.0***	***27.4***	***47.4***	***52.2***	***-3265***	***-13343***
	st.dev			***1.2***	***0.4***	***0.5***	***1.5***	***270***	***1960***
OIL-B, INH-D,100ppm	1	60	15	24.8	25.1	41.1	38.9	-2261	-4739
	2	60	15	24	25.5	38.9	38.9	-2826	-6045
	3	60	15	25.3	26.1	40	42.3	-4398	-8357
	4	60	15	26.1	26.6	39.8	39	-3325	-6575
	5	60	15	24.8	27.2	34.9	47	-3814	-9509
	average			***25.0***	***26.1***	***38.9***	***41.2***	***-3324***	***-7045***
	st.dev			***0.8***	***0.8***	***2.4***	***3.5***	***832***	***1892***
OIL-B, INH- A, 250ppm	1	60	15	24.6	26.7	41.8	48.5	-4196	-13436
	2	60	15	24.3	27.4	----	49.4	-3463	-13982
	3	60	15	24.6	28.5	43.4	49.9	-3853	-15087
	4	60	15	25.2	28.5	44	48.6	-3474	-15618
	average			***24.7***	***27.8***	***43.1***	***49.1***	***-3746***	***-14530***
	st.dev			***0.4***	***0.9***	***1.1***	***0.7***	***350***	***998***
OIL-B, INH-G, 400ppm	1	60	15	21.9	21.9	28.4	25.8	-1109	-1230
	2	60	15	21.9	22.1	25.8	24.8	-1196	-1339
	3	60	15	22.5	22.4	26.6	24.9	-1205	-1401
	4	60	15	23.3	22.5	28.8	25.2	-1231	-1428
	average			***22.4***	***22.2***	***27.4***	***25.2***	***-1185***	***-1349***
	st.dev			***0.7***	***0.3***	***1.4***	***0.5***	***53***	***87***
OIL-B, INH-F, 400ppm	1	60	15	26.9	27.1	46.2	46.5	-2103	-2550
	2	60	15	25.2	26.2	47.1	42.8	-1326	-2274
	3	60	15	25	26.1	48.5	43.2	-1150	-2086
	4	60	15	25.2	25.5	45.4	44.3	-1132	-2075
	5	60	15	25.1	25.6	46.7	----	-1140	-2053
	average			***25.5***	***26.1***	***46.8***	***44.2***	***-1370***	***-2207***
	st.dev			***0.8***	***0.6***	***1.2***	***1.7***	***417***	***210***
OIL-B, INH-E, 400ppm	1	60	15	20.6	21.8	21.5	21.8	-742	-833
	2	60	15	21.1	20.8	21.9	20.8	-778	-953

Continued Table 5-6

Fluid	*Cycle*	*Conditioning T (°C)*	*Destination T (°C)*	*WAT1 (°C)*	*WAT2 (°C)*	*WDT1 (°C)*	*WDT2 (°C)*	*Maximum ΔRF1 (Hz)*	*Maximum ΔRF2 (Hz)*
	3	60	15	21.5	22.3	21.8	22.3	-879	-1033
	4	60	15	22.2	21.7	25	21.7	-915	-1024
	5	60	15	22.1	22.1	24.4	22.1	-960	-1091
	average			***21.5***	***21.7***	***22.9***	***21.7***	***-854***	***-986***
	st.dev			***0.7***	***0.6***	***1.6***	***0.6***	***92***	***99***
OIL-B, INH-H, 400ppm	1	60	15	28.1	----	49.8	----	-17253	----
	2	60	15	28.3	----	49.5	----	-19398	----
	3	60	15	28.6	----	49.3	----	-21052	----
	4	60	15	28.8	----		----	-21638	----
	average			***28.5***	----	***49.5***	----	***-19835***	----
	st.dev			***0.3***	----	***0.3***	----	***1965***	----

Table 5-7. The results and test conditions for both QCM using OIL-C dosed with different inhibitors. Conditioning time for each cycle was 2hrs, and the cooling ramp was 0.5°C/min

Fluid	*Cycle*	*Conditioning T (°C)*	*Destination T (°C)*	*WAT1 (°C)*	*WAT2 (°C)*	*WDT1 (°C)*	*WDT2 (°C)*	*Maximum ΔRF1 (Hz)*	*Maximum ΔRF2 (Hz)*
OIL-C-1	1	50	5	26.2	27.5	41.9	42.8	-13140	-14204
	2	50	5	26.6	26.5	43	42.2	-13690	-14308
	3	50	5	26.8	27.1	41.6	42.7	-13877	-14161
	4	50	5	27.2	27.5	41.6	40.2	-13731	-13788
	5	50	5	27.5	27.7	41.2	40.3	-13341	-12845
	6	50	5	26.3	28.1	39.4	40.8	-12935	-12901
	average			***26.8***	***27.4***	***41.5***	***41.5***	***-13452***	***-13701***
	St.dev			***0.5***	***0.5***	***1.2***	***1.2***	***372***	***665***
OIL-C-2	1	50	5	27.5	----	47.9	----	-18926	----
	2	50	5	27.8	----	48.2	----	-20689	----
	3	50	5	28.2	----	48.1	----	-21492	----
	4	50	5	28.3	----	47.9	----	-21994	----
	5	50	5	28.4	----	47.7	----	-22433	----
	6	50	5	28.5	----	47.4	----	-22433	----
	average			***28.1***	----	***47.9***	----	***-21328***	----
	St.dev			***0.4***	----	***0.3***	----	***1348***	----
OIL-C, INH-C, 350ppm	1	50	5	20	20.2	25.4	21.8	-17030	-15665
	2	50	5	19	19.4	33.6	25.5	-14259	-15021
	3	50	5	19.6	21.1	35.5	33.9	-23131	-15201
	4	50	5	20.3	21.1	38.1	34.4	-23310	-17623
	5	50	5	21.6	21.8	38	34.9	-22920	-17322
	average			***20.1***	***20.7***	***34.1***	***30.1***	***-20130***	***-16166***
	St.dev			***1.0***	***0.9***	***5.2***	***6.0***	***4213***	***1220***
OIL-C, INH-B, 200ppm	1	50	5	23.7	23.7	43.9	42.1	-15297	-16596
	2	50	5	24.2	24	42.3	41.7	-17273	-16675
	3	50	5	24	23.7	41.8	41.8	-16974	-16031
	4	50	5	24	24	39.7	42.3	-16539	-15342
	average			***24.0***	***23.9***	***41.9***	***42.0***	***-16521***	***-16161***
	St.dev			***0.2***	***0.2***	***1.7***	***0.3***	***870***	***617***
OIL-C, INH-A, 250ppm	1	50	5	25.9	25.9	43.6	38.9	-17736	-15805
	2	50	5	25.2	26.3	43.1	35.7	-18011	-16117
	3	50	5	25	26.7	41.7	36	-15737	-15538
	4	50	5	25.1	27.5	43	39.7	-17487	-14545

Continued Table 5-7

Fluid	*Cycle*	*Conditioning T (°C)*	*Destination T (°C)*	*WAT1 (°C)*	*WAT2 (°C)*	*WDT1 (°C)*	*WDT2 (°C)*	*Maximum ΔRF1 (Hz)*	*Maximum ΔRF2 (Hz)*
	5	50	5	26.3	27.7	----	36	-22074	-14378
	average			***25.5***	***26.8***	***42.9***	***37.3***	***-18209***	***-15277***
	St.dev			***0.6***	***0.8***	***0.8***	***1.9***	***2336***	***774***
OIL-C, INH-D, 100ppm	1	50	5	23.8	23.8	42.3	41.9	-15294	-14357
	2	50	5	23.4	25.2	43.1	40.5	-16038	-12665
	3	50	5	23.2	23.7	43.4	42.4	-15505	-12542
	4	50	5	23.3	23.5	43.4	39	-15080	-12480
	5	50	5	23.2	23.2	----	----	-14554	-14454
	average			***23.4***	***23.9***	***43.1***	***41.0***	***-15294***	***-13300***
	St.dev			***0.2***	***0.8***	***0.5***	***1.5***	***546***	***1012***
OIL-C, INH-E, 400ppm	1	50	5	18.7	17.4	19.9	18	-2666	-1946
	2	50	5	17.5	18.5	19.1	21.5	-2836	-2718
	3	50	5	19	18.7	19.4	22.9	-3269	-3779
	4	50	5	18.8	18.7	19.6	25.2	-4230	-6100
	5	50	5	19.5	19.7	20.4	29.2	-5021	-7784
	6	50	5	19.9	19.1	21.7	33.6	-6054	-9343
	average			***18.9***	***18.7***	***20.0***	***25.1***	***-4013***	***-5278***
	St.dev			***0.8***	***0.8***	***0.9***	***5.6***	***1340***	***2946***
OIL-C, INH-F, 400ppm	1	50	5	26	24.87	44.9	38	-27185	-26900
	2	50	5	26	25.5	42.6	40.1	-26622	-22800
	3	50	5	25.6	25.1	42.4	39.4	-22055	-19209
	4	50	5	26.8	25.4	42.6	39.3	-20825	-17662
	5	50	5	26.3	25	----	----	-20435	-16131
	average			***26.1***	***25.2***	***43.1***	***39.2***	***-23424***	***-20540***
	St.dev			***0.4***	***0.3***	***1.2***	***0.9***	***3238***	***4332***
OIL-C, INH-G, 400ppm	1	50	5	20.2	22.2	25.5	32.9	-1324	-1470
	2	50	5	21.5	21.7	35.7	31.2	-1099	-1942
	3	50	5	23.3	24	35.1	33.1	-1009	-2170
	4	50	5	22.3	23.3	35.6	33.8	-1201	-1882
	5	50	5	24	22.9	----	----	-1193	-2156
	average			**22.3**	**22.8**	**33.0**	**32.8**	**-1165**	**-1924**
	St.dev			**1.5**	**0.9**	**5.0**	**1.1**	**118**	**284**
OIL-C, INH-H, 400ppm	1	50	5	27.3	----	49.2	----	-19936	----
	2	50	5	27.7	----	48.5	----	-22610	----
	3	50	5	28.2	----	48.5	----	-23380	----
	4	50	5	28.1	----	48	----	-24138	----
	average			***27.8***	----	***48.6***	----	***-22516***	----
	St.dev			***0.4***	----	***0.5***	----	***1830***	----

Table 5-8. The results and test conditions for QCM using OIL-D dosed with different inhibitors. Conditioning time for each cycle was 2hrs, and the cooling ramp was 0.5°C/min

Fluid	***Cycle***	***Conditioning T (°C)***	***Destination T (°C)***	***WAT (°C)***	***WDT (°C)***	***Maximum ΔRF (Hz)***
OIL-D	1	50	15	31.3	43.2	-34390
	2	50	15	31.5	42.3	-35102
	3	50	15	31.6	44.2	-35494
	4	50	15	31.6	44.4	-35684
	5	50	15	31.6	44.5	-36016
	average			***31.5***	***43.7***	***-35337***
	st.dev			***0.13***	***0.9***	***624***
OIL-D, INH-F, 400ppm	1	50	15	29.5	38.9	-5520
OIL-D, INH-C, 350ppm	1	50	15	30.1	41.9	-31575
OIL-D, INH-E, 400ppm	1	50	15	30.3	36.0	-3223
OIL-D, INH-G, 400ppm	1	50	15	27.0	32.0	-1069
OIL-D, INH-H, 400ppm	1	50	15	31.0	42.2	-29134
	2	50	15	30.8	41.2	-28143
	average			***30.9***	***41.7***	***-28638***
	st.dev			***0.14***	***0.71***	***701***
OIL-D, INH-B, 200ppm	1	50	15	31.2	45.3	-28421
	2	50	15	31.3	45.5	-29414
	3	50	15	31.2	44.5	-29533
	4	50	15	31.3	44.1	-29509
	average			***31.25***	***44.85***	***-29219***
	st.dev			***0.06***	***0.66***	***535***
OIL-D, INH-A, 250ppm	1	50	15	31.2	42.3	-28048
	2	50	15	31.3	43	-28262
	3	50	15	31.2	42.1	-28500
	4	50	15	31.2	42.8	-28749
	average			***31.2***	***42.5***	***-283890***
	st.dev			***0.05***	***0.4***	***302***
OIL-D, INH-D, 100ppm	1	50	15	30	37.8	-6387
	2	50	15	28.8	35.6	-10200
	3	50	15	27.7	37.2	-19997
	4	50	15	26.9	37.5	-23631
	average			***28.35***	***37.02***	***-15054***
	st.dev			***1.3***	***0.98***	***8097***
OIL-D, INH-D, 100ppm	1	50	15	30	35.3	-11880
	2	50	15	29.4	36.2	-18073
	average			***29.7***	***35.75***	***-14976***
	st.dev			***0.4***	***0.64***	***4379***

Figure 5-11 illustrates an example of frequency change in the presence of various inhibitors with OIL-B.

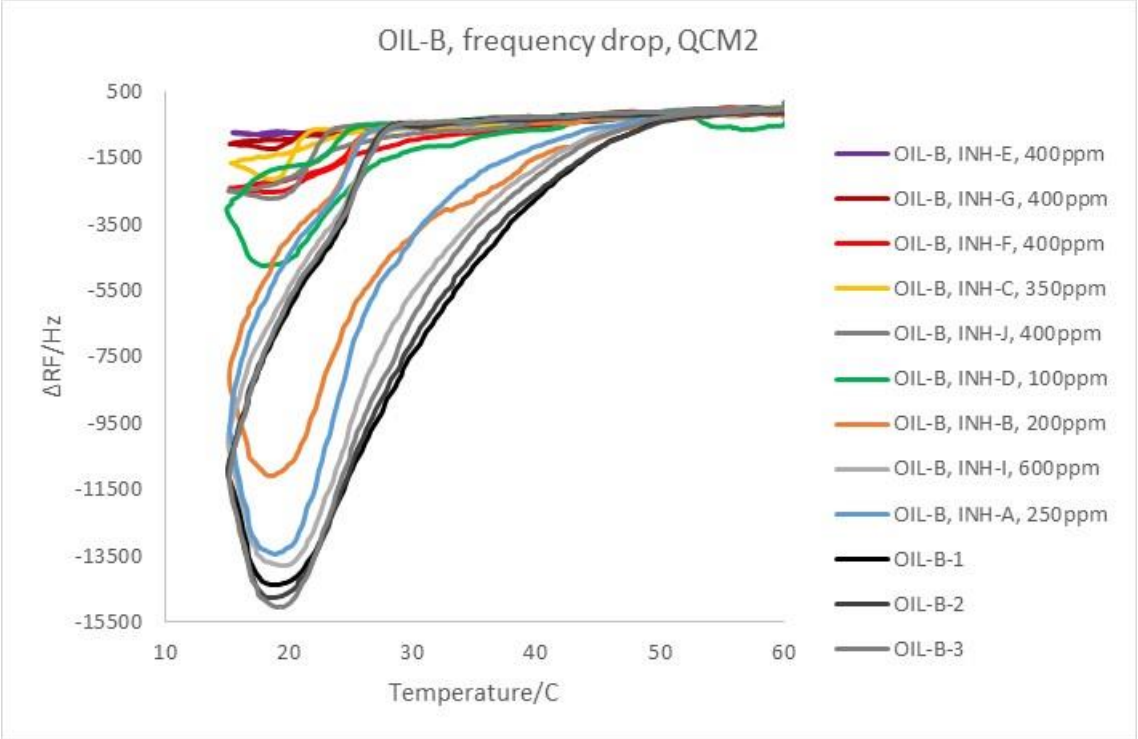

Figure 5-11. Frequency drop in the first cycle measured with QCM2 using OIL-B sample dosed with different inhibitors. The legend ranked top to bottom based on increasing average frequency drop of all runs

In order to improve visual observation for ranking the performance of inhibitors, only the average amount of both frequency drop in all thermal cycles as well as corresponded standard deviation are plotted in Figure 5-12 to Figure 5-15 for the mixtures prepared with OIL-A, OIL-B, OIL-C and OIL-D respectively. The maximum viscosity related to each mixture is also plotted.

As noted earlier in this chapter, viscosity evaluation is not a good way of inhibitor screening in a low viscous sample such as OIL-A. Resonant frequency behaviour, however, resulted a clear view in the presence of inhibitors as illustrated in Figure 5-12. There were only two inhibitors INH-B and INH-D that showed slightly higher frequency drop compared to the blank oil.

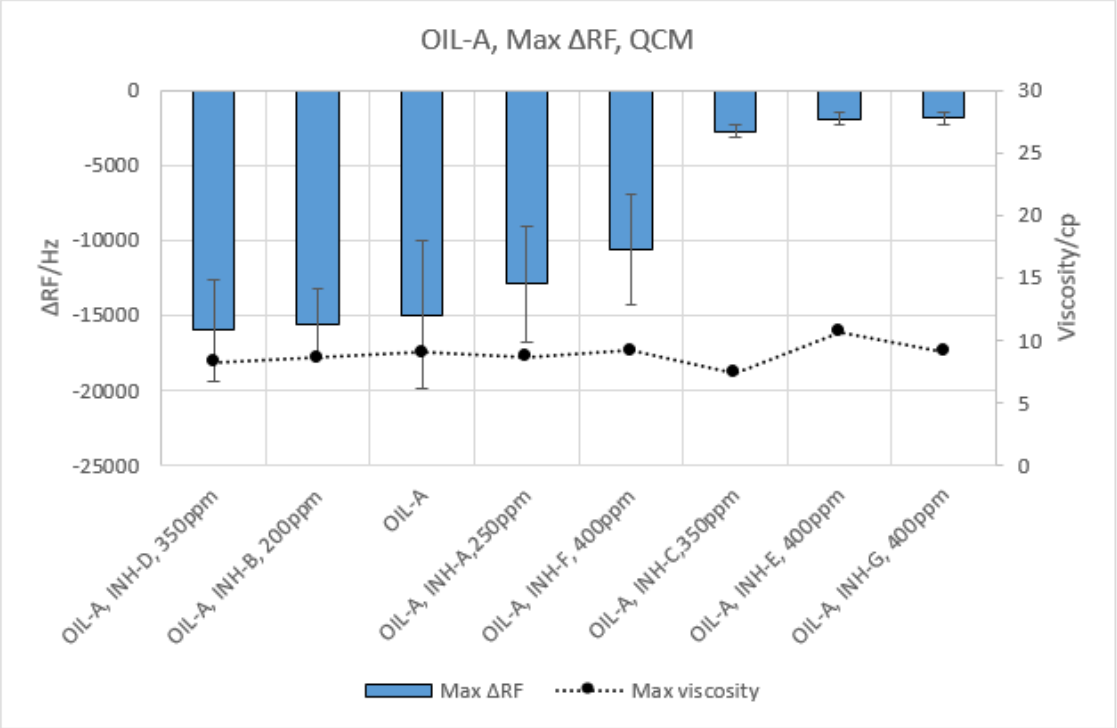

Figure 5-12. Comparison of average frequency reduction measured with two different QCM in several consecutive cycles with maximum viscosity measured by the rheometer using OIL-A dosed with various inhibitors. Plot ranked from left to right based on decreasing average frequency drop.

Figure 5-13, demonstrates a good match between viscosity reduction and decrease in frequency drop for the mixture prepared with OIL-B. The only inhibitor which had higher frequency reduction than blank was INH-H.

Mixtures with OIL-C and OIL-D in the overall trend, imitate the viscosity reduction with some exceptions as shown in Figure 5-14 and Figure 5-15.

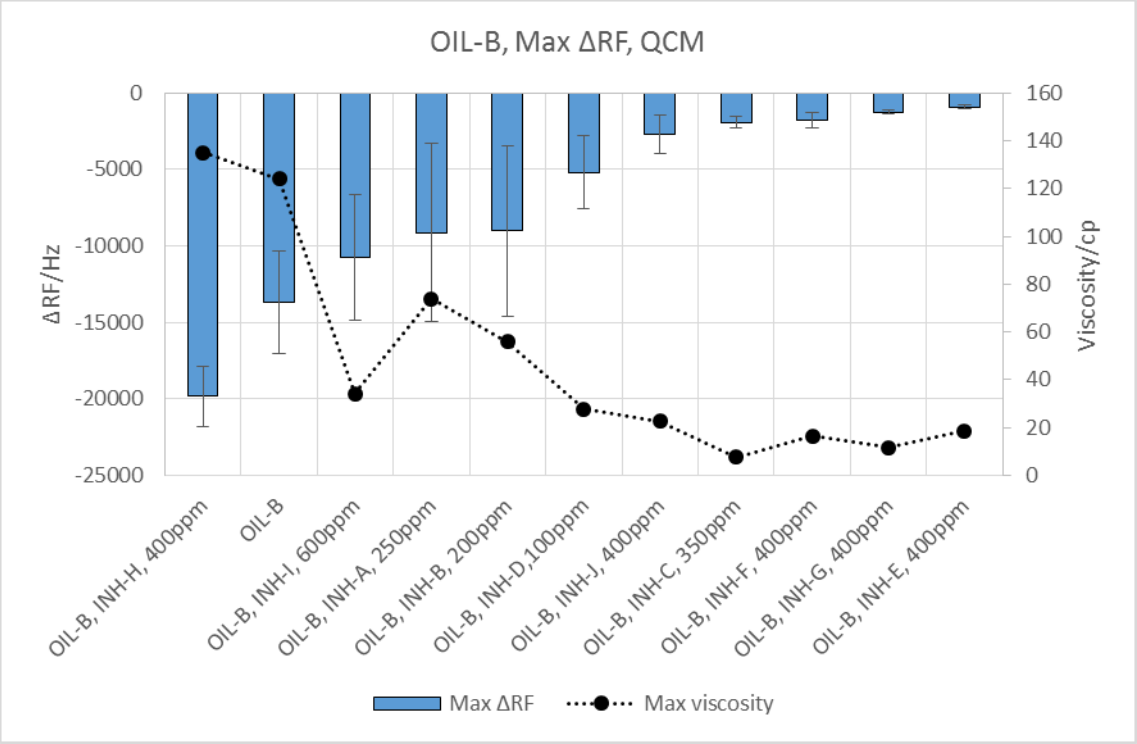

Figure 5-13. Comparison of average frequency reduction measured with two different QCM in several consecutive cycles with maximum viscosity measured by the rheometer using OIL-B sample dosed with various inhibitors. Plot ranked from left to right based on decreasing average frequency drop.

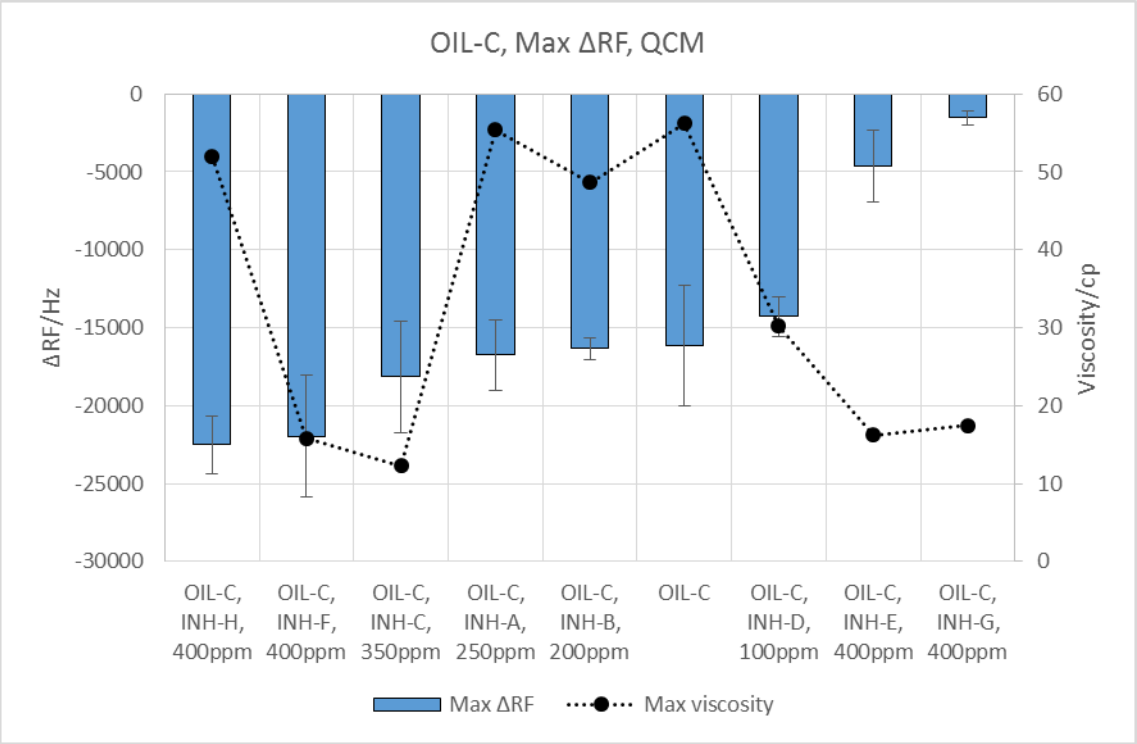

Figure 5-14. Comparison of average frequency reduction measured with two different QCM in several consecutive cycles with maximum viscosity measured by the rheometer using OIL-C sample dosed with various inhibitors. Plot ranked from left to right based on decreasing average frequency drop.

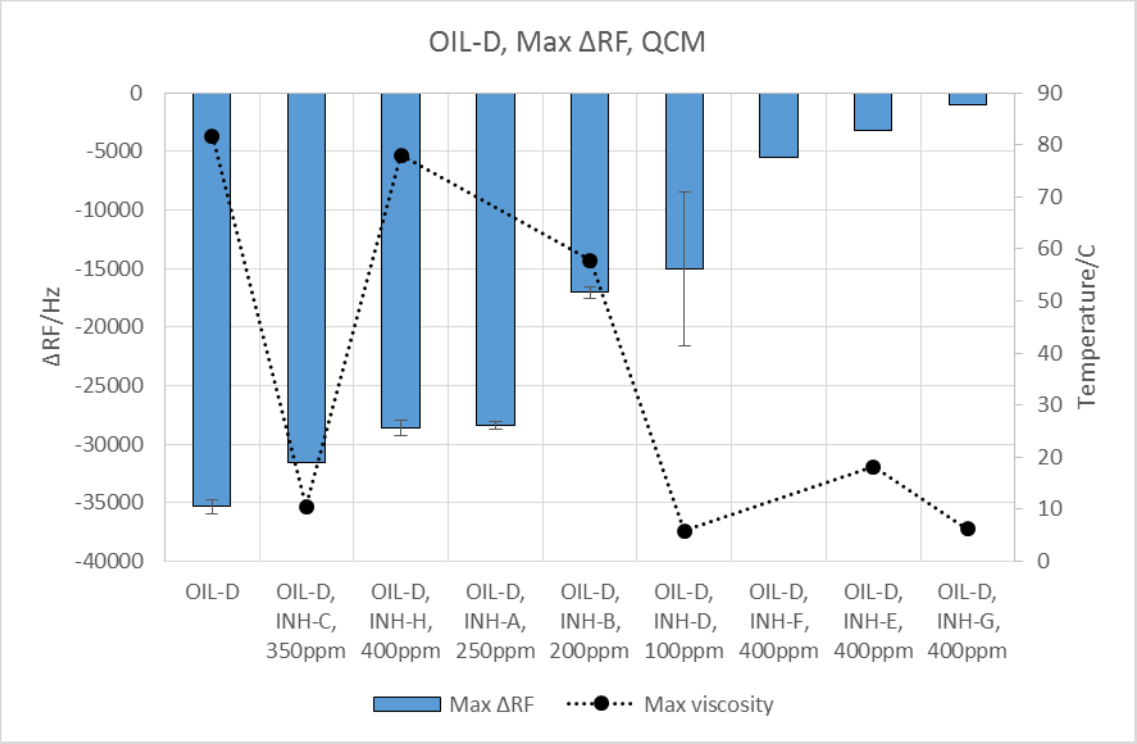

Figure 5-15. Comparison of average frequency reduction measured with two different QCM in several consecutive cycles with maximum viscosity measured by the rheometer using OIL-D sample dosed with various inhibitors. Plot ranked from left to right based on decreasing average frequency drop.

The lower viscosity coupled with lower frequency drop may be due to the fact that the presence of inhibitors might reduce the number of crystals in non-Newtonian region below WAT.

The performance of measured inhibitors in terms of their capability to reduce adhesion tendency (lower resonant frequency drop) to the surface can be categorised into three classes.

1. Significantly low-frequency drop, 2. Slightly lower or higher than blank, and 3. Higher drop than blank.

OIL-A:

Class1) INH- C, E, G

Class2) INH- A, B, D, F

OIL-B:

Class1) INH- C, D, E, F, G, J

Class2) INH- A, B, I

Class3) INH- H

OIL-C:

Class1) INH- E, G

Class2) INH- A, B, C, D, E

Class3) INH- F, H

OIL-D:

Class1) INH- B, D, E, F, G

Class2) INH- A, C, H

Overall, inhibitors INH-C, INH-E and INH-G were found to be the best in terms of adhesion tendency in all oil samples.

5.4 Coaxial cold finger

As explained in the Chapter 3, the coaxial cold finger set up is a modified and more realistic version of the standard cold finger imitate the pipeline to measure deposition with the capability of applied shear rate and controlled differential temperature. There is no fixed ageing time reported in literature, in terms of deposition measurement with coaxial. Test time for measuring deposition in other laboratory equipment has been reported in 3 to 40 hrs [3, 4, 7, 8].

As observed in preliminary measurements, low viscosity oil samples showed a high inconsistency with long ageing time using coaxial equipment, hence making it impossible to screen inhibitors. The first aim of this section was to calibrate the setup and find the best ageing time for waxy low viscous oils such as OIL-A, OIL-B and OIL-C. Three different ageing times were tested, 67hrs, 24hrs and 1hr. All tests were started with the same shear rate, $100s^{-1}$. As found in the section 4.4, the deposited mass in each test could be recycled several times which obtained reliable results if not to be contaminated with inhibitors. The recycled sample was named ‘’used’’ distinguishing it from the original ‘’fresh’’ sample. Oil samples were conditioned at a predetermined temperature obtained from rheometer, then cooled down to fixed temperature where it was held for the desired ageing time.

5.4.1 Evaluation of deposition after 67hrs ageing time

Table 5-9 presents the experimental condition and results of test measured at 67 hrs ageing time using OIL-A dosed with different inhibitors. The differential temperature was set at 40°C.

Table 5-9. Experimental conditions and the results of coaxial tests, using OIL-A dosed with different inhibitors in 67 hrs ageing time, ranked top to bottom based on decreasing deposited mass

Fluid	***Bulk T (°C)***	***Bobbin T (°C)***	***Ageing time (hrs)***	***Shear rate (s^{-1})***	***Deposited mass (gr)***
OIL-A (fresh)	45	5	67	100	5.4558
OIL-A (used)	45	5	67	100	4.5798
OIL-A, INH-A, 250ppm (used)	45	5	67	100	3.9859
OIL-A, INH-C, 350ppm (fresh)	45	5	67	100	3.8199
OIL-A, INH-B, 200ppm (fresh)	45	5	67	100	3.5875
OIL-A (used)	45	5	67	100	3.2927
OIL-A, INH-D, 100ppm (fresh)	45	5	67	100	3.2712

Figure 5-16 demonstrates mass deposition ranked left to right based on decreasing weight. The maximum differential resonant frequency (ΔRF) obtained from QCM is also plotted correspond to each mixture. The dashed line represents the minimum and maximum boundary of measured value for the blank OIL-A. Almost all values were ranked in this boundary, and there is no relation between coaxial and QCM data. It, therefore, seems impossible to screened inhibitors in 67hrs ageing time with applied shear rate $100s^{-1}$ and the temperature used in these tests.

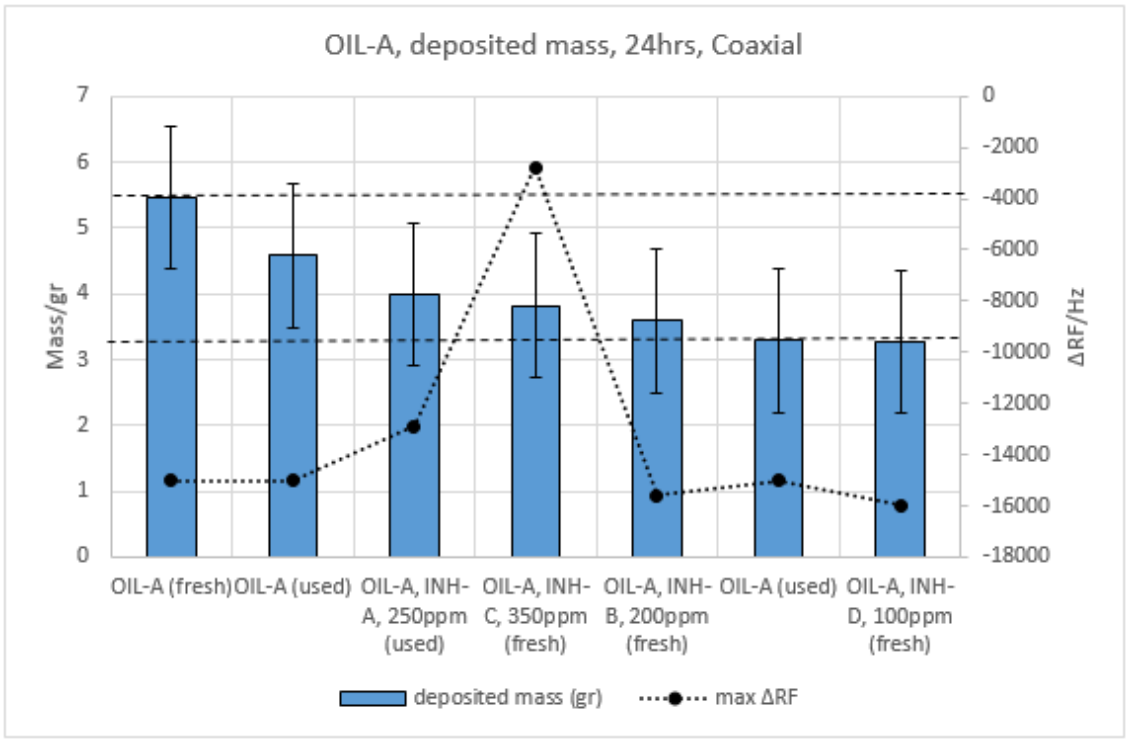

Figure 5-16. Comparison of mass deposition measured with coaxial and maximum frequency drop measured with QCM using OIL-A dosed with different inhibitors in 67 hrs with 100 s^{-1}. The plot ranked from left to right based on decreasing deposited mass. Parallel dashed lines represent the boundary of blank oil results.

The corresponding photos of bobbin covered with layers of deposition were taken after tests are shown in Figure 5-17. Clearly, the scraping wax layers (sloughing) on bobbin surfaces were the reason for the inconsistent results. Visual inspection for blank tests showed that the thickness of untouched deposition layer was almost the same. The standard deviation for selected ageing time, 67hrs was 1.088 gr. It was also observed that there were only two tests free of scraping off deposited layer, first and forth test (blank and dosed with INH-C). These two tests were ranked in the same order as QCM, sample with inhibitor resulted a lower deposition.

Figure 5-17. Visual observation of the mass deposition on bobbin surface of the coaxial using OIL-A dosed with different inhibitors in 67 hrs with 100 s^{-1}. Photos ranked from the left corner down to the right corner based on decreasing deposited mass.

5.4.2 Evaluation of deposition after 24hrs ageing time

To minimise the effect of sloughing, both subcooling and ageing time were reduced for the sample prepared with OIL-A. OIL-B and OIL-C dosed with inhibitors were also run

with 24 hrs ageing time. The differential temperature for the entire measurements was 30°C. The experimental conditions and results are tabulated in Table 5-10, ranked top to bottom based on decreasing deposited mass per each oil sample.

Table 5-10. Experimental conditions and the results of coaxial tests, using different oils dosed with the various inhibitors with 24 hrs ageing time, ranked top to bottom based on decreasing deposited mass of each oil

Fluid	***Bulk T (°C)***	***Bobbin T (°C)***	***Ageing time (hrs)***	***Shear rate (s^{-1})***	***Deposited mass (gr)***
OIL-A, INH-C, 350ppm (fresh)	*45*	*15*	*24*	*100*	*1.3539*
OIL-A, INH-D, 100ppm (fresh)	*45*	*15*	*24*	*100*	*1.3301*
OIL-A, INH-A, 250ppm (fresh)	*45*	*15*	*24*	*100*	*1.3176*
OIL-A, INH-C,350ppm (used)	*45*	*15*	*24*	*100*	*1.2815*
OIL-A, INH-C,700ppm (fresh)	*45*	*15*	*24*	*100*	*1.2699*
OIL-A (fresh)	*45*	*15*	*24*	*100*	*1.1758*
OIL-A (fresh)	*45*	*15*	*24*	*100*	*1.1664*
OIL-A, INH-D, 100ppm (fresh)	*45*	*15*	*24*	*100*	*1.1398*
OIL-A, INH-J, 400ppm (fresh)	*45*	*15*	*24*	*100*	*1.1187*
OIL-A (used)	*45*	*15*	*24*	*100*	*1.116*
OIL-A filtered (fresh)	*45*	*15*	*24*	*100*	*1.1069*
OIL-A filtered, INH-C, 350ppm (fresh)	*45*	*15*	*24*	*100*	*1.0923*
OIL-A, INH-A, 250ppm (fresh)	*45*	*15*	*24*	*100*	*0.9765*
OIL-A, INH-B, 200ppm (fresh)	*45*	*15*	*24*	*100*	*0.9306*
OIL-B (used)	*40*	*10*	*24*	*100*	*1.1802*
OIL-B (fresh)	*40*	*10*	*24*	*100*	*1.0281*
OIL-B, INH-C, 350ppm (fresh)	*40*	*10*	*24*	*100*	*1.0183*
OIL-B, INH-H, 400ppm (fresh)	*40*	*10*	*24*	*100*	*0.9552*
OIL-C (fresh)	*35*	*5*	*24*	*100*	*1.803*
OIL-C, INH-G, 400ppm (fresh)	*35*	*5*	*24*	*100*	*1.7398*
OIL-C, INH-F, 400ppm (fresh)	*35*	*5*	*24*	*100*	*1.6805*
OIL-C, INH-H, 400ppm (fresh)	*35*	*5*	*24*	*100*	*1.305*

Figure 5-18 to Figure 5-20 are plotted ranked left to right based on reducing deposition related to the samples OIL-A, OIL-B and OIL-C respectively. The corresponding maximum viscosity for each mixture is also plotted except for OIL-A where in all cases the change in viscosity was similar. Hence, a maximum differential frequency obtained from QCM was plotted for comparison purposes. Overall, no any relation on ranking among QCM and rheology data was observed.

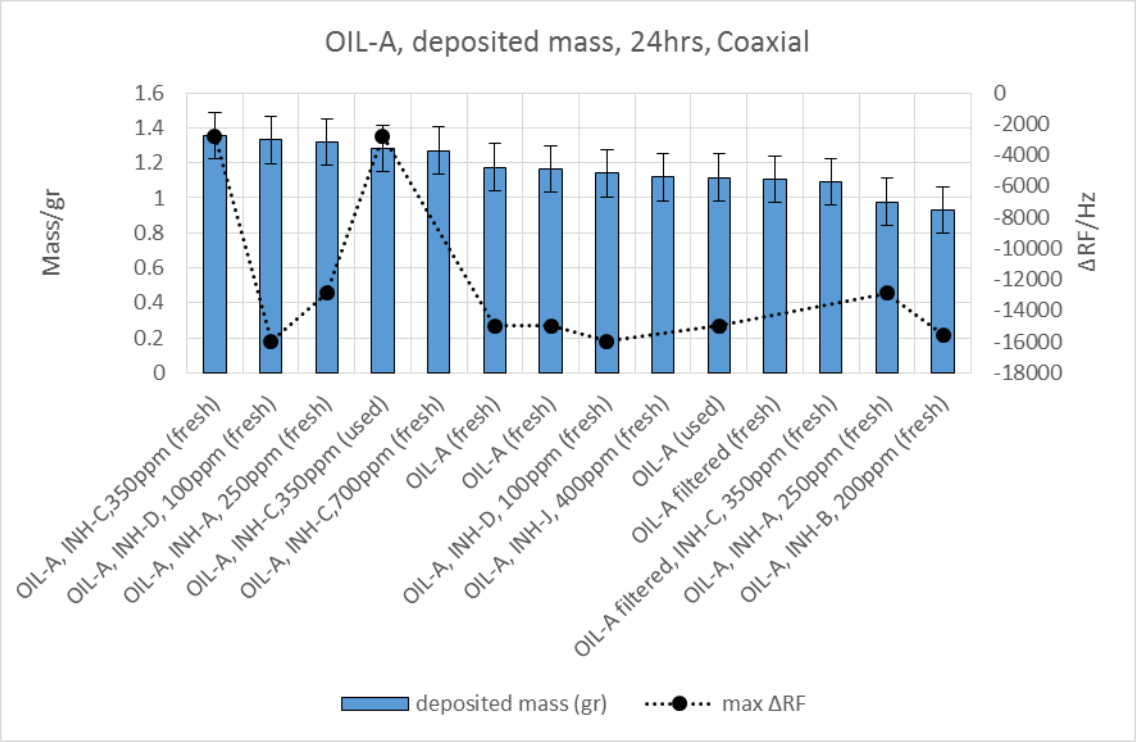

Figure 5-18. Comparison of mass deposition measured with coaxial set up and maximum frequency drop measured with QCM using OIL-A dosed with different inhibitors with 24 hrs with 100 s^{-1}. The plot ranked from left to right based on decreasing deposited mass.

It must be noted that there still appeared to be some effect of sloughing the wax layers in all samples by visual inspection of bobbin surfaces in Figure 5-21 to Figure 5-23. Most probably, the discrepancies between QCM and rheology results were as a consequence of sloughing.

The standard deviation in 24hrs ageing time was measured to be about ±0.1338 gr which still high, making it difficult if not impossible to screen inhibitors in the oil samples used in this study.

In addition, two experiments were launched with filtered OIL-A to eliminate the presence of impurities. The result showed insignificant change after 24 hrs ageing time.

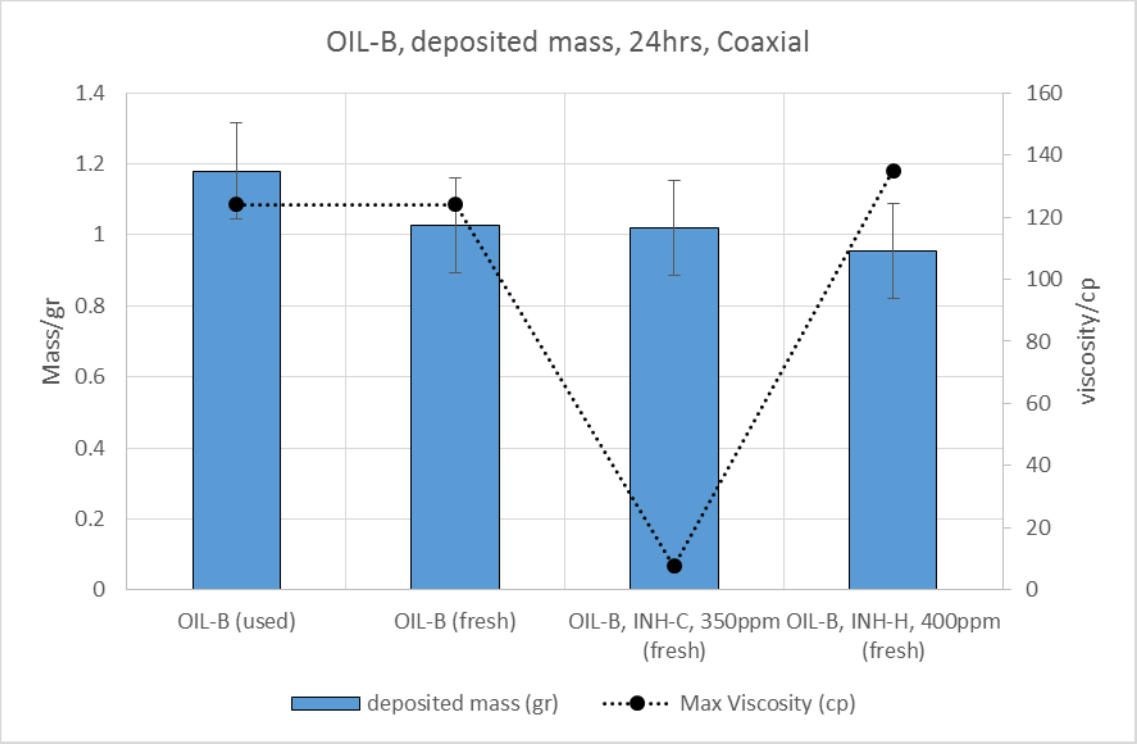

Figure 5-19. Comparison of mass deposition measured with coaxial and maximum viscosity measured with Rheometer using OIL-B dosed with different inhibitors with 24 hrs with 100 s^{-1}. The plot ranked from left to right based on decreasing deposited mass.

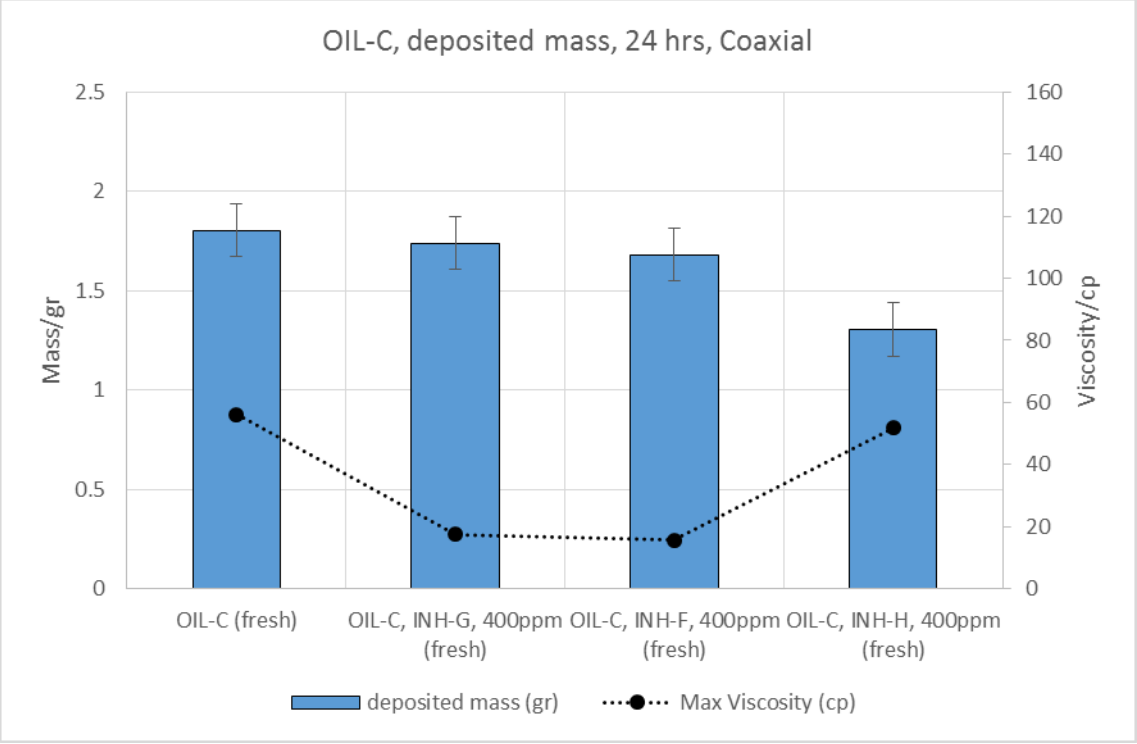

Figure 5-20. Comparison of mass deposition measured with coaxial set up and maximum viscosity measured with Rheometer using OIL-C dosed with different inhibitors with 24 hrs with 100 s^{-1}. The plot ranked from left to right based on decreasing deposited mass.

OIL-A, INH-C, 350ppm (fresh)

OIL-A, INH-D, 100ppm (fresh)

OIL-A, INH-A, 250ppm (fresh)

OIL-A, INH-C, 350ppm (used)

OIL-A, INH-C, 700ppm (fresh)

OIL-A (fresh)

OIL-A (fresh)

OIL-A, INH-D, 100ppm (used)

OIL-A, INH-J, 400ppm (fresh)

Figure 5-21. Visual observation of the mass deposition on bobbin surface of the coaxial using OIL-A dosed with different inhibitors in 24 hrs with 100 s^{-1}. Photos ranked from the left corner down to the right corner based on decreasing deposited mass. Used samples are those tests with the same oil recombined with deposited wax.

Figure 5-22. Visual observation of the mass deposition on bobbin surface of the coaxial set up using OIL-B dosed with different inhibitors with 24 hrs with 100 s^{-1}. Photos ranked from the left corner down to the right corner based on decreasing deposited mass. Used samples are those tests with the same oil recombined with deposited wax.

Figure 5-23. Visual observation of the mass deposition on bobbin surface of the coaxial set up using OIL-C dosed with different inhibitors in 24hrs with 100 s^{-1}. Photos ranked from the left corner down to the right corner based on decreasing deposited mass. Used samples are those tests with the same oil recombined with deposited wax.

5.4.3 Evaluation of deposition with 1hr ageing time

As already discussed, due to the sloughing of wax making it difficult to screen inhibitors, 24hrs was found to be too long. Therefore, it was decided to reduce ageing time as much as possible. Some preliminary measurements were conducted to find out the optimum ageing time with the lowest possible sloughing effect on deposition with the sample under study. It was then observed that 1hr ageing time resulted in reliable data with high accuracy. The standard deviation was obtained ±0.0098 gr.

Table 5-11 presents the test conditions and results which ranked top to bottom based on decreasing deposition mass for each oil samples. All mixtures tested with fresh sample

and differential temperature between bulk oil and bobbin surface likewise, 24hrs ageing was 30°C.

Table 5-11.The experimental conditions and the results of coaxial tests, using different oils dosed with the various inhibitors with 1hr ageing time, ranked top to bottom based on decreasing deposited mass per each oil

Fluid	*Bulk T (°C)*	*Bobbin T (°C)*	*Ageing time (hrs)*	*Shear rate (s^{-1})*	*Deposited mass (gr)*
OIL-A, INH-D, 100ppm (fresh)	*40*	*10*	*1*	*100*	*0.6231*
OIL-A (fresh)	*40*	*10*	*1*	*100*	*0.5289*
OIL-A (fresh)	*40*	*10*	*1*	*100*	*0.5151*
OIL-A, INH-B, 200ppm (fresh)	*40*	*10*	*1*	*100*	*0.5104*
OIL-A, INH-A, 250ppm (fresh)	*40*	*10*	*1*	*100*	*0.4461*
OIL-A, INH-F, 400ppm (fresh)	*40*	*10*	*1*	*100*	*0.4334*
OIL-A, INH-E, 400ppm (fresh)	*40*	*10*	*1*	*100*	*0.4096*
OIL-A, INH-G, 400ppm (fresh)	*40*	*10*	*1*	*100*	*0.3798*
OIL-A, INH-C, 350ppm (fresh)	*40*	*10*	*1*	*100*	*0.3498*
OIL-B, INH-D, 100ppm (fresh)	*40*	*10*	*1*	*100*	*0.6309*
OIL-B (fresh)	*40*	*10*	*1*	*100*	*0.5339*
OIL-B, INH-A, 250ppm (fresh)	*40*	*10*	*1*	*100*	*0.4700*
OIL-B, INH-B, 200ppm (fresh)	*40*	*10*	*1*	*100*	*0.4586*
OIL-B, INH-F, 400ppm (fresh)	*40*	*10*	*1*	*100*	*0.3889*
OIL-B, INH-G, 400ppm (fresh)	*40*	*10*	*1*	*100*	*0.3889*
OIL-B, INH-E, 400ppm (fresh)	*40*	*10*	*1*	*100*	*0.3843*
OIL-B, INH-C, 350ppm (fresh)	*40*	*10*	*1*	*100*	*0.3613*
OIL-C, INH-A, 250ppm (fresh)	*35*	*5*	*1*	*100*	*0.9972*
OIL-C, INH-D, 100ppm (fresh)	*35*	*5*	*1*	*100*	*0.8532*
OIL-C (fresh)	*35*	*5*	*1*	*100*	*0.8530*
OIL-C, INH-H, 400ppm (fresh)	*35*	*5*	*1*	*100*	*0.7675*
OIL-C, INH-B, 200ppm (fresh)	*35*	*5*	*1*	*100*	*0.7092*
OIL-C, INH-E, 400ppm (fresh)	*35*	*5*	*1*	*100*	*0.6561*
OIL-C, INH-G, 400ppm (fresh)	*35*	*5*	*1*	*100*	*0.5789*
OIL-C, INH-C, 350ppm (fresh)	*35*	*5*	*1*	*100*	*0.5077*
OIL-C, INH-F, 400ppm (fresh)	*35*	*5*	*1*	*100*	*0.4675*

Figure 5-24 to Figure 5-26 demonstrate deposition mass which was similarly ranked left to right based on decreasing deposition. As noted earlier, since the viscosity changes with/out inhibitors were negligible, OIL-A was compared with maximum frequency drop obtained from QCM, shown in Figure 5-24.

It was mentioned that a lower ΔRF corresponds to either less wax deposition or lower adhesion tendency of wax to the surface, inferring a good inhibitor. Both QCM results and 1hr ageing time for OIL-A mixtures have a significantly close match with one another. Mixtures with OIL-B and OIL-C, on the other hand, compared with maximum viscosity. The overall trend shows decreasing deposition with decreasing corresponding maximum viscosities.

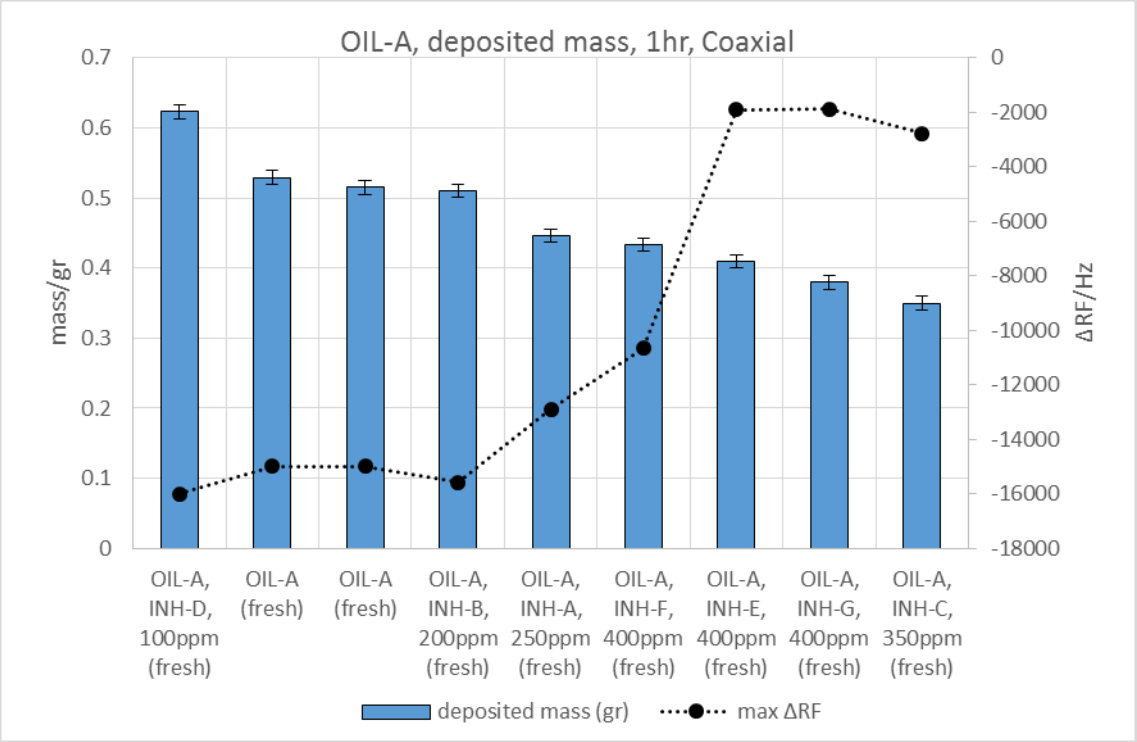

Figure 5-24. Comparison of mass deposition measured with coaxial and maximum frequency drop measured with QCM used OIL-A sample dosed with different inhibitors in 1 hr with 100 s^{-1}. The plot ranked from left to right based on decreasing deposited mass.

Figure 5-27 to Figure 5-29 show the photos taken for visual observation of oil samples OIL-A, OIL-B and OIL-C respectively. It is observed almost no significant sloughing compare to the longer ageing time, reduced deviation results hence easier to screen inhibitors with low viscosity waxy samples.

In addition, a closer look at the deposited crystals show that, by decreasing mass, the smooth layer of deposition converted to coarser, small sphere shape as well as darker colour. It may be a consequence of the crystal modifying nature of specific inhibitors which change plate and needle crystals to mal/amorphous shape.

Furthermore, the top section of bobbin was observed to be free of wax which increased in length with decreasing viscosity as measured by rheometer, ΔRF with QCM and deposition by coaxial.

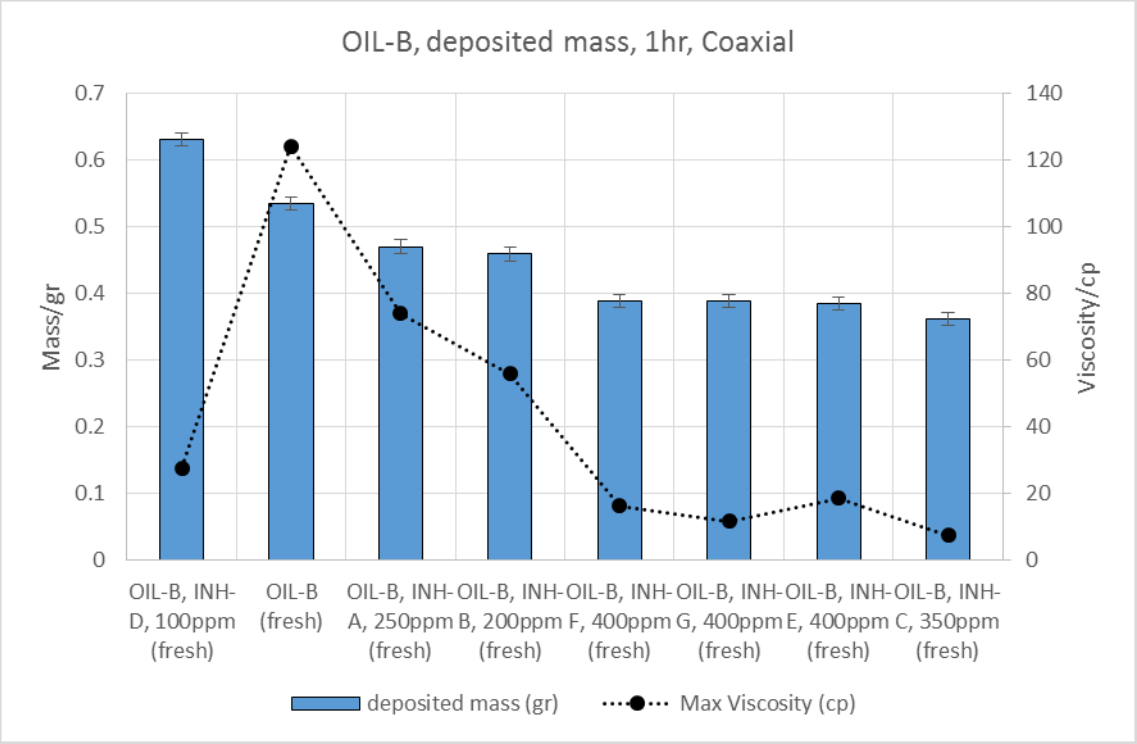

Figure 5-25. Comparison of mass deposition measured with coaxial and maximum viscosity measured with Rheometer used OIL-B sample dosed with different inhibitors in 1 hr with 100 s^{-1}. The plot ranked from left to right based on decreasing deposited mass.

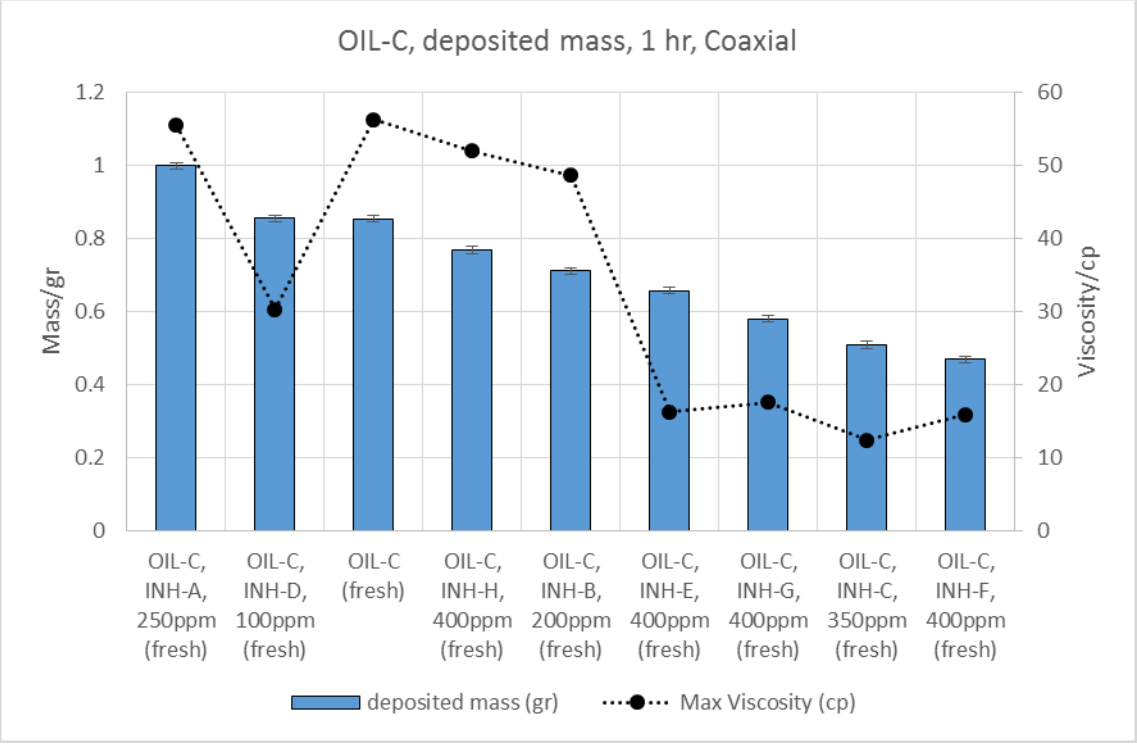

Figure 5-26. Comparison of mass deposition measured with coaxial and maximum viscosity measured with Rheometer used OIL-C sample dosed with different inhibitors in 1 hr with 100 s^{-1}. The plot ranked from left to right based on decreasing deposited mass.

Figure 5-27. Visual observation of the mass deposition on bobbin surface of the coaxial used OIL-A sample dosed with different inhibitors in 1 hr with 100 s^{-1}. Photos ranked from the left corner down to the right corner based on decreasing deposited mass. Used samples are those tests with the same oil recombined with deposited wax.

Figure 5-28. Visual observation of the mass deposition on bobbin surface of the coaxial used OIL-B sample dosed with different inhibitors in 1 hr with 100 s^{-1}. Photos ranked from the left corner down to the right corner based on decreasing deposited mass. Used samples are those tests with the same oil recombined with deposited wax.

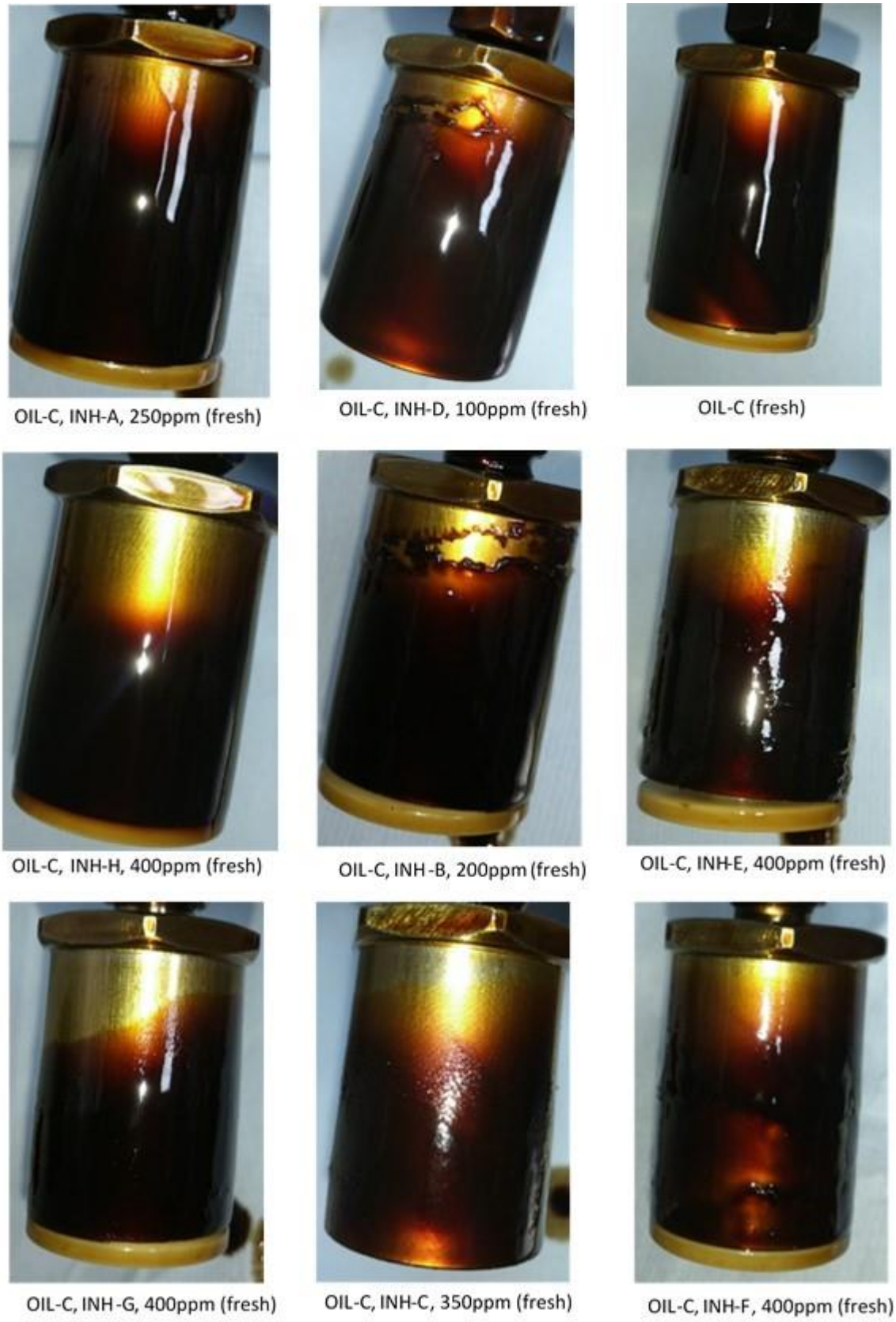

Figure 5-29. Visual observation of the mass deposition on bobbin surface of the coaxial used OIL-C sample dosed with different inhibitors in 1 hr with 100 s^{-1}. Photos ranked from the left corner down to the right corner based on decreasing deposited mass. Used samples are those tests with the same oil recombined with deposited wax.

5.5 Data obtained using the mini benchtop flowloop apparatus

In flow assurance wax studies the most realistic benchtop lab equipment to imitate real field conditions is a flowloop [4]. Therefore, as a part of PhD thesis, a flow loop was fully designed and constructed in this work to simulate a more realistic pipeline condition and produce more realistic results. In this work, several experimental campaigns were performed. These experiments were aimed at investigating the influence of shear rate, subcooling temperature and ageing time on oil dosed with different inhibitors to compare and verify the results with the other applied equipment in this work. In addition, the impact of some specific inhibitors on the existing deposited wax was tested. Furthermore, a series of tests to study the influence of circulation loop on inhibitors was performed. The fluid for all experiments was chosen between OIL-A, OIL-B, OIL-C and OIL-D. Experimental conditions and data obtained from the flowloop are tabulated in all section ranked top to bottom to show decreasing average differential pressure.

The sample fluids were subjected to a thermal cycle circulation path during the test. An appropriate conditioning temperature was required to melt all the wax particles which had already diffused out of the bulk sample at the end of the loop. This particular temperature for each individual oil sample was obtained by the rheometer as explained in detail in the previous chapter.

Most of the tests were done in several sequential cycles and as shown in Figure 5-30, it was observed that there was an increased differential pressure buildup for every cycle. It was thought that the presence of unmelted particles or some impurities, as well as losing light components were the reasons for raising pressure. However, increasing conditioning time even up to 48 hrs or thoroughly cleaning the loops between each cycle and even degassing fluid before present into the loop, did not change the outcome, hence only the first cycle was reported for comparison purposes. One probable reason for this might be due to a change of morphology of wax particles caused by wax thermal memory which was not erased during the conditioning. A fresh sample was then loaded for each individual measurement in the flowloop.

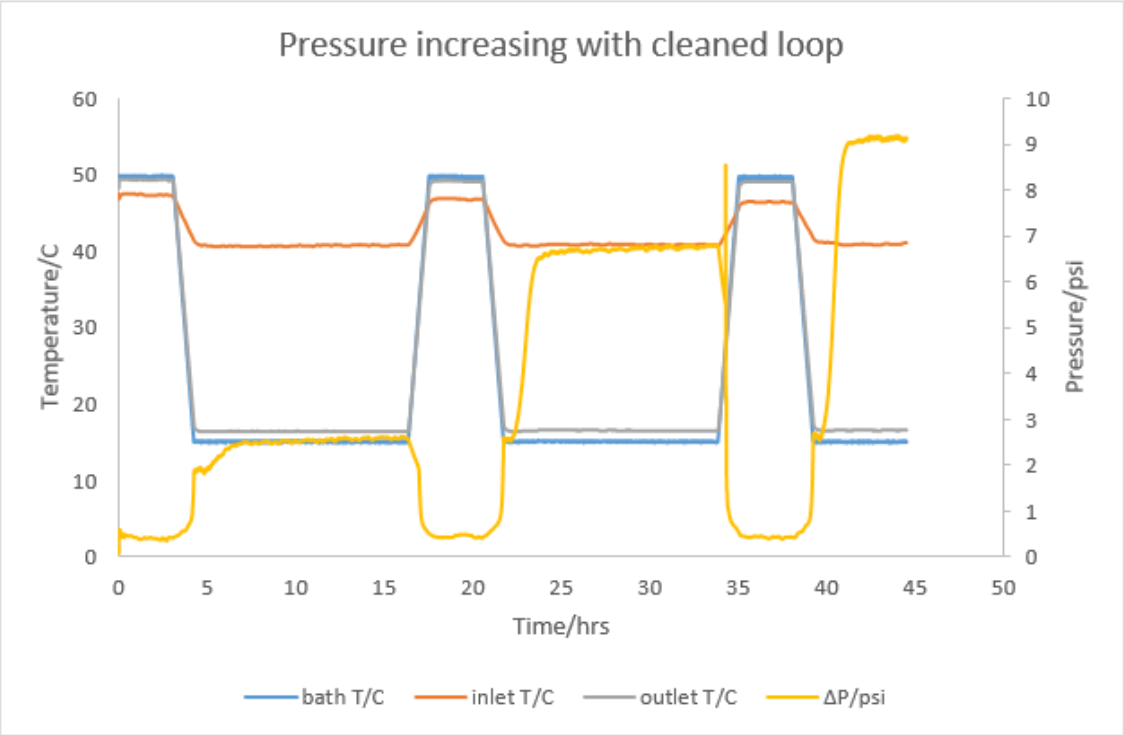

Figure 5-30. A plot of consecutive cycle test by flowloop

Dynamic wax build up and disappearance correspond to WAT/WDT was another data could be obtained by flowloop. Preliminary results of WAT obtained by flowloop showed that it was highly dependent on the accuracy of the pressure transducer and loop diameter which was observed to increase by decreasing loop diameter. It was found to be at least 5-10°C lower than measured WAT by QCM with the diameter of loop in this work, though the ranking was the same as QCM result.

In addition, some other data which seemed unnecessary to the better understanding of this work was ignored including differential pressure at the start of ageing time which was used to determine viscosity and thickness of wax. All measured viscosities, however, were in the same rank with rheometer in the presence of inhibitors.

The average inlet/outlet temperature, differential pressure and thickness for the whole ageing time is tabulated, though it is elaborate to screen inhibitor performance based on these raw data. The best way to organise inhibitor performance was found to be visual assessment by plotting differential pressure and wax thickness versus ageing time.

As discussed in Chapter 3, inlet temperature is important as a basis for smooth injection flow or a failure of the test in this work. However, the primary purpose of using differential temperature was to measure the rate of increase in wax thickness in the loop.

Isolation of temperature sensors with wax by the time leads to reduce differential temperature could be an indication of deposition grow up.

It was also observed that length of the loop was a decisive factor to log the outlet temperature. The inlet temperature in all cases was found to be a constant value. Because the inlet sensor was continuously in contact with the fluid coming through the conditioning bath at the same temperature well above WAT, hence no deposition in the applied ageing time was observed. The differential temperature in two different lengths of loop, 50cm and 300cm, is shown in Figure 5-31. The lower length over the same ageing time showed a lower differential temperature reduction at the same condition. The reason might be explained as follows.

When the fluid sample reached the WAT point wax started to form and diffused out of the solution. Downstream of the WAT point, the oil temperature gradually reduced to equilibrate with surrounding temperature. As mentioned earlier, temperature gradient related to the WAT, plays a predominant role in the wax deposition. The wax deposition disappears when there is no temperature gradient between the oil and the wall, even if the oil temperature is far below WAT. The reason for constant outlet temperature might be due to lack of temperature gradient in a longer loop between the bulk oil and the pipe wall, hence no deposition and insulation of the sensor occurred.

Since almost all the tests were performed in the longer loop, the average inlet/outlet temperature are tabulated without any further discussion.

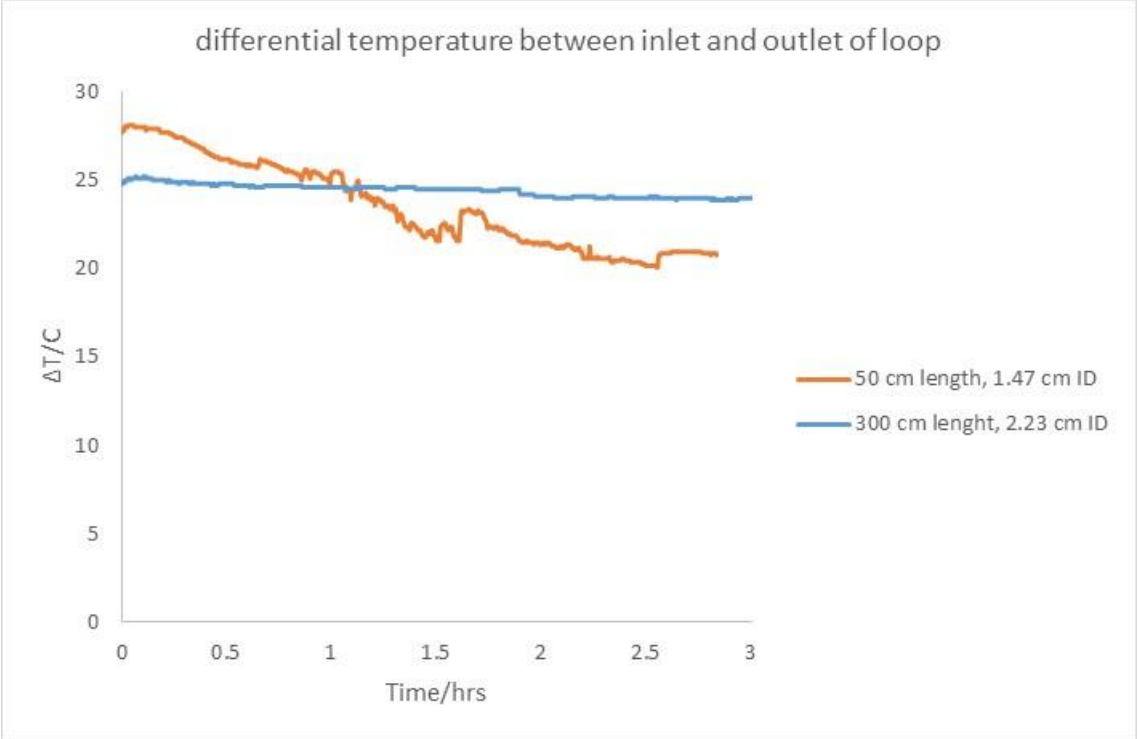

Figure 5-31. Comparison of differential temperature of inlet and outlet of the loop. In both cases, temperatures were set to 50°C and 5°C for both condition bath and test bath respectively.

5.5.1 Impact of shear rate on OIL-A dosed with various inhibitors

Table 5-12 lists two different shear rates applied to OIL-A dosed with various inhibitors.

Table 5-12. Experimental conditions and the results of flowloop, using OIL-A dosed with different inhibitors, ranked top to bottom based on decreasing differential pressure per two different flow rate at 10°C. Loop C was used for all the tests.

Fluid	***Conditioning T (°C)***	***Test T (°C)***	***Flow rate (cc/min)***	***Shear rate (s^{-1})***	***Average ΔP (psi)***	***Average T_{in} (°C)***	***Average T_{out} (°C)***	***Average deposited thickness (μm)***
OIL-A, INH-G, 400ppm	60	10	10	151	882.10	46.85	11.62	889
OIL-A, INH-C,350ppm	60	10	10	151	448.37	47.18	12.57	839
OIL-A, INH-H, 400ppm	60	10	10	151	233.16	46.44	12.41	771
OIL-A	60	10	10	151	175.11	47.06	12.12	755
OIL-A, INH-G, 400ppm	60	10	5	76	46.46	35.12	11.27	674
OIL-A, INH-E, 400ppm	60	10	5	76	34.16	36.31	11.38	627
OIL-A, INH-D, 100ppm	60	10	5	76	47.08	35.19	11.20	637
OIL-A, INH-C, 350ppm	60	10	5	76	23.51	36.49	11.68	566
OIL-A	60	10	5	76	22.33	39.06	12.61	568
OIL-A, INH-A, 250ppm	60	10	5	76	19.86	36.05	11.27	532
OIL-A, INH-B 200ppm	60	10	5	76	16.52	36.75	11.81	521
OIL-A, INH-F, 400ppm	60	10	5	76	5.93	35.13	11.29	383

(Figure 5-32 and Figure 5-34) and (Figure 5-33 and Figure 5-35) illustrate the differential pressure alongside the test loop and correspond wax thickness respectively at both flow rates. Wax thickness is derived by Equation 3.7. Since all mixtures of OIL-A dosed with inhibitors had almost the same viscosity behaviour, the corresponding frequency drop obtained by QCM is included the legends for comparison purposes. The legend information for OIL-A was in the order of, ΔRF, used sample oil, type of inhibitor, the dosage of used inhibitor in the mixture.

Visual inspection in the lower shear rate, likewise rheology assessment for OIL-A, seemed impossible to screen and rank inhibitor performance in terms of overall differential pressure/deposited thickness, due to the high presence of sloughing wax layer. Interestingly, the inconsistency of coaxial as a snapshot of deposition can be understood by this plot. the coaxial data was highly dependent on when the test was stopped, before or after sloughing resulted a big difference as already observed in Figure 5-17 corresponding to a long ageing time, 67hrs.

In this case, inhibitors could be ranked based on decreasing the maximum value of differential pressure approached as shown in the legend of Figure 5-32. It is evident that mixtures with low-frequency drop which were considered to have better performance in QCM, showed higher differential pressure representing lower performance in flowloop.

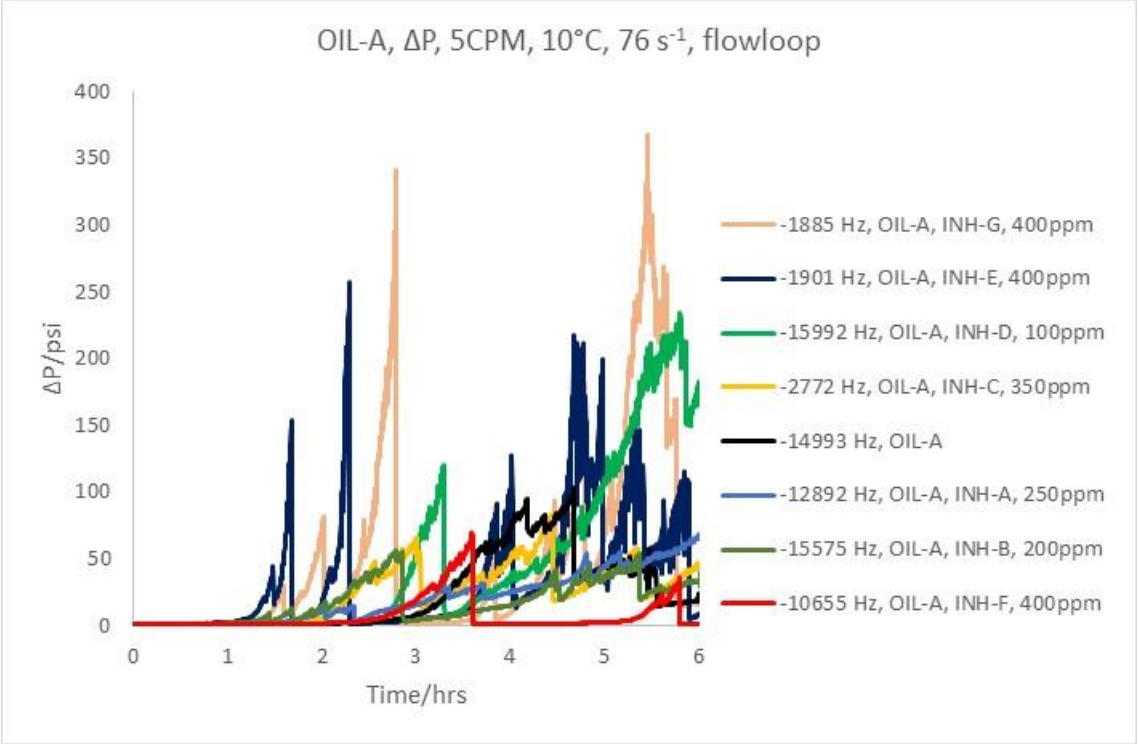

Figure 5-32. Comparison of differential pressure buildup by flowloop using OIL-A sample dosed with different inhibitors in 5CPM with 76 s^{-1}. The legend ranked top to bottom based on decreasing maximum build-up pressure at 10°C.

Comparing the behaviour of wax thickness with time revealed that all treated mixtures reached almost the same thickness of 800µm after which the deposited layers sloughs. However, it was observed that those mixtures which showed higher frequency drop by the QCM, had a delay on deposition growing, Figure 5-33. The legend of thickness was ranked top to bottom based on retarding the start of deposition build up.

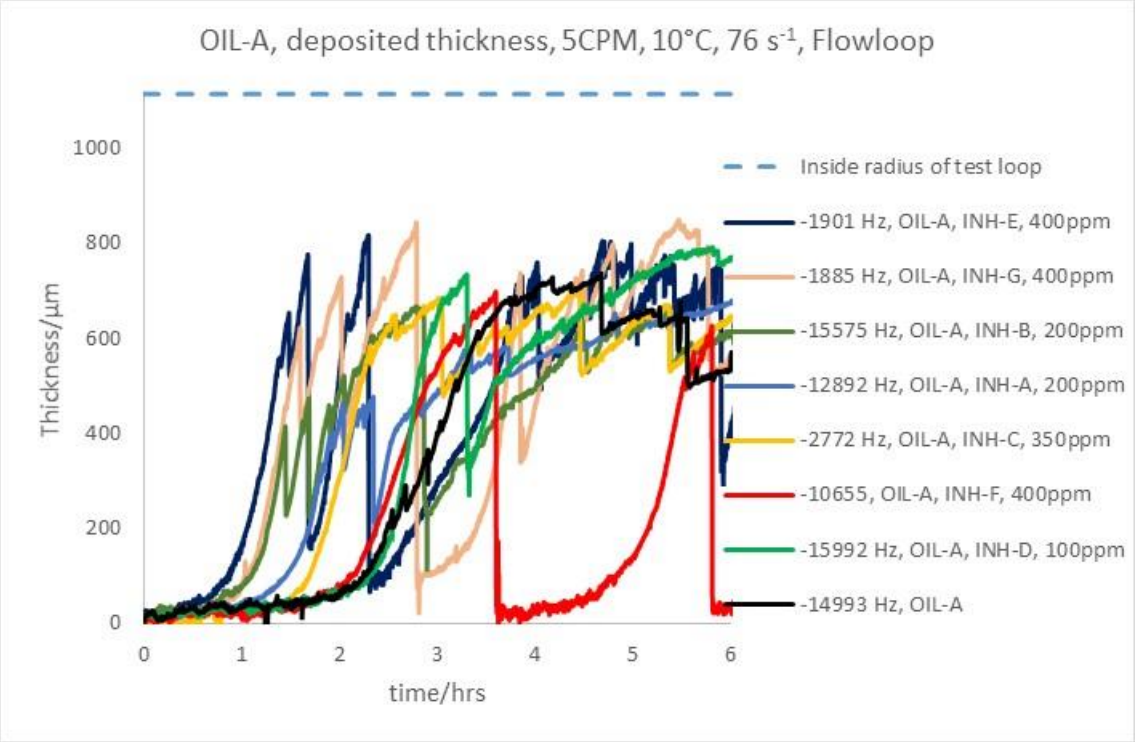

Figure 5-33. Comparison of deposited thickness by flowloop using OIL-A sample dosed with different inhibitors in 5CPM with 76 s^{-1}. The legend ranked top to bottom based on delay in deposited thickness build-up at 10°C.

When the shear rate was doubled, screening inhibitors found to be easier, Figure 5-34 and Figure 5-35. It can be explained that at the higher flow rate, the hardness process of deposition, ageing process, became faster by diffusing out of oil trapped in deposition network hence the scrapping deposited layer decreased and smoother/stabilised differential pressure buildup would occur faster. Surprisingly, mixtures showing less frequency reduction in QCM tests, again showed higher differential pressure and thicker deposition as well.

The test time was around 40 hrs except for the mixture dosed with INH-G where the pump stopped working at around 8hrs because it reached the maximum limited working pressure.

In addition, by comparing thickness in both applied shear rates, Figure 5-33 and Figure 5-35, it was found that with the same subcooling, flowrate did not have a significant influence on the maximum thickness of deposit. Since ageing process forms stable deposition which increases by increasing flowrate, the only difference was observed that the rate of raising deposition would be faster at the higher flow rate.

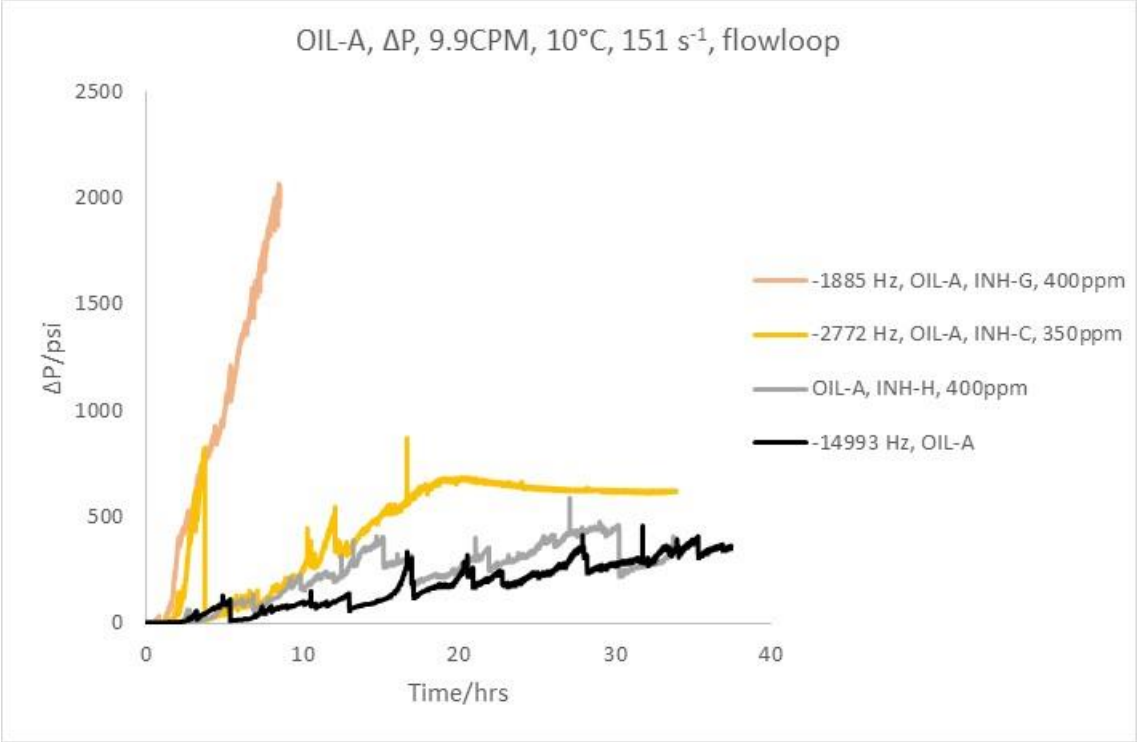

Figure 5-34. Comparison of differential pressure buildup by flowloop using OIL-A sample dosed with different inhibitors in 10CPM with 151 s^{-1}. The legend ranked top to bottom based on decreasing differential build-up pressure at 10°C.

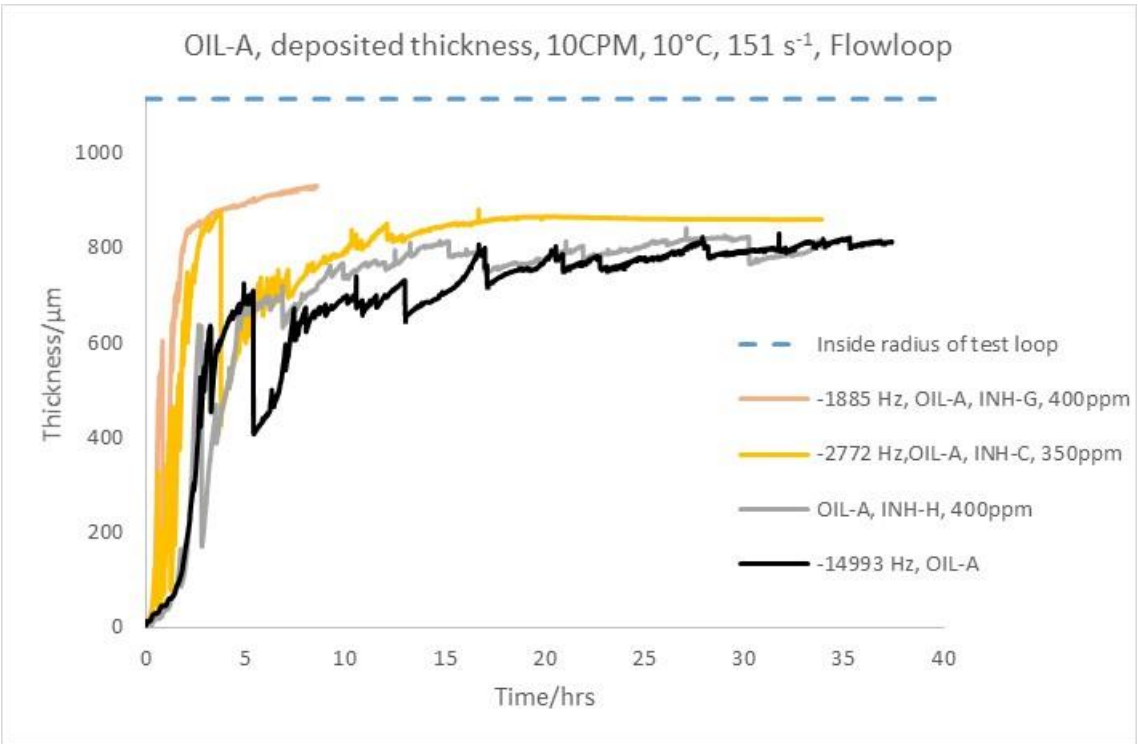

Figure 5-35. Comparison of deposited thickness by flowloop using OIL-A sample dosed with different inhibitors in 10CPM with 151 s^{-1}. The legend ranked top to bottom based on lower deposited thickness at 10°C.

The following measurements were performed using OIL-B, OIL-C and OIL-D, which had previously been screened using the rheometer, hence, they are all ranked with

corresponding maximum viscosities in the legend. In the following graphs, all differential pressures and thicknesses plots are ranked, top to bottom, based on decreasing differential build up pressure and wax thickness respectively. The legends are in the following order:

Maximum viscosity, used sample oil, type of inhibitor, dosage of used inhibitor in the mixture.

5.5.2 Impact of shear rate and subcooling in sample with OIL-B dosed with various inhibitors

Table 5-13 presents the test conditions and results obtained with OIL-B sample at two different shear rates and test temperatures.

Table 5-13. Experimental conditions and the results of flowloop, using OIL-B dosed with different inhibitors, ranked top to bottom based on decreasing differential pressure per two different flow rate. Loop C was used for all the tests.

Fluid	***Conditioning T (°C)***	***Test T (°C)***	***Flow rate (cc/min)***	***Shear rate (s^{-1})***	***Average ΔP (psi)***	***Average T_{in} (°C)***	***Average T_{out} (°C)***	***Average deposited thickness (μm)***
OIL-B, INH-E, 400ppm	*60*	*10*	*5*	*76*	*595.75*	*39.11*	*11.70*	*865*
OIL-B, INH-D, 100ppm	*60*	*10*	*5*	*76*	*357.21*	*37.85*	*11.37*	*801*
OIL-B, INH-C, 350ppm	*60*	*10*	*5*	*76*	*348.65*	*36.82*	*11.57*	*891*
OIL-B, INH-G, 400ppm	*60*	*10*	*5*	*76*	*250.24*	*38.11*	*12.22*	*843*
OIL-B, INH-J ,400ppm	*60*	*10*	*5*	*76*	*214.50*	*39.07*	*11.68*	*793*
OIL-B, INH-F, 400ppm	*60*	*10*	*5*	*76*	*188.40*	*38.83*	*11.70*	*775*
OIL-B, INH-B, 200ppm	*60*	*10*	*5*	*76*	*51.67*	*39.41*	*11.98*	*539*
OIL-B-2	*60*	*10*	*5*	*76*	*21.52*	*37.94*	*11.32*	*498*
OIL-B, INH-A, 250ppm	*60*	*10*	*5*	*76*	*21.50*	*37.55*	*11.30*	*463*
OIL-B-1	*60*	*10*	*5*	*76*	*20.42*	*39.03*	*11.60*	*436*
OIL-B, INH-C,350ppm	*60*	*15*	*10*	*151*	*6.88*	*44.73*	*15.79*	*444*
OIL-B, INH-B, 200ppm	*60*	*15*	*10*	*151*	*4.27*	*44.89*	*15.81*	*310*
OIL-B	*60*	*15*	*10*	*151*	*3.99*	*44.71*	*15.86*	*292*
OIL-B, INH-D, 100ppm	*60*	*15*	*10*	*151*	*3.89*	*45.01*	*15.84*	*290*
OIL-B, INH-J, 400ppm	*60*	*15*	*10*	*151*	*2.69*	*44.93*	*15.81*	*283*

Figure 5-36 and Figure 5-37 demonstrate the differential pressure and thickness with 5CPM flowrate logged in 6 hrs test time.

A close attention in the pressure plot illustrates two different types of pressure decline followed by a gradually increasing differential pressure. An instant reduction which was

most probably due to the sloughing and scraping off the wax layers. Another one was reducing smoothly which was highlighted in the sample dosed with INH-E. A probable reason for this observation could be due to wax-oil gel behaviour and ageing process. The deposition initially consisting of oil entrapped in the gel which was gradually starting to diffuse out of the deposited gel making it harder and thinner hence a lower differential pressure was observed.

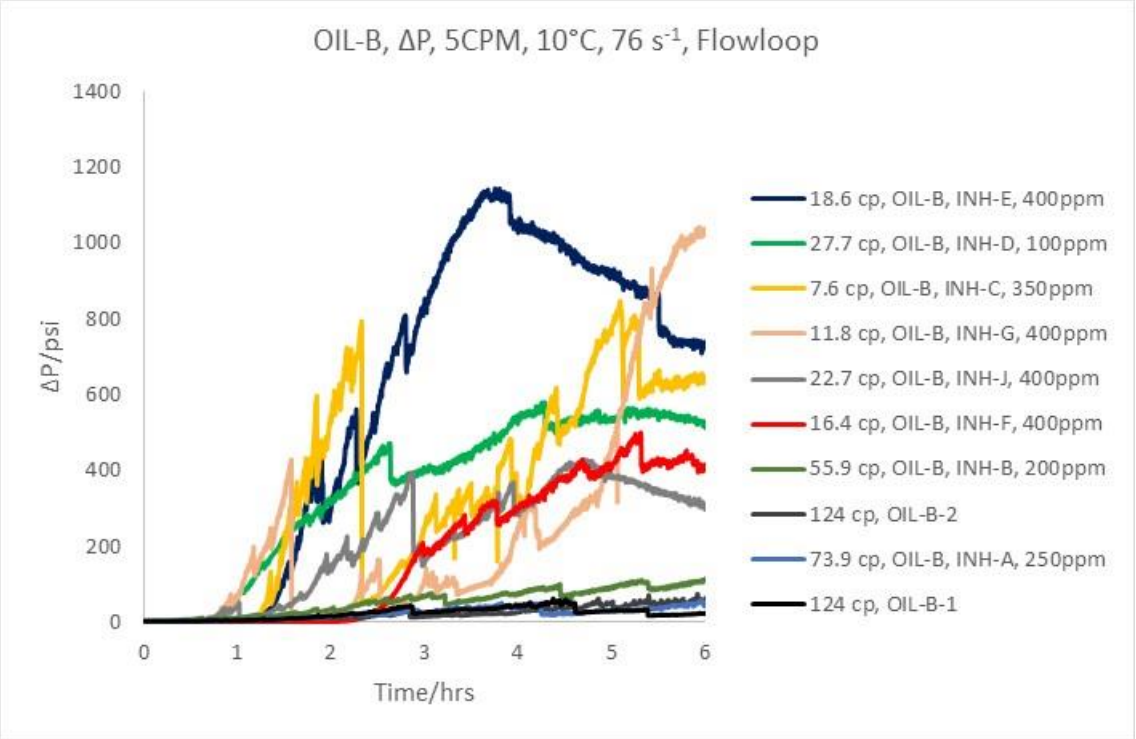

Figure 5-36. Comparison of differential pressure buildup by flowloop using OIL-B sample dosed with different inhibitors in 5CPM with 76 s^{-1}. The legend ranked top to bottom based on decreasing differential build-up pressure at 10°C.

As shown in Figure 5-37, the mixture dosed with INH-F showed a delay compared to other mixture in terms of increasing the deposition wax. The same behaviour was also observed with the sample OIL-A in Figure 5-33. However, by the following test, it was increasing significantly. Therefore, it could be concluded that this inhibitor was only able to prohibit deposition in a limited time in flowing conditions.

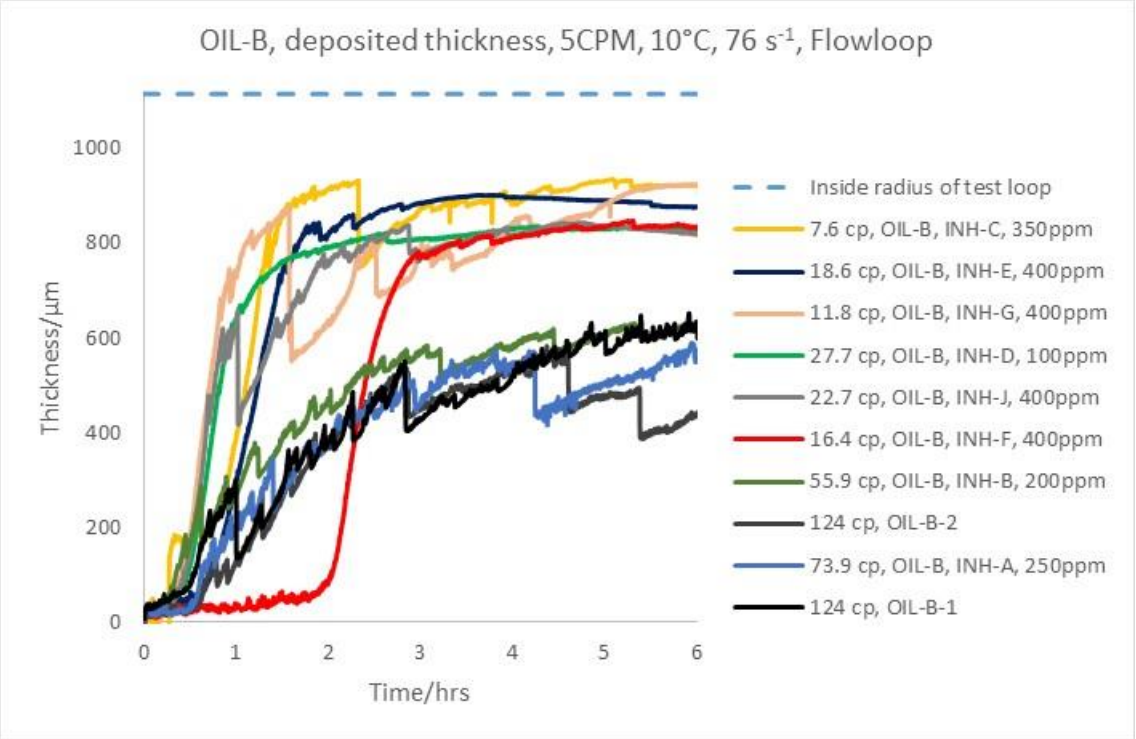

Figure 5-37. Comparison of deposited thickness by flowloop using OIL-B sample dosed with different inhibitors in 5CPM with 76 s^{-1}. The legend ranked top to bottom based on lower deposited thickness at 10°C.

Regarding the inhibitor evaluation, the performance could be categorised in two different classes compare to the blank sample as a reference, 1. No effect and almost the same wax thickness, 2. Higher wax thickness

1. Class 1

   INH- A, B

2. Class 2

   INH- C, D, E, F, G, J

Interestingly Class 1 was those mixtures with the low range of viscosity between 7.6 to 27.7 cP and Class2 had a viscosity range of 55.9 to 124cP. In other words, mixtures which showed a better performance in rheology had the worst performance on flowloop.

Doubling shear rate in addition to decreasing the subcooling was observed to impact on the behaviour of mixtures dosed with INH-D and INH-J, Figure 5-38 and Figure 5-39. These particular inhibitors had low viscosities and already were categorised as Class 2 in terms of performing at higher subcooling and the half shear rate value. In this

condition, these two inhibitors appeared to reduce the pump cost for delivery through the flow lines form similar wax thickness to blank, Figure 5-39.

The sample dosed with INH-C showed a higher differential pressure and wax thickness correspond to lowest maximum viscosity in measured inhibitors.

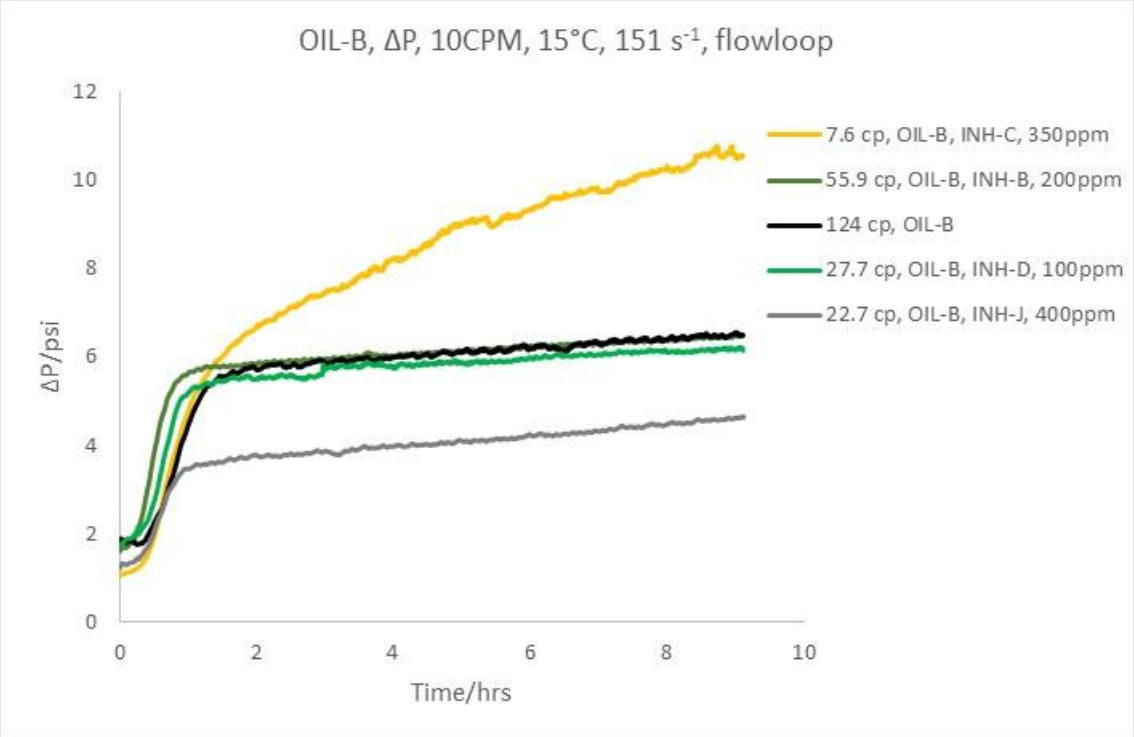

Figure 5-38. Comparison of differential pressure buildup by flowloop using OIL-B sample dosed with different inhibitors in 10CPM with 151 s^{-1}. The legend ranked top to bottom based on decreasing differential build-up pressure at 15°C.

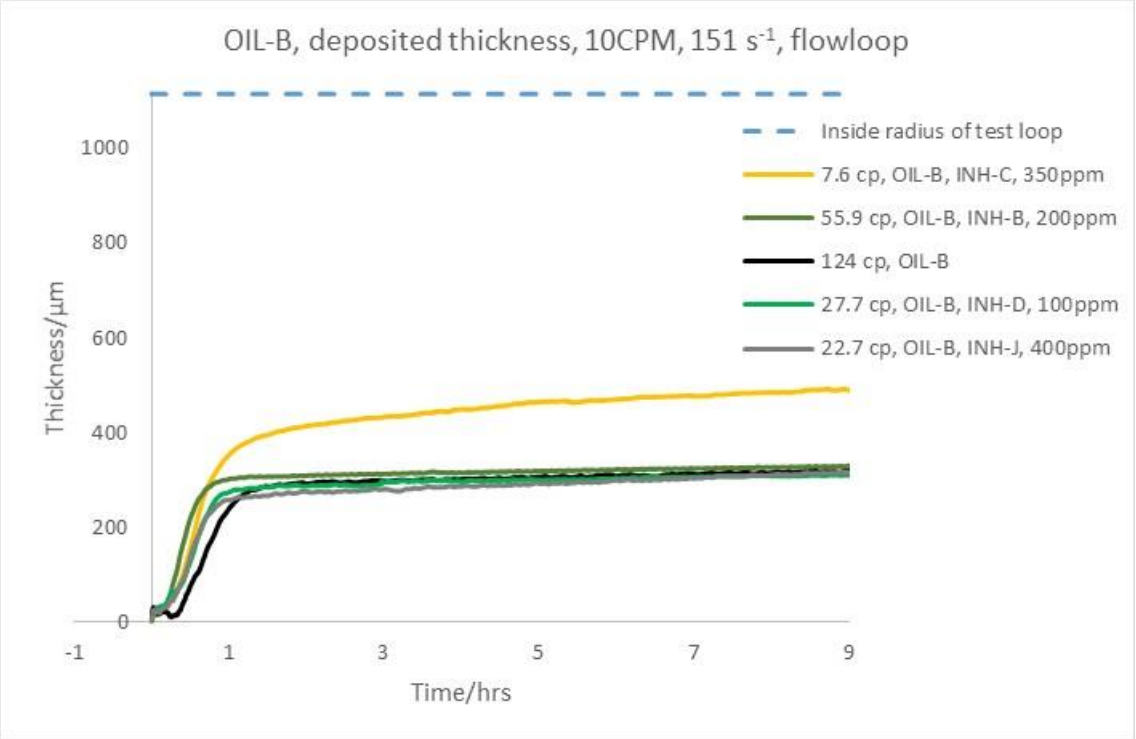

Figure 5-39. Comparison of deposited thickness by flowloop using OIL-B sample dosed with different inhibitors in 10CPM with 151 s^{-1}. The legend ranked top to bottom based on lower deposited thickness at 15°C.

5.5.3 Tests performed with sample OIL-C dosed with various inhibitors

5.5.3.1 Subcooling effect and shear rate

A series of measurements were launched to investigate the impact of subcooling on inhibitor performance. Furthermore, a series of tests was performed in a different sized loop to increase the applied shear rate with the maximum applicable flowrate.

Table 5-14 presents all test conditions and results. In the first section, subcooling test was conducted with the same flowrate of 5CPM at three different test temperatures, 5°C, 15°C and 20°C. It should be pointed out that a limited number of inhibitors as a representative of their classes in terms of viscosity, were evaluated at lower subcooling.

Table 5-14. Experimental conditions and the results of flowloop used OIL-C dosed with different inhibitors in various test temperatures, flow rates and shear rates. Loop C was used for almost all the tests.

Fluid	Conditioning T (°C)	Test T (°C)	Flow rate (cc/min)	Shear rate (s^{-1})	Average ΔP (psi)	Average T_{in} (°C)	Average T_{out} (°C)	Average deposited thickness (μm)
OIL-C, INH-G, 400ppm	50	5	5	76	445	30.78	6.31	809
OIL-C, INH-E, 400ppm	50	5	5	76	424	31.03	6.61	755
OIL-C, INH-G, 1200ppm	50	5	5	76	377	30.48	6.32	840
OIL-C, INH-G, 800ppm	50	5	5	76	376	31.62	6.55	832
OIL-C, INH-F, 400ppm	50	5	5	76	340	30.82	6.6	714
OIL-C, INH-C, 350ppm	50	5	5	76	252	30.31	6.88	734
OIL-C, INH-B, 200ppm	50	5	5	76	15.3	31.27	6.82	244
OIL-C, INH-D, 100ppm	50	5	5	76	12.8	31.95	6.79	205
OIL-C, INH-A, 250ppm	50	5	5	76	5.8	31.37	6.83	98
OIL-C	50	5	5	76	5.4	29.51	6.43	85
OIL-C, INH-E, 400ppm	50	15	5	76	292	33.83	15.81	839
OIL-C, INH-C, 350ppm	50	15	5	76	170	34.27	15.93	808
OIL-C, INH-E, 400ppm	50	15	5	76	120	34.28	16.33	773
OIL-C	50	15	5	76	59	33.76	16.05	665
OIL-C, INH-A, 250ppm	50	15	5	76	17.2	34.88	16.15	512
OIL-C	50	15	5	76	10.6	33.75	15.90	438
OIL-C, INH-F, 400ppm	50	15	5	76	9.4	33.63	15.84	462
OIL-C, INH-G, 400ppm	50	15	5	76	0.85	34.09	15.91	168
OIL-C, INH-C, 350ppm	50	20	5	76	1.13	36.16	20.71	220
OIL-C	50	20	5	76	0.19	35.59	20.61	54
OIL-C, INH-E, 400ppm	50	15	10	151	127	37.73	15.73	743
OIL-C, INH-H, 400ppm	50	15	10	151	34.9	41.32	16.30	565
OIL-C, INH-F, 400ppm	50	15	10	151	32.4	39.40	16.06	569
OIL-C 2	50	15	10	151	18.2	41.67	16.32	478
OIL-C, INH-G, 400ppm	50	15	10	151	13.9	38.82	16.04	504
OIL-C 1	50	15	10	151	10.04	38.46	15.93	382
OIL-C, INH-G, 400ppm	50	5	10	529*	1518	35.04	11.49	549
OIL-C, INH-H, 400ppm	50	5	10	529*	605	35.32	10.79	915
OIL-C	50	5	10	529*	486	36.08	10.83	528
OIL-C, INH-H, 800ppm	50	5	10	529*	181	34.86	9.97	848

*These tests measured with loop A (50cm length and 1.47mm inside diameter)

Figure 5-40 and Figure 5-41 are related to test temperature set at 5°C in 6hrs test time. The performance ranking is observed again to be opposite of viscosities measured with a rheometer. Viscosities lower than 17.5cP raised significantly differential pressure and wax thickness while those with viscosities above 48.6cP had no significant impact on thickness in comparison with the baseline blank sample. Increasing dosage of INH-G was also found to increase wax thickness. The viscosities with higher dosages were not measured, though, most likely would be in the same low viscosity region.

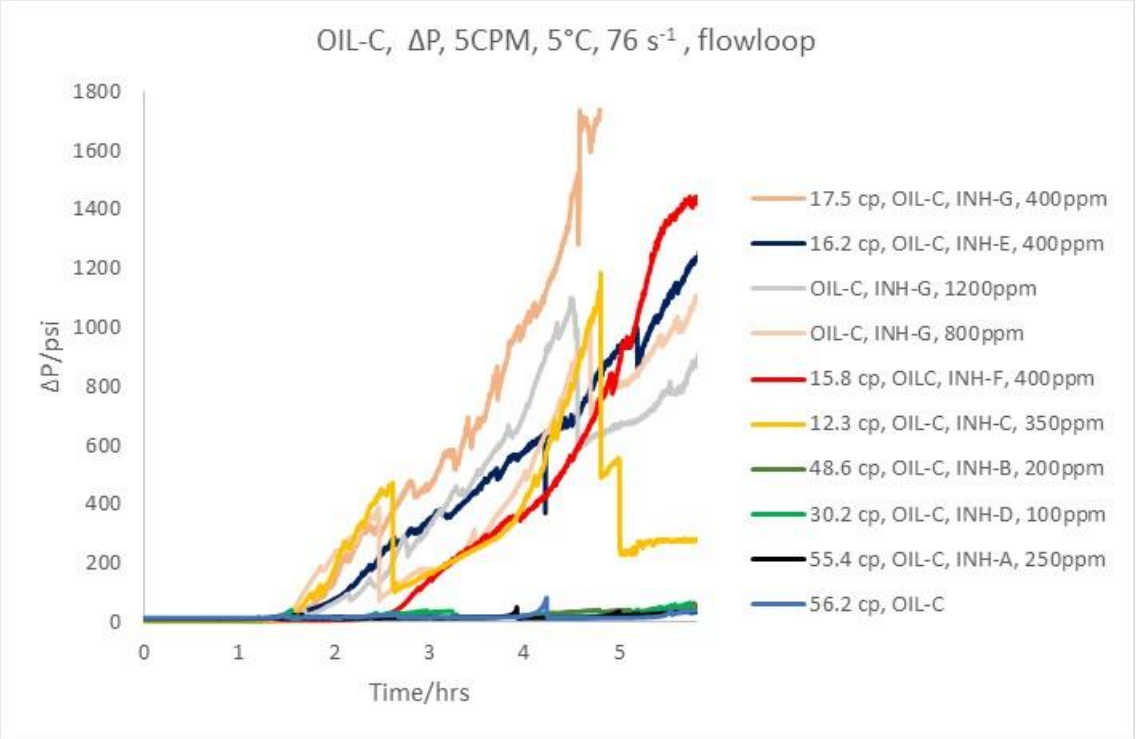

Figure 5-40. Comparison of differential pressure buildup by flowloop using OIL-C sample dosed with different inhibitors in 5CPM with 76 s^{-1}. The legend ranked top to bottom based on decreasing differential build-up pressure at 5°C.

Increasing test temperature to 15°C, as shown in Figure 5-42 and Figure 5-43, seems to have a positive effect when using inhibitor INH-G where it would be able to prohibit deposition growing for at least for 9hrs test time. On the other hand, dosages with inhibitors INH-C and E, still had the same outcome as already observed in low viscosity samples.

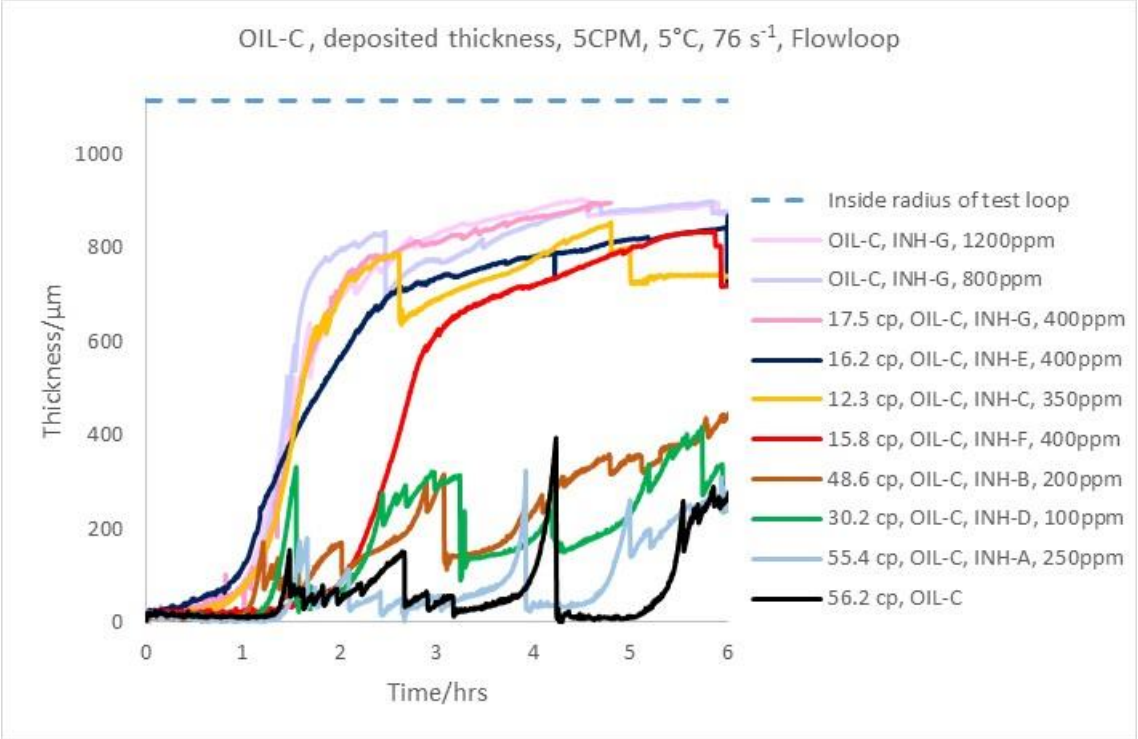

Figure 5-41. Comparison of deposited thickness by flowloop using OIL-C sample dosed with different inhibitors in 5CPM with 76 s^{-1}. The legend ranked top to bottom based on lower deposited thickness at 5°C.

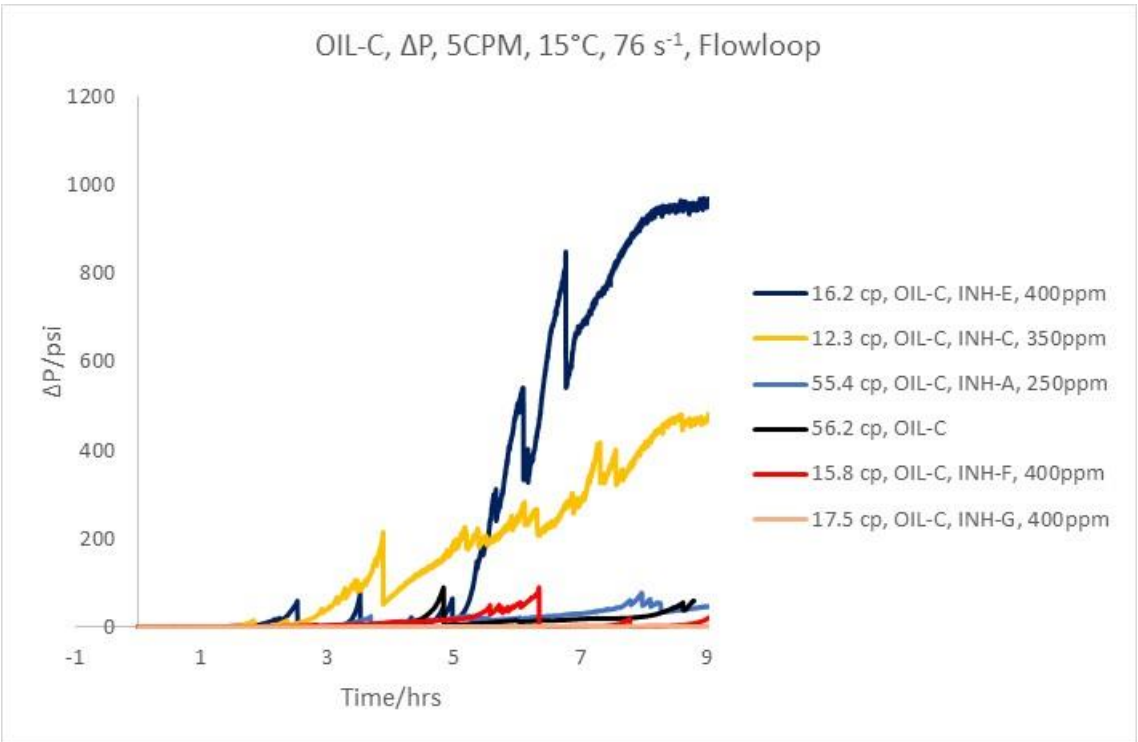

Figure 5-42. Comparison of differential pressure buildup by flowloop using OIL-C sample dosed with different inhibitors in 5CPM with 76 s^{-1}. The legend ranked top to bottom based on decreasing differential build-up pressure at 15°C.

In terms of the impact of lower subcooling on Inhibitor INH-F, it is noted that initially there was a higher deposition than the blank sample followed by a sharp reduction at around 6 hrs probably due to sloughing wax layers.

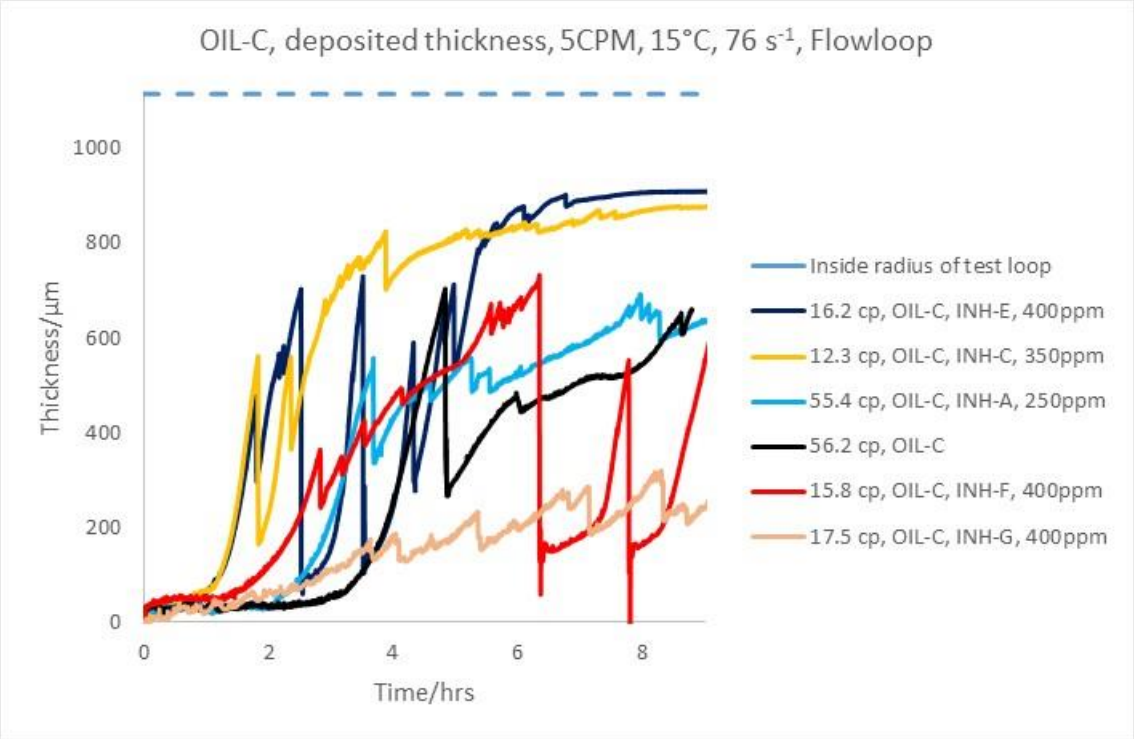

Figure 5-43. Comparison of deposited thickness by flowloop using OIL-C sample dosed with different inhibitors in 5CPM with 76 s^{-1}. The legend ranked top to bottom based on lower deposited thickness at 15°C.

To investigate if the applied test time was sufficient to assess inhibitor performance, INH-E was run for 24 hrs. The conclusions that could be drawn from the results shown in Figure 5-44 and Figure 5-45 are as follows.

A significant divergence in differential pressure was observed in early stages lower than 6 hrs followed by a large sloughing of the deposited layer. The general trend, though, in the following was that less viscous samples still gave higher deposition.

Moreover, Wax layers isolated the inner pipe at around 11 and 13 hrs for blank and dosed inhibitor correspondingly, where no further significant change was monitored.

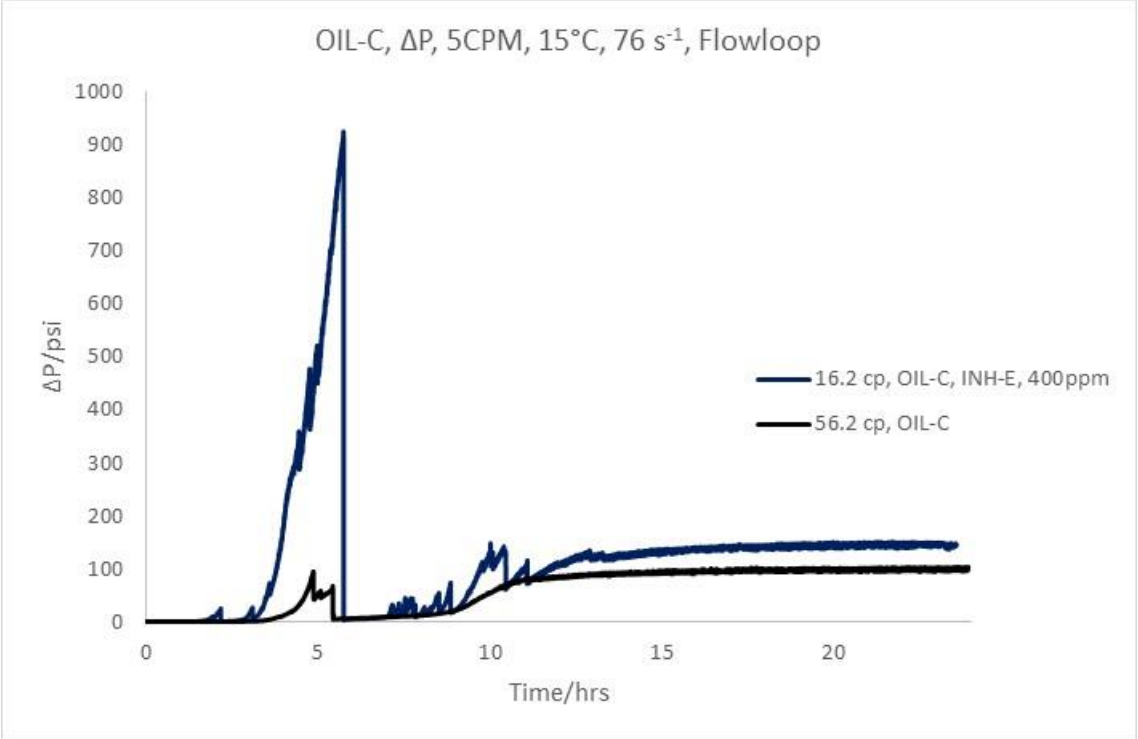

Figure 5-44. Comparison of differential pressure buildup by flowloop using OIL-C sample dosed with different inhibitors in 5CPM with 76 s^{-1}. The legend ranked top to bottom based on decreasing differential build-up pressure at 15°C.

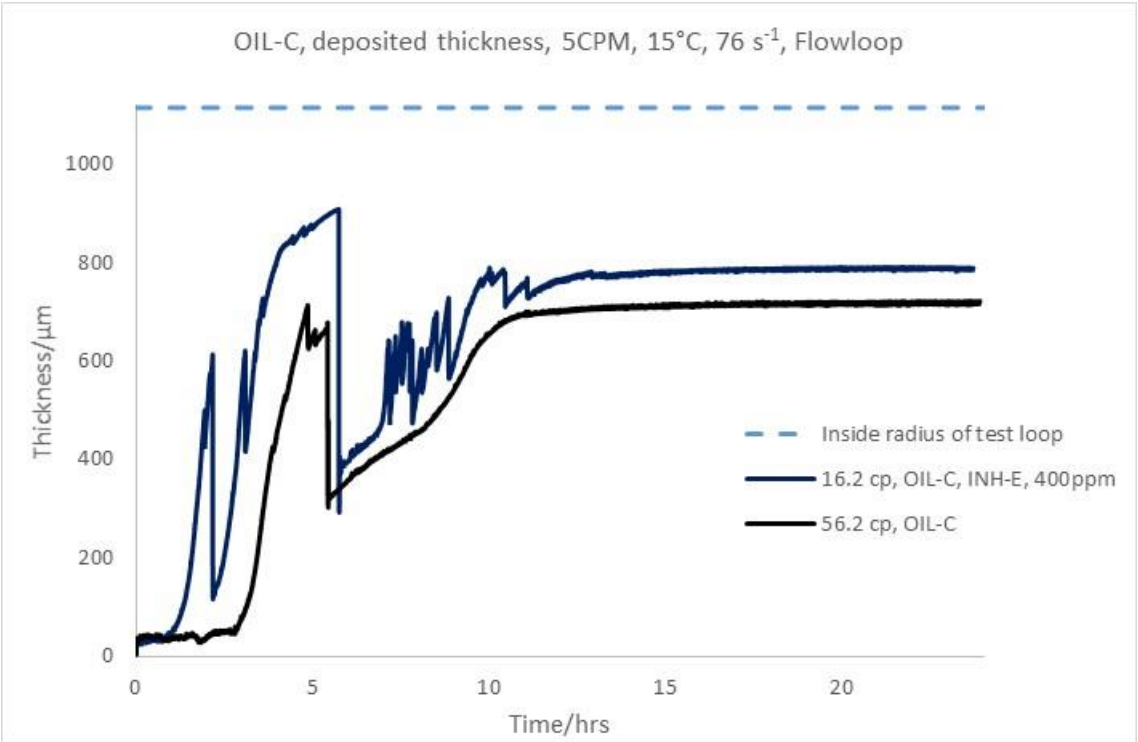

Figure 5-45. Comparison of deposited thickness by flowloop using OIL-C sample dosed with different inhibitors in 5CPM with 76 s^{-1}. The legend ranked top to bottom based on lower deposited thickness at 15°C.

INH-C was tested at low subcooling, 20°C which corresponded to WAT-2 °C for treated and WAT-9 °C for untreated mixtures. Surprisingly, lower viscosity of treated sample dominant the effect of higher subcooling of blank sample which resulted a higher differential pressure and wax thickness.

The following tests were carried out with an increasing shear of $151s^{-1}$, at a test temperature of 15°C with some specified inhibitors, Figure 5-48 and Figure 5-49.

In the early stage, the sample dosed with inhibitor INH-G showed a similar behaviour to lower shear rate tests as shown in Figure 5-42 and Figure 5-43. The strength of inhibition was reliable up to around 11 hrs while it was seen to increase deposition in comparison with the reference blank oil sample. The same action might be expected if the test was continued for a longer time at lower shear rate. Presumably, ranking inhibitors for comparison purposes based on initial behaviour may not be the best option.

Inhibitor INH-F did not also follow the viscosity ranking in this case.

Accordingly, by comparing the results obtained in different test temperature and shear rate, the performance of inhibitors, INH-F and INH-G, seemed to depend on subcooling.

INH-E was still observed to have a higher deposition in comparison with higher viscosity samples.

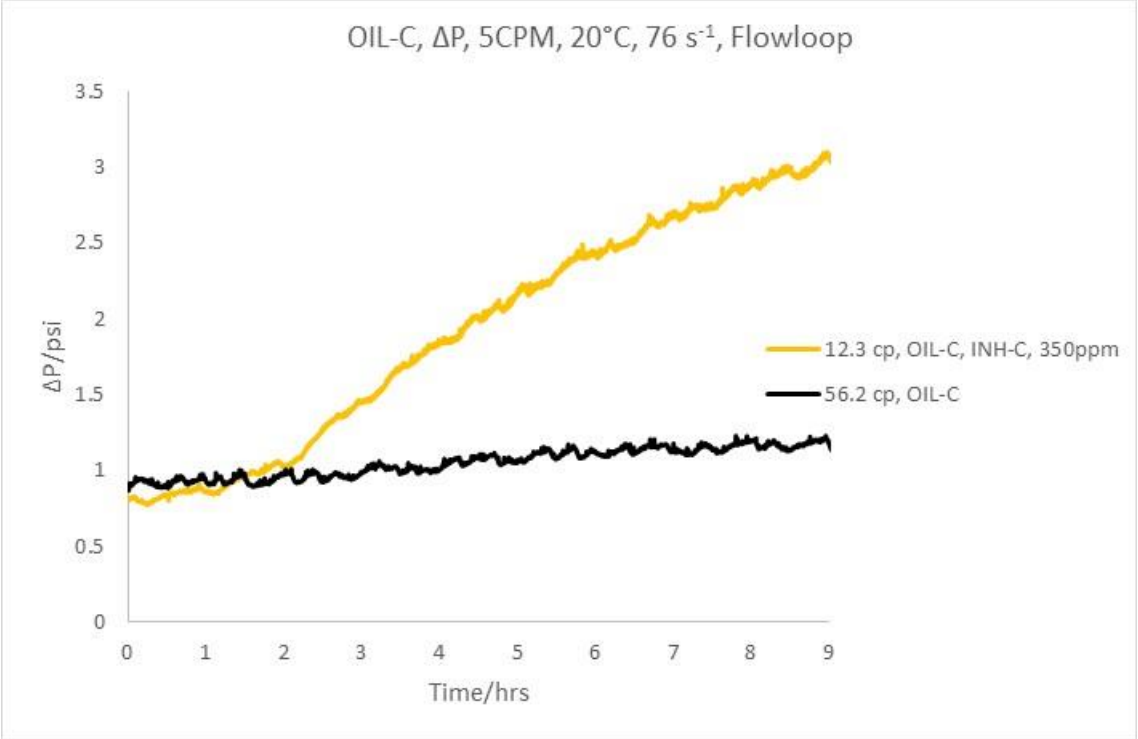

Figure 5-46. Comparison of differential pressure buildup by flowloop using OIL-C sample dosed with different inhibitors in 5CPM with 76 s^{-1}. The legend ranked top to bottom based on decreasing differential build-up pressure at 20°C.

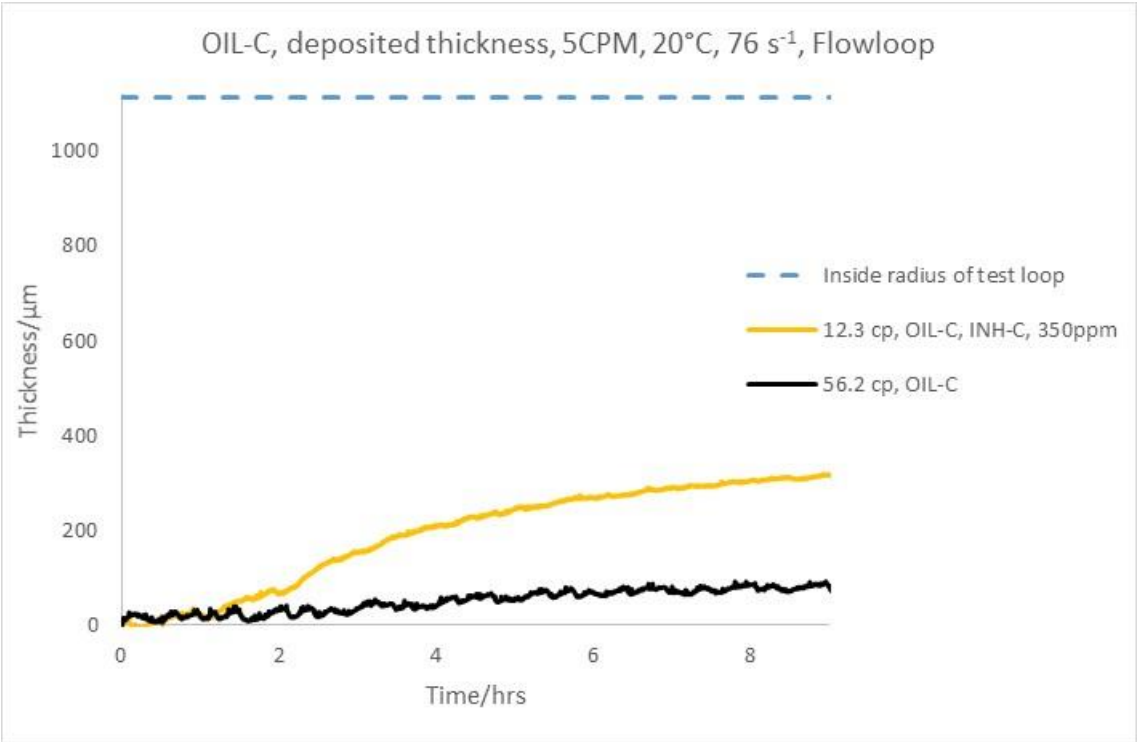

Figure 5-47. Comparison of deposited thickness by flowloop using OIL-C sample dosed with different inhibitors in 5CPM with 76 s^{-1}. The legend ranked top to bottom based on decreasing differential build-up pressure at 20°C.

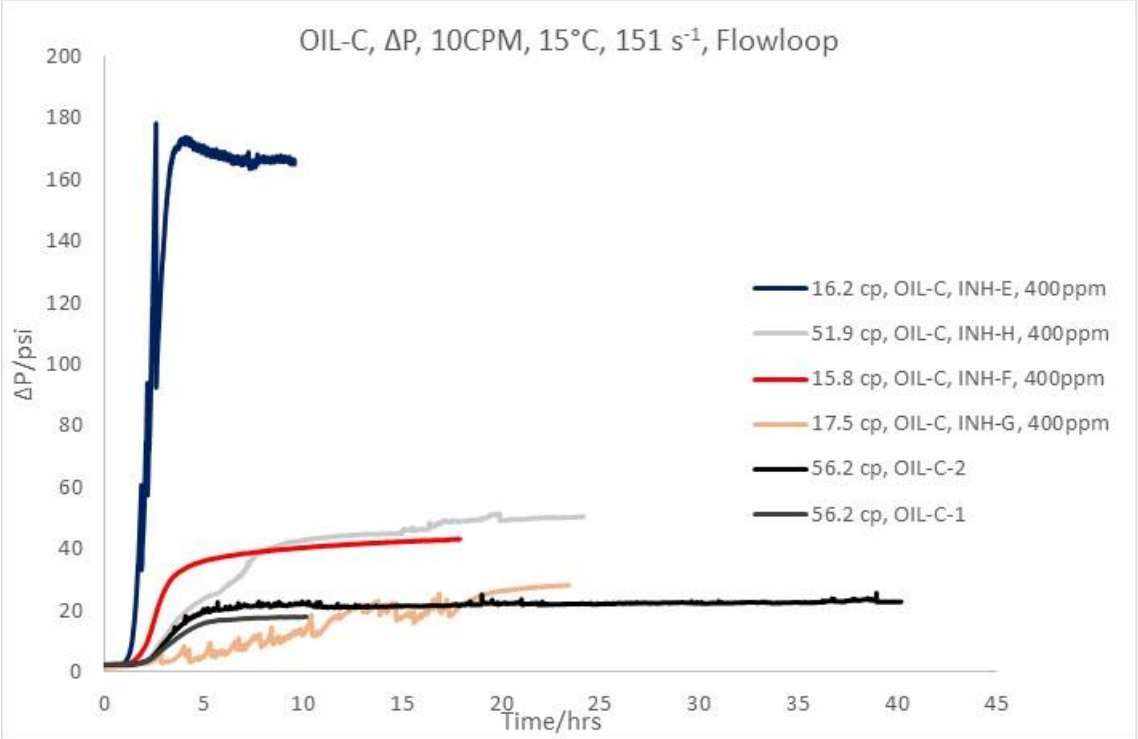

Figure 5-48. Comparison of differential pressure buildup by flowloop using OIL-C sample dosed with the various inhibitors in 10CPM with 151 s^{-1}. The legend ranked top to bottom based on decreasing differential build-up pressure at 15°C.

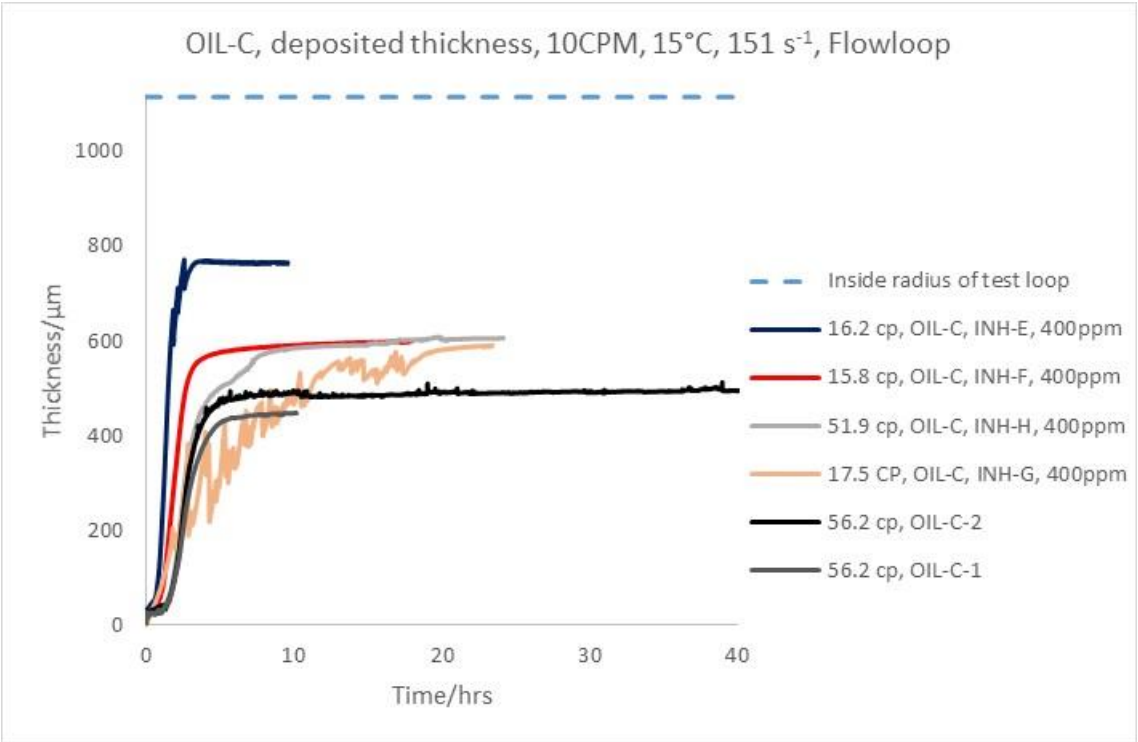

Figure 5-49. Comparison of deposited thickness by flowloop using OIL-C sample dosed with different inhibitors in 10CPM with 151 s^{-1}. The legend ranked top to bottom based on decreasing differential build-up pressure at 15°C.

5.5.3.2 Study of the possible impact of impurities or the loop geometry

In order to investigate the reason for higher deposition in terms of lower viscosity, one feasible option came to mind that accumulation of impurities and heavy composition like Asphaltene and resin could be deposited by gravity segregation in the low viscous laminar flow. The loop in preceding measurements was a cylindrical shape, 3 meters in length, 2.58mm inside diameter with an height of 20cm. Two scenarios were investigated. First, decreasing length, inside diameter and height as much as possible to encourage deposits to move freely out of the loop causing a decrease in differential pressure if this was the case. Another option, loaded the synthetic sample OIL-D which was free of Asphaltene, heavy particles and impurities in the existing loop.

5.5.3.2.1 Different geometry

For the first approach, a loop was made with 50cm length, 1.47 mm inside diameter and a 5cm height. Two different types of inhibitor, INH-G and INH-H, was taken. They were both good at reducing viscosity.

Since inhibitor INH-G was found have a good performance in the low subcooling with a test temperature of 15°C, the test temperature was set at 5°C in the highest possible flow rate 10CPM to obtain the highest possible shear rate expected to flush as much possible as deposition away. The results are plotted in Figure 5-50 and Figure 5-51.

Surprisingly, the outcome was similar, increasing deposition thickness with decreasing viscosity.

It was also observed that in the sample dosed with INH-G there was a sharp differential pressure increase leading to termination of the test at lower than 3hrs test time. As noted earlier, the pump stopped working at the time when the pressure passed the maximum working level. Hence, it never had the chance to slough deposited layer similar to what was observed in Figure 5-44 after about 5 hrs.

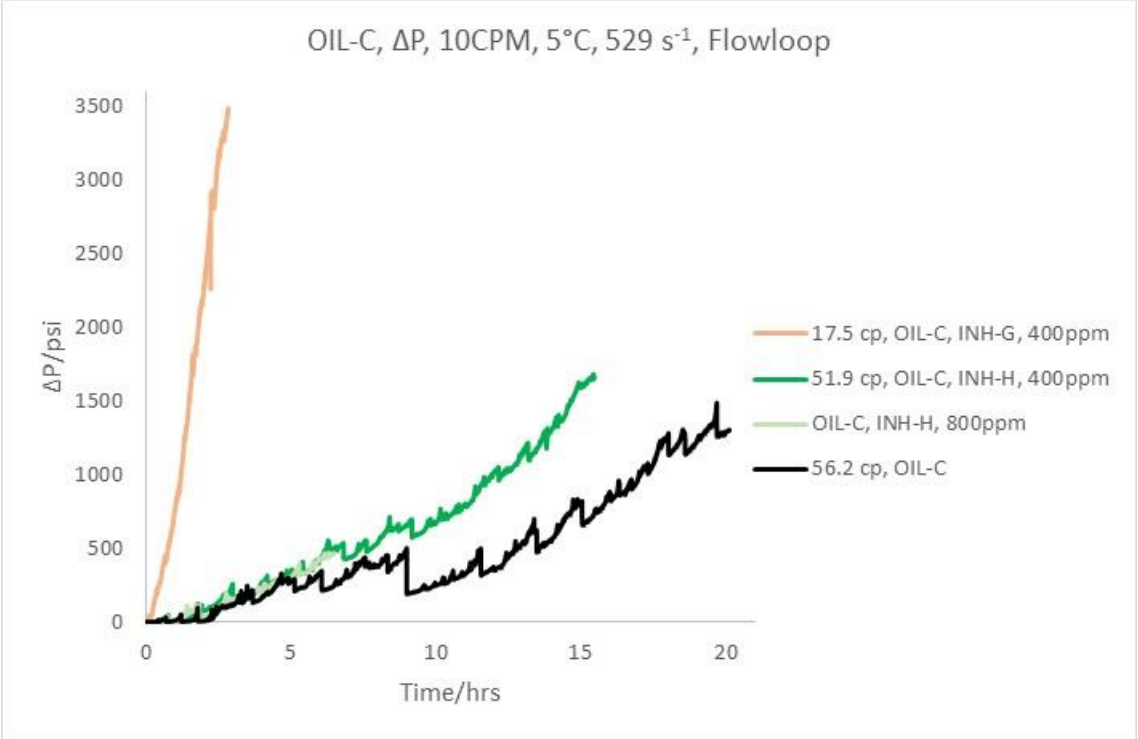

Figure 5-50. Comparison of differential pressure buildup by flowloop using OIL-C sample dosed with the various inhibitors in 10CPM with 529 s^{-1}. The legend ranked top to bottom based on decreasing differential build-up pressure at 5°C.

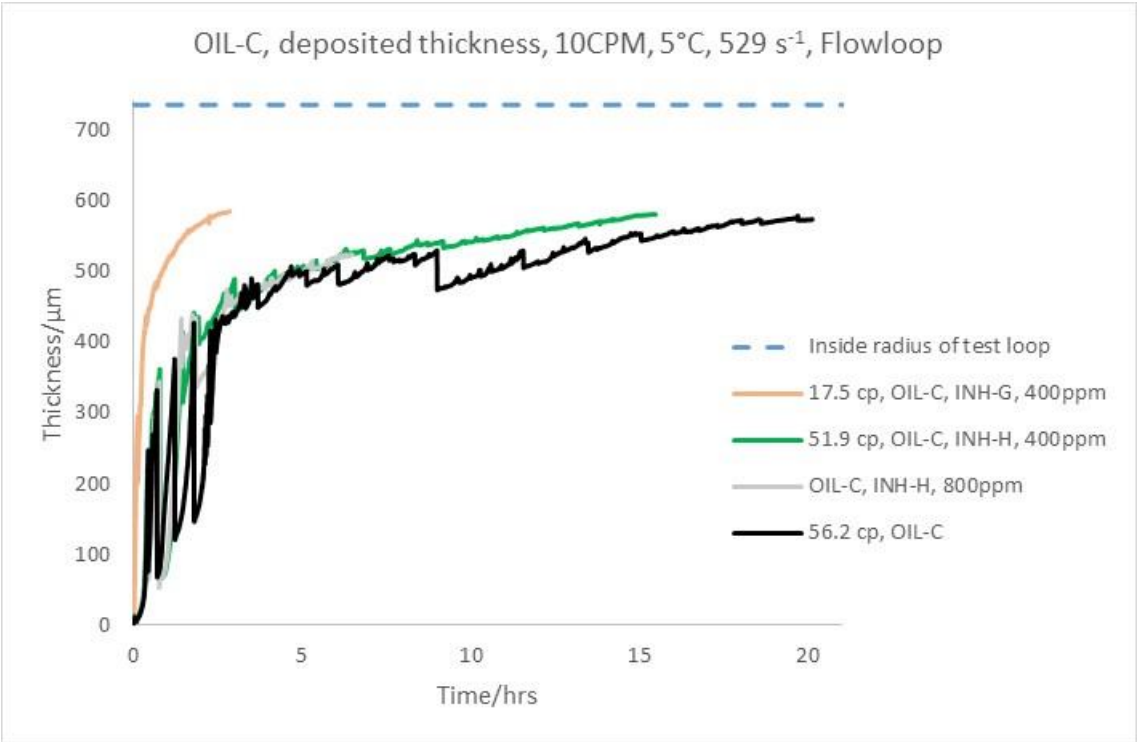

Figure 5-51. Comparison of deposited thickness by flowloop using OIL-C sample dosed with different inhibitors in 10CPM with 529 s^{-1}. The legend ranked top to bottom based on decreasing differential build-up pressure at 5°C.

5.5.3.2.2 Sample free of impurities/ asphaltene

In the second scenario, it was taken OIL-D sample which was made synthetically free of Asphaltene and impurities. It was dosed with four inhibitors in two different class of viscosity reduction. Inhibitors INH-D and INH-G with corresponding viscosities of 5.85 and 6.22cP and inhibitors INH-B and INH-D with 57.8cP and 78cP viscosities respectively.

Test condition and results are presented in Table 5-15.

Table 5-15. Experimental conditions and the results of flowloop, used OIL-D sample dosed with different inhibitor. Loop C was used for all the tests.

Fluid	*Conditioning T (°C)*	*Test T (°C)*	*Flow rate (cc/min)*	*Shear rate (s^{-1})*	*Average ⊿P (psi)*	*Average T_{in} (°C)*	*Average T_{out} (°C)*	*Average deposited thickness (µm)*
OIL-D, INH-D, 100ppm	*50*	*15*	*10*	*151*	*66.6*	*39.50*	*16.38*	*451*
OIL-D, INH-G, 400ppm	*50*	*15*	*10*	*151*	*22.7*	*38.92*	*16.44*	*415*
OIL-D, INH-B, 200ppm	*50*	*15*	*10*	*151*	*16.5*	*39.03*	*16.35*	*310*
OIL-D, INH-H, 400ppm	*50*	*15*	*10*	*151*	*13.3*	*35.67*	*15.92*	*249*
OIL-D	*50*	*15*	*10*	*151*	*18.9*	*36.00*	*16.15*	*279*

As shown in Figure 5-52 and Figure 5-53, interestingly, both differential pressure and deposited thickness increased exactly on the ranking of viscosity reduction.

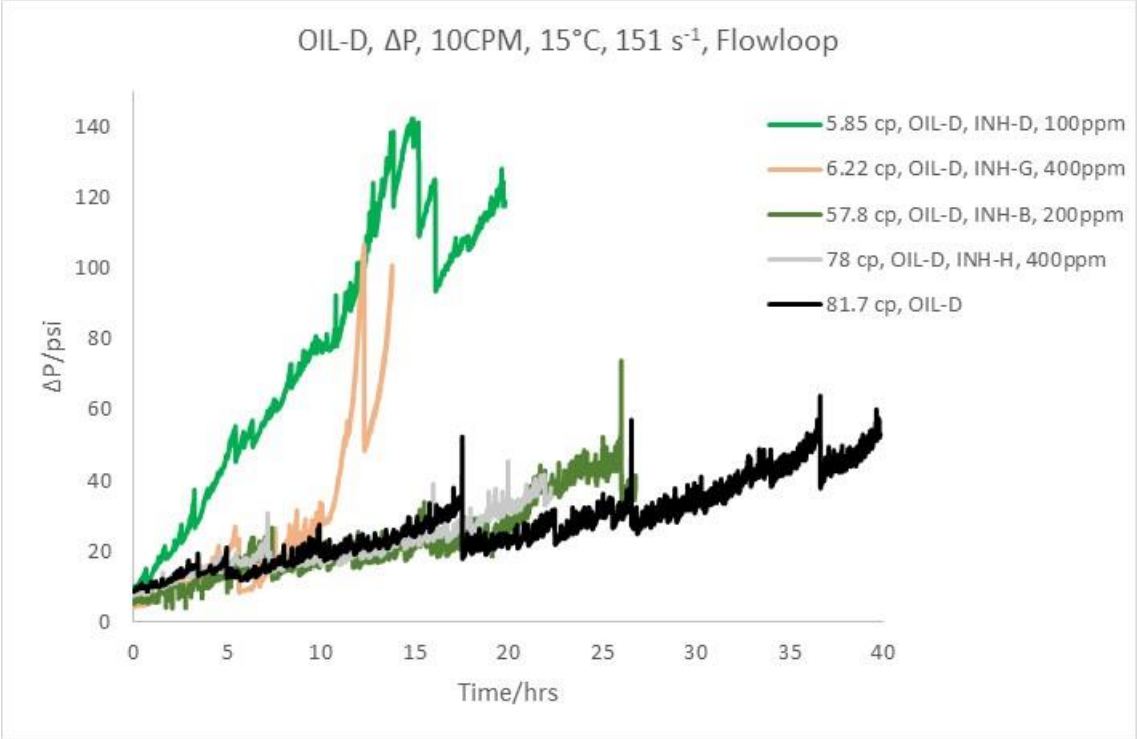

Figure 5-52. Comparison of differential pressure buildup by flowloop using OIL-D sample dosed with different inhibitors in 10CPM with 151 s^{-1}. The legend ranked top to bottom based on decreasing differential build-up pressure at 15°C.

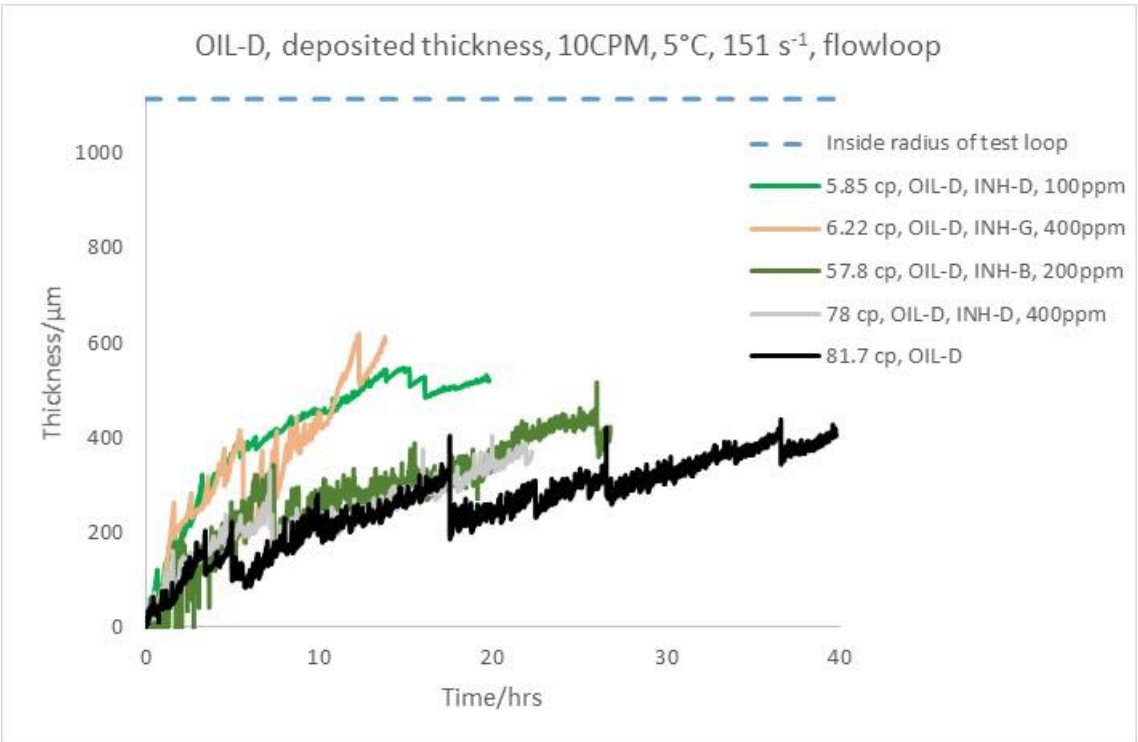

Figure 5-53. Comparison of deposited thickness by flowloop using OIL-D sample dosed with different inhibitors in 10CPM with 151 s^{-1}. The legend ranked top to bottom based on decreasing differential build-up pressure at 15°C.

As can be seen in either scenario, it was found that viscosity had a powerful impact on ranking deposition regardless of loop geometry or presence of Asphaltene/impurities.

5.5.3.3 Addition of inhibitor to the deposited wax or in the presence of a watercut

The routine procedure in terms of inhibitor injection used in this work was far removed from real field conditions. The sample was dosed with predetermined inhibitor loaded in the reservoir while loops were clean and free of any normal deposits. A probable option for increasing deposition in the presence of inhibitors on clean and free of deposition/impurities pipe wall could be due to the surface roughness of the pipe wall acting as a nucleation site overestimate deposition. In addition, the impact of inhibitors on the clean wall, might form an interlock connection between pipe walls and the wax particles, encourage to deposit faster as an artificial nucleation site. The presence of watercut in real flow line was ignored as well. While in reality, inhibitors usually inject in flow line with already deposited wax and/or watercut. This section has investigated the impact of either case on the inhibitor performance. The question arises if, low viscosity mixtures caused higher deposition.

Inhibitor INH-G was chosen based on the best viscosity reducer, using OIL-C with/out 20 % watercut. Table 5-16 contains information employed in this part. Test temperature was set at 5°C with applied shear rate of 151 s^{-1}.

Table 5-16. Experimental conditions and the results of flowloop, using OIL-C sample dosed with INH-G inhibitor added to blank oil with/out watercut. Loop C was used for all the tests.

Fluid	*Conditioning T (°C)*	*Test T (°C)*	*Flow rate (cc/min)*	*Shear rate (s^{-1})*	*Average ΔP (psi)*	*Average T_{in} (°C)*	*Average T_{out} (°C)*	*Average deposited thickness (μm)*
OIL-C, INH-G, 400ppm	*50*	*5*	*10*	*151*	*942*	*34.92*	*5.98*	*847*
Added INH-G, 400ppm to OIL-C	*50*	*5*	*10*	*151*	*602*	*35.27*	*6.84*	
OIL-C	*50*	*5*	*10*	*151*	*503*	*35.71*	*7.53*	*643*
OIL-C, watercut 20%, INH-G, 400ppm	*50*	*5*	*10*	*151*	*331*	*38.84*	*6.93*	*739*
Added INH-G, 400ppm to OIL-C, watercut 20%	*50*	*5*	*10*	*151*	*232*	*39.20*	*6.82*	*543*

5.5.3.4 Inhibitor added to the current deposited wax

As shown in Figure 5-54, the differential pressure for three approaches was compared. A fresh aliquot of blank oil sample was logged for 14 hrs as a baseline reference. Furthermore, a mixture dosed with 400ppm INH-G was loaded in a clean loop, shut the

pump off in about 7 hrs working reached to the maximum working pressure. Following, a blank sample was loaded, start to circulate on the loop, allowed to buildup layers of deposition for about a 4hrs in 5°C test temperature, then dosed with 400ppm INH-G.

It was observed as shown in Figure 5-54, at the start of injection, differential pressure showed a reducing value. The test was continued for about 2hrs then it started to rise sharply until it reached to the maximum working pump pressure. The trend is identical with the mixture loaded in the clean loop, which started to increase for about 2 hrs as well.

As noted, the deposition thickness value depends on the viscosity obtained by differential pressure at the start of holding test temperature, presume no deposition occurred before that point. Hence all the differential pressure contributes to viscosity change. Once the inhibitor was injected, viscosity reduced resulted a dropping in differential pressure. It made it difficult to measure deposition thickness, hence it was not plotted.

The result showed there was no difference among surface roughness and current deposited wax layer on inhibitor performance, at least for the condition and sample used in this study.

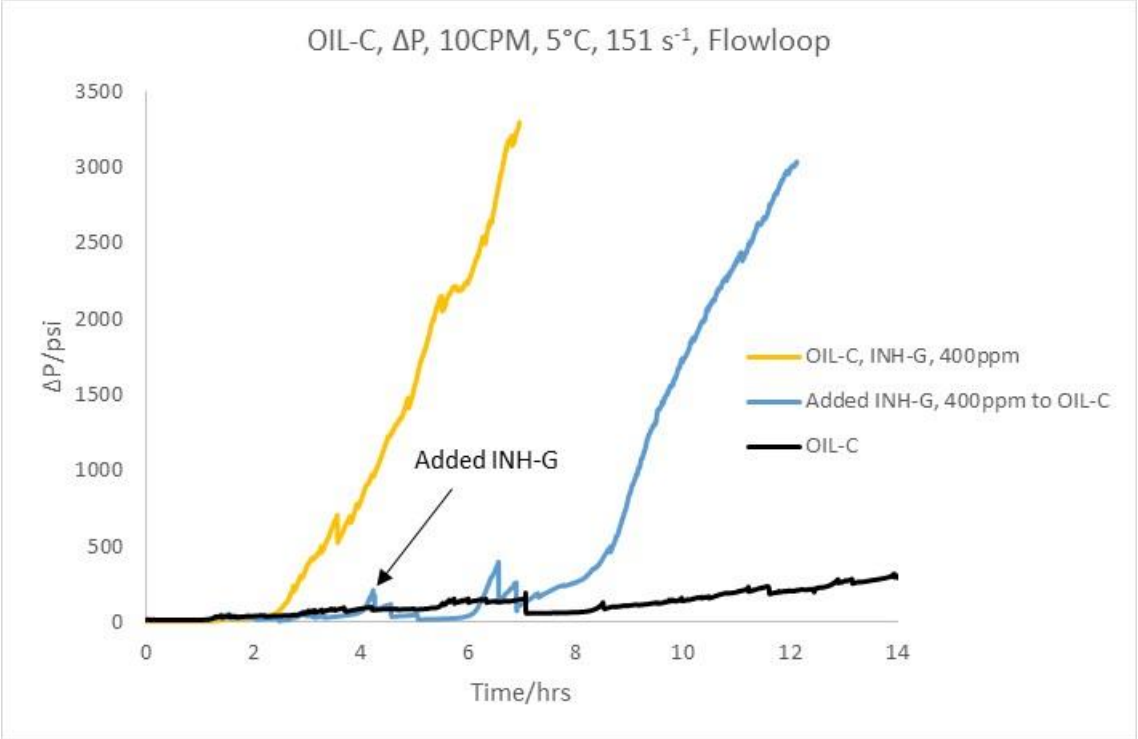

Figure 5-54. Comparison of differential pressure buildup by flowloop using OIL-C sample dosed with different inhibitors in 10CPM with 151 s^{-1}. The legend ranked top to bottom based on decreasing differential build-up pressure at 5°C.

5.5.3.5 Impact of watercut in treated sample

The presence of watercut on wax deposition will be discussed in detail in the following chapter. In essence, samples containing watercut did not show any significant effect at high subcooling where thermal difference play a significant role as a driving force for deposition. At lower subcooling, probably, wettability alteration prevents deposition. As shown in Figure 5-55 and Figure 5-56, both blank sample with/out watercut almost have the same trend in high subcooling. The presence of inhibitor INH-G encouraged deposition; though, presence of water dislodged wax layers continuously.

As has been found so far, viscosity plays a dominant factor in the case of deposition in laminar flow with/out watercut; the presence of water in treated sample only reduced deposition presumably in the same rank without watercut.

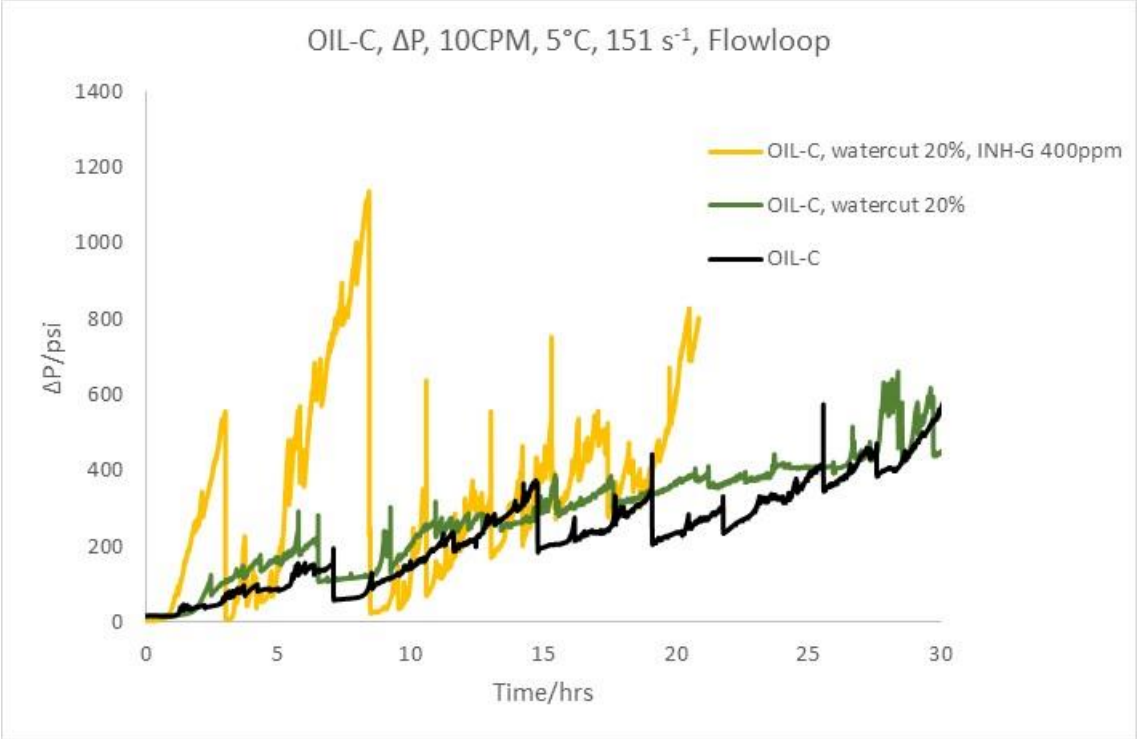

Figure 5-55. Comparison of differential pressure buildup by flowloop using OIL-C sample in 10CPM with 151 s^{-1}. The legend ranked top to bottom based on decreasing differential build-up pressure at 5°C.

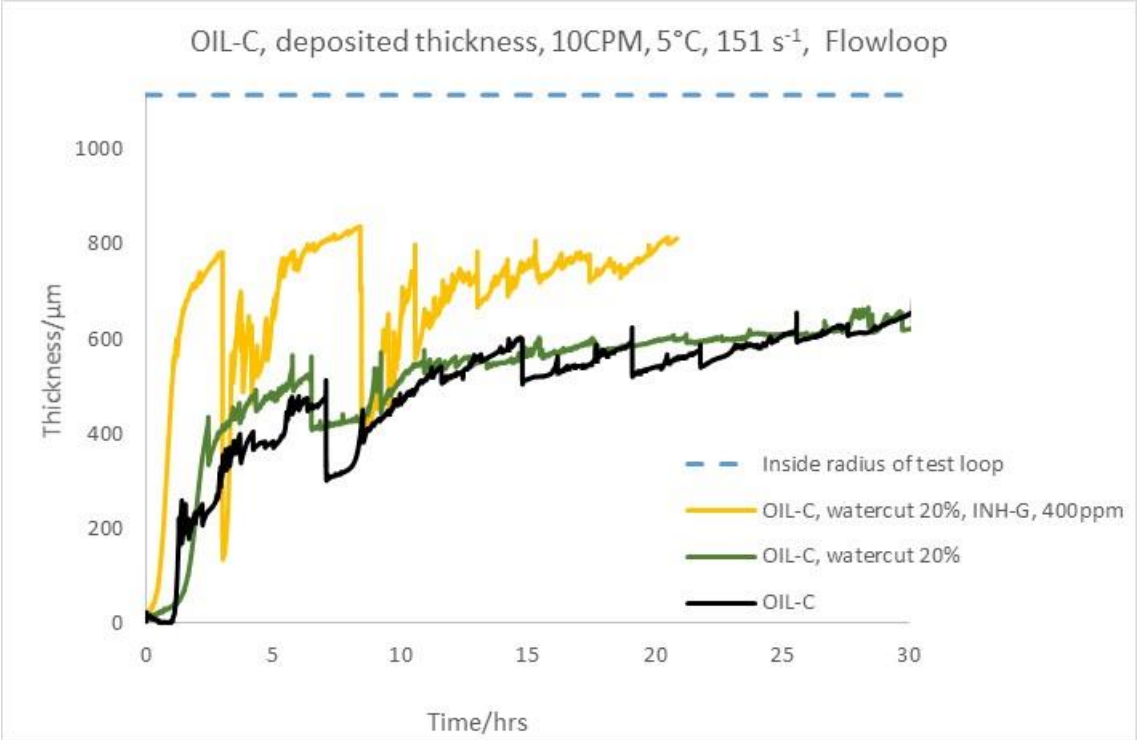

Figure 5-56. Comparison of deposited thickness by flowloop using OIL-C sample in 10CPM with 151 s^{-1}. The legend ranked top to bottom based on decreasing differential build-up pressure at 5°C.

5.5.3.6 Impact of circulation on inhibitor performance

A different approach was also launched to investigate the effect of closed circulation loop where the sample was subjected to a continuous cooling/heating cycle, on the impact of inhibitors. Two inhibitors with a large impact on viscosity were chosen being, INH-C and INH-G compared with a blank sample in a one-way single batch without circulation. The oil sample was then increased to 920cc suited for 3 hrs test time in 5°C at the rate of 5CPM.

To avoid using up oil sample, both dynamic WAT and deposition thickness were not measured. Hence loading was done in a different procedure that did not impact on the deposition rate data. Prior to launching the test, the loop was washed thoroughly with toluene at conditioning temperature, then started to cool down while still toluene circulated in the loop. Sample which is conditioined outside the loop, therefore, replaced with toluene, pushed it away when test loop temperature stabilised at the test temperature. This approach was against previous measurements where it washed with toluene and replaced with oil sample both at conditioning temperature.

Table 5-17 presented the test condition and results of single batched without circulation.

Table 5-17. Experimental conditions and the results of flowloop, using OIL-C sample dosed with different inhibitors in single batched without circulation. Loop C was used for all the tests.

Fluid	*Volume of oil (cc)*	*Condition T (°C)*	*Test T (°C)*	*Flow rate (cc/min)*	*Shear rate (s^{-1})*	*Average ΔP (psi)*	*Average T_{in} (°C)*	*Average T_{out} (°C)*
OIL-C, INH-G, 400ppm	*920*	*50*	*5*	*5*	*76*	*64.93*	*29.50*	*7.36*
OIL-C, INH-C, 350ppm	*920*	*50*	*5*	*5*	*76*	*22.02*	*28.54*	*7.45*
OIL-C	*920*	*50*	*5*	*5*	*76*	*18.12*	*29.77*	*6.27*

Differential pressure over the test temperature is plotted in Figure 5-57. The output surprisingly indicates that the impact of circulation if existed, could not dominant the influence of viscosity reduction. Test with sample dosed with INH-C was failed at around 2 hrs, though it is possible to estimate the trend.

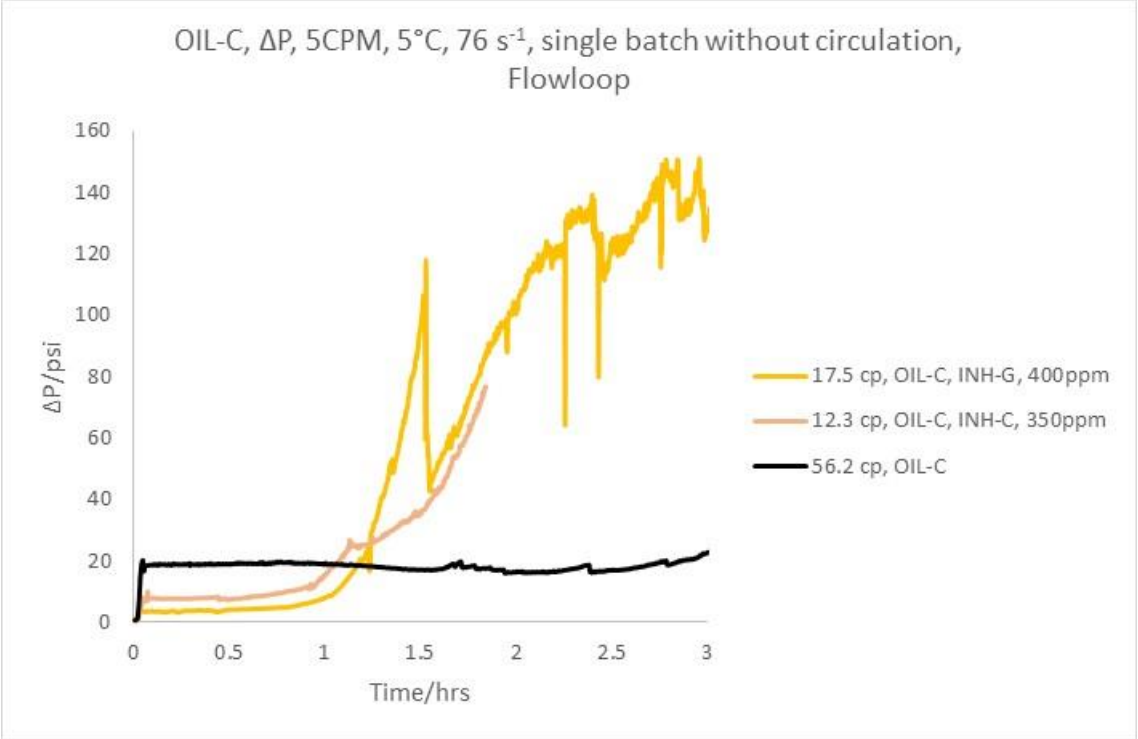

Figure 5-57. Comparison of differential pressure buildup by flowloop using OIL-C sample dosed with different inhibitors in 5CPM with 76 s^{-1}. The legend ranked top to bottom based on decreasing differential build-up pressure at 5°C. Single batched without circulation.

5.6 NIR spectroscopy

The last experimental equipment used in this study was NIR spectroscopy. The capability of NIR in terms of wax study, provide user to measure WAT and precipitation rate. WAT measured with NIR will be discussed in the following section in comparison with QCM and rheometer. As noted, the strength of intensity drop could be attributed to precipitation rate of particles, giving an opportunity to evaluate wax inhibitors. Three different oil samples OIL-B, OIL-C and OIL-D were using in predetermined dosages of various inhibitors. Table 5-18 lists the test conditions and results ranked top to bottom by increasing intensity drop in every individual oil sample. Conditioning temperature was measured using rheometer discussed it in detail in the previous chapter. The cooling rate was set at 0.5°C/min to be in the range of thermal control bath.

Table 5-18. Experimental conditions for NIR using OIL-B dosed with different inhibitors, ranked top to bottom based on decreasing maximum intensity drop

Fluid	*Conditioning temperature (°C)*	*Destination temperature (°C)*	*Cooling ramp (°C/min)*	*WAT (°C)*	*Maximum intensity drop*
OIL-B, INH-A, 250ppm	*60*	*15*	*0.5*	*28.5*	*-358*
OIL-B	*60*	*15*	*0.5*	*30.4*	*-499*
OIL-B, INH-D, 100ppm	*60*	*15*	*0.5*	*29.2*	*-675*
OIL-B, INH-C, 350ppm	*60*	*15*	*0.5*	*22.7*	*-685*
OIL-B, INH-B, 200ppm	*60*	*15*	*0.5*	*26.4*	*-723*
OIL-B, INH-G, 400ppm	*60*	*15*	*0.5*	*22.9*	*-770*
OIL-B, INH-E, 400ppm	*60*	*15*	*0.5*	*21.4*	*-782*
OIL-B, INH-F, 400ppm	*60*	*15*	*0.5*	*25.8*	*-802*
OIL-C, INH-H, 800ppm	*50*	*5*	*0.5*	*25.0*	*-824*
OIL-C	*50*	*5*	*0.5*	*25.1*	*-927*
OIL-C, INH-A, 250ppm	*50*	*5*	*0.5*	*23.1*	*-948*
OIL-C, INH-H, 400ppm	*50*	*5*	*0.5*	*25.8*	*-950*
OIL-C, INH-B, 200ppm	*50*	*5*	*0.5*	*24.4*	*-1016*
OIL-C, INH-D, 100ppm	*50*	*5*	*0.5*	*23.5*	*-1116*
OIL-C, INH-F, 400ppm	*50*	*5*	*0.5*	*22.1*	*-1122*
OIL-C, INH-G, 400ppm	*50*	*5*	*0.5*	*20.4*	*-1345*
OIL-C, INH-E, 400ppm	*50*	*5*	*0.5*	*20.1*	*-1378*
OIL-C, INH-C, 350ppm	*50*	*5*	*0.5*	*21.1*	*-1389*
OIL-D, INH-B, 200ppm	*50*	*15*	*0.5*	*32.0*	*-559*
OIL-D, INH-H, 400ppm	*50*	*15*	*0.5*	*30.3*	*-674*
OIL-D, INH-A, 250ppm	*50*	*15*	*0.5*	*31.5*	*-723*
OIL-D	*50*	*15*	*0.5*	*32.0*	*-900*
OIL-D, INH-C, 350ppm	*50*	*15*	*0.5*	*31.0*	*-1088*
OIL-D, INH-E, 400ppm	*50*	*15*	*0.5*	*31.0*	*-1179*
OIL-D, INH-F, 400ppm	*50*	*15*	*0.5*	*30.1*	*-1228*
OIL-D, INH-G, 400ppm	*50*	*15*	*0.5*	*29.0*	*-1254*
OIL-D, INH-D, 100ppm	*50*	*15*	*0.5*	*30.7*	*-1411*

As an illustration, a typical intensity variation in temperature sweep is plotted in Figure 5-58. Shown in the figure is referred to the oil sample OIL-C in different inhibitor dosages. The legend ranked top to bottom by increasing intensity drop.

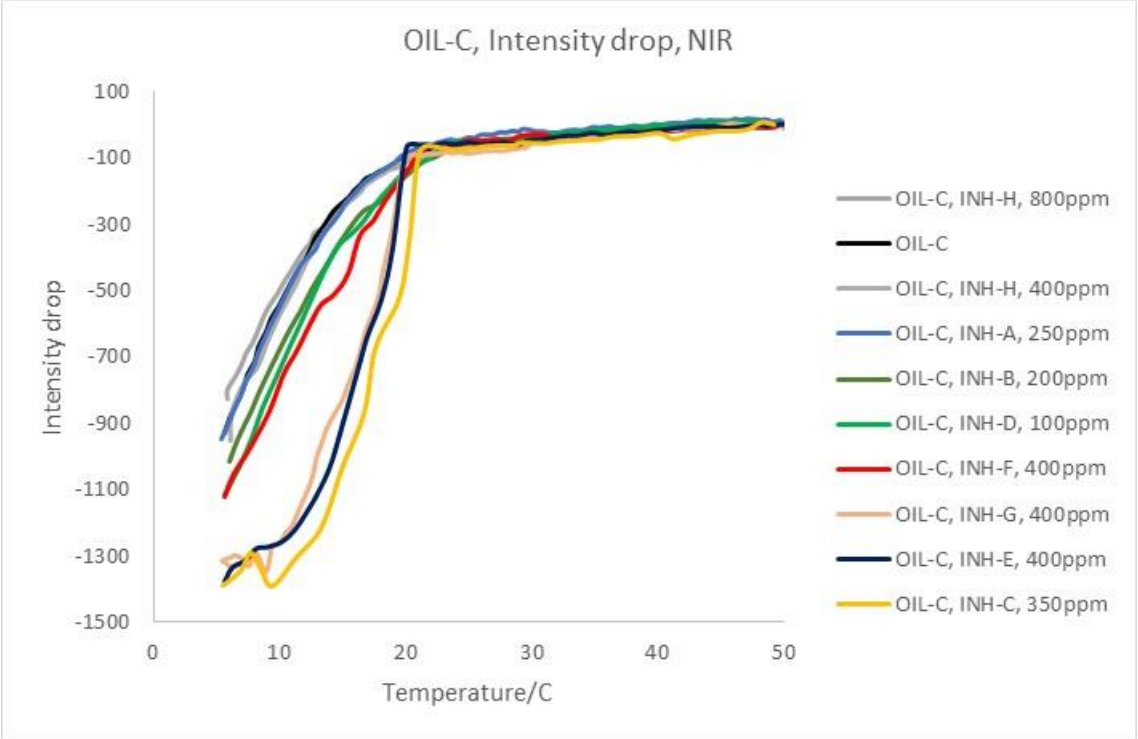

Figure 5-58. Comparison of intensity drop by NIR using OIL-C sample dosed with different inhibitors. The legend ranked top to bottom based on decreasing maximum intensity drop.

For better visual evaluation only the maximum intensity reduction values are demonstrated in Figure 5-59, Figure 5-60 and Figure 5-61 for oil samples OIL-B, OIL-C and OIL-D respectively. The column is ranked left to right by increasing intensity drop attributed to the higher precipitation rates. Corresponding available maximum viscosities are also plotted. Decreasing viscosities was observed to have higher precipitation, likewise what has been found in flowloop in terms of deposition. In a simple word, lower viscosity made higher precipitation rate leading to higher deposition.

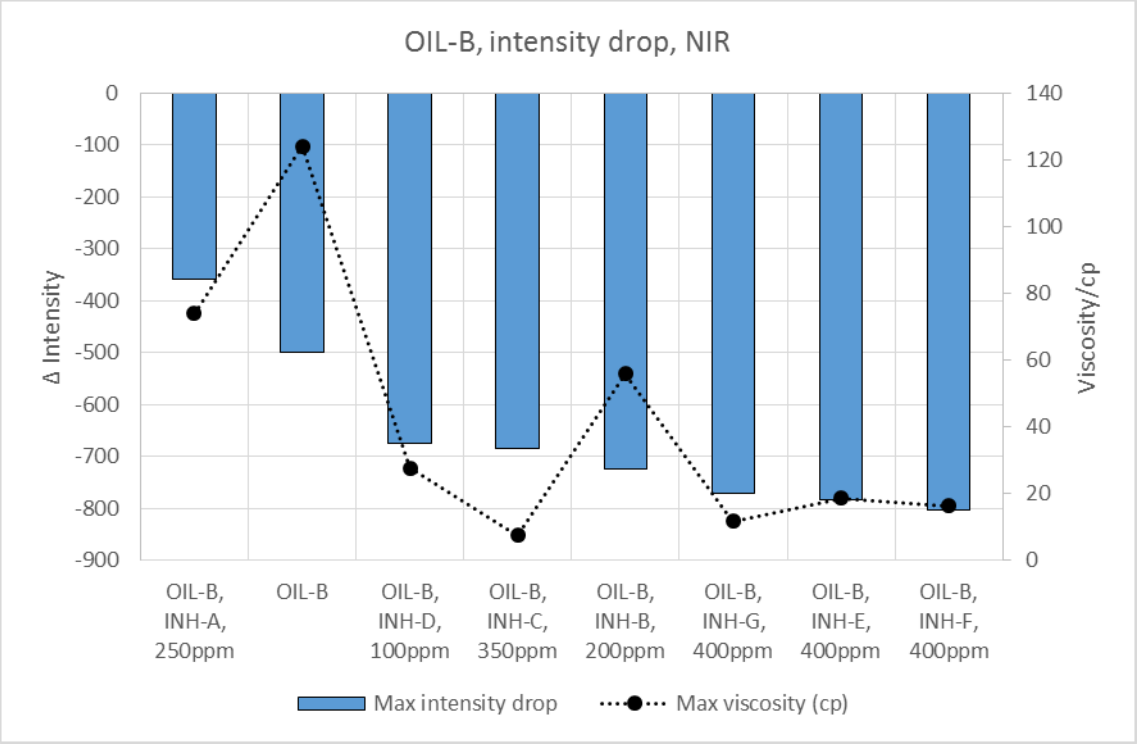

Figure 5-59. Comparison of intensity drop measured with NIR using OIL-B sample dosed with different inhibitors. The plot ranked from left to right based on increasing intensity drop.

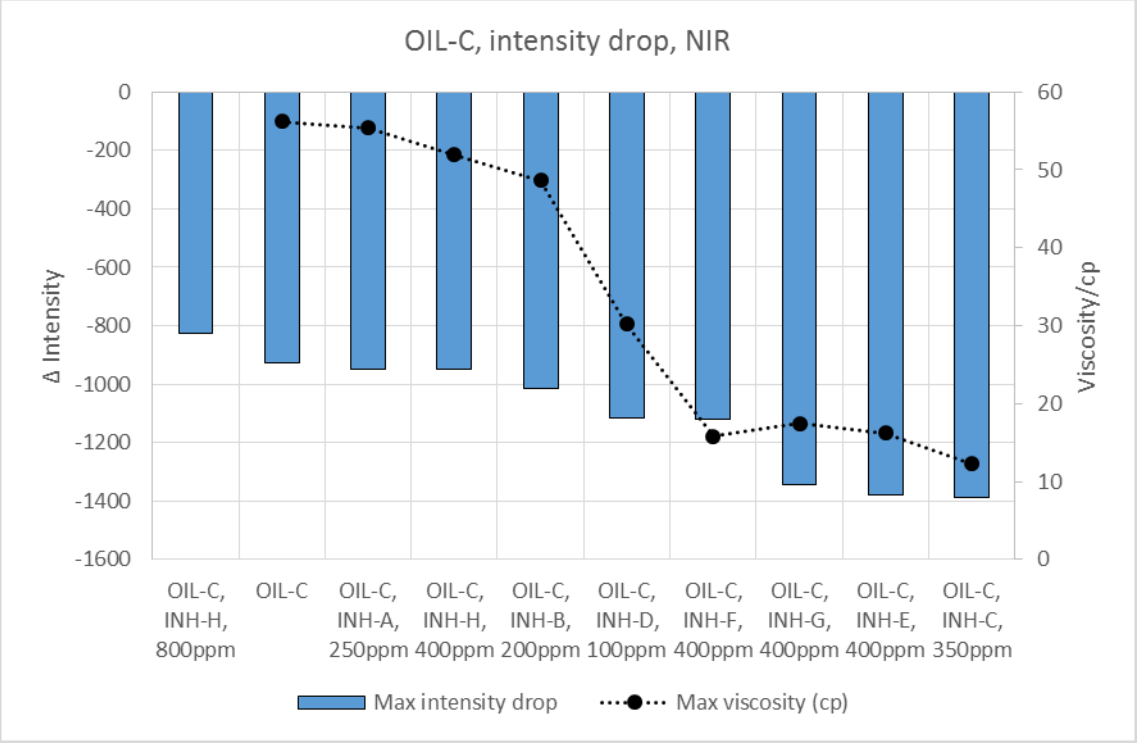

Figure 5-60. Comparison of intensity drop measured with NIR using OIL-C sample dosed with different inhibitors. The plot ranked from left to right based on increasing intensity drop.

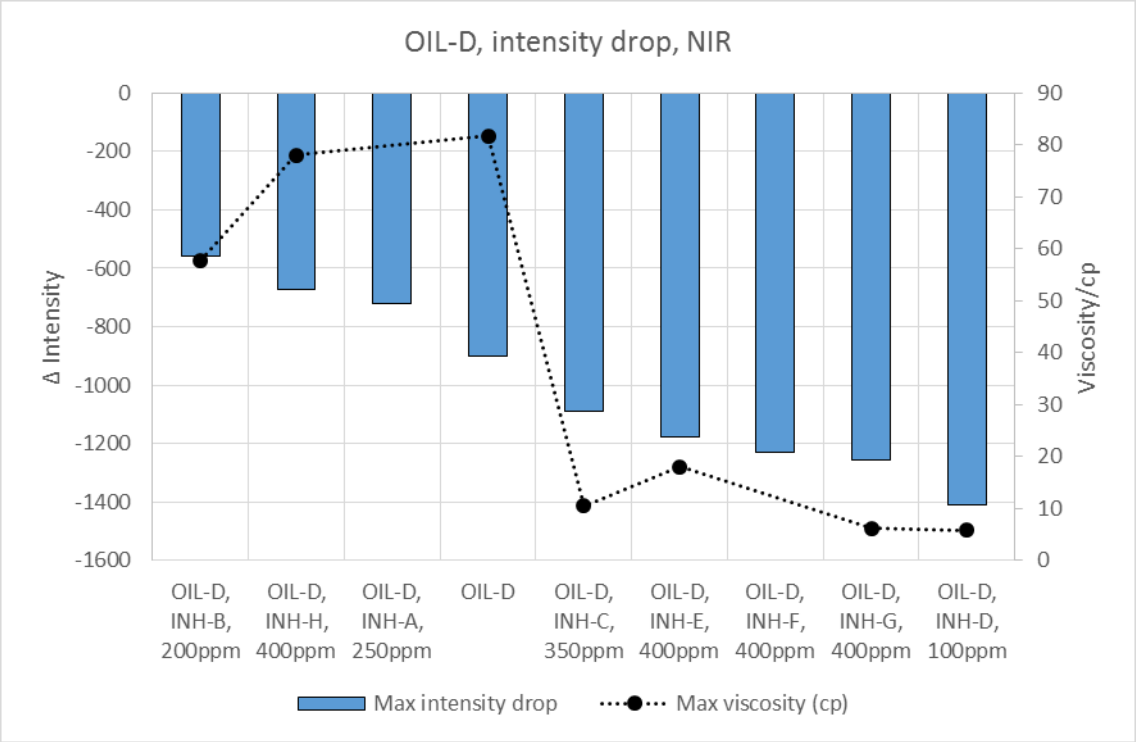

Figure 5-61. Comparison of intensity drop measured with NIR using OIL-D sample dosed with different inhibitors. The plot ranked from left to right based on increasing intensity drop.

5.7 Inhibitor screening by measuring WAT/WDT

Any changes in the wax appearance temperature might be an indication of the impact of wax inhibitors on the wax crystallisation process. Different equipment can experimentally identify this critical point. As hinted earlier, there are no experimental techniques to detect the accurate thermodynamic point of precipitation [9, 10]. In this work, several different independent types of equipment were used with the capability of measuring WAT included: rheometer, QCM, NIR and flowloop. WDT was only measured with QCM.

It was noted that the WAT obtained by flowloop is known as dynamic WAT which showed a low accuracy, highly depended on the inside diameter of loops [11]. Moreover, it was observed that the dynamic WAT had almost with the same rank with the obtained data by the other devices in a deviation up to 10°C in precipitation point, therefore it is not included in this report.

The data for Rheometer, QCM and NIR, has already tabulated in Table 5-2,Table 5-5 to Table 5-8 and Table 5-18 respectively, using oil samples OIL-A, OIL-B, OIL-C and OIL-D. The standard deviation was only determined with QCM for an average of eight different statistical data.

The amount of WAT was averaged and ranked left to right by decreasing in values are plotted in Figure 5-62 to Figure 5-65 corresponding to oil samples OIL-A, OIL-B, OIL-C and OIL-D with different inhibitor dosages.

To further illustrate the relation between WAT/WDT and the other parameters obtained for inhibitor evaluation, WAT/WDT were combined with the corresponding maximum viscosity achieved by the rheometer. Since OIL-A had almost the same viscosity trend in either treated and untreated samples, maximum frequency drop measured by QCM was bundled with WAT/WDT in this case.

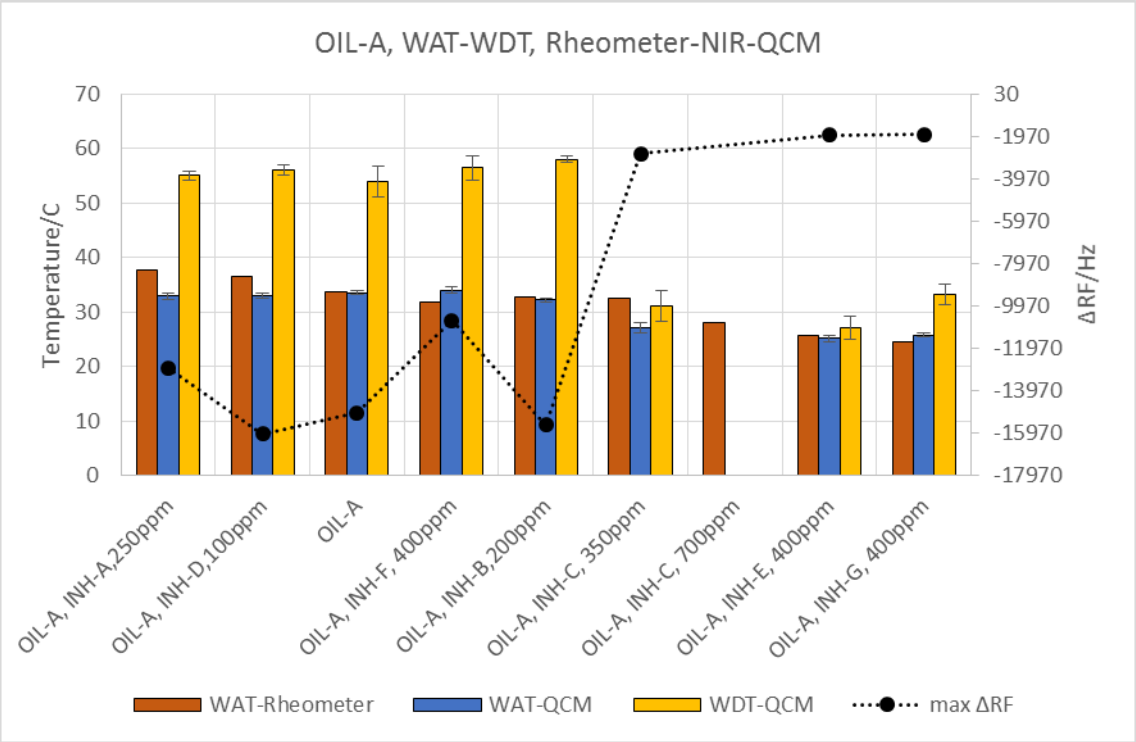

Figure 5-62. Comparison of average WAT-WDT measured with two different QCM in several consecutive cycles with WAT and the maximum viscosity measured with the rheometer using OIL-A sample dosed with various inhibitors. Plot ranked from left to right based on decreasing overall average WAT.

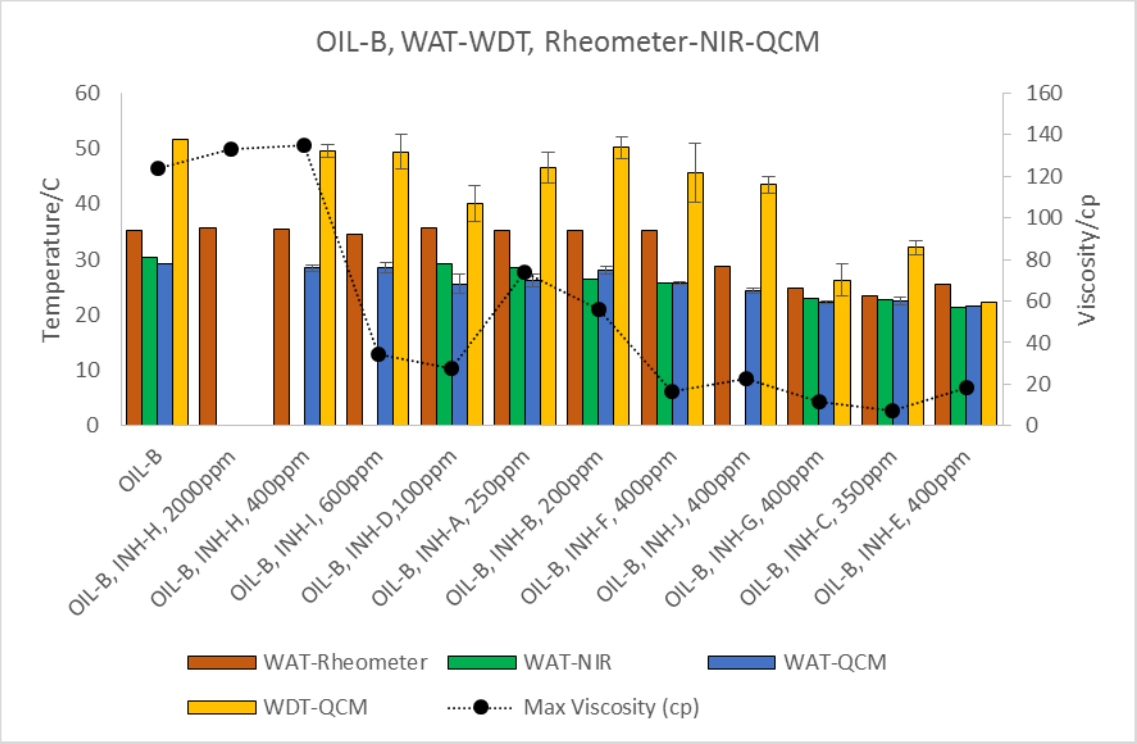

Figure 5-63. Comparison of average WAT-WDT measured with two different QCM, Rheometer and NIR, in several consecutive cycles with maximum viscosity measured with the rheometer using OIL-B sample dosed with various inhibitors. Plot ranked from left to right based on decreasing overall average WAT.

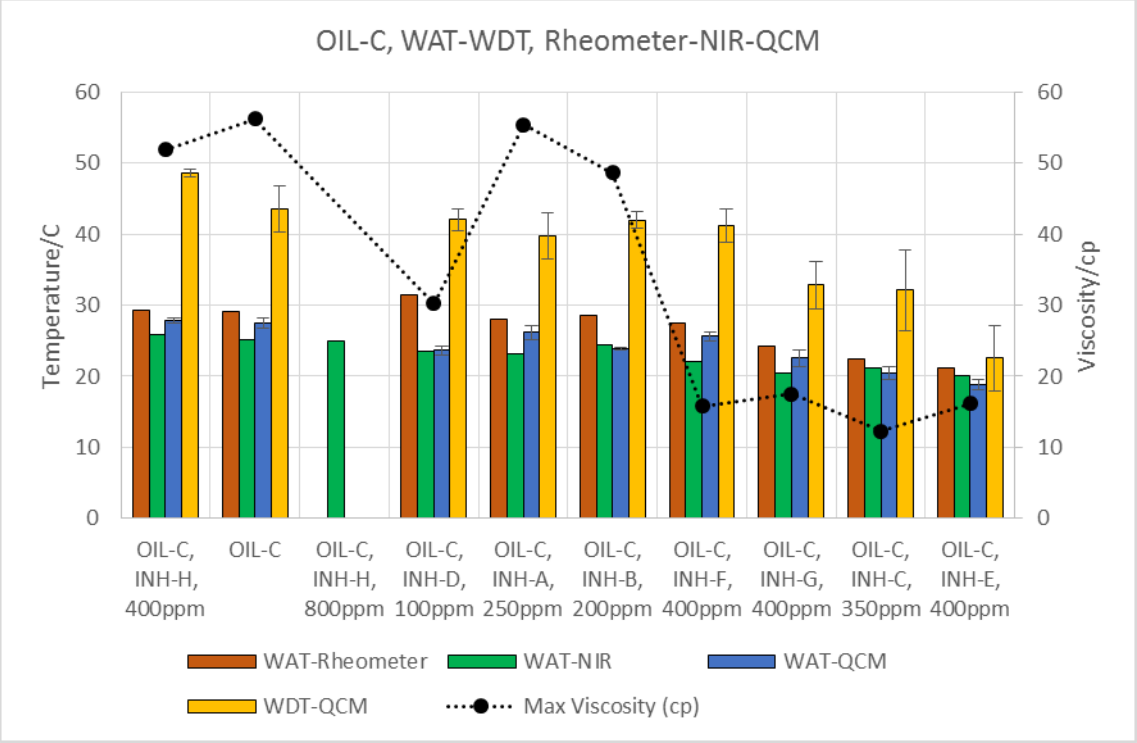

Figure 5-64. Comparison of average WAT-WDT measured with two different QCM, Rheometer and NIR, in several consecutive cycles with maximum viscosity measured with the rheometer using OIL-C sample dosed with various inhibitors. Plot ranked from left to right based on decreasing overall average WAT.

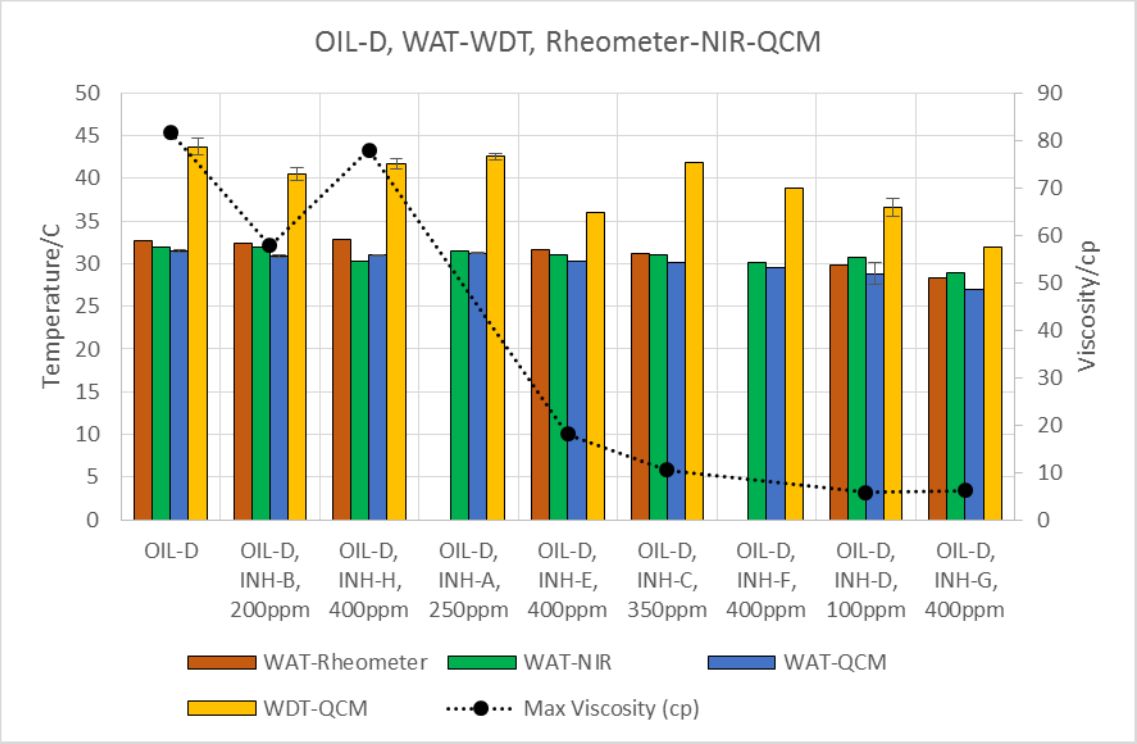

Figure 5-65. Comparison of average WAT-WDT measured with two different QCM, Rheometer and NIR, in several consecutive cycles with maximum viscosity measured with the rheometer using OIL-D sample dosed with various inhibitors. Plot ranked from left to right based on decreasing overall average WAT.

The observations obtained by the plots above are as following:

In general, inhibited samples showed the same or lower WAT in comparison with the blank sample.

In addition, both WAT/WDT was found to decrease by reducing the ΔRF in the same way. The same trend was also observed with the other oil samples which not plotted in here.

Moreover, the higher WAT/WDT coincides with the observation of higher corresponding maximum viscosity for all three oil samples, OIL-B, OIL-C and OIL-D.

Furthermore, the variation of WAT point measured with Rheometer on the treated sample resulted in the higher range up to 11°C in average, rather than other equipment with the lower average point of 6.5°C. The greater range of variation will give an opportunity to assess and rank inhibitor evaluation easily. As a result, rheometer seemed to be a more clear technique on the ranking of performing evaluation in terms of WAT comparison.

Additionally, the rheometer measurement technique, showed a higher value in the WAT point in comparison with the QCM and NIR. As a reminder, wax particles must end up in a large agglomeration, enough size to be detected by rheometer whereas QCM-NIR can detect particles in nanometer size, therefore it was expected to result in lower WAT in rheometer. The most probable reason for this observation may be due to the chance of evaporation of sample during measurement in the atmospheric cone and plate geometry fitted with the rheometer, resulted with a higher WAT point. However, the effect of evaporation seemed negligible in overall results in terms of comparison approach.

Finally, care has to be taken when identifying the wax dissolution point (WDT) with QCM. It highly depends on the cooling/heating rate to allow wax particles equilibrate with applied temperature and the user experience as well. In addition, the presence of impurities was also observed to make some noise on detection; hence, it showed a high statistical deviation. Accordingly, WDT data was found to be not a reliable approach for inhibitor evaluation.

5.8 Visual evaluation approach

In order to deeply understand the reason for discrepancies among commonly used techniques, as well as naked eye visual monitoring of morphological behaviour on treated wax particles, a series of test with a clear sample was performed. Synthetic oil sample OIL-D was taken which was a mixture of diesel and pure paraffin. In addition, it gave an opportunity to neglect the effect of impurities, asphaltene and resin on the result. A typical photo of the samples above WAT is shown in Figure 5-66. It is observed to be entirely clear, free of undissolved particles.

The sample was then mounted on the cooling bath decreased temperature to 15°C corresponded to WAT-17°C. The photos then were taken from the test tubes while after kept it for about a 10 minutes at 15°C, shown in Figure 5-67. The photos are ranked from the left corner down to the right corner based on decreasing cloudiness. The available corresponding viscosities at 15°C are also coupled with photos.

Interestingly, reducing viscosities are in the same line with the strength of depletion as well as decreasing the cloudiness. It was also observed the morphology of the wax particles increased in size and shape by reducing the cloudiness. The discrepancies of the results with the various techniques under study in this work might be explained as following:

5.8.1 Rheometer:

The rheometer cone and plate geometry consists of a stable plate at the bottom and the measuring surface rotating at the top of the sample. This set-up was used for measuring viscosity in this section. Since particular inhibitors such as INH-C, E, F and G cause a higher depletion, it separates the sample into two gravimetrical phases. The lighter phase is stable on the top and in contact with the measuring surface and therefore results in a lower viscosity measurement.

Since the accuracy of WAT and pour point measurement with rheometer translate with the number and size of the particles, and the measured WAT/ pour point was referred to the top layer of the sample where these particles were lower in quantity, therefore, that might be the reason for decreasing WAT/pour point as well as higher variation range of treated samples. It was also observed deviation from Arrhenius equation on these cases was really low and hard to detect WAT point.

5.8.2 QCM

As discussed earlier, QCM surface can respond to adhering particles as well as viscosity and density change of the bulk sample. In addition, QCM surface was observed to respond low accuracy in the presence of macrocrystalline particles due to delicate adhering nature of these particles on the smooth surfaces. QCM was mounted in a middle of test tube without an agitation, so expectedly lower respond in frequency was observed in the presence of inhibitors with the strength of higher viscosity reduction. As mentioned, larger particles in the non-Newtonian region, caused the QCM to detect it harder; hence, QCM detected smaller molecular size components which diffused out of the bulk oil in the lower temperature, showed a lower WAT point.

5.8.3 Coaxial

Since depletion wax particles were found to be the dominant factor in terms of inhibitor injection, and also coaxial bobbin surface are mounted vertically, it could be expected to have a lower wax deposition on the surface. In addition, it could be understood the reason for uneven layer depths of deposition which was thinner or free of wax on the top section of the bobbin.

5.8.4 Flowloop

The observed depletion could be the most probable reason for higher differential pressure and higher wax thickness in the presence of inhibitor with the low viscous outcome. It may be the availability of a greater number of wax and heavy particles in proportion with oil in gel layer of deposition. The lack of oil in gel layer could form the deposition harder and more compact; that’s why it was observed to show lower flake off wax layers in lower viscosity treated samples.

5.8.5 NIR

NIR detector was set at the middle of sample cuvette responding to particle size and behaviour of wax crystallisation. While depletion started in the non-Newtonian region, NIR responded a higher intensity drop coupled with stronger and faster depletion rate which referred to the lower viscosity, etc. lower WAT was also expected where smaller particles formed at the point where detection performed. It's thoughtfully got the different result in WAT point in different location if possible to change the detector position. Hence, it was expected to get a higher WAT point at the bottom of cuvette in presence of inhibitors.

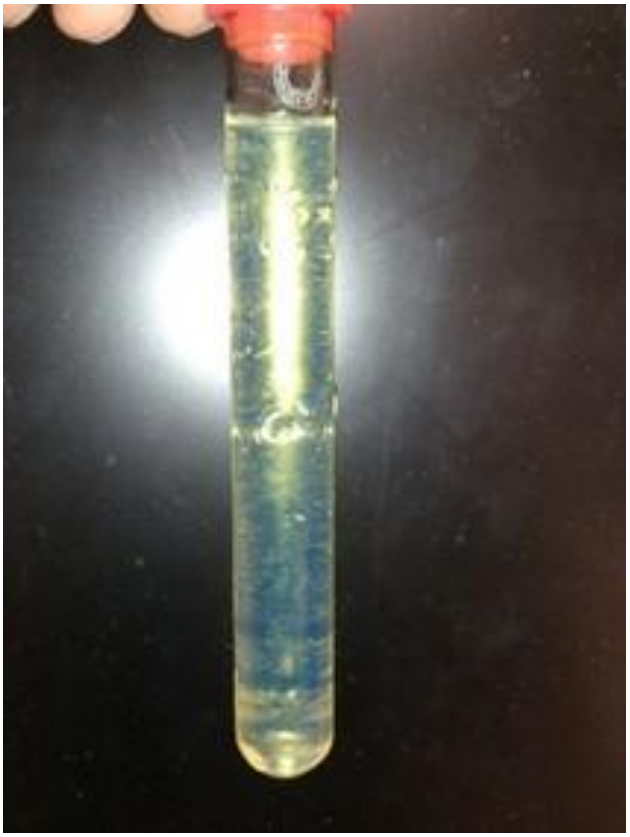

Figure 5-66. Photo of condition for all sample above WAT

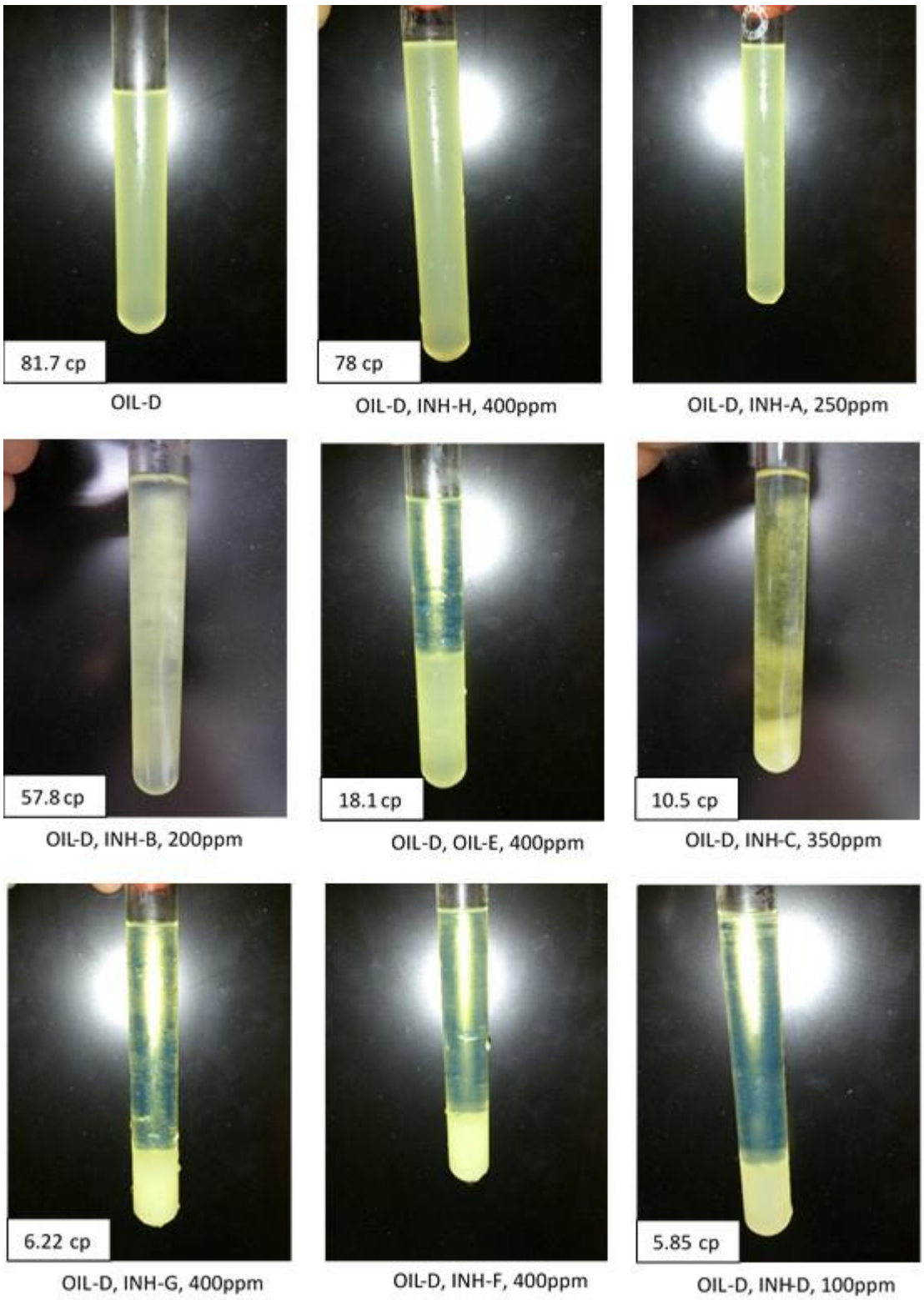

Figure 5-67. Photos of test tubes containing OIL-D sample dosed with different inhibitors under WAT in a static condition. Photos ranked from the left corner down to the right corner based on decreasing cloudiness.

5.9 References

1. Tiratsoo, J.N., *Pipeline pigging technology*. 1992: Gulf Professional Publishing.
2. Jennings, D.W. and K. Weispfennig, *Effects of shear and temperature on wax deposition: Coldfinger investigation with a Gulf of Mexico crude oil.* Energy & fuels, 2005. **19**(4): p. 1376-1386.
3. Burgass, R. and B. Tohidi. *Development and validation of small volume multi-tasking flow assurance tool*. in *SPE Asia Pacific Oil and Gas Conference and Exhibition*. 2011. Society of Petroleum Engineers.
4. Chi, Y., N. Daraboina, and C. Sarica, *Investigation of inhibitors efficacy in wax deposition mitigation using a laboratory scale flow loop.* AIChE Journal, 2016.
5. Marchesini, F.v.H., et al., *Rheological characterization of waxy crude oils: Sample preparation.* Energy & Fuels, 2012. **26**(5): p. 2566-2577.
6. ASTM D97-16, S.T.M.f.P.P.o.P.P., ASTM International, West Conshohocken, PA, 2016, www.astm.org.
7. Burgass, R.W., *Applications of quartz crystal microbalance technology in petroleum engineering, demonstrated by studies of wax, asphaltenes, hydrates, ice, diesel additives and anti-deposition coatings*. 2015, Heriot-Watt University.
8. Garcia, M.d.C., et al., *Paraffin deposition in oil production. Oil composition and paraffin inhibitors activity.* Petroleum science and technology, 1998. **16**(9-10): p. 1001-1021.
9. Hansen, J.H., et al., *A thermodynamic model for predicting wax formation in crude oils.* AIChE Journal, 1988. **34**(12): p. 1937-1942.
10. Coutinho, J.A. and V. Ruffier-Meray, *Experimental measurements and thermodynamic modeling of paraffinic wax formation in undercooled solutions.* Industrial & engineering chemistry research, 1997. **36**(11): p. 4977-4983.
11. IJeomah, C.E., et al., *Measurement of wax appearance temperature under simulated pipeline (dynamic) conditions.* Energy & Fuels, 2008. **22**(4): p. 2437-2442.

Chapter 6: Impact of additives and non-hydrocarbon agents on wax evaluation

6.1 Introduction

In actual industrial processes, several flow assurance challenges may occur coincidentally and as a result may require multiple chemical treatment products introduced in the process at the same time. Therefore, it is important to investigate the compatibility of these products in advance which is the aim of studies in this chapter.

Crude oil production is often commingled with water which normally increases later in the life of a reservoir which could have direct and indirect effects on the wax problem. Water production and changes in the water cut result in changes in the rheological behaviour of the fluid system, which in turn can affect system temperature and shear stress [1]. Furthermore, water production may lead to gas hydrate problem and, due to the temperatures encountered, wax solids may also be present in the process. Hydrates problems can be prevented by injection of hydrate inhibitors during start-ups, shutdowns and/or normal operation. While hydrate inhibitors may resolve hydrate problems when injected at different subcoolings, they may have an adverse effect on the wax problem [2, 3].

Initially, a simple investigation was conducted in this work to study the effect of watercut as well as some thermodynamic hydrate inhibitors such as MEG and methanol on waxy oil samples at different subcooling using the Flowloop set-up. Visual observations suggested that these chemicals have insignificant solubility in oil mainly forming an emulsion, hence are expected to have the same effect at similar test conditions. Moreover, the effect of subcooling on the impact of low dosage hydrate inhibitors, two different commercial anti-agglomerants named as AA-1 and AA-2, on wax deposition was studied using the Flowloop, the QCM and the Rheometer.

Furthermore, oil samples could be contaminated with oil-based mud agents as a result of drilling fluid invasion through the porous and permeable formation. While, industry is trying to minimise the level of contamination using novel techniques and devices [4, 5], there is no systematic investigation on the effect of mud filtrate contamination on wax risk evaluation and prevention strategies. Consequently , the effect of mud filtrate from the initial sampling campaign on the wax related measurements has been studied

in this chapter. Furthermore, a limited study has been conducted to determine/estimate some of the wax related parameters such as WAT, WDT, deposition adherent tendency and viscosity of original/uncontaminated sample with a variety of oils using Rheometer and QCM.

Finally, analysis of frequency reduction measurements in several consecutive thermal cycle tests has shown some level of discrepancies, especially in the case of oil sample OIL-A which was believed to be due to the presence of scale. The different consecutive frequency drop made it difficult to screen inhibitor performance. Therefore, the impact of the presence of scale on QCM reading during wax studies was investigated in this chapter.

Table 6-1 presents an outline of the experimental work presented in this chapter.

Table 6-1. Outline of the experimental work, effect of different subjects on the wax related parameters studied in this chapter

Material	***Type of oil***	***Volume percent (%)***	***Temperature range (°C)***	***Equipment***
Watercut	*OIL-A*	*0, 20*	*60 to 5, 10*	*Flowloop*
	OIL-C	*0, 20*	*50 to 5, 10, 15*	
MEG	*OIL-C*	*0, 21*	*50 to 5, 15*	
Methanol	*OIL-C*	*0, 20, 22% to 22% watercut*	*50-5*	
AA-1	*OIL-C*	*0, 1, 1.96, 2.91*	*50-5*	*Rheometer*
	OIL-C	*0, 1, 1.96, 2.91*	*50-5*	*QCM*
AA-2	*OIL-C*	*0, 1, 1.96, 3.85*	*50-5*	
	OIL-D	*0, 1, 1.96, 3.85*	*50-15*	
	OIL-E	*0, 0.5, .99, 1.72*	*35-5*	
	OIL-F	*0, 0.5, 1, 1.5*	*60-20*	
AA-1	*OIL-C*	*0, 1, 2.91*	*50-5*	*Flowloop*
		0, 0.4, 1, 2.91	*50-15*	
AA-2		*0, 1.96*	*50-5*	
		0, 1.96	*50-10*	
		0, 1, 1.96	*50-15*	
Mud filtrate	*OIL-G*	*0, 4.35, 8.33, 18.52, 24.14*	*60-20*	*Rheometer*
	OIL-G	*0, 4.33, 8.33, 12, 18.52, 24.14*	*60-20*	*QCM*
	OIL-F	*0, 4.76, 9.09, 16.67*	*60-25*	
	OIL-I	*0, 4.76, 9.09, 16.67*	*30-5*	
	OIL-H	*0, 4.76, 9.09, 16.67, 23.08, 28.57*	*50-20*	
	OIL-J	*0, 4.35, 8.33, 15.38, 21.43, 28.57*	*35-5*	
	OIL-E	*0, 4.76, 9.09, 16.67, 23.08, 28.57*	*35-5*	
Scale	*OIL-A, B, C*			

6.2 Subcooling/temperature gradient effect on waxy oil samples in the presence of emulsion

The aim of this section was to study the impact of subcooling on the wax deposition process in the presence of water cut on two different waxy oil samples, known as OIL-A and OIL-C. Additionally, the presence of MEG and Methanol on deposition adherent tendency of waxy oil sample OIL-C was studied. All the measurements were done using flowloop at the same flow rate, 10CPM correspond to 151 s^{-1} imitate the laminar flow condition.

Table 6-2 lists the experimental conditions and the results of the flowloop. Tests were done in different test time, though it did not really impact the trend of the results. The test with OIL-A sample was performed at two different test temperature, 5°C and 10°C which corresponds to subcooling WAT-29°C and WAT-24°C.

Similar test temperature was used for OIL-C in addition to 15°C. Subcooling for OIL-C was at WAT-22°C, WAT-17°C and WAT-12°C in corresponding test temperatures.

The quantity volume of watercut and MEG used was 20% and 21% respectively in all subcooling conditions. Methanol was used in two different approaches, 20% alone in oil and 22% in 22% watercut.

Table 6-2. Experimental conditions and the results of flowloop using OIL-A and OIL-C samples with/out water cut, MEG and methanol in 10CPM with 151 s^{-1} in different ageing temperature. Loop C was used in all tests.

Fluid	***Condition T (°C)***	***Test T (°C)***	***Flow rate (cc/min)***	***Shear rate (s^{-1})***	***Average ΔP (psi)***	***Average T_{in} (°C)***	***Average T_{out} (°C)***	***Average deposited thickness (μm)***
OIL-A	*60*	*5*	*10*	*151*	*151*	*45.38*	*7.32*	*613*
OIL-A, watercut, 20%	*60*	*5*	*10*	*151*	*151*	*47.23*	*7.07*	*680*
OIL-A	*60*	*10*	*10*	*151*	*175*	*47.06*	*12.12*	*755*
OIL-A, watercut, 20%	*60*	*10*	*10*	*151*	*51*	*49.4*	*12.13*	*559*
OIL-C	*50*	*5*	*10*	*151*	*201*	*35.63*	*7.22*	*469*
OIL-C, watercut 20%	*50*	*5*	*10*	*151*	*232*	*39.2*	*6.82*	*543*
OIL-C	*50*	*10*	*10*	*151*	*143*	*40.11*	*12.11*	*616*
OIL-C, watercut 20%	*50*	*10*	*10*	*151*	*26.3*	*41.25*	*12.03*	*364*
OIL-C	*50*	*15*	*10*	*151*	*18.8*	*41.67*	*16.32*	*434*
OIL-C, watercut 20%	*50*	*15*	*10*	*151*	*1.98*	*41.14*	*16.29*	*119*
OIL-C	*50*	*5*	*10*	*151*	*131*	*35.59*	*6.9*	*390*
OIL-C, MEG, 21 V%	*50*	*5*	*10*	*151*	*163*	*38.81*	*6.85*	*477*
OIL-C	*50*	*15*	*10*	*151*	*18.2*	*41.64*	*16.28*	*439*
OIL-C, MEG, 21 V%	*50*	*15*	*10*	*151*	*2.28*	*40.29*	*16.17*	*128*
OIL-C	*50*	*5*	*10*	*151*	*503*	*35.71*	*7.53*	*644*
OIL-C, watercut, 22%, Methanol,	*50*	*5*	*10*	*151*	*133*	*41.2*	*6.88*	*475*

Continued Table 6-2

Fluid	*Condition T (°C)*	*Test T (°C)*	*Flow rate (cc/min)*	*Shear rate (s^{-1})*	*Average ⊿P (psi)*	*Average T_{in} (°C)*	*Average T_{out} (°C)*	*Average deposited thickness (µm)*
22 v% to water								
OIL-C, Methanol, 20 v%	*50*	*5*	*10*	*151*	*67*	*38.95*	*6.73*	*379*

The solubility of water, MEG and methanol in crude oil are negligible hence there are two separate phases without agitation; and form emulsion whenever agitation would be applied to the mixture. The emulsion can be classified into two main categories, ‘’oil in water’’ and ‘’water in oil’’. The latter one is more common type in the oil industry. In addition, it can be described by their droplet size in the continuous phase, micro and macroemulsion which highly depends on the mixing rate. Increasing the mixing rate will cause decreasing droplets making the emulsion tighter [6, 7]. As mentioned, a large stirrer was present in the sample reservoir, fast enough to produce a well-mixed emulsion capable of flowing through the loops. The size, type and other characteristics were not the aims of study in this work, though. All the conditions were kept constant in order to reduce variables which might impact on the wax deposition. The only difference was subcooling temperature, the impact on wax deposition in the presence of some emulsion agent which was the aim of this study.

Different mechanisms of wax deposition may be involved in the presence of emulsion as follows.

As found in the previous chapter, higher viscosity showed lower deposition thickness in terms of using flow loop. Since emulsion shows non-Newtonian behaviour in the presence of shear rate, emulsion viscosity is expected to have a higher value than either two individual fluids forming the emulsion. Therefore, it was expected to have lower differential pressure and correspondingly deposition thickness in the presence of emulsion in comparison with the blank oil sample. In addition, the presence of emulsion droplets might impact on wax thickness acting like a mechanical scraper/cutter, increased shearing stress to the wall, reducing deposition layer. Moreover, the possibility of wettability change, emulsion could produce a film form around the pipeline. These films reduce the adherent tendency of wax crystals hence reduce wax deposition risk. On the other hand, one of the most important driving force in terms of

wax deposition is a differential temperature between bulk oil and pipe walls which plays a significant role in encouraging wax deposition [1, 8-11].

The adherent tendency of crystals on flow line walls might be as a result of these competing phenomenon.

6.2.1 Test temperature of 5°C

Figure 6-1 and Figure 6-2 illustrate the outcome of using OIL-A sample with 20% watercut in 5°C. As shown in the figure, both trends overlaps each other; no significant change is observed.

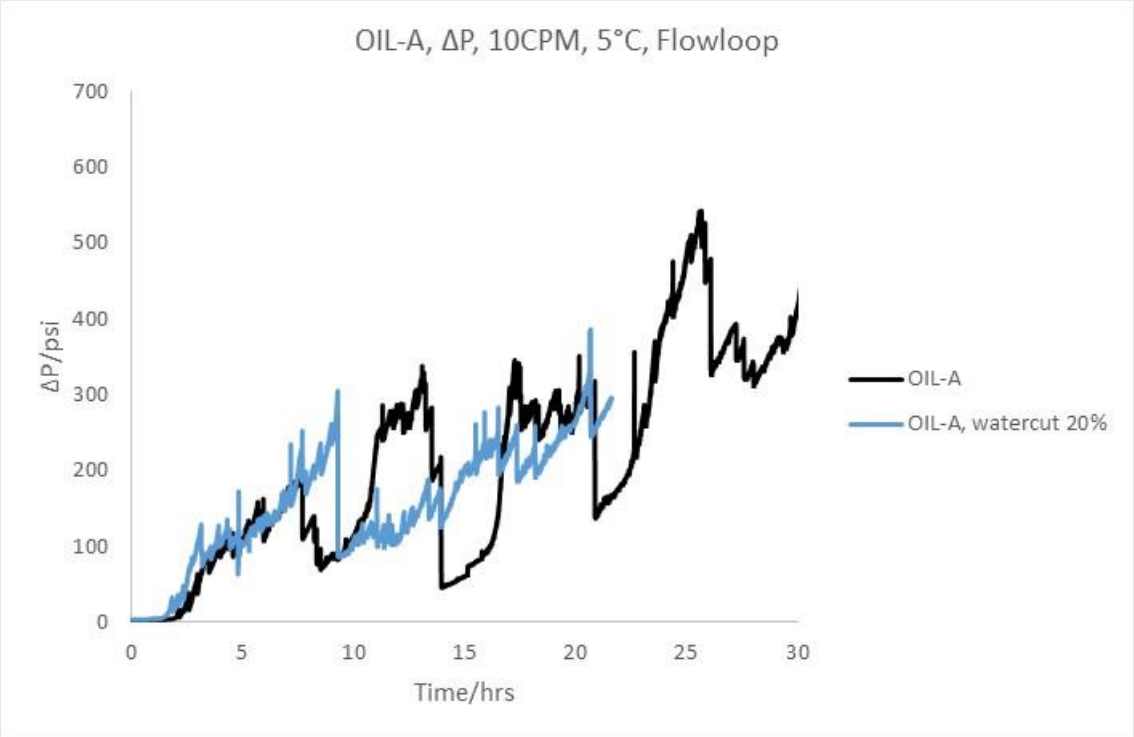

Figure 6-1. Comparison of differential pressure buildup by flowloop using OIL-A sample with/out water in 10CPM with 151 s^{-1}.

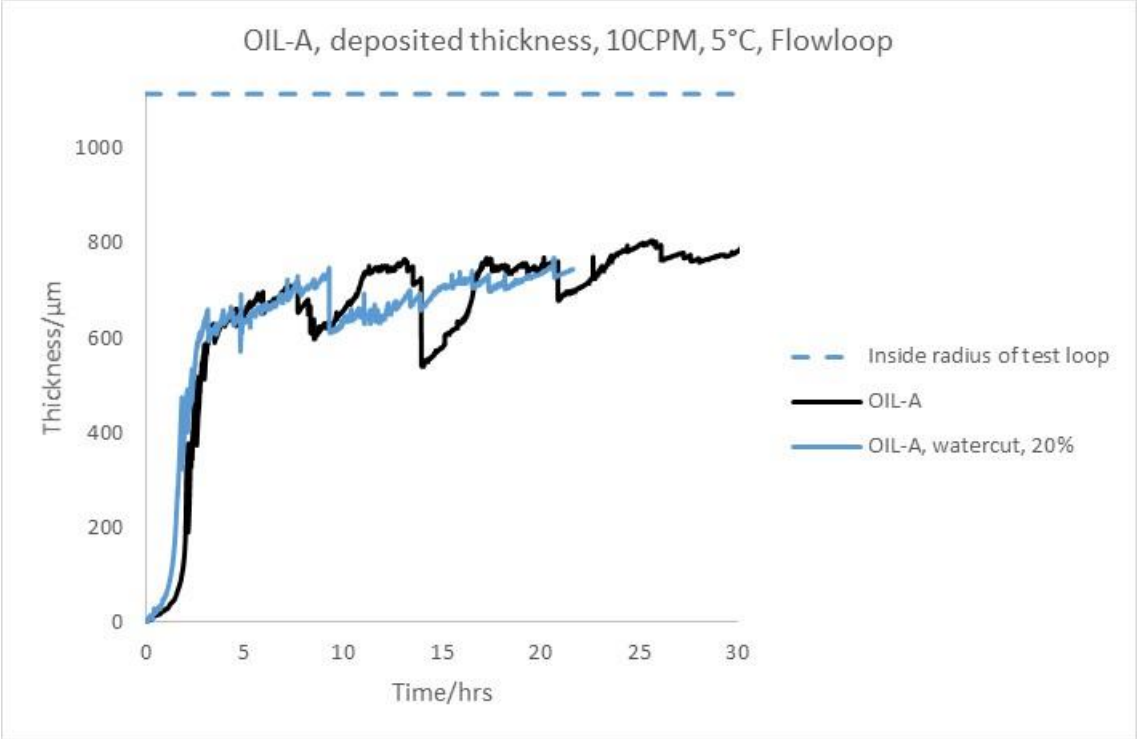

Figure 6-2. Comparison of deposited thickness by flowloop using OIL-A sample with/out water in 10CPM with 151 s^{-1}. The legend ranked top to bottom based on decreasing deposited thickness at 5°C.

Figure 6-3 and Figure 6-4 demonstrate the results with OIL-C in the presence of 20% water cut and 21% MEG in 5°C. In the first 6 hrs test time, either emulsion with MEG and water showed a slightly higher deposition compare to blank, though in following all overlapped one another, a similar trend was observed in long-term test time measurement.

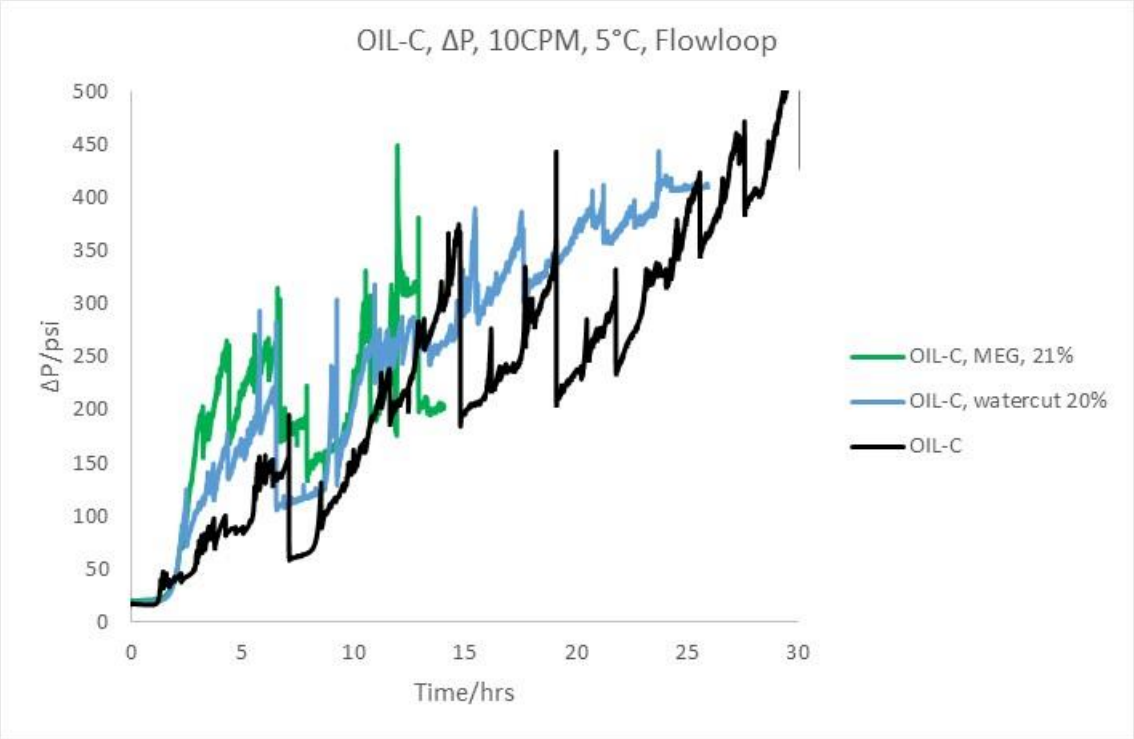

Figure 6-3. Comparison of differential pressure buildup by flowloop using OIL-C sample with/out water in 10CPM with 151 s^{-1}.

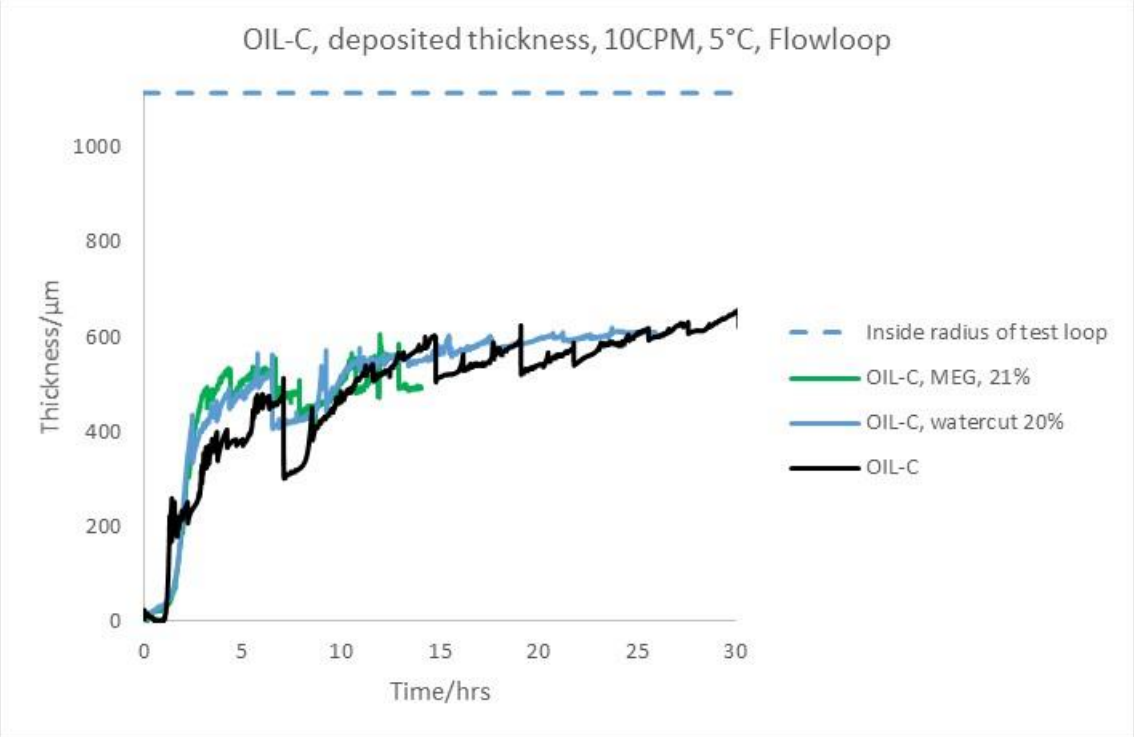

Figure 6-4. Comparison of deposited thickness by flowloop using OIL-C sample with/out water in 10CPM with 151 s^{-1}. The legend ranked top to bottom based on decreasing deposited thickness at 5°C.

Figure 6-5 and Figure 6-6 refer to emulsion formed with methanol and a solution of water/methanol in 5 °C. As evident from the figures in the methanol-oil emulsion

system a slight reduction in differential pressure is observed compared to the oil only system which suggests a lower wax deposition thickness. On the other hand, when water is added to the system and a water-methanol-oil emulsion is formed, this reduction in the differential pressure is no longer observed and the trend of changes in the differential pressure with time remains relatively similar to the oil only system. Since previous results (Figure 6-4) has demonstrated that presence of water alone does not lead to changes in the wax deposition of this oil at this temperature, the contrasting results observed here suggests that either this pattern is due to the difference in the type of emulsion formed in these two systems or it is due to the fact that the results of the methanol-oil emulsion experiments are effected by the evaporation of the methanol before the test loop which causes in a non-representative pressure reading at this point and therefore a non-realistic differential pressure reading across the loop. The possible difference in the type of emulsion could be the result of the methanol particles floating on top of the oil which could prevent the formation of an emulsion as tight as the water-oil emulsion even at the same stirrer speed. On the other hand, the evaporation of the methanol which was also suspected as the reason behind the observed trend is further supported by the lower amount of methanol detected at the end of the measurement. It should be noted that the pressure sensors are placed in small chambers positioned higher than the flow loop and perpendicular to the flow direction. Furthermore, the flowloop is completely sealed and therefore it is very likely for the evaporated methanol particles to concentrate and fill these chambers resulting in the pressure sensors to read underestimated pressures.

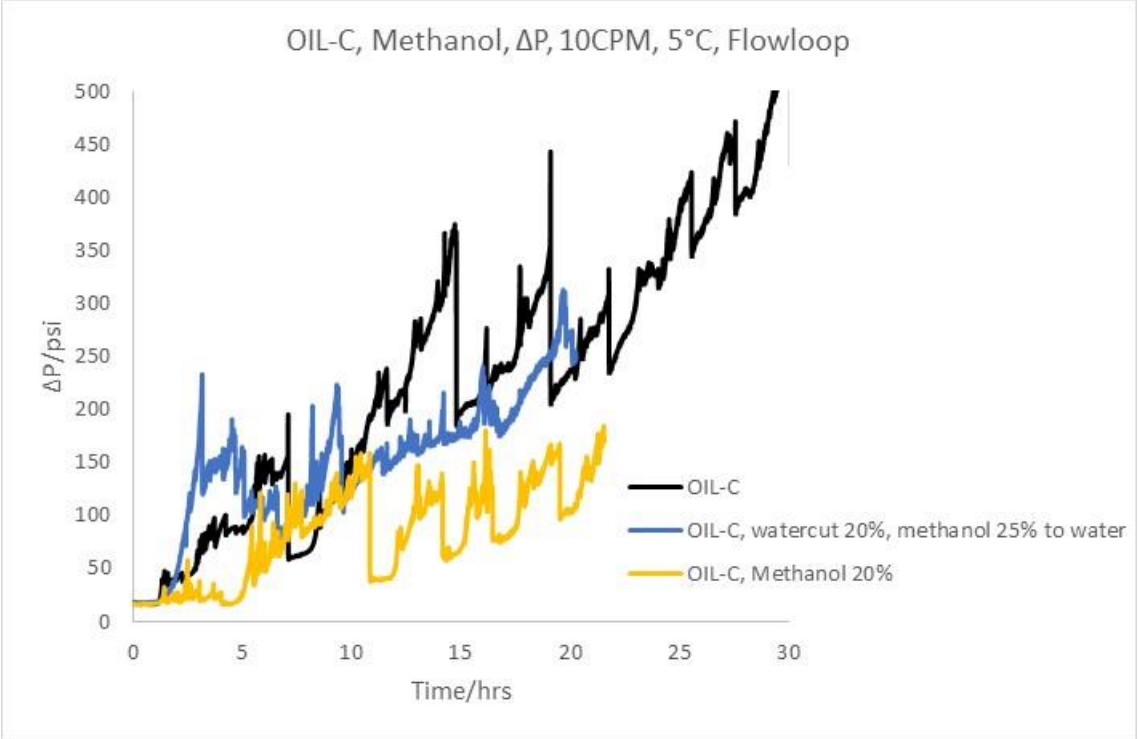

Figure 6-5. Comparison of deposited thickness by flowloop using OIL-C sample in the presence of methanol with/out water cut in 10CPM with 151 s^{-1}. The legend ranked top to bottom based on decreasing deposited thickness at 5°C.

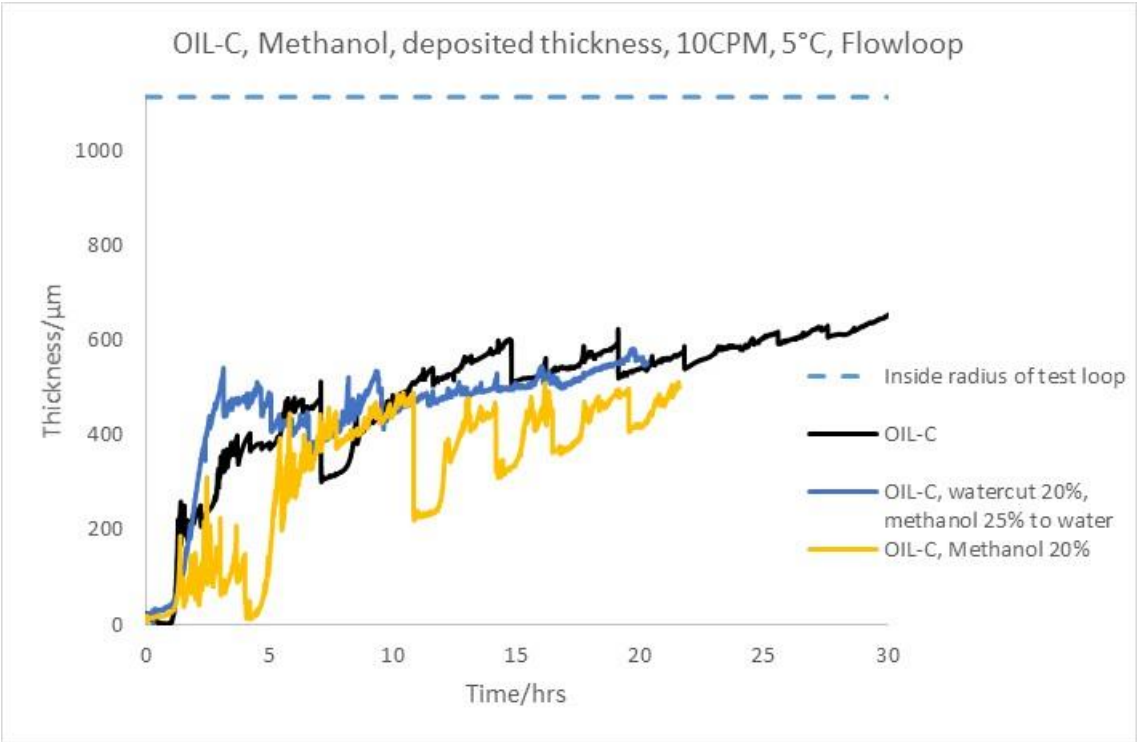

Figure 6-6. Comparison of deposited thickness by flowloop using OIL-C sample in the presence of methanol with/out water cut in 10CPM with 151 s^{-1}. The legend ranked top to bottom based on decreasing deposited thickness at 5°C.

As shown overall, the subcooling/temperature gradient effect at 5°C for both oil sample OIL-A and OIL-C, seemed to be the driving force as opposed to wettability change and higher viscosity in the presence of all emulsions.

6.2.2 Test temperature of 10°C

The test temperature was then increased and set at 10°C for both oil samples OIL-A and OIL-C contained 20% watercut shown in (Figure 6-7 and Figure 6-8) and (Figure 6-9 and Figure 6-10) correspondingly. In either test, samples showed an overlapping trend up to around 10 hrs test time, after which the trend start to diverge, low differential pressure and thickness found in the presence of emulsion. Perhaps it could be explained by thermal diffusion playing a dominant effect in early stages. This effect continued as long as a certain layer of wax thickness insolates the inside pipe wall. The insolation reduced differential temperature between bulk oil and the pipe wall. Increasing the temperature of the bulk oil in the loop, increased the thermal energy of the emulsion droplets; hence, drop collision rate towards deposition layer increased avoid further deposition to occur.

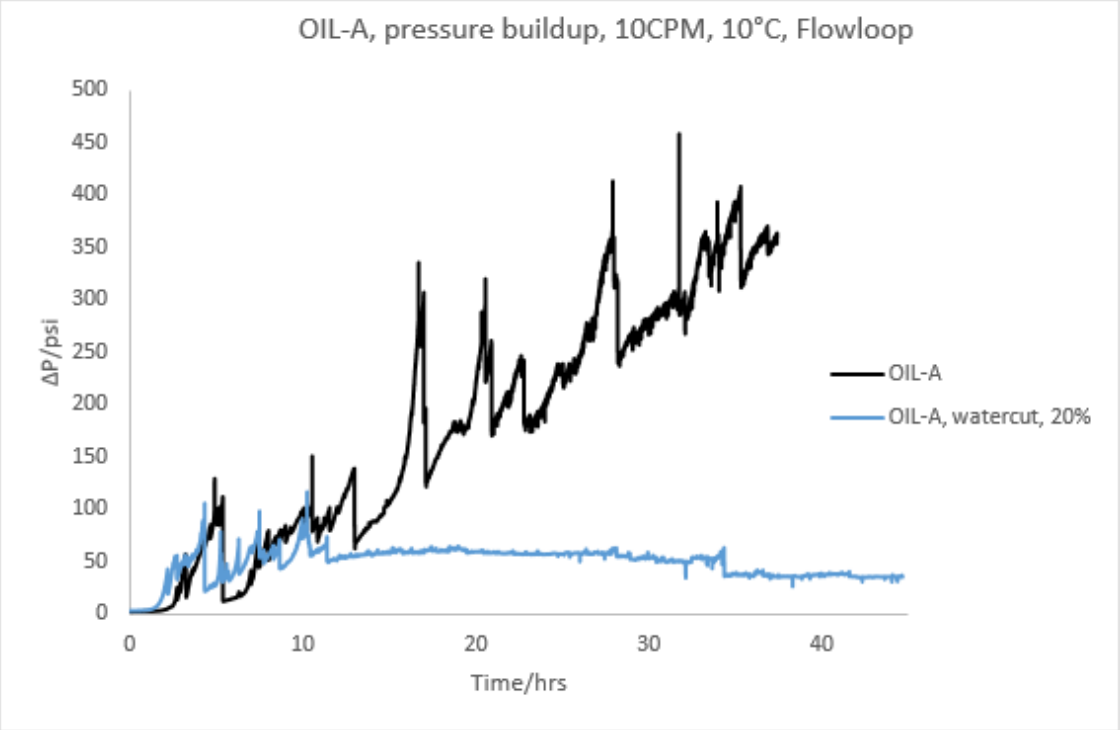

Figure 6-7. Comparison of differential pressure buildup by flowloop using OIL-A sample with/out water in 10CPM with 151 s^{-1}. The legend ranked top to bottom based on decreasing maximum build-up pressure at 10°C.

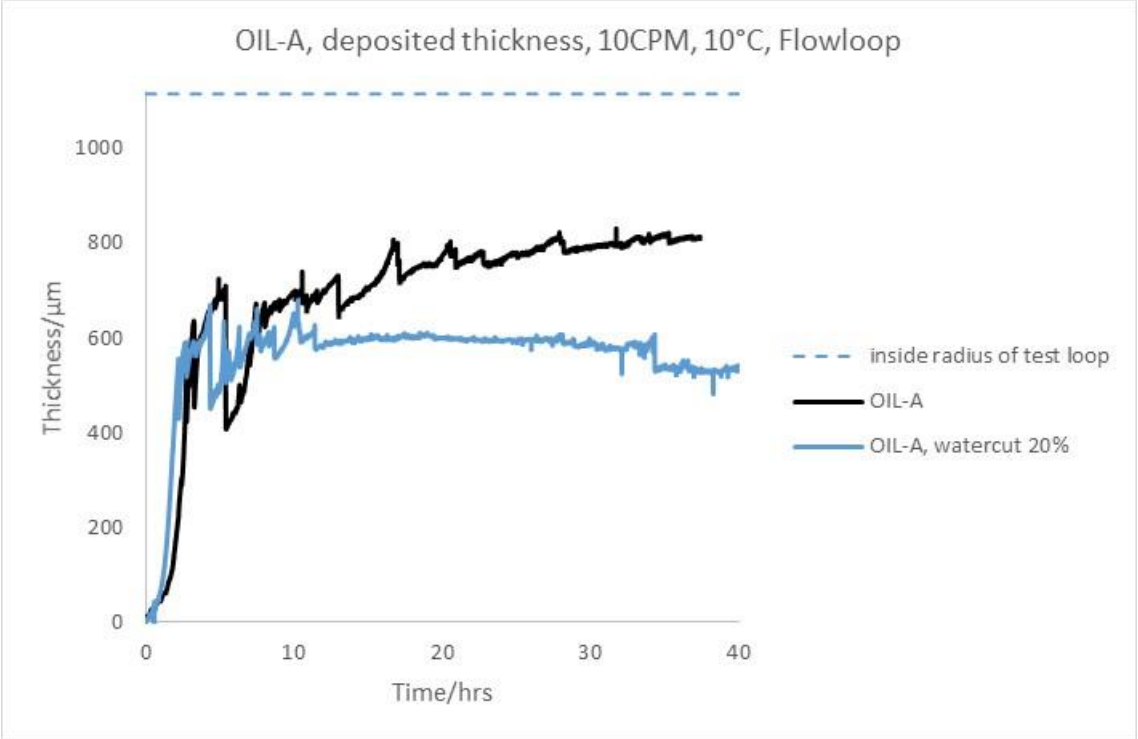

Figure 6-8. Comparison of deposited thickness by flowloop using OIL-A sample with/out water in 10CPM with 151 s^{-1}. The legend ranked top to bottom based on decreasing deposited thickness at 10°C.

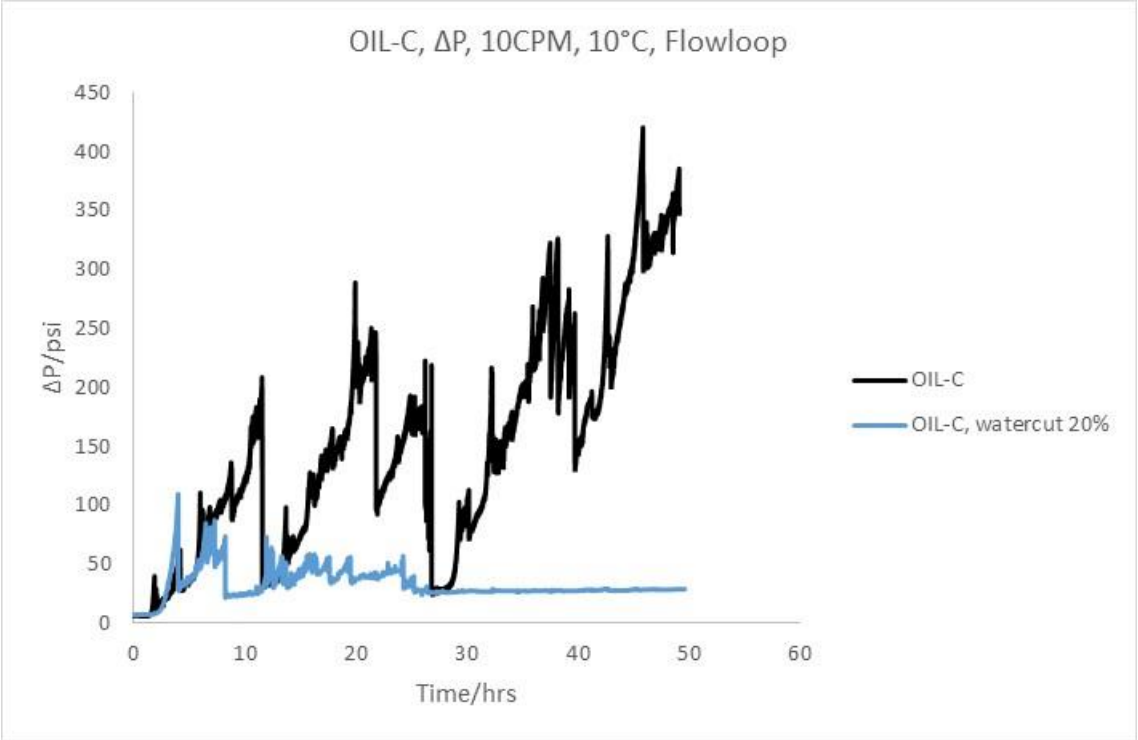

Figure 6-9. Comparison of differential pressure buildup by flowloop using OIL-C sample with/out water in 10CPM with 151 s^{-1}. The legend ranked top to bottom based on decreasing maximum build-up pressure at 10°C.

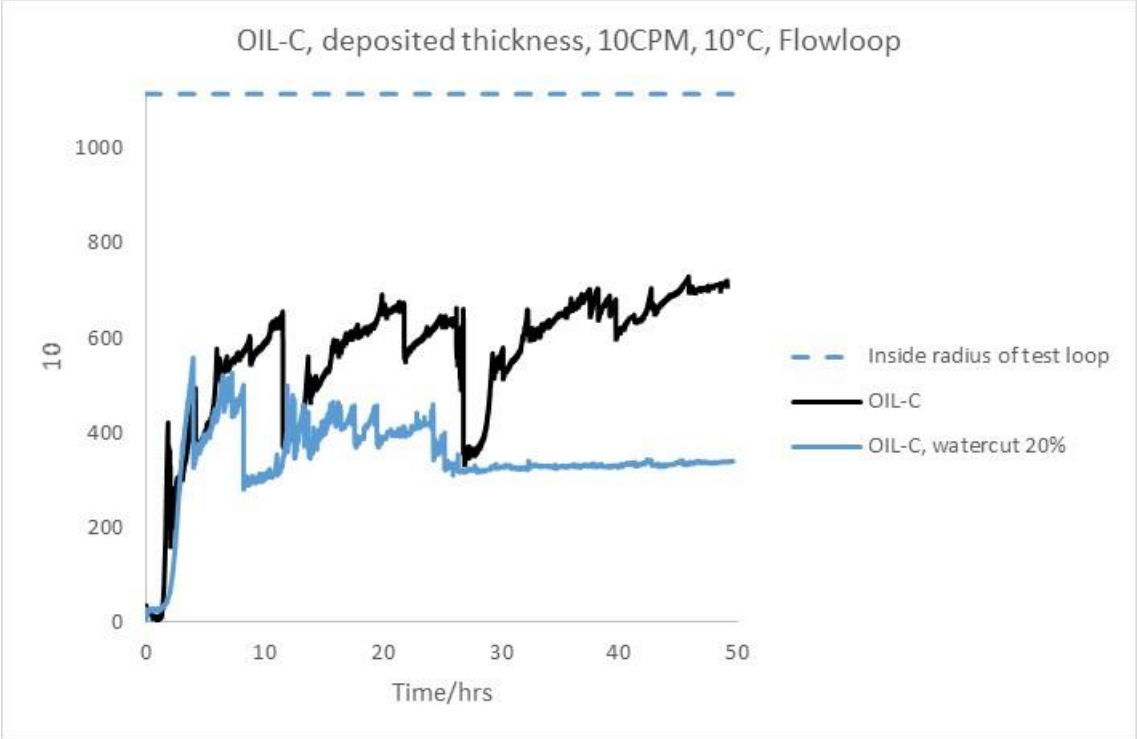

Figure 6-10. Comparison of deposited thickness by flowloop using OIL-C sample with/out water in 10CPM with 151 s^{-1}. The legend ranked top to bottom based on decreasing deposited thickness at 10°C.

6.2.3 Test temperature of 15°C

A test at 15°C was only performed with oil sample OIL-C in the presence of emulsion formed by 20% watercut and 21% MEG separately, in the results are presented in Figure 6-11 and Figure 6-12. Both emulsions showed the same deposited thickness in a similar way. This behaviour confirmed that the only effective parameter was the physical property of emulsion no matter of forming agent. A lower significant deposition, in either case, was observed at the whole test temperature. Most probably, subcooling differential temperature were not able to overcome either wettability change and/or increasing droplet collision (as a result of higher temperature) at this test temperature.

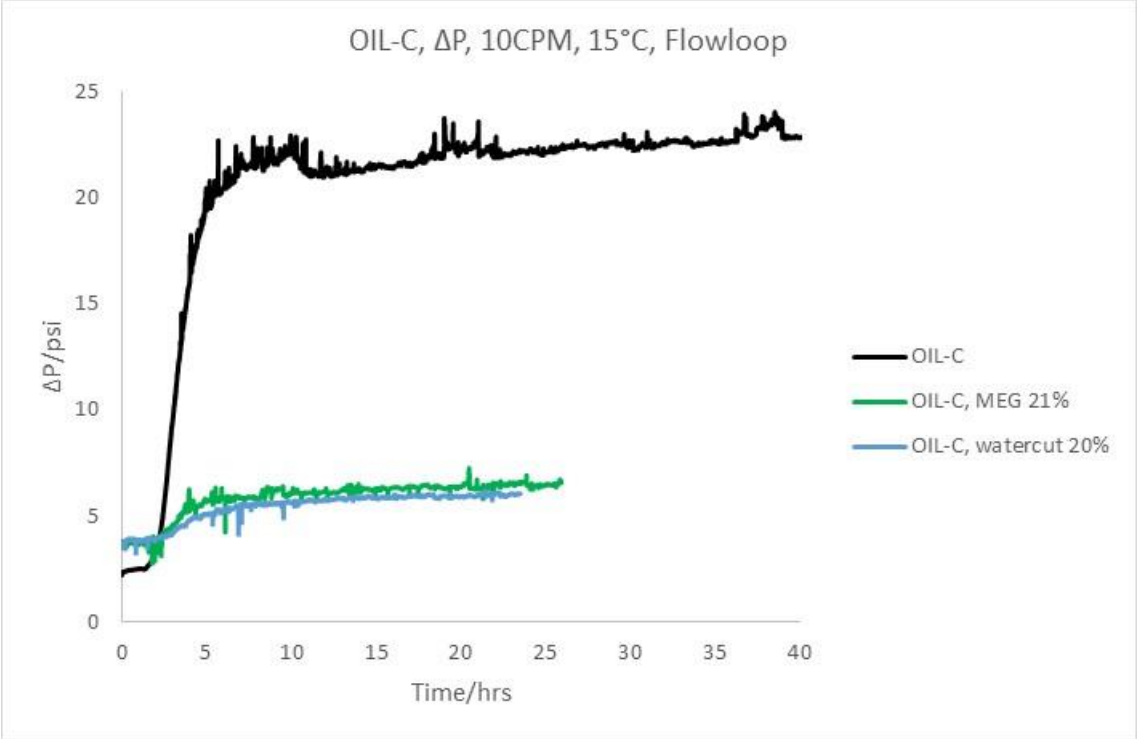

Figure 6-11. Comparison of differential pressure buildup by flowloop using OIL-C sample with/out water in 10CPM with 151 s^{-1}. The legend ranked top to bottom based on decreasing maximum build-up pressure at 15°C.

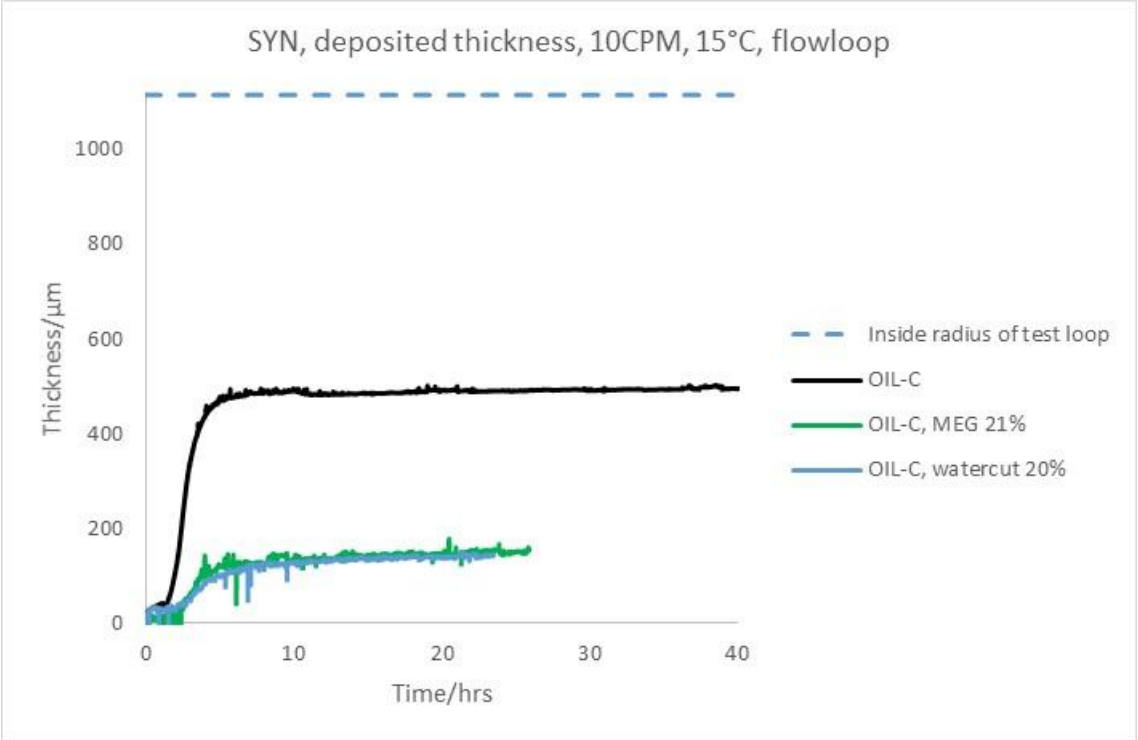

Figure 6-12. Comparison of deposited thickness by flowloop using OIL-C sample with/out water in 10CPM with 151 s^{-1}. The legend ranked top to bottom based on decreasing deposited thickness at 15°C.

6.3 Effect of hydrate anti-agglomeration additives on wax deposition

Anti-agglomeration (AA) is a commonly used technology giving the ability to control hydrate plugging in the deep-water production facilities and pipelines. In contrast to thermodynamic inhibitors which inhibit hydrate formation, AAs which mainly consist of ammonium salts, allow hydrates to form but prevent the agglomeration of hydrate particles. The exact pattern to which AAs inhibit hydrate agglomeration is yet to be understood, however it is believed that AAs change the morphology of the hydrate particle network which results in the existing hydrates to convert into fine, well-dispersed particles in addition to reducing the viscosity of the slurry making it easy to transport [12, 13].

As mentioned earlier, wax formation is likely to accompany hydrate formation, and there is no studies found in the literature to see the impact of using hydrate inhibitors such as AA on wax deposition tendency. A short study was then conducted to investigate the effect of two different commercial AA with different dosages known as AA-1 and AA-2, purely on wax deposition without watercut and hydrate formation.

6.3.1 Rheology investigation

In the first instance, rheology of different dosages AA-1 added to oil sample OIL-C was performed in a temperature sweep, as shown in Figure 6-13. Table 6-4 presents results and experimental condition using an atmospheric cone and plate geometry by the rheometer. Similar conditioning temperature was set discussed it in detail in the previous chapter. As shown in the table below, the presence of AA did not have any impact on wax appearance temperature up to 2.91% dosage AA-1.

Table 6-3. The condition and results of rheometer to measure viscosity, using OIL-C sample with different AA dosage, ranked top to bottom based on decreasing overall viscosity

Fluid	***Condition T (°C)***	***Destination T (°C)***	***Cooling rate (°C/min)***	***Shear rate (s^{-1})***	***Minimum Viscosity (cP)***	***Maximum Viscosity (cP)***	***WAT (°C)***
OIL-C	*50*	*5*	*1*	*10*	*2.42*	*56.2*	*29.1*
OIL-C, AA-1, 1%	*50*	*5*	*1*	*10*	*2.64*	*52.4*	*28.7*
OIL-C, AA-1, 1.96%	*50*	*5*	*1*	*10*	*2.32*	*45.4*	*28.9*
OIL-C, AA-1, 2.91%	*50*	*5*	*1*	*10*	*2.39*	*40.7*	*28.9*

As shown in Figure 6-13, increasing AA dosages in the lack of watercut reduced the viscosity of the mixture in the non-Newtonian region below WAT point. However, viscosity change effect was expected in the presence of watercut where AA reduces the emulsion effect, resulting in a viscosity reduction.

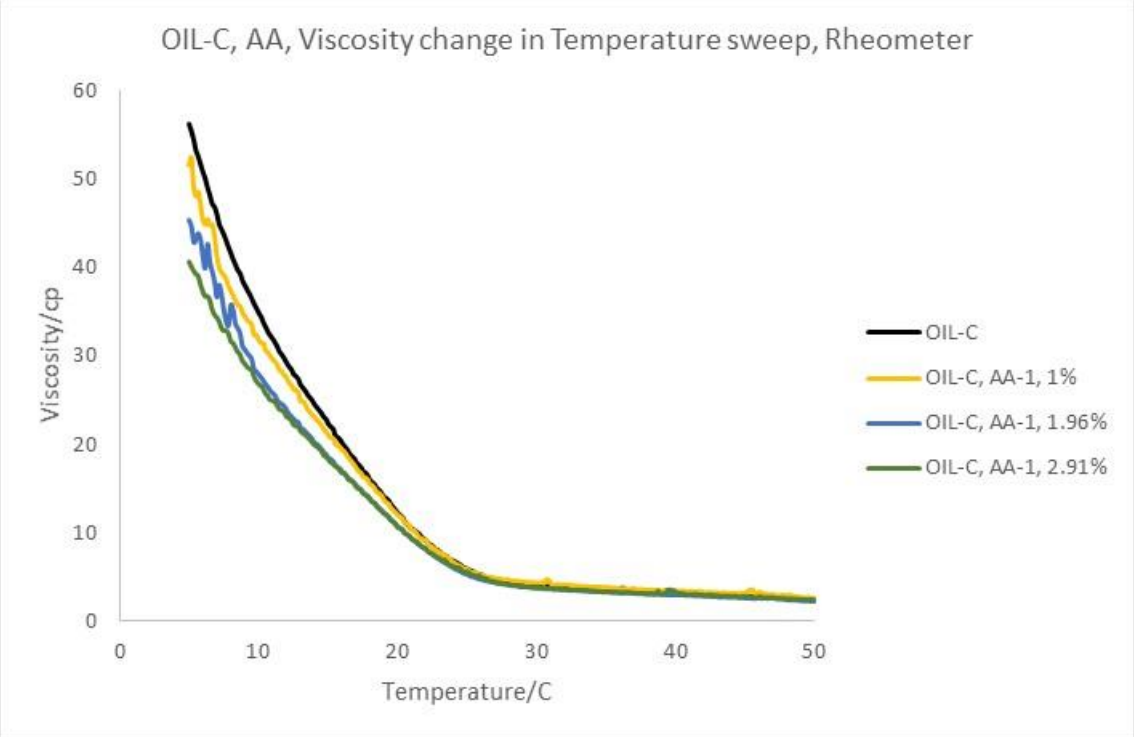

Figure 6-13. Variation of viscosity in temperature sweep measured with rheometer using OIL-C sample with different AA dosage. The legend ranked top to bottom based on decreasing overall viscosity

6.3.2 QCM study

Further work was conducted using QCM technology capable of assessing wax adhesion tendency as well as WAT/WDT for both AA with various oil samples. AA-1 only was added to oil sample OIL-C while AA-2 was mixed with oil samples OIL-C, OIL- D, OIL-E and OIL-F. Some dosages were repeated in different thermal cycles. Table 6-4 lists the experimental conditions and the overall results. The standard deviation was measured in some limited cases showing a reasonable repeatability.

Table 6-4. The results and condition of QCM using for measuring the effect of AA on WAX

Fluid	AA dosage (V%)	Cycle	Conditioning T (°C)	Destination T (°C)	WAT (°C)	WDT (°C)	Maximum ΔRF (Hz)
OIL-C	0	1	50	5	27.5	47.9	-18926
		2	50	5	27.8	48.2	-20689
		3	50	5	28.2	48.1	-21492
		4	50	5	28.3	47.9	-21994
		5	50	5	28.4	47.7	-22433
		6	50	5	28.5	47.4	-22433
		average			**28.1**	**47.9**	**-21328**
		st.dev			**0.39**	**0.29**	**1348**
OIL-C, AA-1	1	1	50	5	28	32.7	-16257
	1.96	1	50	5	28.3	33.4	-16481
		2	50	5	28.1	34.3	-16037
		3	50	5	28.4	33.3	-15283
		4	50	5	28.7	33.4	-14914
		average			**28.02**	**33.42**	**-15794**
		st.dev			**0.82**	**0.57**	**667**
	2.91	1	50	5	28	----	-8504
		2	50	5	28.2	----	-8148
		average			**28.1**	**----**	**-8326**
		st.dev			**0.14**	**----**	**252**
OIL-C, AA-2	1	1	50	5	28.8	----	-19959
	1.96	1	50	5	28.9	35.2	-15163
		2	50	5	28.6	34	-14191
		3	50	5	28.7	33.6	-12870
		4	50	5	28.8	33.3	-12040
		average			**28.8**	**34**	**-14845**
		st.dev			**0.44**	**0.83**	**3100**
	3.85	1	50	5	29.4	29.6	-8981
OIL-D, AA-2	0	1	50	15	31.3	43.2	-34390
	1	1	50	15	31.7	----	-25946
	1.96	1	50	15	31.7	42.8	-20933
	3.85	1	50	15	31.8	41.3	-8246
OIL-E, AA-2	0	1	35	5	13	19.9	-5190
	0.5	1	35	5	13.2	18.8	-5595
	0.99	1	35	5	14.5	20.9	-6795
	1.72	1	35	5	15	20.8	-7417
	1.72	1	35	5	15.1	23.7	-7815
OIL-F, AA-2	0	1	60	20	38.3	54.6	-9365
	0.5	1	60	20	38.5	51	-9671
		2	60	20	38.4	53	-11180
		3	60	20	38.5	54	-11886
		average			**38.5**	**52.7**	**-10912**
		st.dev			**0.06**	**1.53**	**1131**
	1	1	60	20	41.4	55.4	-18214
		2	60	20	39.3	53.9	-16869
		3	60	20	38.8	52.8	-17674
		4	60	20	39.5	53.2	-19069
		average			**39.75**	**53.83**	**-17957**
		st.dev			**1.14**	**1.14**	**925**
	1.5	1	60	20	41.6	52.3	-19663

Figure 6-14 to Figure 6-18 illustrate frequency change measured with different dosages of AAs in a variety of oil samples. Two distinct mechanisms were observed with the presence of AAs on QCM results.

In the first approach, increasing AA dosages was found to have no significant impact on WAT/WDT point with oil samples OIL-C and OIL-D, similar to what was observed in the rheometer. It could be justified that no solubility change occurred in presence of AAs. On the other hand, it was found to decrease frequency drop, shifting it up gradually as shown in Figure 6-14 to Figure 6-16. As discussed earlier, frequency shift could be due to the adherent tendency of particles, here, wax crystals on the gold electrode surfaces. The frequency does not translate to the amount of deposition, though, gives an opportunity in terms of quality evaluation in line with comparison purposes. The frequency reduction might be due to the effect of viscosity reduction caused by gravity depletion reducing the quantity of wax crystals around QCM surface as was observed in the previous chapter. In addition, the presence of AA might change the wettability of the surface prohibiting wax deposition, reducing frequency reduction.

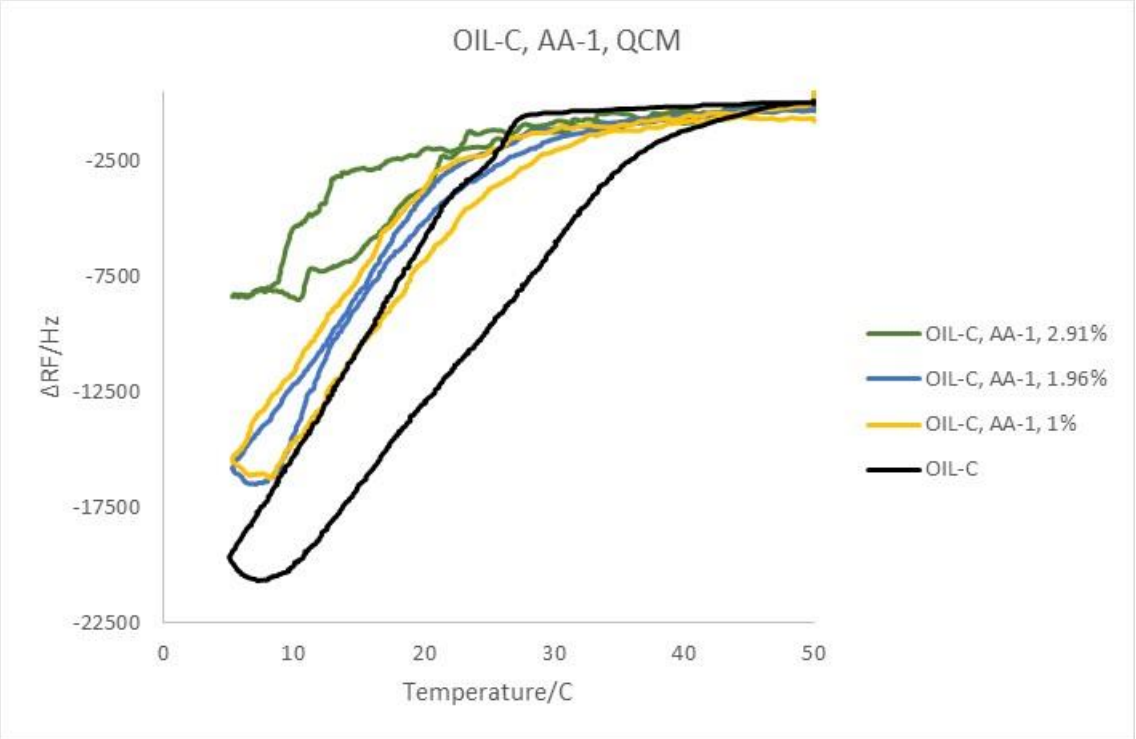

Figure 6-14. Frequency drop measured with QCM using OIL-C sample with different AA-1 dosage. The legend ranked top to bottom based on increasing average frequency drop.

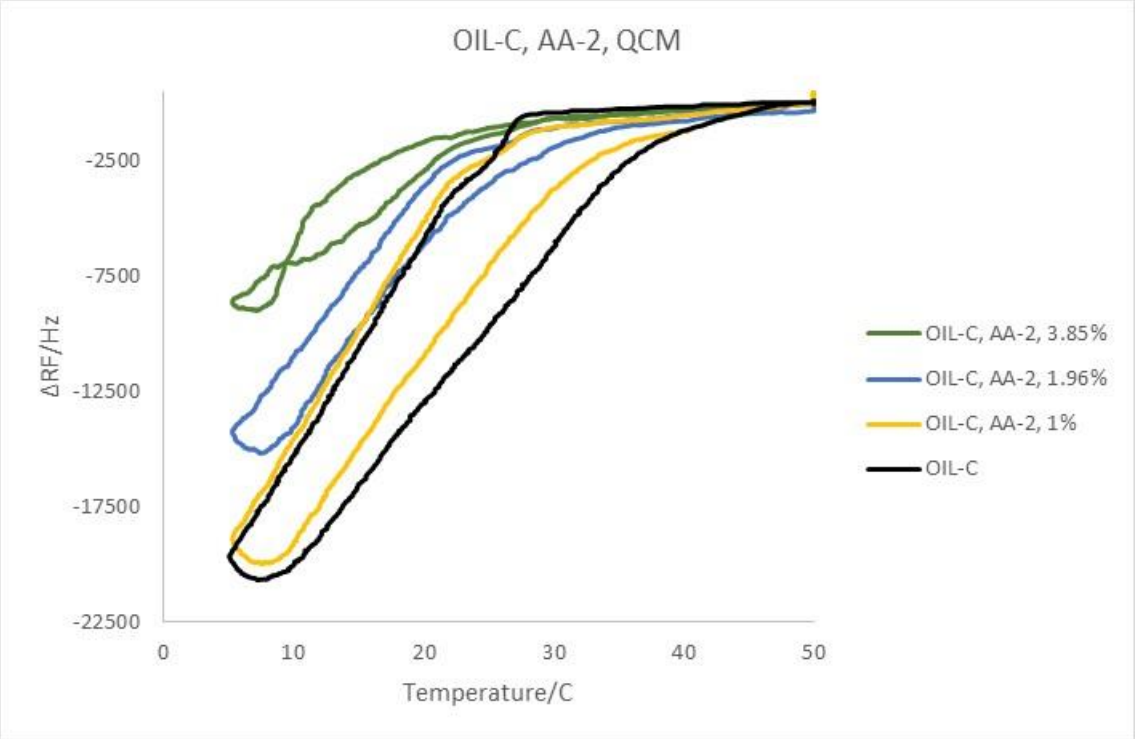

Figure 6-15. Frequency drop measured with QCM using OIL-C sample with different AA-2 dosage. The legend ranked top to bottom based on increasing average frequency drop.

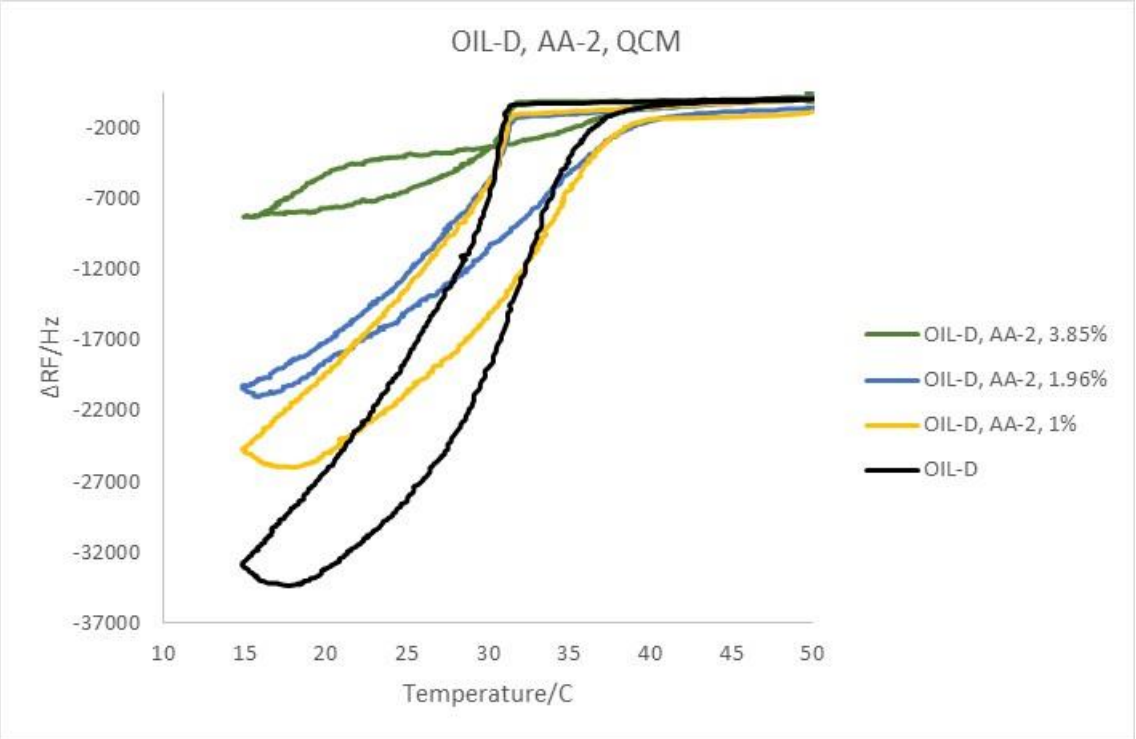

Figure 6-16. Frequency drop measured with QCM using OIL-D sample with different AA-2 dosage. The legend ranked top to bottom based on increasing average frequency drop.

Another behaviour was found in the presence of the different dosages with oil samples OIL-E and OIL-F, Figure 6-17 and Figure 6-18. Presented 1.72% and 1.5% AA-2 into the oil samples OIL-E and OILF shifted WAT 2.1°C and 3.3°C respectively. In

addition, the reverse effect on frequency drop was observed where increasing dosages increased frequency drop. A possible option for this type of behaviour was thought to be due to the solubility change of the samples. Additionally, based on the observation in the previous chapter, this solubility probably increased viscosity so then a higher amount of wax particles exists around QCM surface lower than WAT point, causing higher frequency reduction as a result of more wax deposition. Another option might be due to morphological change of the crystals, converting macro to microcrystalline particles with a higher adherent tendency to the QCM surface causing higher frequency reduction.

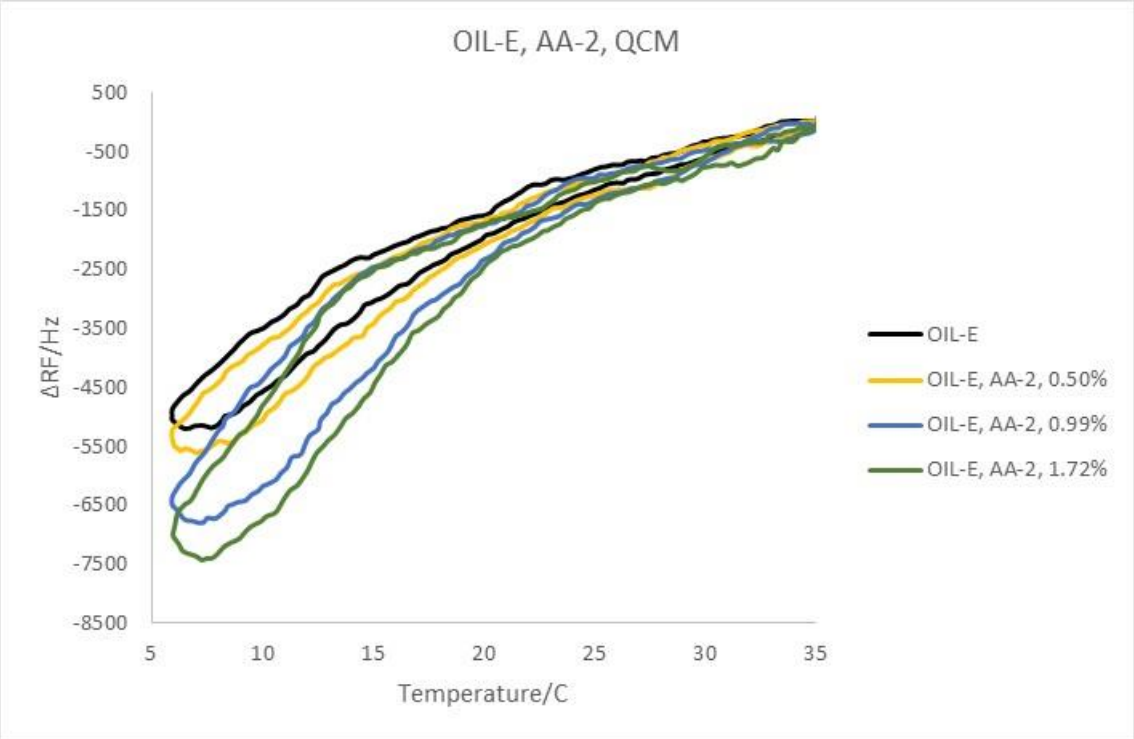

Figure 6-17. Frequency drop measured with QCM using OIL-E sample with different AA-2 dosage. The legend ranked top to bottom based on increasing average frequency drop.

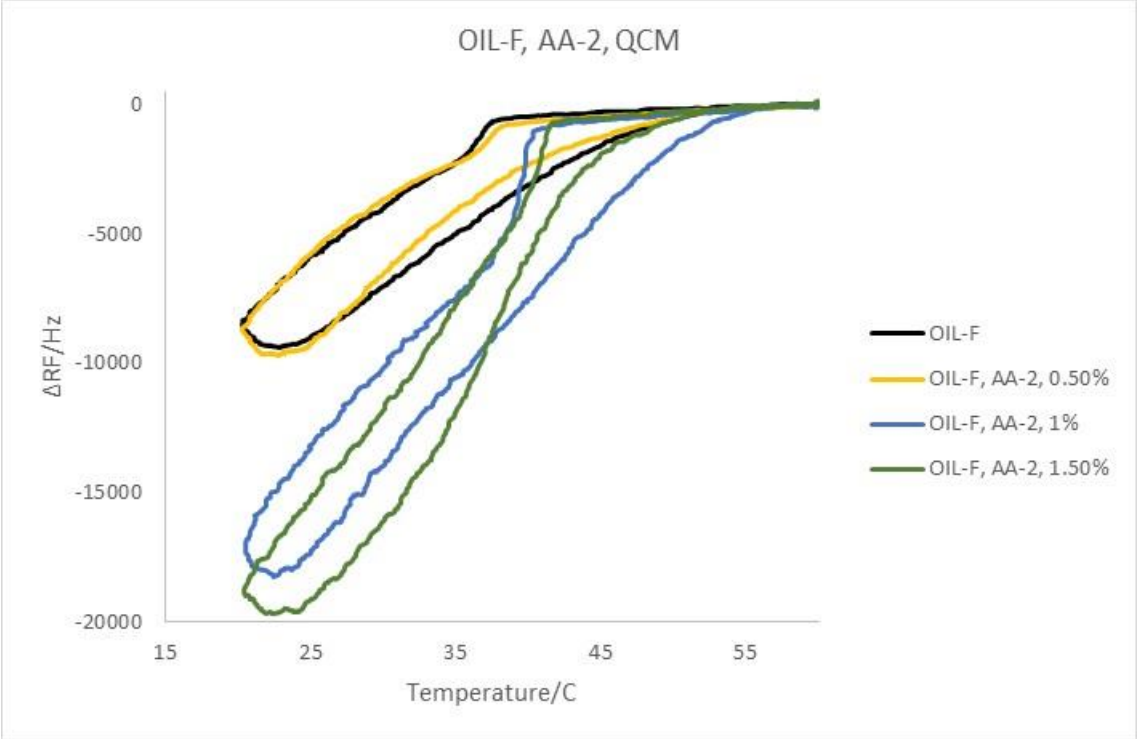

Figure 6-18. Frequency drop measured with QCM using OIL-F sample with different AA-2 dosage. The legend ranked top to bottom based on increasing average frequency drop.

6.3.3 Flowloop technique

One of the flow assurance issues associated with wax is the build-up of deposits in flow lines. In this work, the mini flowloop approach was used to determine experimentally the wax build-up tendency in the presence of hydrate anti-agglomeration imitating basic assumptions in real field conditions. A number of measurements were performed with different dosages of AA-1 and AA-2 using oil sample OIL-C without any watercut. Flow loop experiments were conducted at constant flow rate of 10CPM corresponding to a shear rate of 151 s^{-1} for all tests. Table 6-5 presents the required information about experimental conditions and results. These tests were conducted at different set temperatures, 5°C, 10°C and 15°C corresponded to subcooling of WAT-22°C, WAT-17°C and WAT-12°C.

As noted, the mechanism of AA working on hydrate has not been fully understood hence it was necessary to interpret the behaviour in the presence of wax particles. Perhaps, different mechanisms on wax deposition with the shear rate in flowline might be involved in the presence of AAs in addition to differential temperature driving force. AAs may function as a surface acting agent, reduced the wax deposition adherent

tendency on the walls. Furthermore, the nature of AAs as a viscosity reducer may adversely impact on wax deposition, increasing build up of deposits.

Table 6-5. Experimental condition and the results of flowloop, using OIL-C with/out AA in 10CPM with 151 s^{-1} in different ageing temperature. Loop C was used for all the tests.

Fluid	***Conditioning T (°C)***	***Test T (°C)***	***Flow rate (cc/min)***	***Shear rate (s^{-1})***	***Average ΔP (psi)***	***Average T_{in} (°C)***	***Average T_{out} (°C)***	***Average deposited thickness (µm)***
OIL-C	50	5	10	151	159	35.58	7.03	426
OIL-C, AA-1, 1%	50	5	10	151	116	38.31	6.67	437
OIL-C, AA-1, 2.91%	50	5	10	151	97	37.61	6.87	305
OIL-C, AA-1, 2.91%	50	15	10	151	19.1	39.83	16.36	390
OIL-C, AA-1, 1%	50	15	10	151	20.9	40.6	16.79	435
OIL-C, AA-1, 400ppm	50	15	10	151	19.8	41.11	16.25	491
OIL-C	50	15	10	151	15.2	41.67	16.32	406
OIL-C	50	5	10	151	174	35.71	7.53	446
OIL-C, AA-2, 1.96%	50	5	10	151	132	38.11	6.86	451
OIL-C, AA-2, 1.96%	50	10	10	151	264	39.5	11.92	671
OIL-C	50	10	10	151	144	40.11	12.11	616
OIL-C, AA-2, 1.96%	50	15	10	151	59	40.62	16.26	618
OIL-C, AA-2, 1%	50	15	10	151	32	40.68	16.24	548
OIL-C	50	15	10	151	17	41.63	16.26	430

6.3.3.1 Test temperature of 5°C

Figure 6-19 and 6-20 illustrate the results of differential pressure and deposited thickness with oil sample OIL-C without and with AA-1 at dose rates of 1 and 2.91 volume%. As can be seen, increased dose rate of AA-1 slightly reduced deposition. The same result was observed with AA-2 at a dose rate of 1.96 volume% shown in Figure 6-21 and Figure 6-22. It seems the surface acting property had a dominant impact on deposition at this subcooling.

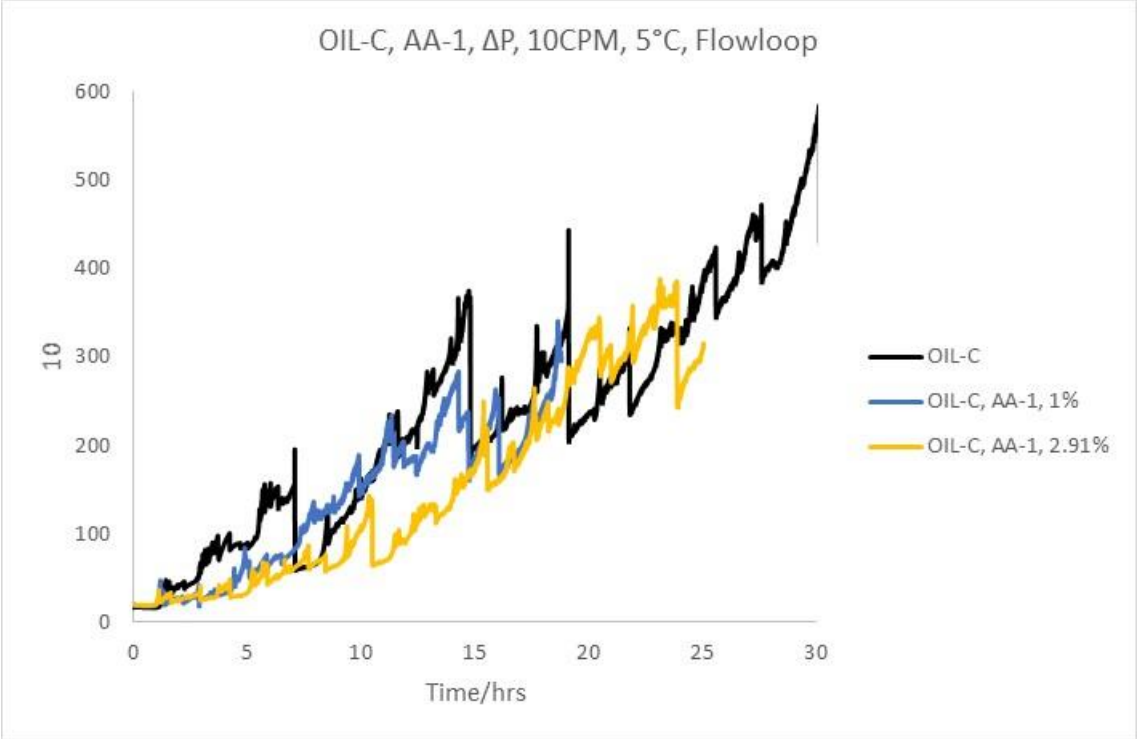

Figure 6-19. Comparison of differential pressure buildup by flowloop using OIL-C sample with/out AA-1 in different dosage in 10CPM with 151 s^{-1}.

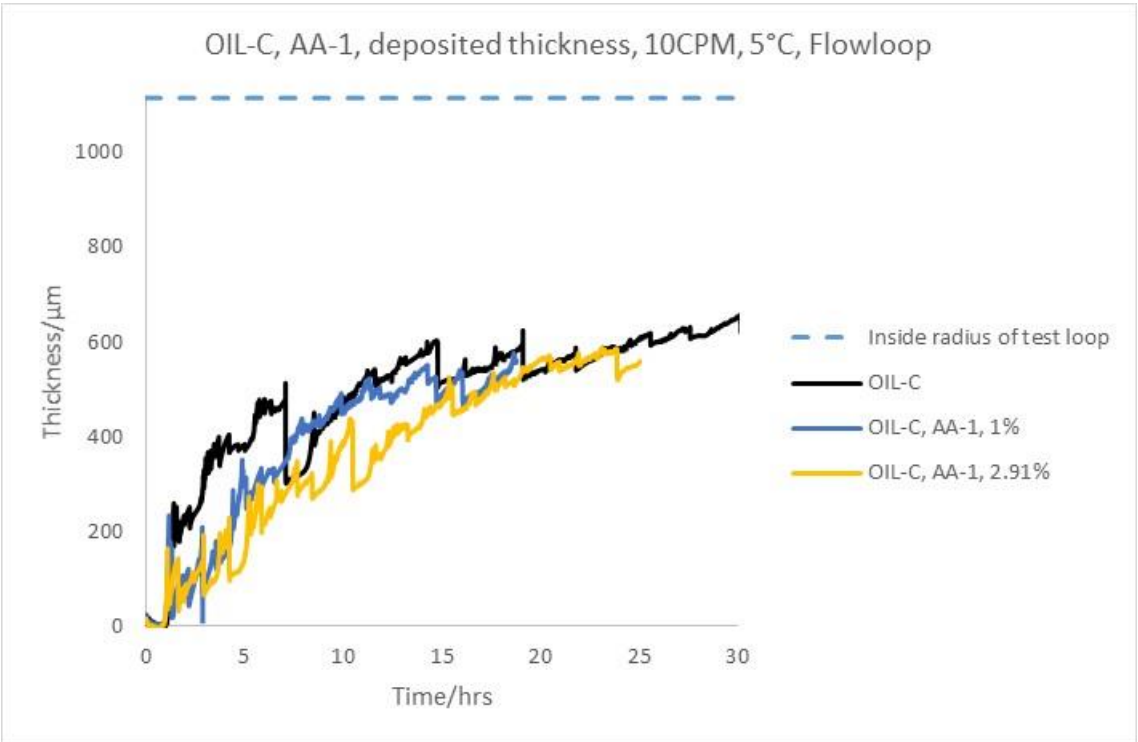

Figure 6-20. Comparison of deposited thickness by flowloop using OIL-C sample with/out AA in different dosage in 10CPM with 151 s^{-1}.

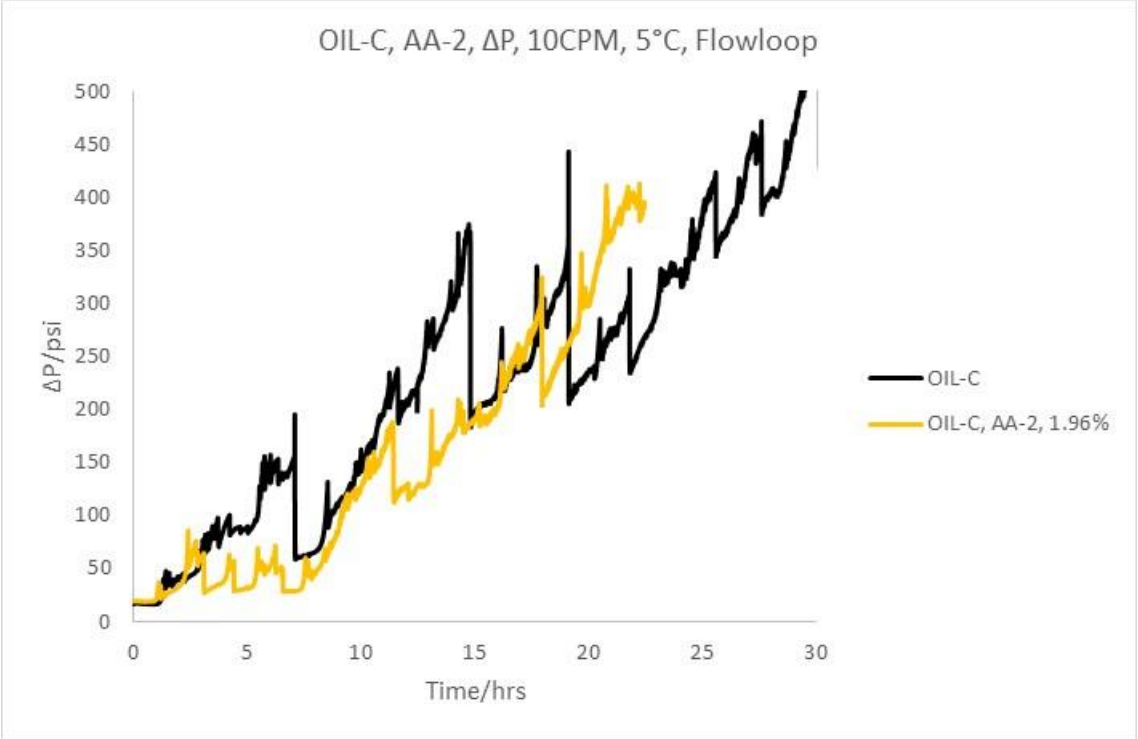

Figure 6-21. Comparison of differential pressure buildup by flowloop using OIL-C sample with/out AA-2 in 10CPM with 151 s^{-1}. The legend ranked top to bottom based on decreasing deposited thickness at 5°C.

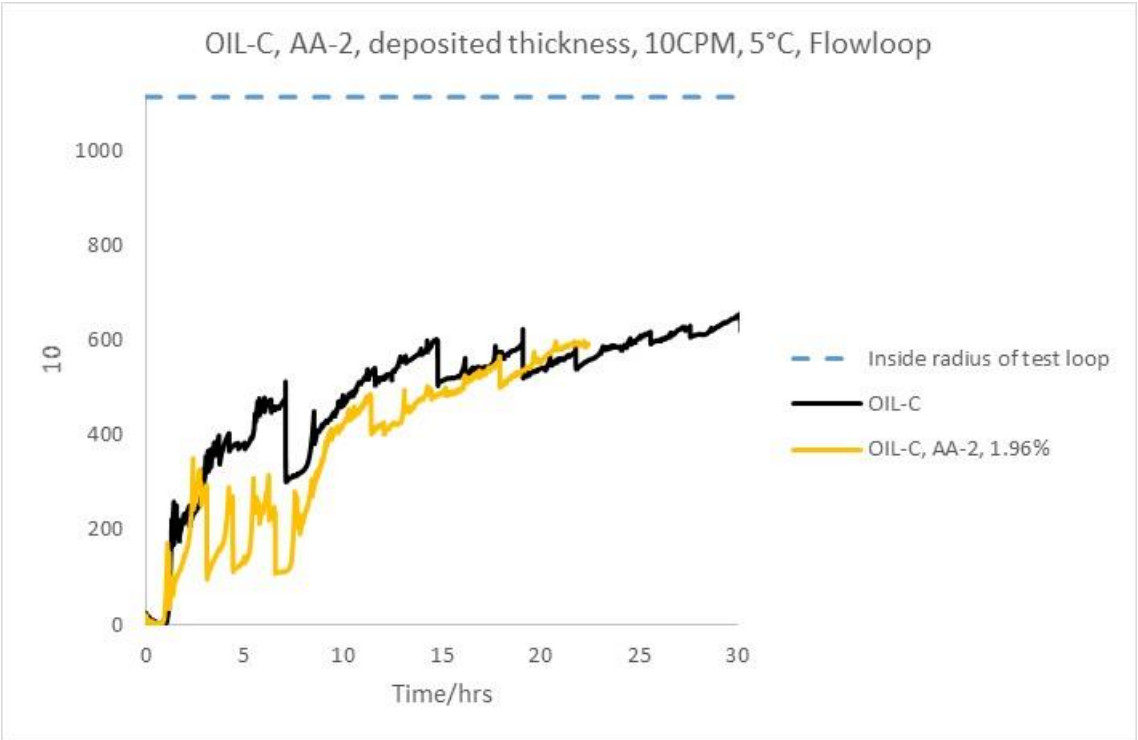

Figure 6-22. Comparison of deposited thickness by flowloop using OIL-C sample with/out AA in 10CPM with 151 s^{-1}. The legend ranked top to bottom based on decreasing deposited thickness at 5°C.

6.3.3.2 Test temperature of 10°C

From Figure 6-23 and Figure 6-24, it is clear that the test with the lower subcooling run at 10°C in dosage with 1.96% AA-2, resulted in a similar pattern of differential pressure and deposition thickness for about 24 hrs test time. Deposition in the blank oil was then sloughed and the differential pressure and thickness started to diverge. The deposition of sample with AA-2 increased continuously to the end of the test for about the next 24hrs.

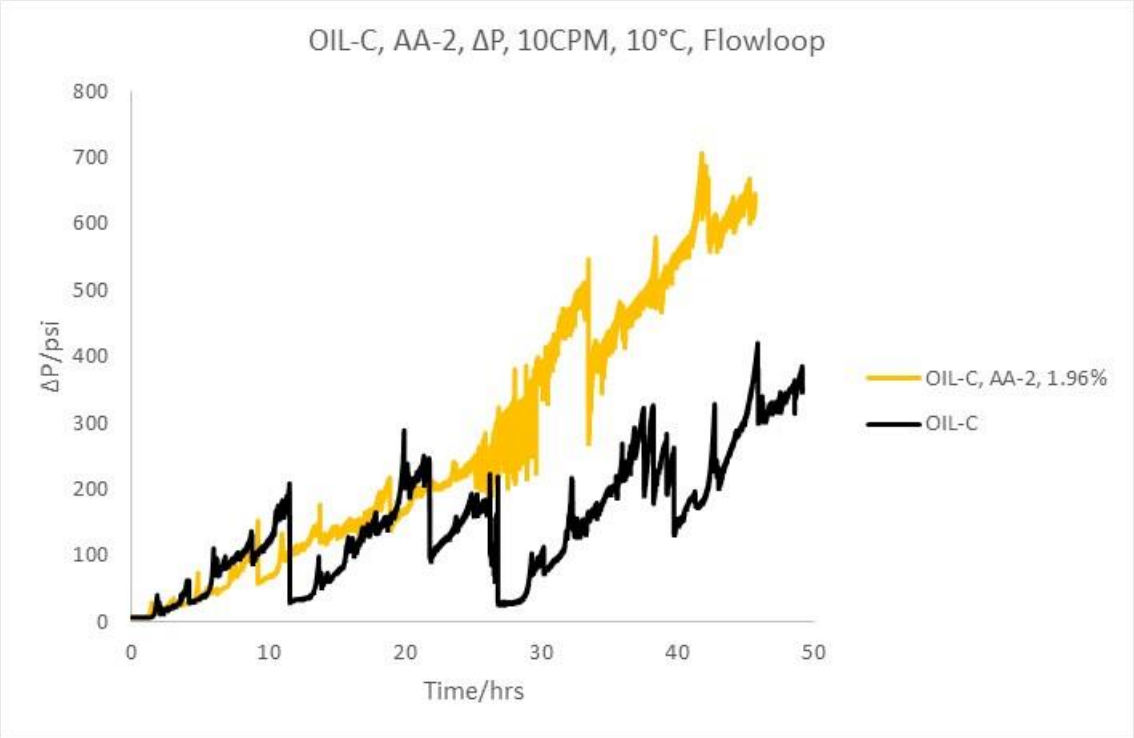

Figure 6-23. Comparison of deposited thickness by flowloop using OIL-C sample with/out AA in 10CPM with 151 s^{-1}. The legend ranked top to bottom based on decreasing deposited thickness at 10°C.

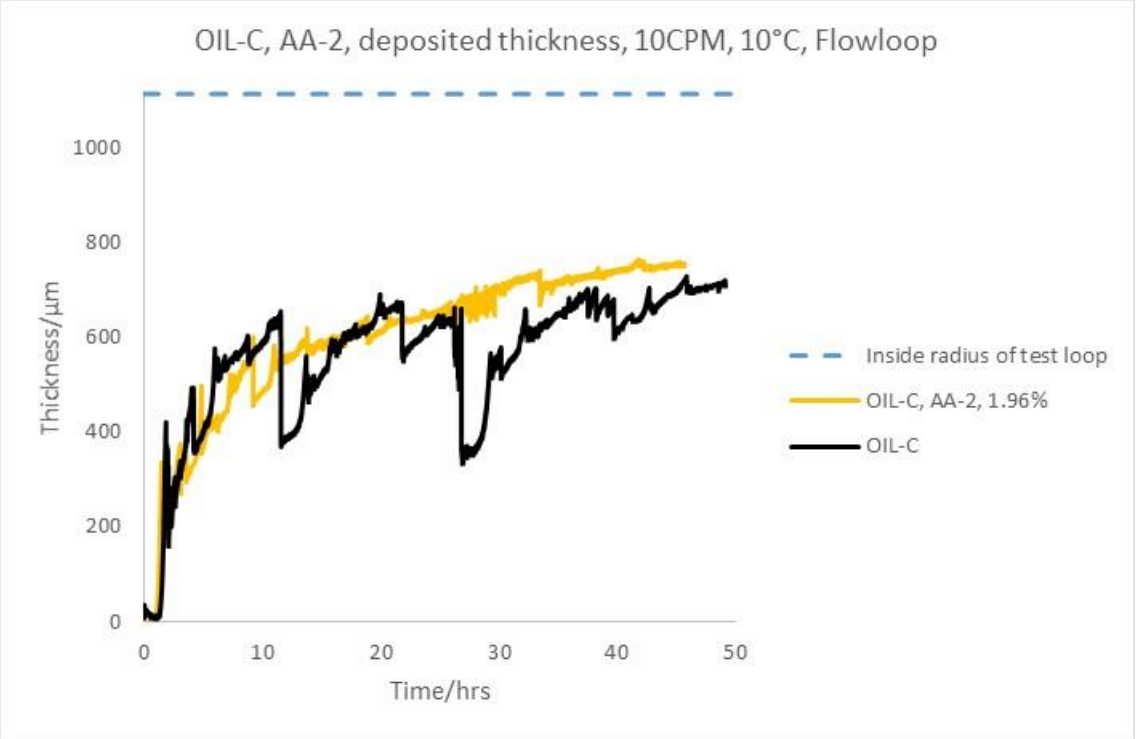

Figure 6-24. Comparison of deposited thickness by flowloop using OIL-C sample with/out AA in 10CPM with 151 s^{-1}. The legend ranked top to bottom based on decreasing deposited thickness at 10°C.

6.3.3.3 Test temperature of 15°C

Finally, the test was conducted at 15°C dosed with both AA-1 and AA-2 in various concentrations. Figure 6-25 and Figure 6-26 demonstrate give the results indicating that the deposition adherent tendency was ranked in terms of AA dosages only at the early stages of 5hrs measuring time. The rank of inhibition was then scattered after this point where shear stress probably was sloughing the layers of deposition.

The trend in 5 hrs test time shows that the overall differential pressure and thickness increased with increasing dosages. In addition, a sharp increase was observed in trends with both 1 and 2.91 v% dosages then fell down, most probably due to sloughing the deposition layer. It seemed presence of AA-1 modified the microstructure of wax particles making a loose deposit with a large amount of oil in the wax network which was broken down at around 5hrs.

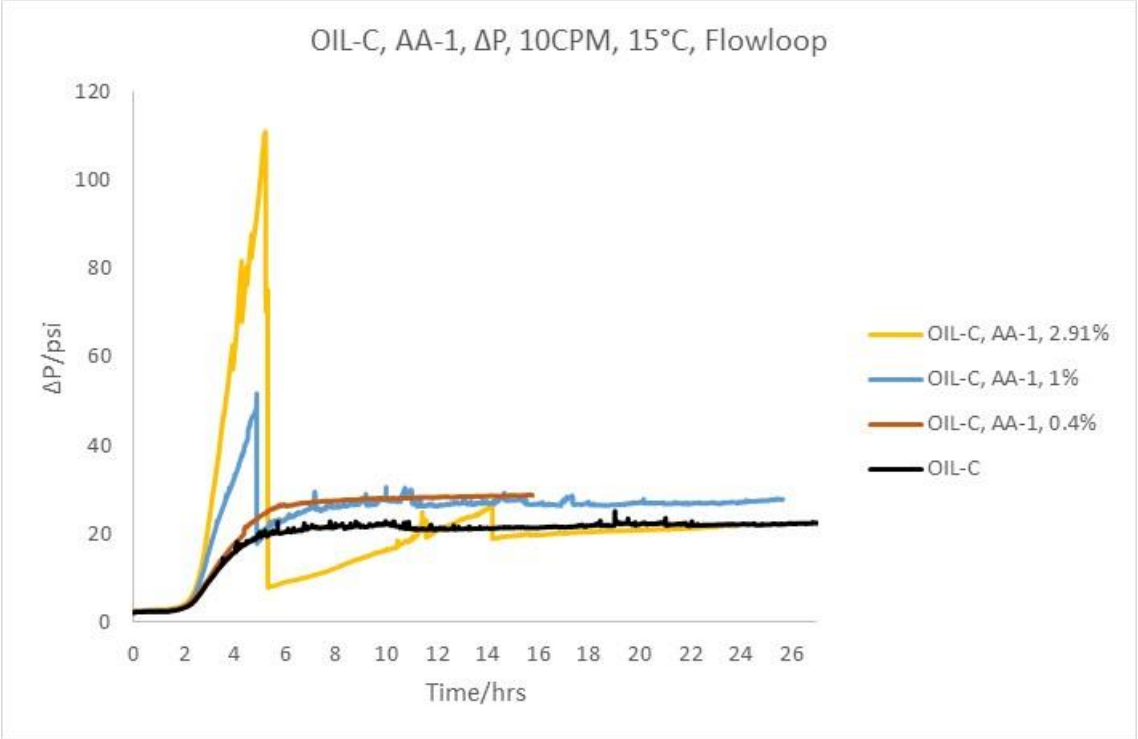

Figure 6-25. Comparison of differential pressure buildup by flowloop using OIL-C sample with/out AA in different dosage in 10CPM with 151 s^{-1}. The legend ranked top to bottom based on decreasing maximum build-up pressure at 15°C.

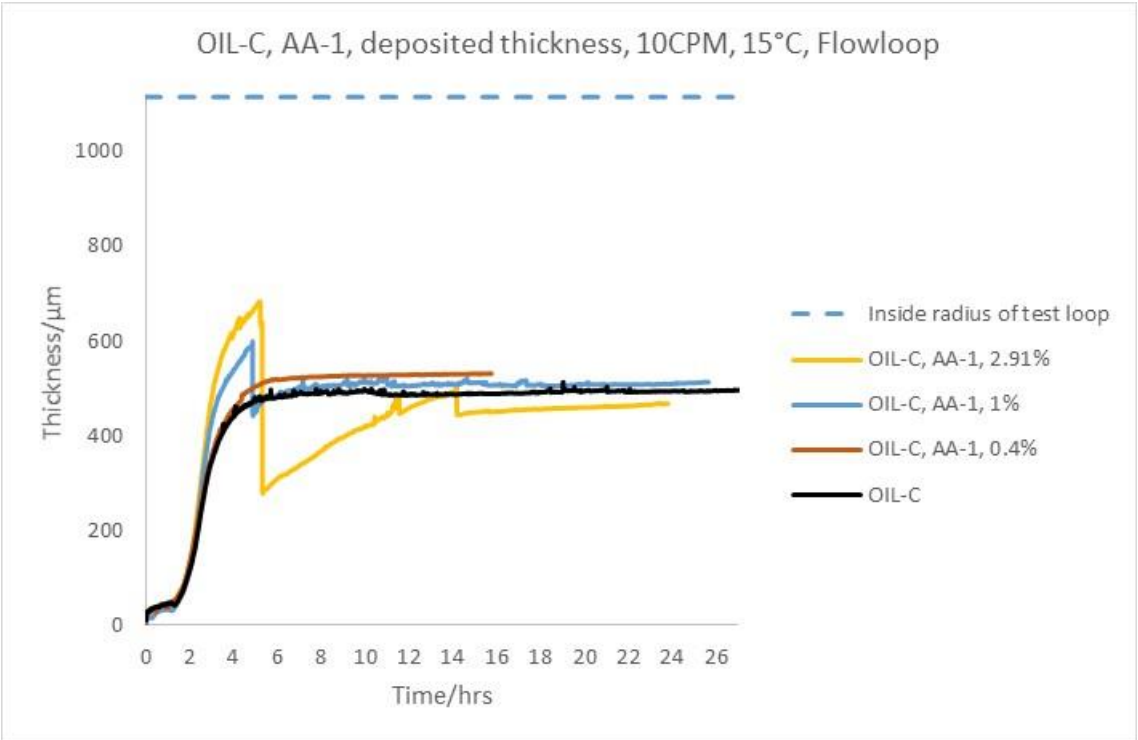

Figure 6-26. Comparison of deposited thickness by flowloop using OIL-C sample with/out AA in different dosage in 10CPM with 151 s^{-1}.

Figure 6-27 and Figure 6-28 indicate a sharp increase in trends followed by a plateau for all samples with and without AA-2.

Since the trends increased in the same patterns with increasing dosages without any flake off layers, morphological change of crystals was less likely. Since viscosity reduced with increasing temperature and also the effect of subcooling was low enough, viscosity reduction property of AA seemed to have a dominant factor at this temperature. As observed in the last chapter, lower viscosity had higher deposition tendency in the presence of wax inhibitors.

Overall it was found that using AAs at higher subcooling resulted in a better performance in terms of inhibition of wax deposition at least for AAs studied in this work.

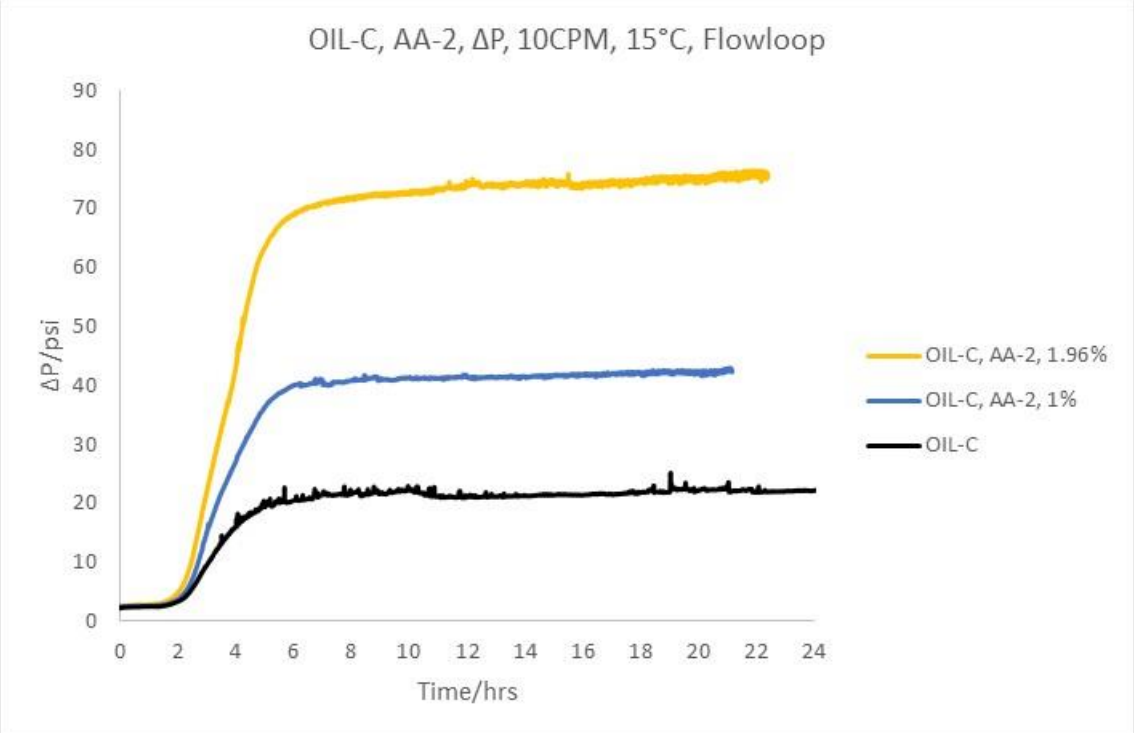

Figure 6-27. Comparison of differential pressure buildup by flowloop using OIL-C sample with/out AA in different dosage in 10CPM with 151 s^{-1}. The legend ranked top to bottom based on decreasing maximum build-up pressure at 15°C.

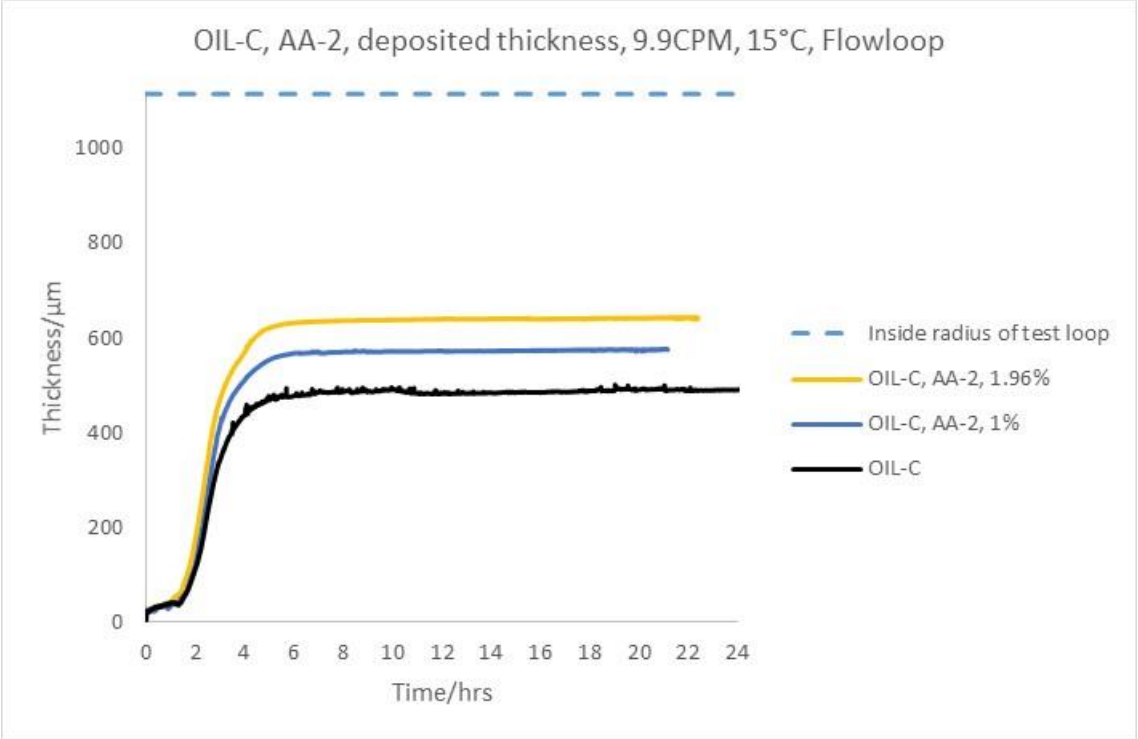

Figure 6-28. Comparison of deposited thickness by flowloop using OIL-C sample with/out AA in different dosage in 10CPM with 151 s^{-1}. The legend ranked top to bottom based on decreasing deposited thickness at 15°C.

6.4 The impact of oil-based mud fluid on the wax properties

Oil based mud is an expensive type of drilling fluid applied in shale layers, high temperature, water soluble and production zone. A significant disadvantage of these kinds of fluids could be the risk of filtration towards core and oil around wellbore zone. Initial sampling of these wells then may have a degree of contamination, resulted in some non-representative values [4, 5, 14].

The purpose of the current study was to investigate the ability to predict some wax properties such includes WAT, WDT, viscosity and wax deposition tendency of the uncontaminated samples. Six different oil samples were used to measure with QCM. One sample was taken to measure rheology behavior in a temperature sweep by the rheometer.

A simple approach was conducted, using a different concentrations of oil based fluid looking for a trend, useful for estimating the properties of any contamination level. A commercial oil-based fluid was used with a range of components C9 to C19.

6.4.1 Rheological investigation

The experimental conditions and some general results using rheometer are listed in Table 6-6 for oil sample OIL-G. Different concentration of oil based fluid was mixed with blank oil sample all at the same experimental condition.

Table 6-6. The condition and results of rheometer to measure viscosity, using OIL-G with different oil based mud dosage, ranked top to bottom based on decreasing overall viscosity

Oil based mud (volume %)	***Conditioning T (°C)***	***Destination (°C)***	***Cooling rate (°C/min)***	***Shear rate (s^{-1})***	***WAT (°C)***	***WDT (°C)***	***Minimum Viscosity (cP)***	***Maximum Viscosity (cP)***
0	*60*	*20*	*1*	*10*	*34*	*45*	*5.07*	*129*
4.35	*60*	*20*	*1*	*10*	*33*	*44*	*4.62*	*87.8*
8.33	*60*	*20*	*1*	*10*	*31.5*	*43.9*	*4.39*	*58.6*
18.52	*60*	*20*	*1*	*10*	*28.8*	*41*	*3.52*	*23.2*
24.14	*60*	*20*	*1*	*10*	*27*	*40.6*	*3.1*	*14.8*

A semi log variation of viscosities versus temperature sweep in a thermal cycle trend is demonstrated in Figure 6-29. Increasing dosages led to a reduced viscosity, with lower viscosity over the entire thermal cycle path. The viscosity reduction is more significant at lower temperatures, less than WAT point; the reason for this behaviour could be attributed to the presence of a higher proportion of aromatic components in the oil-based fluid which functioned as a solvency parameter reducing the amount of wax particles in lower WAT hence lower viscosity was obtained. The same explanation could be given for higher temperatures where floating heavy components such as asphaltene and un-dissolved heavy wax particles exist.

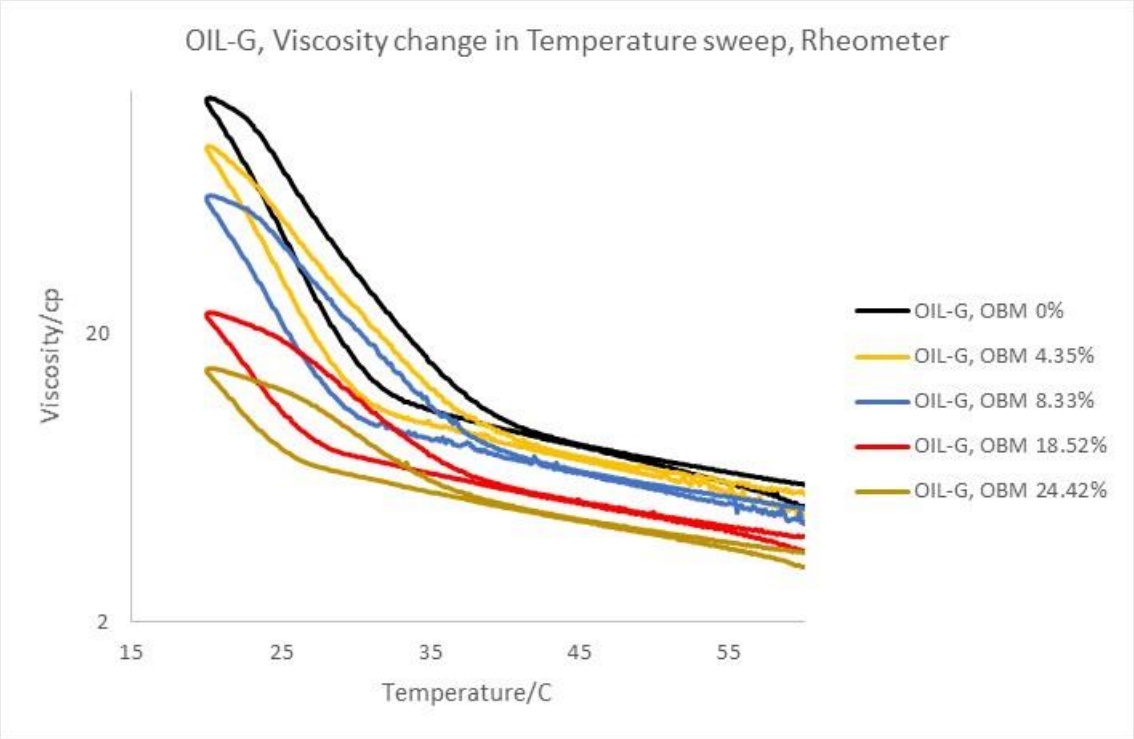

Figure 6-29. Semilog variation of viscosity in temperature sweep measured with rheometer using OIL-A sample dosed with different inhibitors. The legend ranked top to bottom based on decreasing overall viscosity

A linear relation between WAT, WDT and semi log relation in maximum viscosity obtained by rheometer is plotted in Figure 6-30. The amount of variation from a straight line is shown with R-squared to indicate how close the data are to the fitted line. Generally, the higher r-squared close to 1, the better the data fits the straight line. All trends illustrate very high close to 1 r squared, so then it would make it easy to predict WAT-WDT and viscosity of uncontaminated sample by using the rheometer. WAT and WDT slightly reduced with increasing dosages which again could be attributed to the presence of a higher proportion of aromatic components as a solvency agent.

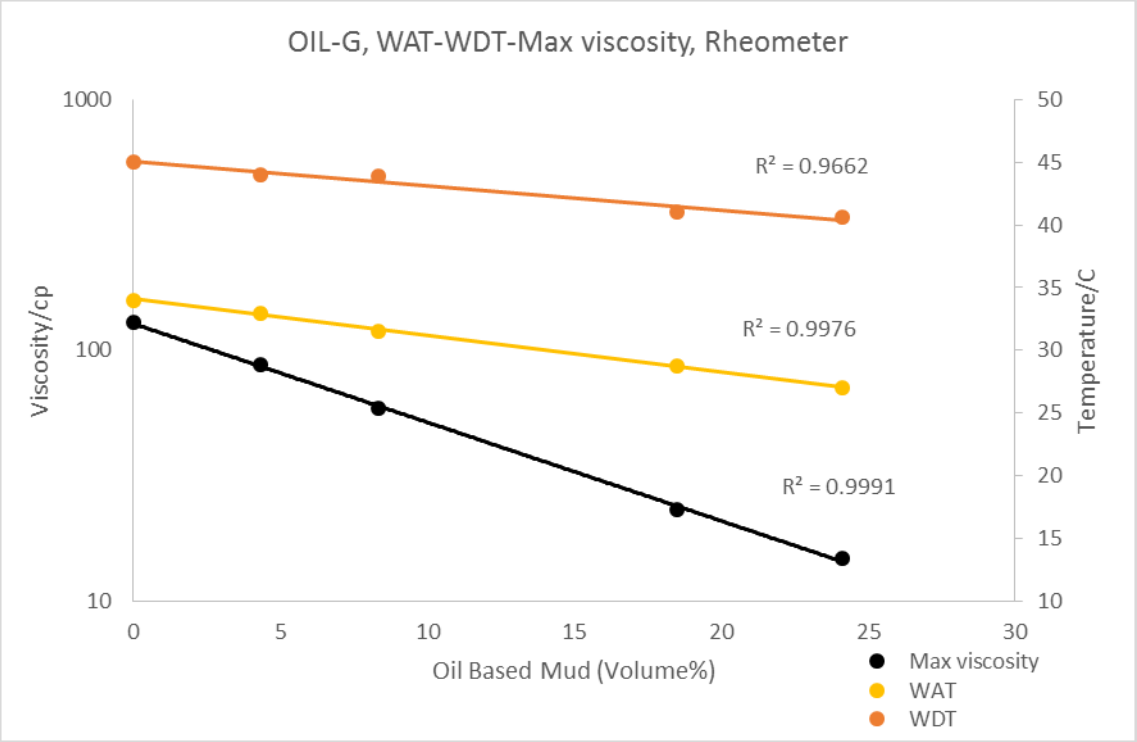

Figure 6-30. Comparison of WAT-WDT and the maximum viscosity measured with the rheometer using OIL-G sample with different oil based mud dosage. The solid line is of the form y = x and is not associated with a fit of the data series.

6.4.2 QCM technique

A series of measurements was carried out with different oil samples OIL-E, OIL-F, OIL-G, OIL-H, OIL-I and OIL-J in various oil based fluid concentration. All tests except OIL-G were conducted with two different QCM surfaces to monitor repeatability and reliability of trends. Tests condition and result are tabulated in Table 6-7. Starting conditioning temperature was set with respect to the rheometer for which results were discussed in detail in Chapter 4.

For each individual sample in one of the applied QCM surface, Figure 6-31 to Figure 6-36 demonstrate the frequency change in a thermal cycle test. The legends ranked top to bottom based on increasing average frequency drop which is shown in the figures below. In general, increasing dosages caused the overall thermal cycle trends to shrink.

Table 6-7. The results and conditions of two different QCMs using for analysing the effect of oil-based mud on various oil samples.

Fluid	Conditioning T (°C)	Destination T (°C)	Oil based mud (volume %)	WAT1 (°C)	WAT2(°C)	WDT1 (°C)	WDT2(°C)	maximum ΔRF1 (Hz)	maximum ΔRF2 (Hz)
OIL-E	35	5	0.00	13.7	12.6	24.9	23.3	-7528	-7617
			4.76	13.0	12.7	24.3	24.3	-7135	-6980
			9.09	11.2	10.7	21.5	22.6	-6524	-6691
			16.67	9.1	10.7	19.4	20.7	-4866	-4708
			23.08	8.8	8.7	19.5	20.8	-4083	-3590
			28.57	7.8	8.1	18.8	20.8	-3678	-2777
OIL-F	60	25	0.00	38.1	38.4	54.5	53.8	-7156	-6407
			4.76	36.2	36.2	53.4	47.7	-5175	-3843
			9.09	36.6	35.5	52.5	47.7	-4648	-3906
			16.67	35.1	34.2	51.1	47.8	-4057	-3292
OIL-G	60	20	0.00	26.2	----	47.0	----	-15052	----
			4.35	25.6	----	45.2	----	-14585	----
			8.33	25.2	----	44.4	----	-13342	----
			12.00	24.6	----	43.8	----	-14640	----
			18.52	23.8	----	42.1	----	-11227	----
			24.14	23.3	----	42.5	----	-8865	----
OIL-H	50	20	0.00	34.9	34.9	39.5	39.5	-12603	-7206
			4.76	34.1	34.1	38.4	38.6	-7585	-5190
			9.09	34.2	34.2	41.6	41.6	-7304	-4728
			16.67	33.1	33.9	41.4	40.0	-5513	-3817
			23.08	32.3	32.3	37.5	40.1	-4613	-3147
			28.57	31.6	31.8	41.0	40.1	-4349	-3080
OIL-I	30	5	0.00	11.7	11.7	27.3	21.5	-29935	-27522
			4.76	11.6	11.4	25.9	21.4	-25952	-23966
			9.09	10.9	10.9	25.0	23.5	-22203	-19689
			16.67	10.1	9.9	25.2	19.7	-13659	-13543
OIL-J	35	5	0.00	16.9	17.9	28.0	29.1	-10866	-10586
			4.35	16.0	16.0	27.1	29.2	-10601	-10501
			8.33	15.1	14.7	27.9	28.5	-10951	-11020
			15.38	13.1	13.1	27.1	29.1	-10592	-10616
			21.43	10.8	10.9	26.8	28.2	-11708	-10850
			28.57	9.9	10.1	28.2	28.0	-9673	-9920

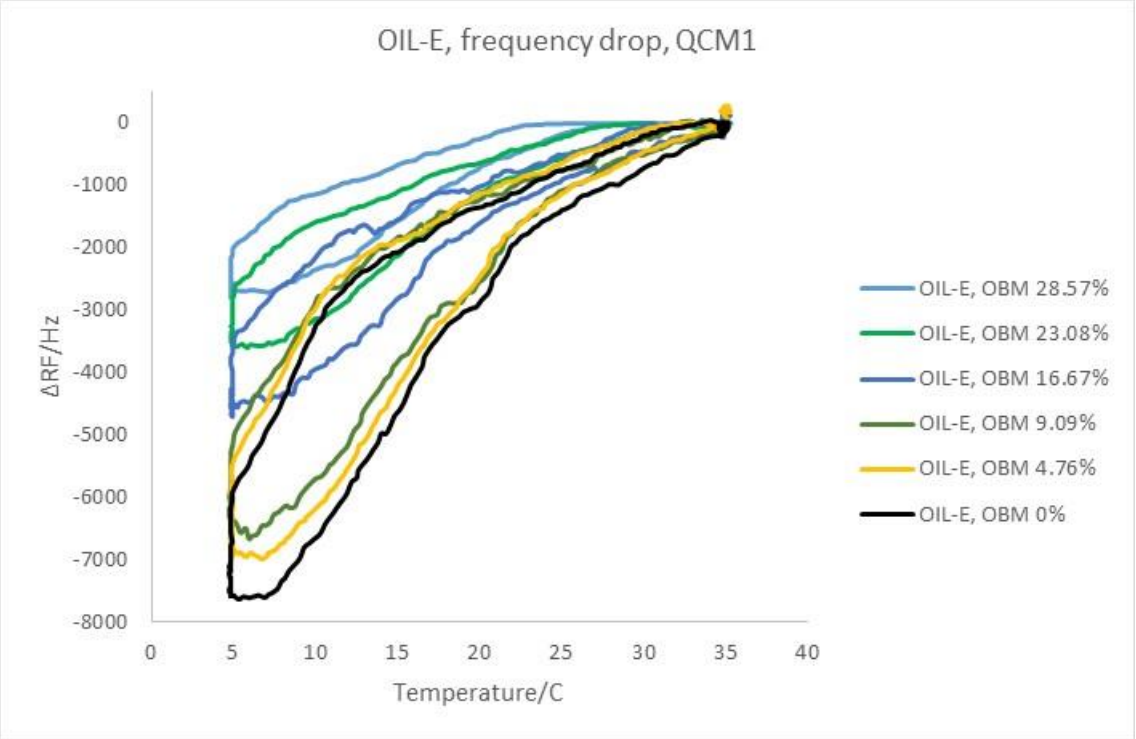

Figure 6-31. Frequency drop measured with QCM1 using OIL-E sample with different oil based mud dosage. The legend ranked top to bottom based on increasing average frequency drop.

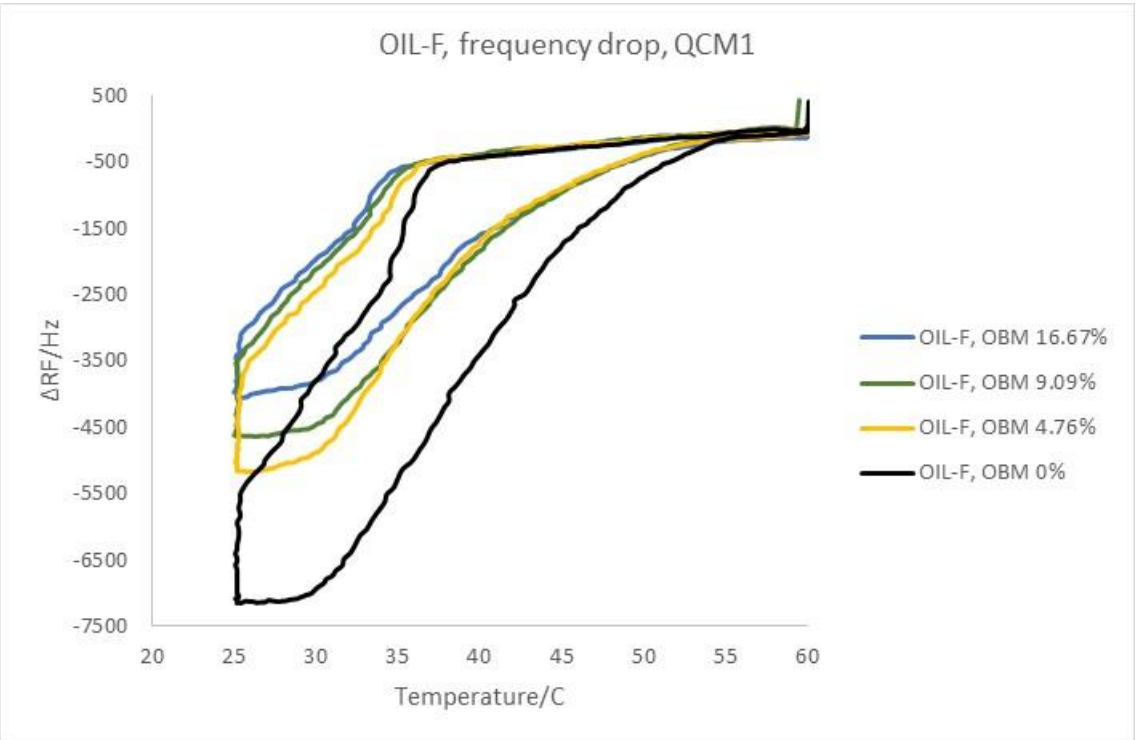

Figure 6-32. Frequency drop measured with QCM1 using OIL-F sample with different oil based mud dosage. The legend ranked top to bottom based on increasing average frequency drop.

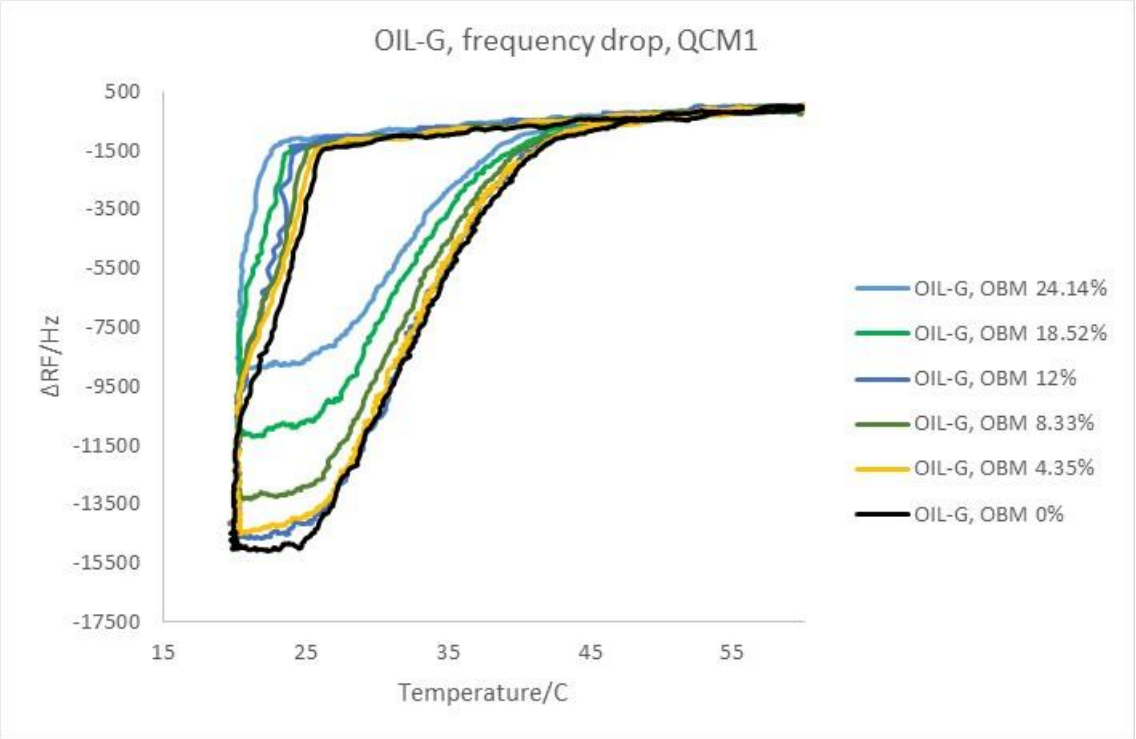

Figure 6-33. Frequency drop measured with QCM1 using OIL-G sample with different oil based mud dosage. The legend ranked top to bottom based on increasing average frequency drop.

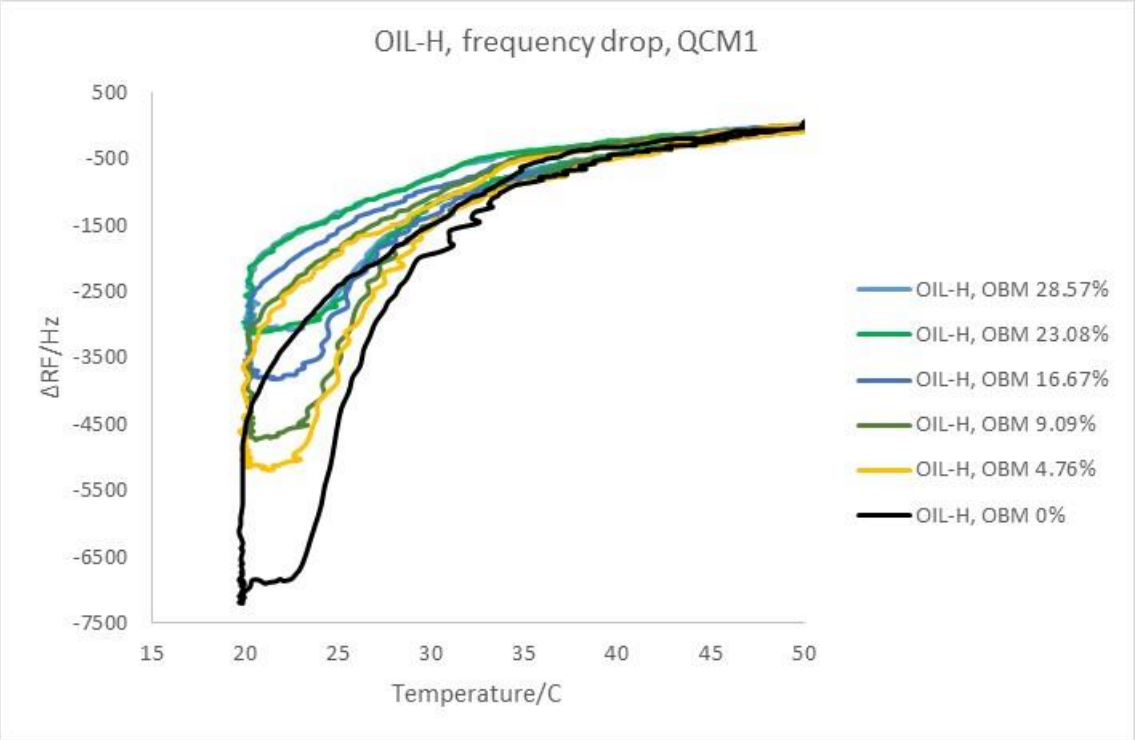

Figure 6-34. Frequency drop measured with QCM1 using OIL-H sample with different oil based mud dosage. The legend ranked top to bottom based on increasing average frequency drop.

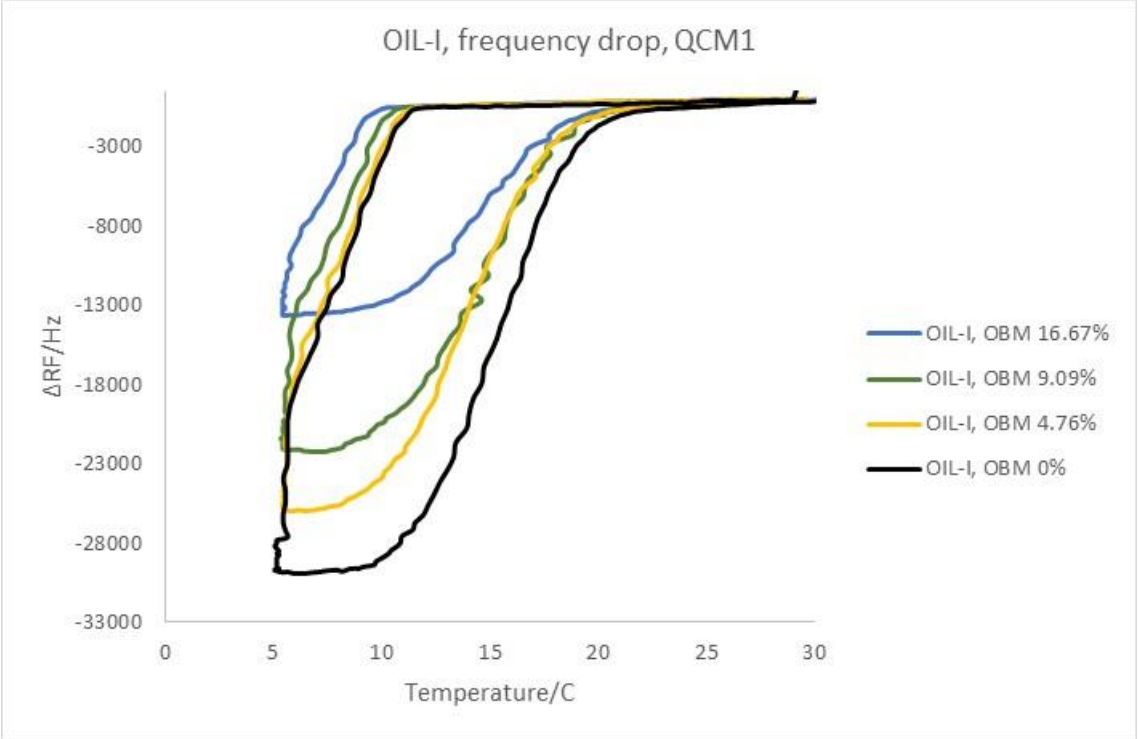

Figure 6-35. Frequency drop measured with QCM1 using OIL-I sample with different oil based mud dosage. The legend ranked top to bottom based on increasing average frequency drop.

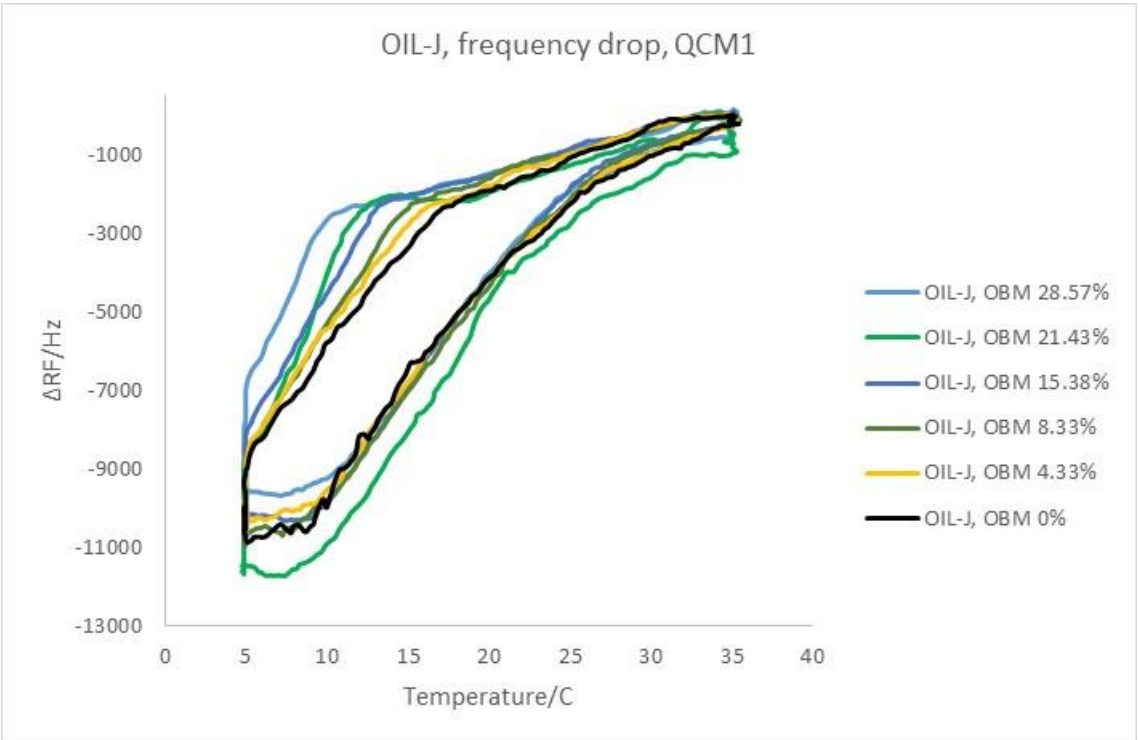

Figure 6-36. Frequency drop measured with QCM1 using OIL-J sample with different oil based mud dosage. The legend ranked top to bottom based on increasing average frequency drop.

Figure 6-37, Figure 6-38 and Figure 6-39 show plots of WAT, WDT and maximum frequency reduction respectively. All the points were in the order of linear trend quite close to 1 r-squared which made it possible to predict WAT-WDT and frequency drop

in any sample with different contamination level using QCM. WAT and WDT decreased slightly which could be due to the increasing solubility.

As mentioned earlier, frequency reduction could be attributed to the change in viscosity, density, and adherent tendency of the sample. Frequency reduction decreased with increasing oil based fluid which is observed in the figure below. Frequency reduction might be due to the gravity depletion of wax particles as already found in the last chapter (due to viscosity reduction and resulted in wax depletion). In addition, this drop might be as a consequence of increasing solubility. Higher solubility decreased the number of wax particles which exist at lower WAT point hence less deposition occurred, which leads to less frequency reduction.

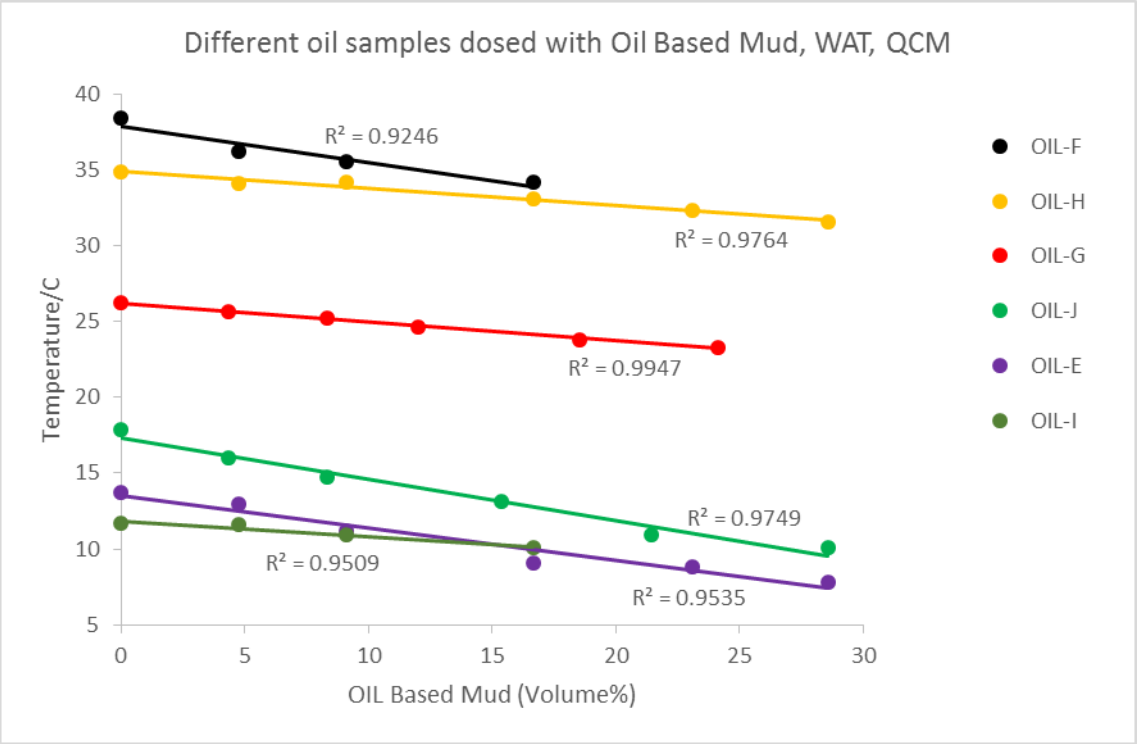

Figure 6-37. Average WAT measured with 2 different QCM used different samples with different oil based mud dosage. The legend ranked top to bottom based on decreasing WAT. The solid line is of the form y = x and is not associated with a fit of the data series.

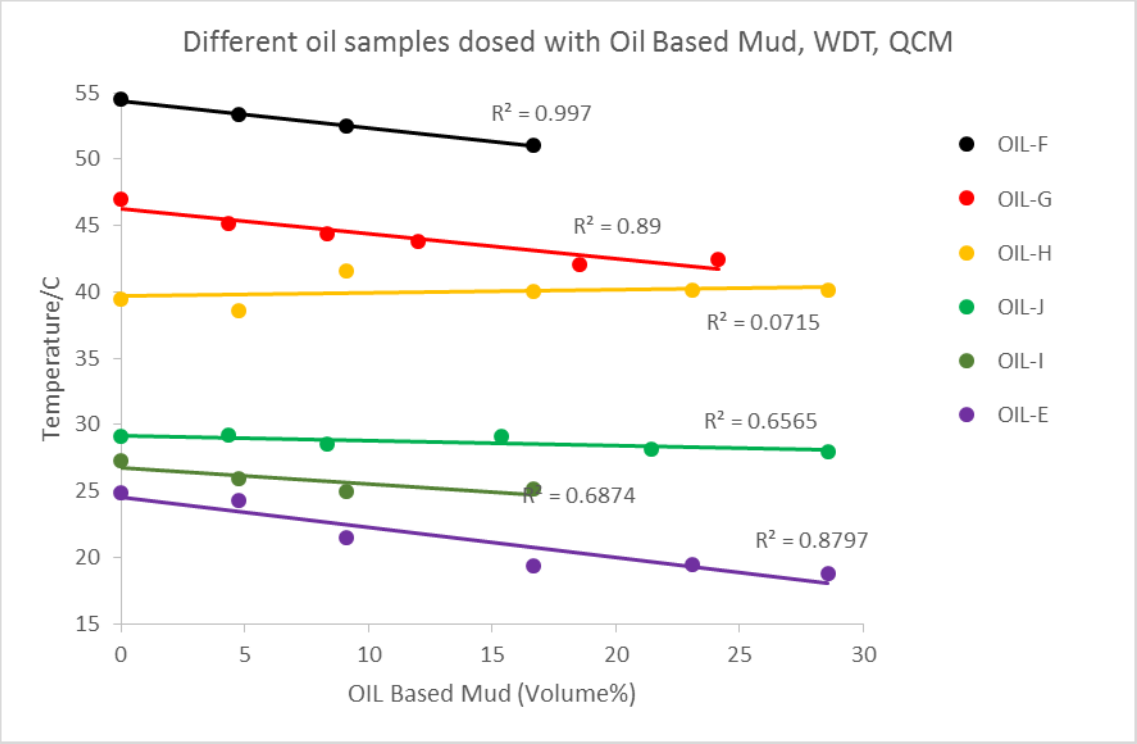

Figure 6-38. Average WDT measured with 2 different QCM used different samples with different oil based mud dosage. The legend ranked top to bottom based on decreasing WDT. The solid line is of the form y = x and is not associated with a fit of the data series.

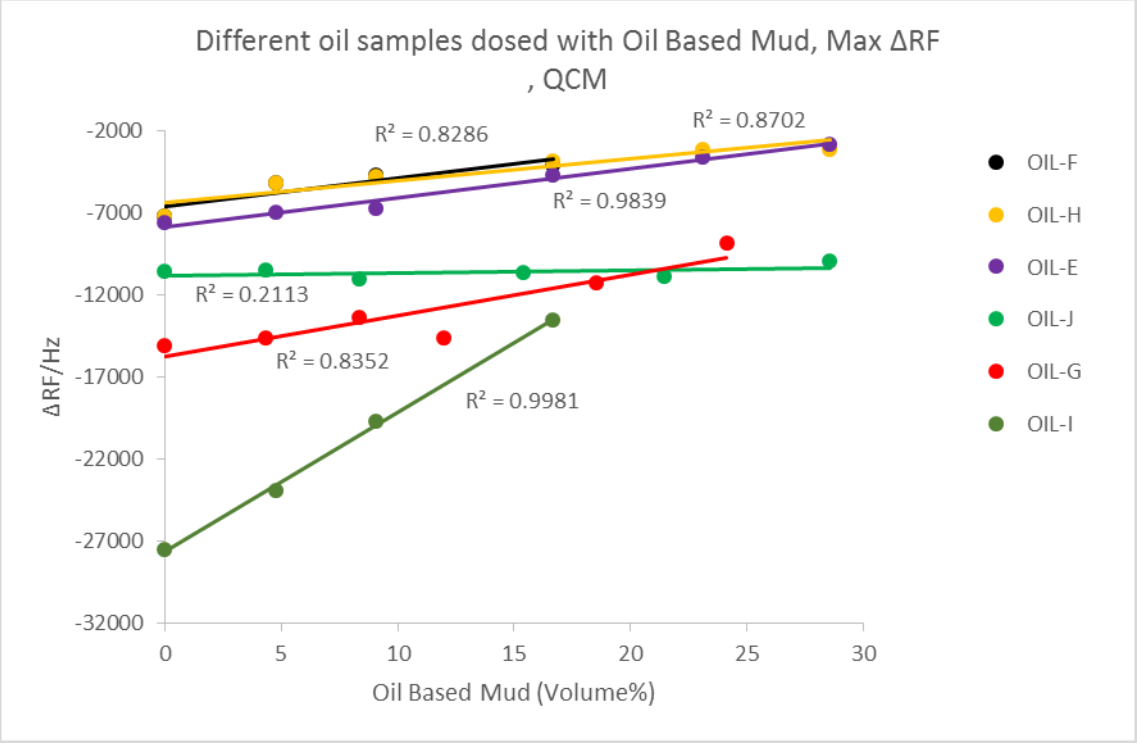

Figure 6-39. Average maximum frequency drop measured with 2 different QCM used different oil samples with different oil based mud dosage. The legend ranked top to bottom based on increasing frequency drop. The solid line is of the form y = x and is not associated with a fit of the data series.

6.5 Effect of scale on QCM reading in wax study

The capability of QCM in terms of wax study, provide an opportunity to measure WAT/WDT and the adherent tendency of wax crystals [2]. In order to validate the repeatability of data and the impact of the morphological change of crystals on QCM detectors, the majority of measurements were repeated several times in a thermal cycle (cooling/heating) test for each loaded sample. It was usually conditioned for a duration of 1 to 3 hrs between each cycle. WAT and WDT in all the blank samples without inhibitors had a very good repeatability and no any significant change was observed even after 10 different cycles with different condition time between 0 and 24 hrs. It was also observed using a different QCM surface the same WAT/WDT was obtained. The average deviation in various QCM for the sample under study in this work was resulted around 0.5°C and 1°C for WAT and WDT correspondingly. Therefore, there would be no concern if the QCM surface was broken during measurements in terms of comparative purposes.

However, a different story was observed for frequency reduction. Using a single QCM didn't show a repeatable frequency behaviour if an appropriate conditioning temperature was not used. The best way to measure optimum conditioning temperature was discussed in Chapter 4 using rheometer. In addition, different QCM surface might result in a significantly different frequency drop. Furthermore, material on the surface was realised to be sensitive to any scratch. It was also observed any change in the position of the electrical connection to the surface would make a significant impact on the frequency reading. Hence, must be taken into account using one single QCM for the whole comparative measurements without any disturbance.

Of course, while meet all the requirements using the same QCM without any disturbance showed a repeatable trend in thermal cycle path but, it showed scattered results on the maximum frequency drop. The variation for the waxy blank oils used in this work was found to be around 1000 Hz.

As an example, Figure 6-40 demonstrates up to six consecutive thermal cycles with oil sample OIL-C. The frequency drop variation is probably due to the occurrence of the gradual dissolution of wax crystals which modify the microstructure of particles from one cycle to another. In addition, the existence of some particles such as asphaltene and heavy components might co-crystallize with wax particles causing these discrepancies.

As noted, the only difference in all these cases was observed in maximum frequency drop, not the path frequency trend behaviour in thermal cycles. The only exception was found in OIL-A sample in all measurements with/out inhibitors, the first cycle, as shown in Figure 6-41, was observed to be a clearly different pattern to the subsequent cycles.

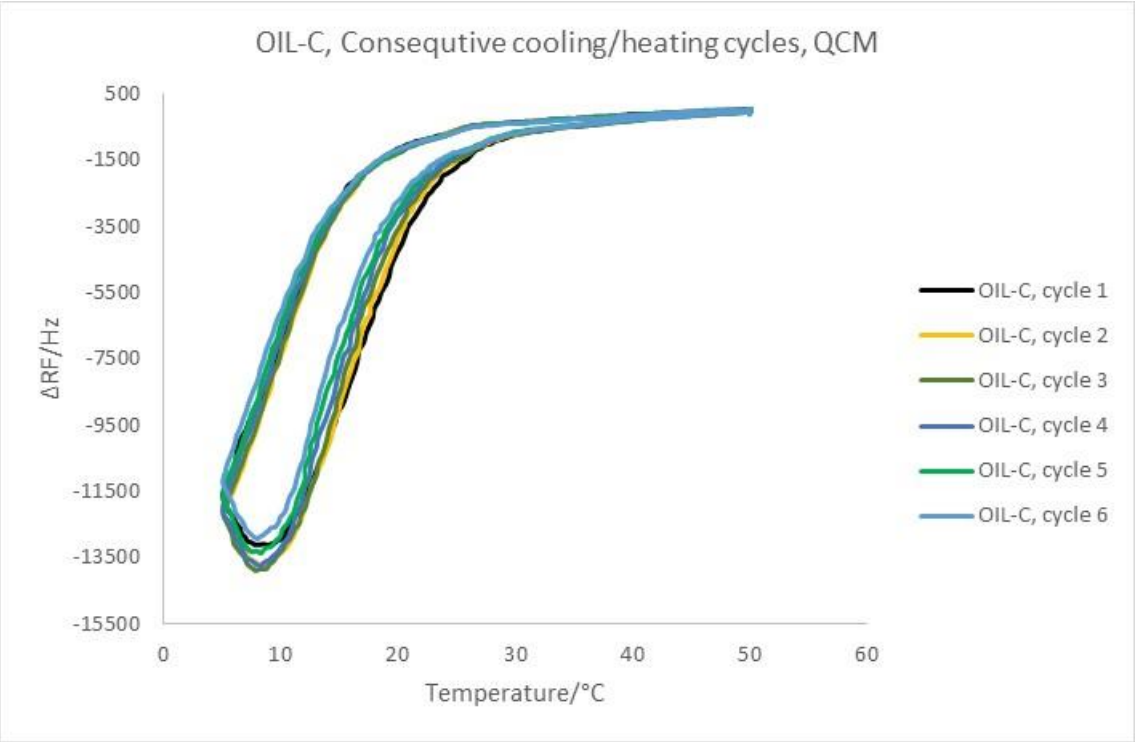

Figure 6-40. Consecutive cycles of QCM in the test tube with OIL-C sample, 3 hours conditioning between cycles.

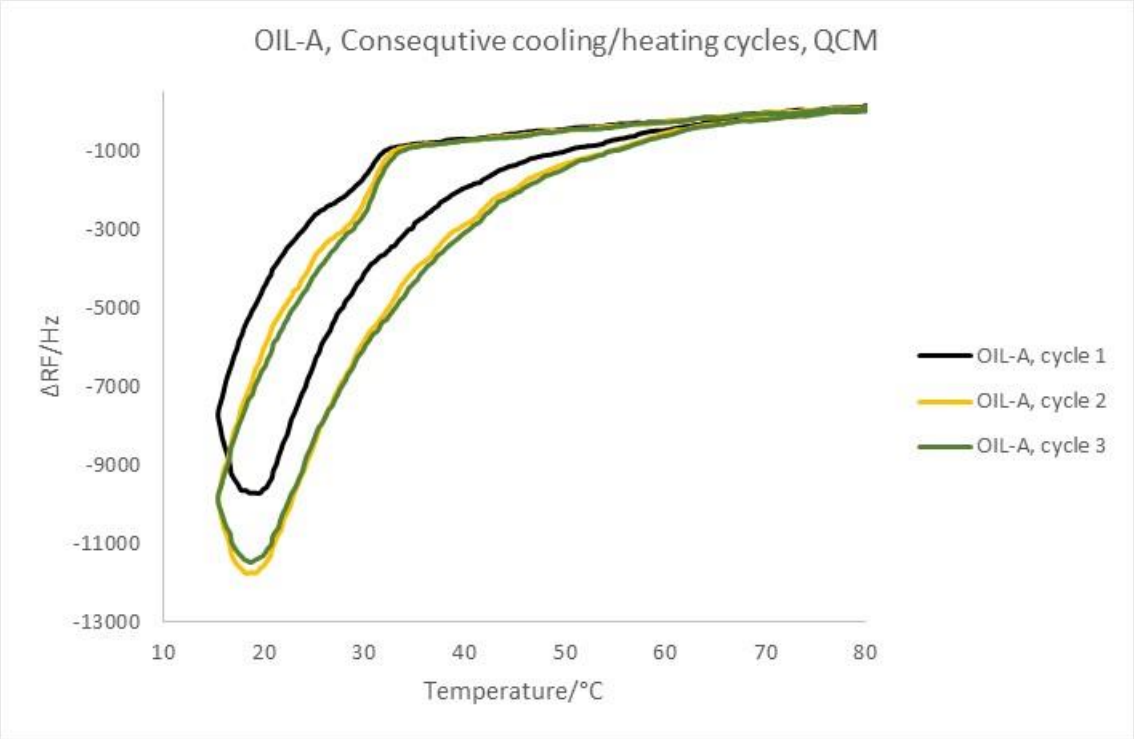

Figure 6-41. Consecutive cycles of QCM in the test tube with OIL-A sample, 3 hours conditioning between cycles.

It was considered that the presence of some impurities might be the reason for this behaviour, so then it was decided to filter OIL-A and to repeat the same cycle. Oil-A was then filtered above WAT point at high-pressure using filter paper with 22-micron pore size. The filter paper was then washed thoroughly with heptane and toluene to remove any hydrocarbon residual then analysed with scanning electron microscope (SEM). Figure 6-42 demonstrates the filter paper after the test, after washing with a mixture of toluene/heptane and a sample photo of SEM. Scanning electron microscopy on the filtered residue found that the oil contained solid particulate matter composed of predominantly barium sulphate and iron oxide. The latter one is probably due to the presence of corrosion in oil reservoir tank. In the test shown in Figure 6-43, the filtered sample was conducted in the same thermal condition where all the frequency trend overlaps one another.

Figure 6-42. Photos of filter paper after OIL-A filtration, filter paper after washed with Heptane and Toluene and a part of SEM analysis picture respectively from left to right.

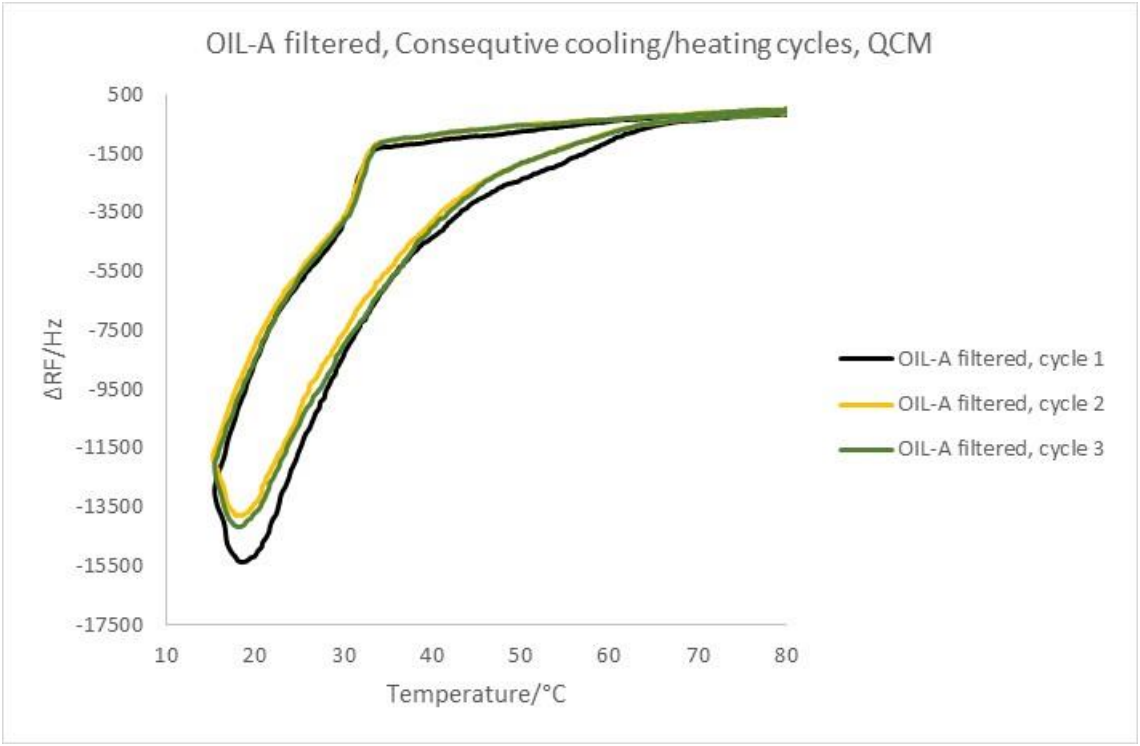

Figure 6-43. Consecutive cycles of QCM in the test tube with OIL-A filtered oil, 3 hours conditioning between cycles.

To confirm the impact of scale on frequency reading, a random sample was chosen, OIL-B, where all cycles were almost repeatable, Figure 6-44. Then some barium sulphate was added to OIL-B which it was observed the first cycle was different with subsequent cycles, shown in Figure 6-45. These observations confirmed the presence of impurities such as scale made a big discrepancy between first and the other cycles which must be taken into account in terms of inhibitor evaluation.

The reason might be due to the fact that below WAT when wax particles formed, they tend to gather around the nucleation site which was barium sulphate, in this case, so then the amount of crystals presented around the shiny surface of QCM reduced. Hence lower chance of deposition translated a lower frequency change in the first cycle. In static condition without any agitation, impurities started to settle down by gravity

depletion. In the next heating and following cycles, only wax particles which already diffused out of the bulk, dissolved and came back to the solution. It was also observed using stirrer or shaking sample between each cycle, encourage impurities to be involved in all cycles resulted in scattered values. Therefore, the best approach to deal with such oil in terms of wax evaluation is recommended to filter samples or ignore the first cycle without any agitation.

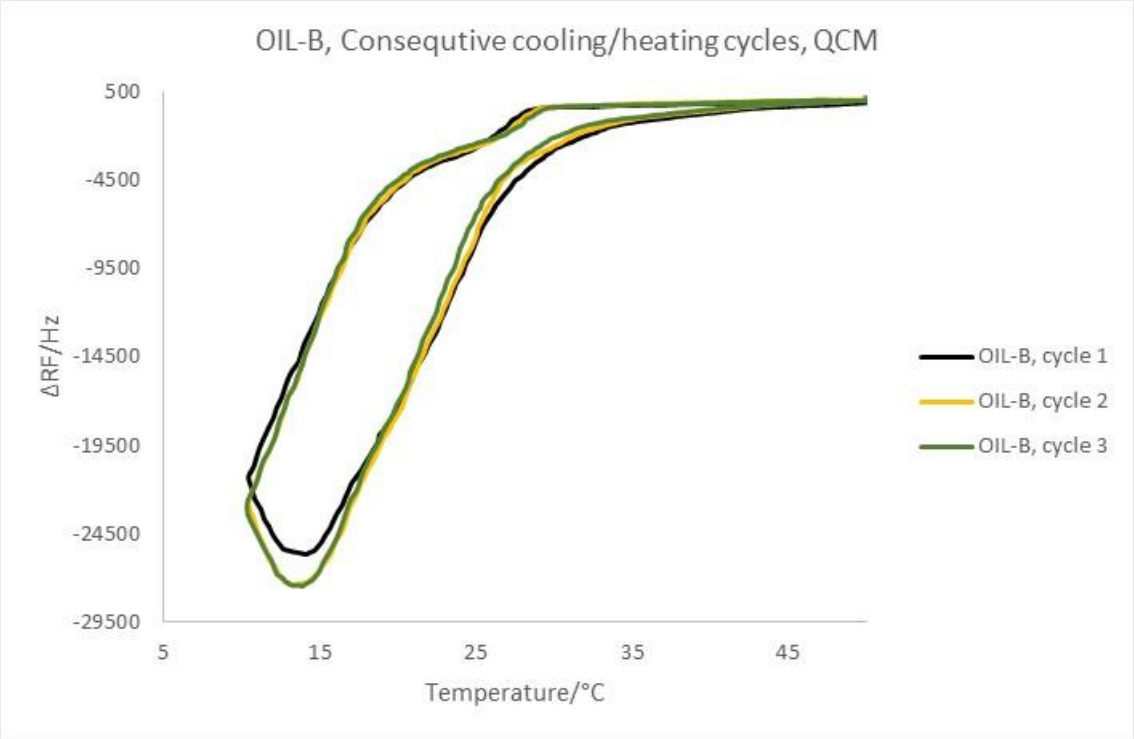

Figure 6-44. Consecutive cycles of QCM in the test tube with OIL-B sample, 3 hours conditioning between cycles.

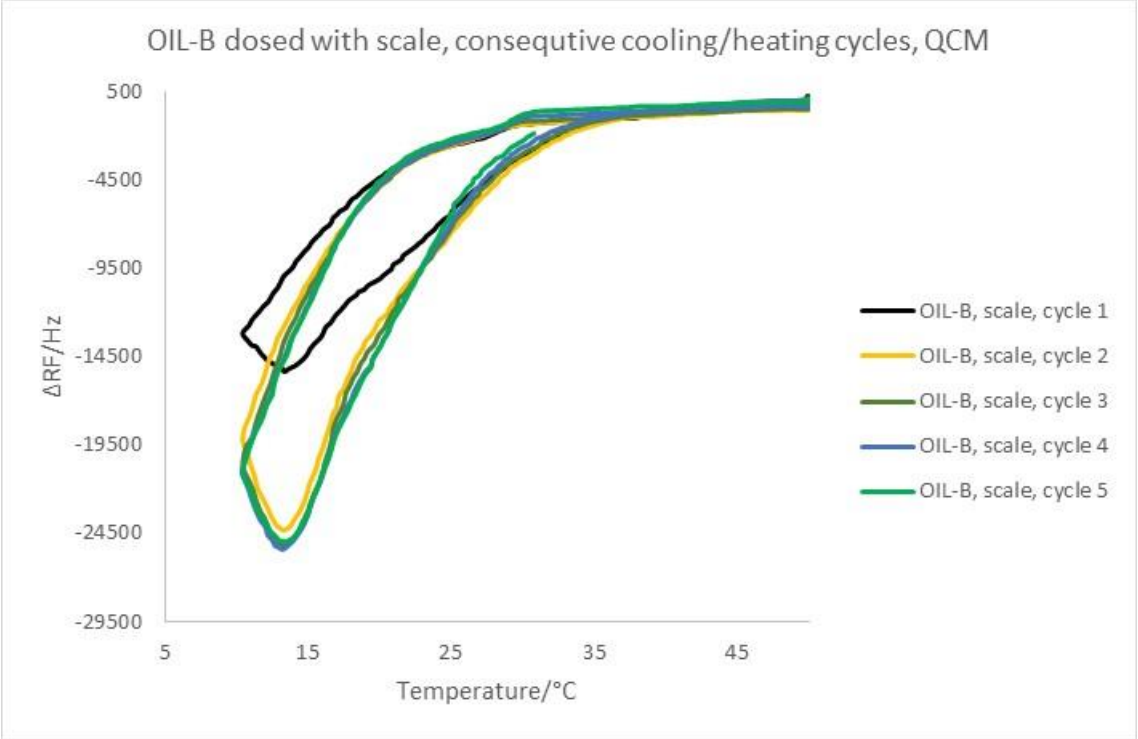

Figure 6-45. Consecutive cycles of QCM in the test tube with OIL-B sample includes barium sulphate particles, 3 hours conditioning between cycles.

6.6 References

1. Kasumu, A.S., *An Investigation of Solids Deposition from Two-Phase Wax–Solvent–Water Mixtures*. 2014, University of Calgary.
2. Burgass, R.W., *Applications of quartz crystal microbalance technology in petroleum engineering, demonstrated by studies of wax, asphaltenes, hydrates, ice, diesel additives and anti-deposition coatings*. 2015, Heriot-Watt University.
3. Kelland, M.A., *History of the development of low dosage hydrate inhibitors.* Energy & Fuels, 2006. **20**(3): p. 825-847.
4. Hsu, K., Hegeman, P., Dong, C., Vasques, R. R., O'Keefe, M., & Ardila, M. (2008, January 1). *Multichannel Oil-Base Mud Contamination Monitoring Using Downhole Optical Spectrometer*. Society of Petrophysicists and Well-Log Analysts.
5. Bybee, Karen. "*Entrance Pressure of Oil-Based Mud Into Shale.*" Journal of Petroleum Technology 61, no. 11 (2009): 63-64.
6. Trallero, J., C. Sarica, and J. Brill, *A study of oil-water flow patterns in horizontal pipes.* SPE Production & Facilities, 1997. **12**(03): p. 165-172.
7. Kokal, S.L., *Crude oil emulsions: A state-of-the-art review.* SPE Production & facilities, 2005. **20**(01): p. 5-13.
8. Becker, J., *Crude oil waxes, emulsions, and asphaltenes*. 1997: Pennwell Books.
9. Singh, P., et al., *Formation and aging of incipient thin film wax-oil gels.* AIChE Journal, 2000. **46**(5): p. 1059-1074.
10. Jennings, D.W. and K. Weispfennig, *Effects of shear and temperature on wax deposition: Coldfinger investigation with a Gulf of Mexico crude oil.* Energy & fuels, 2005. **19**(4): p. 1376-1386.
11. Zhang, Y., et al., *Effect of emulsion characteristics on wax deposition from water-in-waxy crude oil emulsions under static cooling conditions.* Energy & Fuels, 2009. **24**(2): p. 1146-1155.
12. Huo, Z., et al., *Hydrate plug prevention by anti-agglomeration.* Chemical Engineering Science, 2001. **56**(17): p. 4979-4991.
13. Kelland, M.A., T.M. Svartås, and L.D. Andersen, *Gas hydrate anti-agglomerant properties of polypropoxylates and some other demulsifiers.* Journal of Petroleum Science and Engineering, 2009. **64**(1): p. 1-10.
14. Davies, J., et al., *Environmental effects of the use of oil-based drilling muds in the North Sea.* Marine Pollution Bulletin, 1984. **15**(10): p. 363-370.

Chapter 7: Results and future works

The conclusions that can be made from the work presented in this thesis are summarised below. Following are some recommendations for future work in this area of research.

7.1 Results

The first section of this wax study, **Section 4.2,** described a proposed method to identify the lowest possible initial conditioning temperature which is identified as the Optimum Temperature in this work. The Optimum Conditioning Temperature was chosen to be the temperature at which the maximum viscosity starts to decrease and a sharp change in pour point occurs. Studies in this section conclude that overall changes in the maximum viscosity appears to be a more reliable indicator of the optimum conditioning temperature compared to changes in the pour point. Furthermore, it was found that increasing the starting temperature up to a certain temperature may cause the activation of the natural pour point depressant components which will disturb the wax crystals and as a result decrease the oil viscosity/pour point. On the other hand, the starting temperature had no significant impact on the reduction/inhibition of WAT point; it was observed that as expected increasing the conditioning temperature led to increasing both WAT and WDT. Furthermore, while literature has concluded that injection of some paraffin inhibitors into the well should be done at relatively high temperatures so that minimum viscosity is achieved, this study has concluded that high temperatures do not necessarily give highest viscosity reduction. Consequently, if reduction of viscosity is presumed to be the determining factor for the highest inhibitor performance, the most effective temperature for paraffin inhibitor injection should be the Optimum Temperature which is the lowest temperature and results in the lowest viscosity.

In **Section 4.3** an investigation to determine the impact of cooling/heating rate on WAT/WDT and viscosity measurements using a rheometer was presented. Studies of this chapter concluded that generally a slow cooling rate results in higher measured values for WAT and WDT. Moreover, the maximum viscosity, viscosity value at lowest test temperature, for a light waxy oil sample has a linear increase when increasing the cooling rate. On the contrary, for a heavy waxy oil sample this maximum viscosity has a linear decreasing trend with increasing the cooling rate. This result will help take into

account and/or eliminate the cooling rate effect when comparing results of different test techniques with varying cooling rates.

In **Section 4.4**, a series of measurements using a coaxial cold finger apparatus was conducted to study the impact of ageing time and shear rate on a blank oil sample. It was found that re-combining the collected wax and oil could be employed as a method to re-use the wax and bulk oil from previous tests; hence, it would be possible to perform series of subsequent tests without using large quantities of oil. In addition to that, recombining can reduce the uncertainty between two different samples for comparison purposes in tests such as inhibitor evaluation. Furthermore, the impact of so-called 'ageing' of the wax on the hardness of deposition was observed by scraping and weighing the wax from the bob at the end of each test. For those tests with longest experimental times, wax gradually became harder. Also, it did appear that the thermal insulation of deposition caused the wax deposition rate to decrease for times over 150 hrs, in an applied shear rate of 100 s^{-1}. Furthermore, results of this section revealed a maximum deposition value with increasing shear rate in the laminar flow region. Wax deposition increased with increasing shear rate before approaching the shear strength of the deposited wax, after which it started to decrease with increasing the shear rate. It was observed that the deposited wax was thicker at the base of the bob compared to the top of the bob, which was increasingly apparent at shear rates over 250 s^{-1}. In experiments under static conditions it was difficult to identify deposited wax (if any) from the bulk oil.

The objective of the work in **Section 4.5** was to investigate the impact of temperature gradient as a driving force on the performance of inhibitors in terms of wax deposition using the coaxial setup. As expected, a higher degree of subcooling corresponds to the greater driving force for crystallization, covering a larger range for involving more components that can cause deposition; hence, higher deposition was formed. The performance of inhibitors was highly selective and INH-C showed the highest dependency on temperature gradient, giving a better performance at lower subcooling. In addition, in all samples except INH-C, which appeared to show a crystal modifier behaviour, decreasing subcooling resulted in a smoother layer of deposition. Furthermore, the presence of impurities resulted in some erroneous value making it difficult to screen inhibitors; these impurities might adhere to the surface even at higher WAT points.

The aim of **Chapter5** was to explain a series of screening techniques, comparing and evaluating the wax inhibition performance of a number of commercially available wax inhibitors. The equipment included, rheometer, QCM, coaxial cold finger, flowloop and NIR.

Section 5.2 describes two different approaches using the rheometer for screening inhibitors. The first approach was based on viscosity assessment. The efficiency of an additive was evaluated based on reduction of non-Newtonian viscosity. Viscosity was found to be an appropriate approach in terms of inhibitor screening apart from those samples with a low maximum viscosity lower than 10cP, OIL-A and OIL-F in this study. Overall it was concluded that polymeric inhibitors reduced viscosity in the non-Newtonian region. On the other hand, the tested non-polymeric inhibitor, INH-H, slightly increased viscosity. The second successful approach was based on measuring the pour point with an accuracy of ±0.2°C using the rheometer. Pour point reduction provides a reference to evaluate the effectiveness of inhibitors. Since the accuracy of pour point measurements by the rheometer is about ±0.2°C, it was possible to use pour point reduction to evaluate inhibitors in the sample with low maximum viscosity such as OIL-A, lower than 10cP. Generally, the pour point reduction of inhibitors follow a similar sequence as inhibitor viscosity reduction which means that inhibitors which reduce the pour point most are the ones that reduce the viscosity most and vice versa. Furthermore, in **Section 5.2**, the strength of inhibitor under several consecutive thermal cycle tests, as well as long conditioning time was studied using high-pressure geometry with rheometer. It could be concluded that the possibility of inhibitor deterioration or morphological change in the thermal cycles and long conditioning time were insignificant, at least for the tested inhibitor. It was also observed that increasing inhibitor dosage doesn't necessarily guarantee improving the performance. Hence, dosage evaluation is important. Moreover, it was observed that measuring sample viscosity in the presence of impurities should be used with caution as these impurities can influence viscosity measurements. In this case, it should not rely on the initial viscosity at a constant temperature, even after 5 hrs stabilising test time as impurities do not settle until after the first thermal cycle. For this reason, it was found that an initial thermal cycle is necessary and viscosity measurements and recordings should be done after this and preferably in the second cycle during which deterioration has yet not occurred. In addition to that, it was found that the presence of inhibitor may cause some unexpected behaviour such as instability of viscosity in the middle of the heating process in a thermal cycle test.

The aim of **Section 5.3** was to compare resonant frequency drop as an indication of wax deposition with viscosity in each individual treated sample. Generally, there was a good match between viscosity reduction and decrease in frequency drop.

As observed in preliminary measurements, low viscosity oil samples showed a high inconsistency with long ageing time using coaxial equipment, making it impossible to screen inhibitors. Hence, the first aim of **Section 5.4** was to calibrate the coaxial setup and find the best ageing time for waxy low viscous oils. Three different ageing times were tested, 67hrs, 24hrs and 1hr. It was then observed that 1hr ageing time resulted in reliable data with high accuracy. No significant sloughing was observed compared to the longer ageing time, reducing deviation in results hence allowing easier screening of inhibitors with low viscosity waxy samples. The standard deviation obtained was ±0.0098gr. The overall trend showed decreasing deposition with decreasing corresponding maximum viscosities and lower ΔRF. In addition to that, a closer look at the deposited crystals show that, larger masses of deposition form a smooth layer on the bobbin surface whereas smaller masses of deposition form a rough, coarse and uneven layer with small sphere particles that has an overall darker colour. Furthermore, the top section of the bobbin was observed to be free of wax which was found to be larger at lower viscosities measured by rheometer, ΔRF with QCM and lower deposition measured by the coaxial.

Several experimental campaigns are presented in **Section 5.5** using an in-house built mini benchtop flowloop. Preliminary measurements were aimed at studying the impact of thermal cycle on the results. In this study it was observed that there was an increased differential pressure buildup in several sequential cycles. Increasing conditioning time even up to 48 hrs or thoroughly cleaning the loops between each cycle and even degassing fluid before injecting into the loop, did not change the outcome, hence, only the first cycle should be reported for comparison purposes. Moreover, the best technique for ranking inhibitor performance was found to be visual assessment by plotting differential pressure and wax thickness versus ageing time. It was also observed that length of the loop was a decisive factor to log the outlet temperature. The inlet temperature in all cases was found to be a constant value. Overall, it was found that viscosity had a powerful impact on ranking inhibitors; lower viscosity resulted in higher deposition regardless of following campaigns:

- Testing at different subcooling

- Testing with a different geometry, decreasing length, inside diameter and tuned height as low as possible to encourage deposition move freely out of the loop.
- Using a synthetic sample which was free of asphaltene, heavy particles and impurities.
- Adding Inhibitor to pre deposited wax.
- Testing in the presence of a watercut
- Testing without accounting for the effect of a closed circulation loop, using a single batch fresh sample through the loops.

Furthermore, in **Section 5.5**, evaluation of inhibitors was studied at two different shear rates of 76 s^{-1} and 151 s^{-1} for OIL-A which showed a very low maximum viscosity. Visual inspection at the lower shear rate, made it impossible to screen and rank inhibitor performance in terms of overall differential pressure/deposited thickness. Moreover, it was found that at the same subcooling, flowrate did not have a significant influence on the maximum thickness of the deposit. Since the ageing process forms a stable deposition which increases with increasing flowrate, the only difference observed was that this rate of increase in deposition is faster at the higher flow rate.

Section 5.6 describes NIR spectroscopy results. The strength of intensity reduction could be attributed to precipitation rate of particles, giving an opportunity to evaluate wax inhibitors. Decreasing viscosity was observed to show higher precipitation, in keeping with what was found in flowloop in terms of deposition. Overall, lower viscosity lead to higher precipitation rate leading to higher deposition.

Any changes in the wax appearance temperature might be an indication of the impact of wax inhibitors on the wax crystallisation process. In **Section 5.7,** inhibitor screening by measuring WAT/WDT was discussed. Several different independent types of equipment were used with the capability of measuring WAT. These included rheometer, QCM, NIR and flowloop. WDT was only measured with QCM. In general, inhibited samples showed the same or lower WAT in comparison with the blank sample in all equipment. WAT obtained by flowloop is known as dynamic WAT which showed a low accuracy, highly depended on the inside diameter of loops. However, it was observed that the dynamic WAT of samples with different inhibitors follow an almost similar order of ranking to the obtained data by the other devices although with a deviation of up to 10°C in the precipitation point. Both WAT/WDT were found to decrease by reducing the ΔRF obtained by QCM in the same way. Moreover, the higher WAT/WDT

coincides with the observation of higher corresponding maximum viscosities. Furthermore, the variation of rheometer measured WAT point of the treated sample resulted in the higher range of up to 11°C in average, rather than measurements using other equipment with the lower average point of 6.5°C. The greater range of variation will give an opportunity to assess and rank inhibitors more easily. As a result, rheometer seemed to be a more clear technique on the ranking of inhibitor performance in terms of WAT comparison. Additionally, the rheometer WAT measurement technique, showed a higher value in the WAT point in comparison with the QCM and NIR. Finally, measuring WDT with QCM, highly depends on the cooling/heating rate to allow wax particles to equilibrate with applied temperature, as well as the user experience. Moreover, the presence of impurities was observed to make some noise on WDT detection; hence, WDT measurements showed a high statistical deviation. Accordingly, WDT data obtained by QCM was not found to be a reliable approach for inhibitor evaluation.

In order to deeply understand the reason for discrepancies between commonly used techniques, as well as naked eye visual monitoring of morphological behaviour on treated wax particles, a series of tests with a clear sample was performed as described in **Section 5.8**. It was observed that the morphology of the wax particles increased in size and shape reducing the cloudiness. Overall, depletion of wax particles was found to be a dominant mechanism in the presence of inhibitor injection. Wax depletion can be used to explain the discrepancies of the results with the various techniques under study in this work. The strength of depletion and reducing the cloudiness of sample under WAT was in order with:

- Reducing viscosities and pour point (rheometer, flowloop)
- Increasing the morphology of the wax particles in size and shape (coaxial, visual observation)
- Reducing the WAT point in all measuring equipment
- Reducing the frequency drop (QCM)
- Lower wax deposition on the bobbin surface (coaxial)
- The higher wax thickness and lower flake off wax layers (flowloop)
- Higher intensity drop (NIR)

The aim of **Section 6.2** was to study the impact of subcooling on the wax deposition process in the presence of water, MEG and Methanol using flowloop. They all have insignificant solubility in oil mainly forming an emulsion, hence were expected to have the same effect at similar test conditions. The impact was found to be highly dependent on subcooling. At low temperature, there was no significant difference in deposition thickness; once subcooling reduced, the deposited wax thickness also started to reduce regardless of emulsion acting agent.

A short study is presented in **Section6.3** on the effect of two different commercial AA with different dosages, purely on wax deposition without watercut and hydrate formation using rheometer, QCM and flowloop. It was observed that increasing AA dosages reduced the viscosity of the mixture in the non-Newtonian region below WAT point. The impact on the wax was found to be oil dependent on QCM reading. Two distinct mechanisms were observed. In some oils, increasing AA dosages were found to have no significant impact on WAT/WDT point and decreased the wax adherent tendency to the surface. Another behaviour was observed with some other oils, increasing AA dosages reduced WAT point and increased the wax adhesion tendency to the surface. The overall result using flowloop showed that AAs at higher subcooling resulted in a better performance in terms of inhibition of wax deposition. In low subcooling, increasing dosages encouraged higher wax deposition

A simple approach is discussed in **Section 6.4**, to investigate the ability to predict some wax properties including WAT, WDT, viscosity and wax deposition tendency of the uncontaminated samples from oil-based mud using both rheometer and QCM. In general, a linear relation between WAT, WDT, wax adhesion tendency and a semilog relation in viscosity was found. All the points were in the order of linear trend quite close to 1 r-squared which made it possible to predict the wax relation parameters in any sample with different contamination level using rheometer and QCM.

Section 6.5 discussed the impact of impurities on the QCM reading as well as repeatability and reliability of using different QCM surface on wax properties. It was observed that WAT and WDT were independent of QCM surface, impurities, thermal cycles and condition time. The average deviation in various QCM for the sample under study in this work was resulted around 0.5°C and 1°C for WAT and WDT correspondingly. However, a different story was observed for frequency reduction. The amount of frequency reduction was observed to be highly dependent on QCM surface,

thermal cycles, condition time, cooling rate, the position of the electrical connection to the surface, surface roughness and any other external disturbance to the surface. Hence, one single QCM should be used for the whole comparative measurements without any disturbance. In addition, the same frequency trend was observed in all cycles without impurities; the only difference was in the maximum frequency drop with a reasonably average deviation of 1000 Hz. In the presence of impurities on the other hand, the first cycle pattern was completely different from the other subsequent cycles. It was also observed using stirrer or shaking sample between each cycle, encouraged impurities to be involved in all cycles resulting in scattered values. Therefore, the best approach to deal with such oil in terms of wax evaluation is to filter samples or ignore the first cycle without any agitation.

Following is a short summary of the most important developments and findings in this thesis:

- A technique has been developed using the rheometer for finding the Optimum Conditioning Temperature to mimic the worst possible results in the field. This Optimum Conditioning Temperature has also been found to be the optimum temperature for maximising injected paraffin inhibitor performance.

- In wax studies, cooling rate has shown a notable impact on WAT-WDT and viscosity measurements. Therefore, it is important to optimize this parameter in order to compare results of different test techniques.

- An intensive wax study on coaxial cold finger, Quartz Crystal Microbalance, mini-benchtop flowloop (build and developed as a part of this thesis), rheometer and Near Infra-Red setup was performed on various parameters, wax inhibitors and different types of oil in terms of gravity which can easily be referenced by the other researchers.

- Developed a novel technique using the rheometer to measure pourpoint with an accuracy of ±0.2°C.

- It was found that viscosity has a pronounced impact on ranking wax inhibitors.

- Depletion of wax particles was found to be a dominant mechanism in the presence of wax inhibitor injection which can be used to explain the discrepancies of the results with various techniques.

- Subcooling was found to have a predominant impact on the wax deposition in the presence of water and some hydrate inhibitors including MEG, Methanol and two different commercial low dosage anti-agglomeration.

- A novel and straightforward technique was described to predict the wax properties (WAT, WDT, viscosity and wax adhesion tendency) of uncontaminated samples from oil-based mud.

7.2 Future work

The effect of conditioning temperature was only reported for rheometer using blank oil sample with some inhibitors. It is recommended to employ other equipment with different starting conditions. In addition, adding different dosages of asphaltene/resin from the same source of sample oil extracted by SARA fraction to find the lowest possible concentration which might have an impact on wax parameters.

The cooling rate study was performed in the range of 0.2 to 1 °C/min measuring WAT/WDT and viscosity behaviour using atmospheric cone and plate rheometer where evaporation might have some impact on the results. It is then suggested to use high pressure geometry to avoid evaporation in addition to using higher range of cooling rate. QCM technique can also be used to determine WAT/WDT and wax adherent tendency with various cooling rates. Moreover, it was observed that decreasing cooling rate resulted in a lower maximum viscosity except for OIL-E sample which was the heaviest oil in comparison with the other samples under study. It is speculated that the applied shear rate of $10s^{-1}$ was not high enough to break down the wax microstructure. It is therefore recommended to use higher shear rate with the same condition.

It was observed that the deposited wax was thicker at the base of the coaxial bob compared to the top of the bob, it was then concluded that the wax depletion in presence of inhibitor was the reason. Therefore, it would be a good idea to change the coaxial position in a horizontal way following the same approach.

Coaxial and flowloop test was employed in a constant differential temperature in this work. It is suggested to run a series of tests where both bulk oil and wall temperature will be reduced gradually in the same constant differential temperature simulating real conditions along the flowline. For this purpose, there is the need to optimize both devices. Thermal jacket on coaxial should be optimized to be able to control and log

data. Furthermore, using another controlled bath is necessary between conditioning bath and test bath for flowloop.

The gap between the lower and upper test plates in rheometer was set at 0.1mm. Oil with very low max viscosity resulted a low deviation in temperature sweep which made it difficult to assess inhibitor performance. It could be attributed to the low wax content or small wax particle size. Consequently, it is recommended to reduce the gap as much as possible. A new calibration with the measured gap is then necessary.

Flowloop tests were done in laminar flow where gravity depletion is found to have a dominant impact on deposition, resulting in a reverse ranking in comparison with QCM, rheometer and coaxial equipment. Using samples in turbulent flow condition helps identify what the best approach is for screening inhibitors.

It was observed that there was an increased differential pressure buildup in several sequential thermal cycles using flowloop. Increasing conditioning time, cleaning the loops between each cycle and degassing fluid did not change the outcome. Further investigation is suggested.

It was observed that the presence of impurities resulted in a significant impact especially in flowing condition where a long time is required to settle down and remove particles from the bulk oil. Filtration or using centrifuged samples in temperatures higher than the WAT point will give a clearer assessment of inhibitor screening.